



15432

ON-BOARD VEHICLE OPERATING PARAMETER MEASUREMENTS AND VEHICLE EMISSIONS MODELING

Final Report

Contracts Number S-C92101 and S-C92029
SOUTH COAST AIR QUALITY MANAGEMENT DISTRICT.

Principal Investigator

Arthur M. Winer

Researchers

Michael J. St. Denis
Pablo Cicero-Fernández

ENVIRONMENTAL SCIENCE AND ENGINEERING PROGRAM
DEPARTMENT OF ENVIRONMENTAL HEALTH SCIENCES
SCHOOL OF PUBLIC HEALTH
UNIVERSITY OF CALIFORNIA
LOS ANGELES, CALIFORNIA 90024

MARCH 1994

ABSTRACT

To aid in resolving critical questions about the accuracy of mobile source emissions models (e.g. EMFAC and MOBILE), this study provided a direct evaluation of real-time, on-road vehicle and engine operating parameters, and investigated their relationship to rich open loop emissions and driving pattern characteristics. Data were collected using a 1991 Ford Taurus equipped with a computerized on-board data collection system which was connected to the stock electronic engine controller. More than 200,000 seconds of data were collected driving the test vehicle both "conservatively" and "aggressively" in morning and evening commute hours over a matrix of eight freeway and eight urban routes in California's South Coast Air Basin. Dynamometer emissions measurements were conducted for the Federal Test Procedure (FTP), the Highway Fuel Economy Test (HFET), and three new driving schedules developed for this study. Two modal emissions models were developed; one based on modeling emissions as a function of acceleration and speed and one based on modeling emissions as a function of load and speed. Emissions rate data from the dynamometer emissions tests were used as a data base for modeling of on-road emissions for the driving pattern data collected on-road in the SoCAB.

The average on-road speed was 31.2 mph compared to 20.7 mph for the FTP and the maximum acceleration rate on-road was 10.0 mph s^{-1} compared to 3.3 mph s^{-1} for the FTP. Rich open loop operation was not observed during the FTP or HFET, however, it was observed an average of 0.005% of the time on-road for conservative driving and 0.77% of the time for aggressive driving. Rich open loop operation was approximately twice as frequent on urban routes as it was on freeway routes. Other factors which increased rich open loop operation were up-hill grades, merging and free flowing traffic conditions. Emission rates during rich open loop operation were ≈ 100 times higher than the closed loop emission rate for HC (0.038 g s^{-1} during open loop operation), ≈ 1700 times the closed loop emission rate for CO (3.17 g s^{-1}) and ≈ 80 times the closed loop emission rate for NO_x (0.106 g s^{-1}).

Two new vehicle emissions models were developed and tested, the UCLA Acceleration-Based Vehicle Emission (UAVE) Model and the UCLA Load-Based Vehicle Emission (ULVE) Model. Of the two, the load- and speed-based model was found to be the most accurate. Emission rates for the driving pattern data recorded on-road in the SoCAB were modeled using the load-based model. Aggressive driving was found to cause higher emission rates of CO and NO_x than conservative driving (6.8 versus 3.1 g mi^{-1} and 0.49 versus 0.26 g mi^{-1} respectively) but essentially no difference in the HC emission rate (0.29 versus 0.28 g mi^{-1}). With the exception of the NO_x emission rate during aggressive driving, all of the modeled on-road emission rates were lower than the current certification emissions standards, but they were also all greater than the emission rates measured for the FTP (33% for HC, 190% for CO and 120% for NO_x).

The higher emission rates on-road versus the FTP were attributed to the occurrence of rich open loop operation on-road but not during the FTP, as well as differences between current driving patterns and the Urban Dynamometer Driving Schedule used in

the FTP. For CO, $\approx 70\%$ of the increase in the emission rate was determined to have come from open loop operation, and for both HC and NO_x, $\approx 40\%$ of the increase was attributed to open loop operation with the remainder attributed to differences between the FTP and on-road driving patterns.

The results of the modeling studies suggest emissions from rich open loop operation, because they are not included in the FTP, may account for a portion of the under-estimation of current mobile source emissions models. However, because the emissions modeling was only conducted for a single vehicle, it is difficult to draw conclusions about the entire in-use fleet. Much more needs to be known about the frequency of rich open loop operation on-road and the emission rates during this operation for a variety of vehicles. If rich open loop operation is not included in the emissions measurements which are used as inputs to emissions models, and if the emissions from these events account for a significant proportion of the total vehicle emissions, there will continue to be discrepancies between on-road emissions and the emissions predicted by emissions models. New emissions testing procedures need to be developed which will include all possible operations of on-road vehicles, and new vehicle emissions models need to be developed which can weight the emissions data in a manner representative of current driving conditions.

TABLE OF CONTENTS

ABSTRACT	i
ACKNOWLEDGEMENTS	viii
DISCLAIMER	ix
LIST OF FIGURES	x
LIST OF TABLES	xxi
GLOSSARY OF TERMS, ABBREVIATIONS AND SYMBOLS	xxiv
EXECUTIVE SUMMARY	1
1. Introduction	1
2. On-Road Conservative and Aggressive Driving versus the FTP	2
3. Frequency of Open Loop Operation	4
4. Dynamometer Emissions Experiments and Emissions During Open Loop Operation	4
5. Modeling of On-Road Emissions and Comparison to the FTP	5
6. Conclusions and Recommendations	7
1.0 - INTRODUCTION	9
1.1 Background	9
1.2 The Use of Airshed Models in the Development of Air Pollution Control Strategies	10
1.3 Emissions Inventories	10
1.3.1 The Federal Test Procedure (FTP)	11

1.3.1.1	Development of the Urban Dynamometer Driving Schedule	15
1.3.2	The ARB's Emissions Factor Model, EMFAC	18
1.4	Sources of Under-Estimation in Mobile Source Emissions Inventories	18
1.4.1	"Gross Emitters"	21
1.4.2	Rich Open Loop Operation	23
1.5	Objectives	34
2.0	EXPERIMENTAL	35
2.1	Hardware Description	35
2.1.1	Test Vehicle	35
2.1.2	Vehicle Instrumentation and Data Collection System	35
2.2	Data Collection Procedures	42
2.3	On-Road Experiments	43
2.3.1	Start, Idle and Cool Down	43
2.3.2	Acceleration and Deceleration	43
2.3.3	Effects of Variation in Load	44
2.3.4	Repeated Freeway Route	44
2.3.5	Conservative Driving Freeway and Urban Route Matrix	45
2.3.6	Aggressive Driving Freeway and Urban Route Matrix	46
2.4	Data Analysis Software	49
2.5	Dynamometer Emissions Tests	55
2.5.1	Development of Dynamometer Driving Schedules	55
2.5.2	Dynamometer Emissions Measurements	56
2.6	On-Road Emissions Modeling	71
2.6.1	Development of Emissions Binning Models	81
2.6.2	Development of Emissions Estimating Models	81
2.6.3	Validation of the Models	82
2.6.4	Modeling of On-Road Emissions	85

3.0 - RESULTS AND DISCUSSION	87
3.1 Limitations on the Scope of the Study	87
3.2 On-Road Experiments	87
3.2.1 Vehicle Operating Parameters During Start, Idle and Shut Down.	87
3.2.1.1 Starts	87
3.2.1.2 Idle	98
3.2.1.3 Cool Down	98
3.2.2 Maximum Operating Envelope	102
3.2.2.1 Comparison to the FTP	104
3.2.3 Development of Modes of Operation	107
3.2.4 Effect of Variations in Load	107
3.2.5 Repeated Freeway Experiment	113
3.2.6 Comparison of Conservative Driving to the FTP	120
3.2.7 Comparison of Aggressive Driving to the FTP and Conservative Driving	139
3.2.8 Open Loop Operation	166
3.2.8.1 Lean Open Loop Operation	166
3.2.8.2 Rich Open Loop Operation	170
3.3 Dynamometer Emissions Experiments	181
3.3.1 Comparison of UCLA Freeway and Urban Driving Schedules to On-Road Driving Patterns and the FTP	181
3.3.2 Comparison of Bag Emissions to Second-by-Second Emissions	183
3.3.3 Comparison of Bag Emissions to Emissions Certification Standards	190
3.3.4 Frequency and Emission Rates of Open Loop Operation During the Dynamometer Emission Tests	196
3.4 Emissions Modeling	218
3.4.1 Model Validation	218
3.4.2 Predicted On-Road Emissions and Comparison to Certification Emissions Standards	220

4.0 - CONCLUSIONS AND RECOMMENDATIONS	233
REFERENCES	236
APPENDICES	241
A.1 Data Analysis Programs	242
A.1.1 VDAS Data Analysis Program ANLYS50C.FOR	243
A.1.2 Velocity and Acceleration Probability Binning Program VABINNEW1.FOR	264
A.2 Emissions Modeling Programs	268
A.2.1 Acceleration and Speed-based Emissions Binning Program EMMODE.FOR	269
A.2.2 Acceleration and Speed-based Emissions Averaging Program AVGM.FOR	279
A.2.3 Acceleration and Speed-based Emissions Estimating Program MODEIO.FOR	285
A.2.4 Load and Speed-based Emissions Binning Program EMLOAD.FOR	294
A.2.5 Load and Speed-based Emissions Averaging Program AVGL.FOR	303
A.2.6 Load and Speed-based Emissions Estimating Program LOADIO.FOR	309
A.2.7 One Second Emissions Analysis Program EMOUT.FOR	317
A.3 List of File Extension Definitions	319
A.4 Occurrences of Open Loop Operation On-Road	320
A.4.1 Repeated Freeway Experiment Lean Open Loop Events	321
A.4.2 Repeated Freeway Experiment Rich Open Loop Events	322
A.4.3 Conservative Driving Experiments Lean Open Loop Events ...	323
A.4.4 Conservative Driving Experiments Rich Open Loop Events ...	324
A.4.5 Aggressive Driving Experiments Lean Open Loop Events	325
A.4.6 Aggressive Driving Experiments Rich Open Loop Events	326

A.5	UCLA Developed Dynamometer Driving Schedules	327
A.5.1	UCLA Freeway Dynamometer Driving Schedule	328
A.5.2	UCLA Urban Dynamometer Driving Schedule	332
A.5.3	UCLA Acceleration Dynamometer Driving Schedule	336
A.6	Determination of Emission Rates During Rich Open Loop Operation	340
A.6.1	Analysis of Rich Open Loop Emission Rates During Cold Start Bag of UCLA Acceleration Cycle	341
A.6.2	Analysis of Rich Open Loop Emission Rates During Hot Running Bag of UCLA Acceleration Cycle	347
A.6.3	Analysis of Rich Open Loop Emission Rates During Warm Start Bag of UCLA Acceleration Cycle	353
A.6.4	Summary of the Analysis of Rich Open Loop Emission Rates by Speed of the UCLA Acceleration Cycle	359
A.7	Estimated and Measured Emission Rates For Dynamometer Driving Patterns	360
A.8	Estimated Emission Rates For On-Road Driving Patterns	361
A.8.1	Estimated Emission Rates For Conservative Driving On-Road Patterns With a Cold Start Added	362
A.8.2	Estimated Emission Rates For Conservative Driving On-Road Patterns With No Starts	363
A.8.3	Estimated Emission Rates For Conservative Driving On-Road Patterns With a Warm Start Added	364
A.8.4	Estimated Emission Rates For Aggressive Driving On-Road Patterns With a Cold Start Added	365
A.8.5	Estimated Emission Rates For Aggressive Driving On-Road Patterns With No Starts	366
A.8.6	Estimated Emission Rates For Aggressive Driving On-Road Patterns With a Warm Start Added	367

ACKNOWLEDGEMENTS

The important role of Dr. Alan Lloyd (SCAQMD) and Professor Joseph Norbeck (UC Riverside) in the conception of this project is gratefully acknowledged. This project was conducted in collaboration with James W. Butler and Gerald Jesion at Ford Motor Company Scientific Research Laboratories (FMCSRL), Dearborn without whom this study could have not been completed.

The authors would like to thank David Chock, Chris Gierczak, and John Pitak of FMCSRL, Virginia Smith of Ford Engine and Electronic Engineering, Matthew Barth of UCR and Jon Leonard of SCAQMD for helpful discussions. John Piatak of FMCSRL developed the instrumentation system used in the test vehicle and worked with John Mulrine and Jim Augestine of FMCSRL on the installation of the instruments in the vehicle. Bill Larkin of UCLA aided in the maintenance of the instruments and the test vehicle. Dynamometer emissions tests were conducted at the beginning of the study with the assistance of Tom Kornisky and John Weir at the FMCSRL test facility and at the end of the study by William Cooley and Elizabeth Zaldivar at the Ford Gas Turbine Laboratory dynamometer facility.

We wish to thank the South Coast Air Quality Management District for support of this research under Contracts S-C92101 and S-C92029 (Alan Lloyd, Chief Scientist; Jon Leonard, Project Manager).

DISCLAIMER

This report was prepared as a result of work sponsored by the South Coast Air Quality Management District (DISTRICT). The opinions, findings, conclusions, and recommendations are those of the authors and do not necessarily represent the views of DISTRICT. DISTRICT, its officers, employees, contractors, and subcontractors make no warranty, expressed or implied, and assume no legal liability for the information in this report. DISTRICT has not approved or disapproved this report, nor has DISTRICT passed upon the accuracy or adequacy of the information contained herein.

LIST OF FIGURES

Figure 1.3.1.1	Speed versus time trace of the Urban Dynamometer Driving Schedule (UDDS).	14
Figure 1.3.1.2	Speed versus time trace of the Highway Fuel Economy Test (HFET).	16
Figure 1.3.1.1.1	The LA 4 on-road driving route.	17
Figure 1.3.2.1	ARB's motor vehicle emissions inventory process (Horie, 1992).	19
Figure 1.4.1.1	Schematic of General Motors instrumentation for roadside measurements of vehicle exhaust CO (Stephens and Cadle, 1991).	22
Figure 1.4.1.2	Cumulative VMT versus cumulative CO emissions for Los Angeles remote sensing data and EMFAC7E model predictions (Pollack, 1992).	24
Figure 1.4.1.3	Fraction of cars and CO emissions by model year (Stephens and Cadle, 1991).	25
Figure 1.4.1.4	Mean emissions rates of passenger cars by model year (Stephens and Cadle, 1991).	25
Figure 1.4.2.1	Emissions control system types: a. Oxidation catalyst; b. Dual-bed catalyst; and, c. Three-way catalyst (Alder, 1985b).	27
Figure 1.4.2.2	Chemistry of oxidation of CO and HC and reduction of NO _x on catalyst surface (Alder, 1985b).	28
Figure 1.4.2.3	Ignition and fuel metering control system of a modern production vehicle (Alder, 1986b).	29
Figure 1.4.2.4	Pre-catalyst (a) and post-catalyst (b) relative emissions rates of CO, HC and NO _x as a function of air/fuel ratio (c), (Lies, 1989).	30

Figure 1.4.2.5	Schematic diagram of lambda closed-loop operation (1985b).	31
Figure 1.4.2.6	Limiting factors in the development of a vehicle strategy and calibration.	33
Figure 2.1.1.1	1991 FFV Ford Taurus test vehicle.	36
Figure 2.1.2.1	Vehicle data collection system.	37
Figure 2.1.2.2	RCON connected to EEC behind passenger side front seat (top view).	39
Figure 2.1.2.3	RCON connected to EEC behind passenger side front seat (side view).	39
Figure 2.1.2.4	Remote laptop computer on passenger side front seat.	40
Figure 2.1.2.5	Placement of horiba air-to-fuel ratio analyzer and accelerometer transducer in trunk of test vehicle.	41
Figure 2.1.2.6	Placement of horiba AFR sensor and pre- and mid-bed catalyst thermocouples.	41
Figure 2.3.5.1	On-road freeway route matrix.	47
Figure 2.3.5.2	On-road urban route matrix.	48
Figure 2.4.1	Flow chart for analysis of on-road VDAS data.	50
Figure 2.4.2	The first page of the data analysis output from the program ANLYS50C.FOR.	52
Figure 2.4.3	The second page of the data analysis output from the program ANLYS50C.FOR.	53
Figure 2.4.4	The third page of the data analysis output from the program ANLYS50C.FOR.	54
Figure 2.5.1.1a	On-road freeway driving pattern used as basis for UCLA Freeway Dynamometer Driving Schedule continued (deleted sections shown marked out).	57
Figure 2.5.1.1b	On-road freeway driving pattern used as basis for UCLA Freeway Dynamometer Driving Schedule continued (deleted sections shown marked out).	58

Figure 2.5.1.1c	On-road freeway driving pattern used as basis for UCLA Freeway Dynamometer Driving Schedule continued (deleted sections shown marked out).	59
Figure 2.5.1.1d	On-road freeway driving pattern used as basis for UCLA Freeway Dynamometer Driving Schedule continued (deleted sections shown marked out).	60
Figure 2.5.1.2	Time versus speed trace of the UCLA Freeway Dynamometer Driving Schedule.	61
Figure 2.5.1.3a	On-road urban driving pattern used as basis for UCLA Urban Dynamometer Driving Schedule continued (deleted sections shown marked out).	62
Figure 2.5.1.3b	On-road urban driving pattern used as basis for UCLA Urban Dynamometer Driving Schedule continued (deleted sections shown marked out).	63
Figure 2.5.1.3c	On-road urban driving pattern used as basis for UCLA Urban Dynamometer Driving Schedule continued (deleted sections shown marked out).	64
Figure 2.5.1.3d	On-road urban driving pattern used as basis for UCLA Urban Dynamometer Driving Schedule continued (deleted sections shown marked out).	65
Figure 2.5.1.3e	On-road urban driving pattern used as basis for UCLA Urban Dynamometer Driving Schedule continued (deleted sections shown marked out).	66
Figure 2.5.1.4	Time versus speed trace of the UCLA Urban Dynamometer Driving Schedule.	67
Figure 2.5.1.5	Time versus speed trace of the ARB Acceleration Dynamometer Driving Schedules (Long, 1992a).	68
Figure 2.5.1.6	Time versus speed trace of the UCLA Acceleration Dynamometer Driving Schedule.	69

Figure 2.6.1	Predicted versus actual HC speed correction factors for carbureted and throttle-body fuel injected vehicles.	72
Figure 2.6.2	Predicted versus actual HC speed correction factors for multi-point fuel injected vehicles.	73
Figure 2.6.3	Predicted versus actual CO speed correction factors for carbureted and throttle-body fuel injected vehicles.	74
Figure 2.6.4	Predicted versus actual CO speed correction factors for multi-point fuel injected vehicles.	75
Figure 2.6.5	Predicted versus actual NO _x speed correction factors for carbureted and throttle-body fuel injected vehicles.	76
Figure 2.6.6	Predicted versus actual NO _x speed correction factors for multi-point fuel injected vehicles.	77
Figure 2.6.7	Flow diagram of the emissions modeling process.	80
Figure 2.6.1.1	ASBVE model binned emissions for CO, HC and NO _x	83
Figure 2.6.1.2	LSBVE model binned emissions for CO, HC and NO _x	84
Figure 3.2.1.1.1	Open loop flag, engine coolant temperature and catalyst temperature during a cold start at an ambient temperature of 72°F.	88
Figure 3.2.1.1.2	Vehicle speed, open loop flag, and lambda during cold start at an ambient temperature of 19°F.	90
Figure 3.2.1.1.3	Engine coolant temperature, ambient temperature and catalyst temperature during cold start at an ambient temperature of 19°F.	91
Figure 3.2.1.1.4	Duration of open loop operation as a function of engine coolant temperature at start.	92
Figure 3.2.1.1.5	Duration of open loop operation as a function of catalyst temperature at start.	93
Figure 3.2.1.1.6	Duration of open loop operation as a function of ambient temperature at start.	94

Figure 3.2.1.1.7	Duration of open loop operation as a function of engine air charge temperature at start.	95
Figure 3.2.1.1.8	Duration of open loop operation as a function of engine coolant temperature 15 seconds after start.	96
Figure 3.2.1.1.9	Duration of open loop operation as a function of engine coolant temperature 51 seconds after start.	97
Figure 3.2.1.2.1	Engine load, engine coolant temperature, and catalyst temperature during 1500 second idle.	99
Figure 3.2.1.2.2	Engine load, engine coolant temperature, and air conditioning flag during 360 second idle.	100
Figure 3.2.1.3.1	Engine coolant temperature, exhaust gas temperature, and catalyst temperature for first 1500 seconds after engine shut down.	101
Figure 3.2.2.1	Speed, braking flag, and open loop flag during acceleration, deceleration, and coasting experiment.	103
Figure 3.2.2.2	One second speed and acceleration data from the acceleration/deceleration/coasting experiments.	105
Figure 3.2.2.3	Speed, acceleration and gear during a 0 to 80 mph acceleration experiment.	106
Figure 3.2.2.1.1	One second FTP data points and operating envelope.	108
Figure 3.2.3.1	Acceleration as a function of speed showing divisions used to define light and medium accelerations.	109
Figure 3.2.3.2	Deceleration as a function of speed showing divisions used to define hard and medium decelerations.	110
Figure 3.2.3.3	Deceleration as a function of speed from coasting experiment used to determine natural rate of deceleration.	111
Figure 3.2.4.1	Speed, open loop flag, and throttle position during downhill trip on 5 mile 6% grade.	114

Figure 3.2.4.2	Load, lambda, and fuel injector pulse width during downhill trip on 5 mile 6% grade.	115
Figure 3.2.4.3	Speed, open loop flag, and throttle position during uphill trip on 5 mile 6% grade.	116
Figure 3.2.4.4	Load, lambda, and fuel injector pulse width during uphill trip on 5 mile 6% grade.	117
Figure 3.2.4.5	Speed, open loop flag, and throttle position during uphill trip on 5 mile 6% grade with cruise control set at 65 mph. . . .	118
Figure 3.2.4.6	Load, lambda, and fuel injector pulse width during uphill trip on 5 mile 6% grade with cruise control set at 65 mph. . . .	119
Figure 3.2.5.1	Time of travel, percent time open loop and fuel economy for repeated freeway experiment by direction of travel.	122
Figure 3.2.6.1	Comparison of the freeway, urban, and combined freeway and urban on-road matrix data with the FTP by vehicle operating parameter.	125
Figure 3.2.6.2	Comparison of on-road data to the FTP by percent time in acceleration based modes of operation.	129
Figure 3.2.6.3	Probability plot of the UDDS, bags 1 and 2.	141
Figure 3.2.6.4	Probability plot of conservative freeway driving pattern data.	142
Figure 3.2.6.5	Probability plot of conservative morning freeway driving pattern data.	143
Figure 3.2.6.6	Probability plot of conservative evening freeway driving pattern data.	144
Figure 3.2.6.7	Probability plot of conservative urban driving pattern data.	145
Figure 3.2.6.8	Probability plot of conservative morning urban driving pattern data.	146
Figure 3.2.6.9	Probability plot of conservative evening urban driving pattern data.	147

Figure 3.2.6.10	Probability plot of combined conservative freeway and urban driving pattern data.	148
Figure 3.2.6.11	Probability plot of FTP minus combined conservative freeway and urban driving pattern data.	149
Figure 3.2.7.1	Comparison of vehicle operating parameters for the FTP, conservative driving and aggressive driving on-road data.	151
Figure 3.2.7.2	Comparison of the FTP, conservative driving and aggressive driving on-road data by mode of operation.	153
Figure 3.2.7.3	Probability plot of aggressive freeway driving pattern data.	160
Figure 3.2.7.4	Probability plot of aggressive morning freeway driving pattern data.	161
Figure 3.2.7.5	Probability plot of aggressive evening freeway driving pattern data.	162
Figure 3.2.7.6	Probability plot of aggressive urban driving pattern data.	163
Figure 3.2.7.7	Probability plot of aggressive morning urban driving pattern data.	164
Figure 3.2.7.8	Probability plot of aggressive evening urban driving pattern data.	165
Figure 3.2.7.9	Probability plot of combined aggressive freeway and urban driving pattern data.	167
Figure 3.2.7.10	Probability plot of FTP minus combined aggressive freeway and urban driving pattern data.	168
Figure 3.2.7.11	Probability plot of combined conservative freeway and urban driving on-road data minus combined aggressive freeway and urban driving pattern data.	169
Figure 3.2.8.1.1	Occurrences of lean open loop operation for conservative driving freeway and urban matrix routes.	172
Figure 3.2.8.1.2	Occurrences of lean open loop operation for aggressive driving freeway and urban matrix routes.	173

Figure 3.2.8.1.3	Occurrences of lean open loop operation for repeated freeway experiment.	174
Figure 3.2.8.2.1	Occurrences of rich open loop operation for conservative driving freeway and urban matrix routes.	176
Figure 3.2.8.2.2	Occurrences of rich open loop operation for aggressive driving freeway and urban matrix routes.	177
Figure 3.2.8.2.3	Occurrences of rich open loop operation for repeated freeway experiment.	179
Figure 3.3.1.1	UCLA Freeway Dynamometer Driving Schedule as a function of probability of driving as a specific speed and acceleration.	184
Figure 3.3.1.2	UCLA Urban Dynamometer Driving Schedule as a function of probability of driving as a specific speed and acceleration.	185
Figure 3.3.1.3	UCLA Freeway Dynamometer Driving Schedule minus on-road freeway conservative driving data.	186
Figure 3.3.1.4	UCLA Urban Dynamometer Driving Schedule minus on-road urban conservative driving data.	187
Figure 3.3.1.5	Average of the UCLA Freeway and Urban Dynamometer Driving Schedules.	188
Figure 3.3.1.6	Average of the UCLA Freeway and Urban Dynamometer Driving Schedules minus average on-road freeway and urban conservative driving data.	189
Figure 3.3.2.1	Differences between bag calculated and hertz calculated emission rate data for HC by test schedule.	192
Figure 3.3.2.2	Differences between bag calculated and hertz calculated emission rate data for CO by test schedule.	193
Figure 3.3.2.3	Differences between bag calculated and hertz calculated emission rate data for NO _x by test schedule.	194
Figure 3.3.4.1a	Speed, lambda, and open loop flag during driving of the FTP, cold start and hot running bags.	197

Figure 3.3.4.1b	Emission rates of HC, CO, and NO _x during driving of the FTP, cold start and hot running bags.	198
Figure 3.3.4.2a	Speed, lambda, and open loop flag during driving of the UCLA Freeway Dynamometer Driving Schedule, cold start bag.	199
Figure 3.3.4.2b	Emission rates of HC, CO, and NO _x during driving of the UCLA Freeway Dynamometer Driving Schedule, cold start bag.	200
Figure 3.3.4.3a	Speed, lambda, and open loop flag during driving of the UCLA Urban Dynamometer Driving Schedule, cold start bag.	202
Figure 3.3.4.3b	Emission rates of HC, CO, and NO _x during driving of the UCLA Urban Dynamometer Driving Schedule, cold start bag.	203
Figure 3.3.4.4a	Speed, lambda, and open loop flag during driving of the UCLA Acceleration Dynamometer Driving Schedule, cold start bag.	204
Figure 3.3.4.4b	Load, exhaust gas temperature, and catalyst temperature during driving of the UCLA Acceleration Dynamometer Driving Schedule, cold start bag.	205
Figure 3.3.4.4c	Emission rates of HC, CO, and NO _x during driving of the UCLA Acceleration Dynamometer Driving Schedule, cold start bag.	206
Figure 3.3.4.4d	Catalyst efficiency for HC, CO, and NO _x during driving of the UCLA Acceleration Dynamometer Driving Schedule, cold start bag.	207
Figure 3.3.4.5a	Speed, lambda, and open loop flag during driving of the UCLA Acceleration Dynamometer Driving Schedule, hot running bag.	208

Figure 3.3.4.5b	Load, exhaust gas temperature, and catalyst temperature during driving of the UCLA Acceleration Dynamometer Driving Schedule, hot running bag.	209
Figure 3.3.4.5c	Emission rates of HC, CO, and NO _x during driving of the UCLA Acceleration Dynamometer Driving Schedule, hot running bag.	210
Figure 3.3.4.5d	Catalyst efficiency for HC, CO, and NO _x during driving of the UCLA Acceleration Dynamometer Driving Schedule, hot running bag.	211
Figure 3.3.4.6a	Speed, lambda, and open loop flag during driving of the UCLA Acceleration Dynamometer Driving Schedule, warm start bag.	212
Figure 3.3.4.6b	Load, exhaust gas temperature, and catalyst temperature during driving of the UCLA Acceleration Dynamometer Driving Schedule, warm start bag.	213
Figure 3.3.4.6c	Emission rates of HC, CO, and NO _x during driving of the UCLA Acceleration Dynamometer Driving Schedule, warm start bag.	214
Figure 3.3.4.6d	Catalyst efficiency for HC, CO, and NO _x during driving of the UCLA Acceleration Dynamometer Driving Schedule, warm start bag.	215
Figure 3.4.1.1	Percent difference between dynamometer measured and load based modeled HC emissions for five driving patterns.	221
Figure 3.4.1.2	Percent difference between dynamometer measured and acceleration based modeled HC emissions for five driving patterns.	222
Figure 3.4.1.3	Percent difference between dynamometer measured and load based modeled CO emissions for five driving patterns.	223

Figure 3.4.1.4	Percent difference between dynamometer measured and acceleration based modeled CO emissions for five driving patterns.	224
Figure 3.4.1.5	Percent difference between dynamometer measured and load based modeled NO _x emissions for five driving patterns. . . .	225
Figure 3.4.1.6	Percent difference between dynamometer measured and acceleration based modeled NO _x emissions for five driving patterns.	226
Figure 3.4.2.1	FTP measured and modeled on-road HC emission rates by model.	229
Figure 3.4.2.2	FTP measured and modeled on-road CO emission rates by model.	230
Figure 3.4.2.3	FTP measured and modeled on-road NO _x emission rates by model.	231

LIST OF TABLES

Table 1.3.1	Summary of emissions by major category in the SoCAB for 1987, average annual day (tons/day), (SCAQMD, 1991). . . .	12
Table 1.3.1.1	California gasoline and diesel vehicle exhaust emission standards for passenger vehicles at 50,000 miles (CARB, 1991).	13
Table 1.4.1	Comparison of emissions rates measured in the tunnel study and emission factors calculated from EMFAC7C (Ingalls, 1989).	21
Table 1.4.2.1	Chronology of vehicle emissions control technology in California.	26
Table 2.2.1	Measured vehicle/engine operating parameters.	42
Table 2.3.5.1	On-road freeway and urban driving matrix routes.	45
Table 2.5.1.1	Comparison of the UCLA Freeway and Urban Driving Schedules to the average of the on-road data.	56
Table 2.6.1.1	Acceleration and load based modes.	82
Table 3.2.2.1	Acceleration/deceleration/coasting experiments results. . . .	104
Table 3.2.4.1	Summary of up- and down-hill grade experiments results with and without the use of cruise control.	113
Table 3.2.5.1	Repeated freeway experiment driving parameter summary. . .	121
Table 3.2.6.1	Driving parameter data for the FTP and the HFET.	123
Table 3.2.6.2	Driving parameter data for on-road conservative driving experiments.	124
Table 3.2.6.3	Percent time in acceleration-based modes for the FTP and the HFET.	127
Table 3.2.6.4	Percent time in acceleration-based modes for on-road conservative driving experiments.	128

Table 3.2.6.5	Average time in acceleration-based modes for the FTP and the HFET (seconds).	130
Table 3.2.6.6	Average time in acceleration-based modes for on-road conservative driving experiments (seconds).	131
Table 3.2.6.7	Percent time in load-based modes for the FTP and the HFET.	132
Table 3.2.6.8	Percent time in load-based modes for on-road conservative driving experiments.	133
Table 3.2.6.9	Average vehicle operating parameter data for the FTP and the HFET.	135
Table 3.2.6.10	Average vehicle operating parameter data for on-road conservative driving experiments.	136
Table 3.2.6.11	Maximum vehicle operating parameter data for the FTP and the HFET.	137
Table 3.2.6.12	Maximum vehicle operating parameter data for on-road conservative driving experiments.	138
Table 3.2.6.13	Minimum vehicle operating parameter data for the FTP and the HFET.	139
Table 3.2.6.14	Minimum vehicle operating parameter data for on-road conservative driving experiments.	140
Table 3.2.7.1	Driving parameter data for on-road aggressive driving experiments.	150
Table 3.2.7.2	Percent time in acceleration-based modes for on-road aggressive driving experiments.	152
Table 3.2.7.3	Average time in acceleration-based modes for on-road aggressive driving experiments.	154
Table 3.2.7.4	Percent time in load-based modes for on-road aggressive driving experiments.	155
Table 3.2.7.5	Average vehicle operating parameter data for on-road aggressive driving experiments.	156

Table 3.2.7.6	Maximum vehicle operating parameter data for on-road aggressive driving experiments.	157
Table 3.2.7.7	Minimum vehicle operating parameter data for on-road aggressive driving experiments.	158
Table 3.2.8.1.1	Summary of on-road lean open loop operation.	171
Table 3.2.8.2.1	Summary of on-road rich open loop operation.	175
Table 3.2.8.2.1.1	Comparison of experimental conditions vs. GM enrichment condition for the Taurus.	180
Table 3.3.1.1	Comparison of UCLA Freeway and Urban Dynamometer Driving Schedules to the on-road routes they were developed from.	182
Table 3.3.2.1	Comparison of emissions data from summed one second emissions measurements and bag emissions measurements.	191
Table 3.3.3.1	Total distance and weighted emission rates from the UCLA Dynamometer Driving Schedules, the FTP and HFET.	195
Table 3.3.4.1	Rich open loop emission rates measured during driving of the UCLA Acceleration Driving Schedule on a dynamometer.	219
Table 3.4.1.1	Comparison of percent differences between measured emissions for five driving patterns driven on a dynamometer and modeled emissions from two models.	220
Table 3.4.2.1	Predicted emissions by acceleration- and load-based models for conservative and aggressive on-road driving patterns.	228
Table 3.4.2.2.	Difference between measured and modeled on-road emission rates compared to the calculated increase due to rich open loop operation.	232

GLOSSARY OF TERMS, ABBREVIATIONS AND SYMBOLS

AFR	Air-to-Fuel Ratio
APRAC	Air Pollution Research Activities Committee
AQMP	Air Quality Management Plan
ARB	California Air Resources Board
ASCII	American Standard Code for Information Interchange
°C	Degrees centigrade
CAA	Federal Clean Air Act
CCAA	California Clean Air Act
CFR	Code of Federal Regulations
CO	Carbon Monoxide
CO ₂	Carbon Monoxide
CRC	Coordinating Research Council
EEC	Electronic Engine Controller
EMFAC	Emissions Factor Model
°F	Degrees fahrenheit
FMCSRL	Ford Motor Company Scientific Research Laboratory
FTIR	Fourier Transform Infrared spectrometer
FTP	Federal Test Procedure
g	Grams
GM	General Motors Company
GVDAS	Graphical display for Vehicle Data Acquisition System Data
HC	Hydrocarbons
HFET	Highway Fuel Economy Test
Hz	Hertz
I/M	Inspection and Maintenance Program
Lambda	Measured air/fuel ratio divided by the stoichiometric air/fuel ratio
MOBILE	US EPA Mobile Source Emissions Model

mph	Miles per hour
NAAQS	National Ambient Air Quality Standards
NO	Nitric Oxide
NO ₂	Nitrogen Dioxide
NO _x	Oxides of Nitrogen
PM ₁₀	Particulates, 10µm or less
PPMC	Parts Per Million Concentration
psi	Pounds per square inch
RCON	Research Console
ROG	Reactive Organic Gases
s	Seconds
SCAQMD	South Coast Air Quality Management District
SCAQS	Southern California Air Quality Study
SIP	State Implementation Plan
SO ₂	Sulfur Dioxide
SoCAB	South Coast Air Basin
UAM	Urban Airshed Model
UCLA	University of California Los Angeles
UCR	University of California Riverside
UDDS	Urban Dynamometer Driving Schedule
US EPA	United States Environmental Protection Agency
V5CVT	Version 5 of Data Conversion Utility
VDAS	Vehicle Data Acquisition System
VMT	Vehicle Miles Traveled
λ	Lambda, measured air/fuel ratio divided by the stoichiometric air/fuel ratio

EXECUTIVE SUMMARY

1. Introduction

Among the most urgent problems concerning the development of effective air pollution control programs in the 1990's is a fundamental discrepancy between emission inventories of ROG and CO based on models of mobile source emissions (e.g. EMFAC and MOBILE) vs. experimentally measured ambient air concentrations and dynamometer, roadside, and tunnel measurements of emissions from motor vehicles. Focus on this problem has emerged, in part, from the growing sophistication of research techniques for characterizing the actual emissions of the motor vehicle fleet during on-road operation.

To resolve important questions about the accuracy of past and present mobile source emissions models, a critical need exists to determine the representativeness of the Federal Test Procedure (FTP) with respect to driving patterns in the California South Coast Air Basin (SoCAB) and the frequency of so-called "off-cycle" or "open-loop" emissions corresponding to rich engine operation and elevated emissions. A limitation to current vehicle emissions models is the reliance on emissions measurements from a single test pattern [the Urban Dynamometer Driving Schedule (UDDS) used in the Federal Test Procedure] to predict the emissions from the entire fleet. Despite efforts to develop a test pattern which is "more representative" of current on-road driving conditions in order to increase the representativeness of the emissions estimates from such tests, a single pattern of reasonable length cannot represent all of the driving conditions observed on-road. For this reason, a modal vehicle emissions model needs to be developed which can be used with many on-road driving patterns to increase the representativeness of modeled on-road emissions.

This study provided a direct evaluation of real-time, on-road vehicle and engine operating parameters, and investigated their relationship to rich open loop emissions and driving pattern characteristics. Data were collected using a 1991 Ford Taurus equipped with a computerized on-board data collection system which was connected to the stock electronic engine controller. The vehicle was driven both "passively" and "aggressively"

in morning and evening commute hours over a matrix of eight freeway and eight urban routes in California's South Coast Air Basin. From the driving pattern data collected on-road, two new dynamometer driving schedules were developed which were representative of current driving conditions in the basin. Dynamometer emissions measurements were conducted for the FTP, the HFET, the two new driving schedules and a high acceleration rate driving schedule which was developed to cause rich open loop operation. Data from the dynamometer emissions tests were used to determine the magnitude of rich open loop emissions and to compare emissions from the new more representative driving schedules to the FTP.

Emissions rate data from the dynamometer emissions test were also used as a data base for modeling of on-road emissions for the driving pattern data collected on-road in the SoCAB. Two modal emissions models were developed; one based on modeling emissions as a function of acceleration rate and speed and one based on modeling emissions as a function of load and speed. Because the new emissions models are not reliant on a specific driving schedule but can be used to estimate emissions from many measured on-road driving patterns, they should produce more representative on-road emission rate estimates.

2. On-Road Conservative and Aggressive Driving versus the FTP

Significant differences were observed between on-road driving patterns and the UDDS used in the FTP which affect emissions. The one-second speed versus acceleration data for the UDDS used in the FTP are plotted in Figure 1 with the measured maximum operating envelope of the vehicle on a level road. The figure shows that accelerations greater than 3.3 mph s^{-1} and speeds greater than 56 mph are not tested during the FTP, but that the vehicle operates under a wide range of conditions outside those tested in the FTP. Comparison of the on-road driving pattern data to the UDDS shows the average on-road speeds were 29.3 mph for conservative driving and 33.1 mph for aggressive driving compared to 20.7 mph for the FTP. The maximum acceleration rates on-road were 8.0 mph s^{-1} for conservative driving and 10.0 mph s^{-1} for aggressive driving

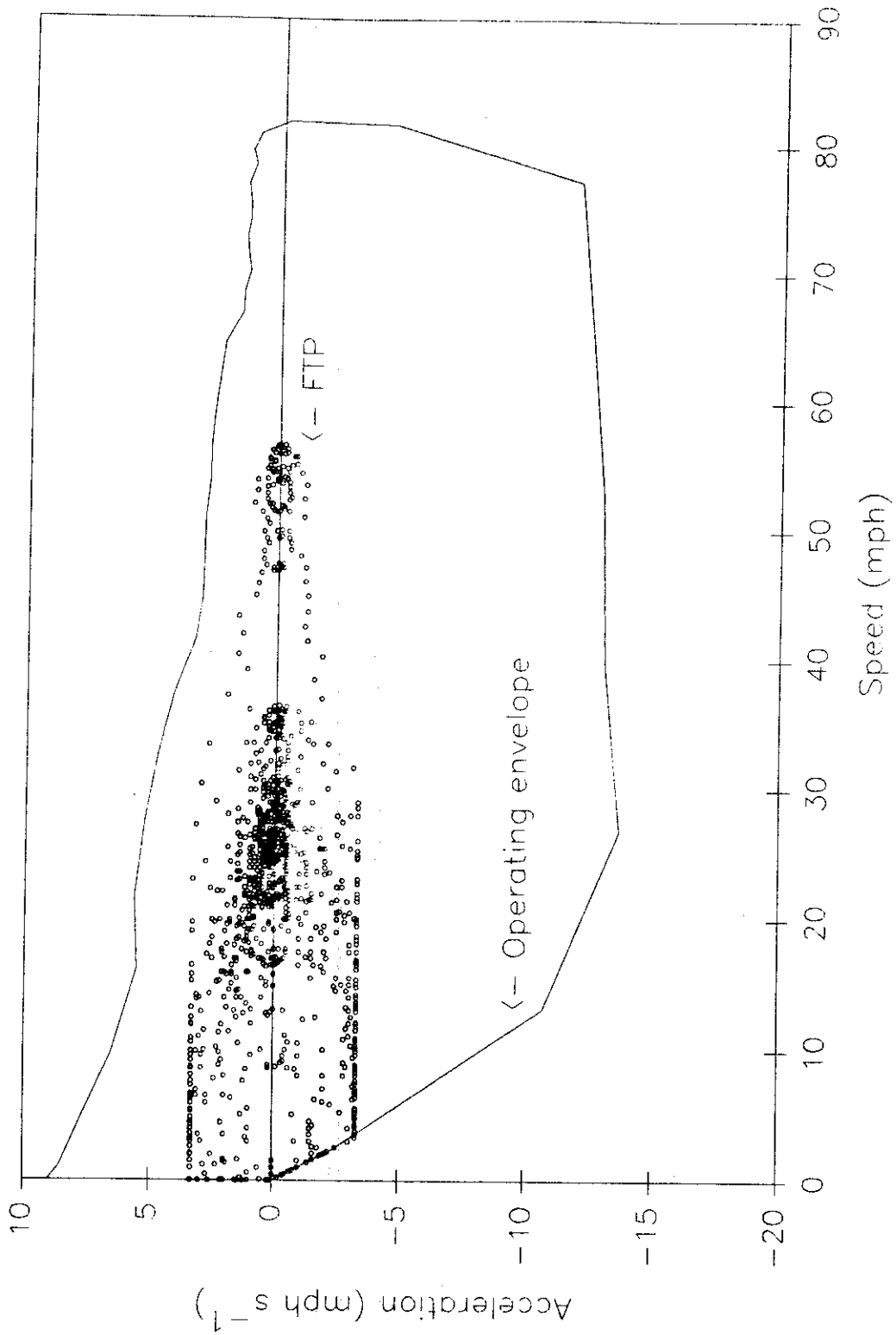


Figure 1. Plot of the FTP speed and acceleration data in the vehicle maximum operating envelope.

compared to 3.3 mph s^{-1} for the FTP. Higher speeds and higher acceleration rates can cause high emission rates. The fuel economy measured on-road for both conservative and aggressive driving (28.6 and 24.7 mpg) was higher than during the FTP (23.1 mpg). The average distance per stop was greater on-road for both conservative and aggressive driving (2.8 and 3.7 miles per stop) compared to the FTP (0.46 miles per stop).

3. Frequency of Open Loop Operation

The frequencies of rich open loop operation measured during FTP and HFET tests and on-road in the SoCAB are listed in Table 1 for the Ford Taurus test vehicle. Rich open loop operation was not observed during the FTP or HFET, however, it was observed while driving on-road in a conservative manner in congested traffic conditions (0.003 on freeway routes and 0.007% of the time on urban routes). On-road aggressive driving experiments, also conducted in congested traffic conditions, found aggressive driving to greatly increase the frequency of rich open loop operation relative to conservative driving (0.44% of the time on freeway routes and 1.1% of the time on urban routes). Up-hill grades and merging were also found to raise the frequency of rich open loop operation due to the increased load on grades and due to the high rates of acceleration necessary while merging. Rich open loop operation was also found to occur more frequently in free flowing traffic than in congested or grid-locked traffic, probably due to the low velocities and close proximity of the vehicles in grid-lock.

4. Dynamometer Emissions Experiments and Emissions During Open Loop Operation

Emissions tests were conducted with the Ford Taurus test vehicle using the FTP, HFET and two new UCLA dynamometer driving schedules which were developed from the measured on-road driving pattern data to be representative of the current freeway and urban driving patterns in the SoCAB (the UCLA Freeway and Urban Dynamometer Driving Schedules). The averaged emission rates from the UCLA freeway and urban driving schedules of HC, CO and NO_x were all higher than from the FTP (0.17 versus 0.15 g mi^{-1} for HC, 2.73 versus 1.72 g mi^{-1} for CO and 0.22 versus 0.12 g mi^{-1} for NO_x).

Table 1. Measured frequency of rich open loop operation on-road in the SoCAB.

Experiment	Percent time in Rich Open Loop
Federal Test Procedure	0.0
Highway Fuel Economy Test	0.0
Conservative freeway driving	0.003
Conservative urban driving	0.007
Aggressive freeway driving	0.44
Aggressive urban driving	1.1

In addition to the FTP, HFET and the UCLA freeway and urban driving schedules, emissions tests were conducted using a special high acceleration rate driving schedule (the UCLA Acceleration Dynamometer Driving Schedule) which was developed to cause open loop operation to occur. Emission rates measured during rich open loop operation and during closed loop operation (near stoichiometry) are given in Table 2. Emission rates during open loop operation were ≈ 100 times higher than the closed loop emission rate for HC (0.038 g s^{-1} during open loop operation), ≈ 1700 times the closed loop emission rate for CO (3.17 g s^{-1}) and ≈ 80 times the closed loop emission rate for NO_x (0.106 g s^{-1}).

5. Modeling of On-Road Emissions and Comparison to the FTP

Two new vehicle emissions models, the UCLA Acceleration-Based Vehicle Emissions (ASBVE) Model and the UCLA Load-Based Vehicle Emissions (LSBVE) Model, were developed to test the feasibility of acceleration or load based modeling. The emissions rates data recorded during the dynamometer tests were used as the emissions input data to the two models to predict emission rates. The accuracy of the models was tested by modeling the emissions for the driving patterns used in the emissions test previously discussed. Of the two, the LSBVE model which models emissions as

Table 2. Rich open loop emission rates measured during driving of the UCLA Acceleration Driving Schedule on a dynamometer.

Phase	HC g mi ⁻¹	CO g mi ⁻¹	NO _x g mi ⁻¹
Rich open loop	0.0376	3.167	0.1059
Closed loop	0.0004	0.0018	0.0013
Increase over closed loop	≈100	≈1700	≈80

a function of vehicle load and speed, was found to be the most accurate. The LSBVE model under-predicted the actual emission rates of all three pollutants (-28.1% for HC, -55.4% for CO and -8.2% for NO_x). The under-prediction of the model was possibly due to the limited resolution in the model which was necessary because of the limited emission rate data used as the model input.

Emission rates for the driving pattern data recorded on-road with the Taurus in the SoCAB were modeled using the ULVE model. The results of the modeling showed aggressive driving caused higher emission rates of CO and NO_x than conservative driving (6.8 versus 3.1 g mi⁻¹ and 0.49 versus 0.26 g mi⁻¹ respectively) but approximately no difference in the HC emission rate (0.29 versus 0.28 g mi⁻¹). Comparison of the results for freeway versus urban routes found the HC emission rate was higher for urban routes (0.24 versus 0.33 g mi⁻¹ respectively), the CO emission rate was higher for freeway routes (5.2 versus 4.7 g mi⁻¹ respectively), and there was essentially no difference in the emission rate of NO_x between freeway and urban routes (0.38 versus 0.37 g mi⁻¹ respectively). With the exception of the NO_x emission rate during aggressive driving, all of the modeled on-road emission rates were lower than the current certification emissions standards, but they were also all greater than the emission rates measured for the FTP (33% for HC, 190% for CO and 120% for NO_x).

The cause of the higher emission rates on-road than for the FTP was attributed to the occurrence of rich open loop operation on-road but not during the FTP as well as

Table 3. Difference between measured and estimated on-road emission rates compared to the calculated increase due to rich open loop operation (g mi⁻¹).

Pollutant	FTP measured (g mi ⁻¹)	On-road average (g mi ⁻¹)	Difference (g mi ⁻¹)	Increase due to rich open loop (g mi ⁻¹)
HC	0.21	0.28	+ 0.07 (33%)	0.03 (40%)
CO	1.7	4.9	+ 3.2 (190%)	2.3 (70%)
NO _x	0.17	0.37	+ 0.20 (120%)	0.08 (40%)

differences between current driving patterns (represented by the UCLA driving schedules) and the Urban Dynamometer Driving Schedule used in the FTP. For CO, 70% of the increase in the emission rate was determined to have come from open loop operation, with the remainder due to differences in the driving patterns (see Table 3). For both HC and NO_x, 40% of the increase was attributed to open loop operation with the remaining 60% attributed to differences between the FTP and on-road driving patterns.

6. Conclusions and Recommendations

The results of the modeling studies suggest emissions from rich open loop operation, because they are not included in the FTP, may account for a portion of the under-estimation of current mobile source emissions models. However, because the emissions modeling was only conducted for a single vehicle, it is difficult to draw conclusions about the entire in-use fleet. Comparison of the present results to the only other data available on the frequency of and emissions during rich open loop operation suggest there can be large variations in the frequency of open loop operation between manufacturers. In general, much more needs to be known about the frequency of rich open loop operation on-road and the emission rates during this operation for a variety of vehicles.

If rich open loop operation is not included in the emissions measurements which are used as inputs to emissions models, and if the emissions from these events account for a significant proportion of the total vehicle emissions, there will continue to be discrepancies between the emissions predicted by emissions models and real on-road emissions. New emissions testing procedures need to be developed which will include all possible operation of on-road vehicles and new vehicle emissions models need to be developed which can weight the emissions data to be representative of current driving conditions.

1.0 - INTRODUCTION

1.1 Background

Over the past two decades, there have been great advances in our knowledge of the detailed chemical transformations leading to the formation of photochemical air pollution (Finlayson-Pitts and Pitts, 1986; Atkinson, 1988; Seinfeld, 1986, 1989; National Research Council, 1991). In particular, the precursor role of reactive organic gases (ROG) and oxides of nitrogen (NO_x) has been elucidated, although the detailed photooxidation mechanisms of certain classes of organic compounds (eg. aromatics) remain to be characterized. At the same time, there have been important advances in the development of urban airshed models which permit investigation of the relative efficacy of various mobile and stationary source emission control strategies designed for reducing photochemical smog. Finally, introduction of new control technologies for ROG and NO_x for both mobile (eg. 3-way catalysts) and stationary sources has occurred. Because of these advances, significant progress has been made in some areas of the United States (eg. California's South Coast Air Basin) over the past 15 years in improving ambient air quality although reductions in fine particulate have been limited, and in much of the country (eg. eastern United States) there has been little improvement in ozone levels (National Research Council, 1991).

Ozone is an atmospheric pollutant of significant consequence to public health and welfare. Even prior to the establishment of the National Ambient Air Quality Standards (NAAQS) under the 1970 Clean Air Act, it had been identified as an important factor in the smog episodes that plagued urban areas which had hot and sunny climates, were prone to meteorological air stagnations, and had high motor vehicle emission densities. The lack of success of current control programs for ozone in many U.S. airsheds, and recent evidence of the importance of ozone in affecting human health as well as its effects on vegetation and materials, have highlighted the necessity that the factors affecting its formation must be more thoroughly understood.

One of the most urgent problems with current control strategies is the growing

recognition of fundamental discrepancies between emission inventories of ROG and carbon monoxide (CO), based in part on models of mobile source emissions (e.g. EMFAC and MOBILE), and experimentally measured ambient air concentrations and dynamometer, roadside, and tunnel measurements of emissions from motor vehicles. While the absence of systematic, long-term ambient air measurements of hydrocarbons has made it difficult to reach definitive conclusions concerning this important issue, focus on this problem has grown, in part, from the increasing sophistication of research techniques for characterizing the actual emissions of the motor vehicle fleet during on-road operation as described below.

1.2 The Use of Airshed Models in the Development of Air Pollution Control Strategies

The South Coast Air Quality Management District (SCAQMD) in Southern California is responsible for regional air pollution control in the South Coast Air Basin (SoCAB). The SCAQMD uses models such as the Urban Airshed Model (UAM) to study the capacity of air pollution control strategies which are part of their Air Quality Management Plan (AQMP), (SCAQMD, 1991) to fulfill the requirements of the federal Clean Air Act (CAA) and the California Clean Air Act (CCAA) for development of State (or regional) Implementation Plans (SIPs). These models combine emissions inventories with data on transport and meteorology and the chemistry of the pollutants in the atmosphere. Changes in the input inventories can be made to test the effects of air pollution control strategies. However, if the emissions inventories which are used as inputs to the models are incorrect, then the results from the model may not correctly predict the impacts of the control strategies and the control strategies, if applied, may not produce the desired effects.

1.3 Emissions Inventories

The emissions inventories which are used as inputs to air pollution models are divided into mobile and stationary sources. The 1987 summary of emissions by major

category in the SoCAB are shown in Table 1.3.1 (SCAQMD, 1991). Data on emissions from stationary sources are divided into emissions from point sources (e.g. power plants, refineries) and from area sources (e.g. residential water heaters, architectural coatings). Point sources whose emissions of any of the criteria air pollutants (CO, NO₂, lead, SO₂, or PM₁₀) exceed 18 tons per year (an average of ≈100 pounds per day) report their emissions directly to SCAQMD. Emissions for point sources of less than 18 tons per year, are estimated from SCAQMD's Automated Equipment Information System data base. Emissions from area sources are divided into more than 200 categories which are individually estimated by SCAQMD and the California Air Resources Board (ARB).

Mobile sources are divided into on-road and off-road sources. They include emissions from all forms of combustion based transportation; cars, trucks, buses, trains, planes, and sea vessels. Because of the immense quantity and the variety of these sources, as well as inherent difficulties in monitoring mobile sources, the mobile source emission inventory is calculated through the use of socio-economic data provided by the Southern California Association of Governments (SCAG), spatial distribution of vehicles data from the Direct Travel Impact Model (DTIM) developed by Caltrans, and the ARB's EMFAC (EMissions FACTor) model (CARB, 1991) of vehicle emissions (the US EPA uses their own emissions factor model, MOBILE (US EPA, 1991)). Off-road emissions are modeled as area sources and include trains and ships. Currently, on-road motor vehicle emissions in the SoCAB are calculated to comprise approximately 50% of the total ozone precursor emissions (ROG and NO_x) and 98% of CO emissions (SCAQMD, 1991).

1.3.1 The Federal Test Procedure (FTP)

The Federal Test Procedure (Federal Register, 1990) is used to test vehicles for compliance with exhaust emissions standards for hydrocarbons (HC), CO and NO_x, compliance with evaporative emissions standards for HC, and to determine urban fuel economy. The Highway Fuel Economy Test (HFET) is used to determine freeway fuel economy. The FTP specifies the vehicle preparation and testing conditions including rest

Table 1.3.1 Summary of emissions by major category in the SoCAB for 1987, average annual day (tons/day), (SCAQMD, 1991).

Source Category	ROG	NO _x	CO	SO _x	PM ₁₀
Stationary Sources					
Fuel Combustion	17	267	78	23	14
Waste Burning	1	2	3	0	1
Solvent Use	464	0	0	0	1
Petroleum Process, Storage and Transfer	107	9	6	19	3
Industrial Processes	41	12	7	8	45
Miscellaneous Processes	57	1	5	0	942
Total Stationary Source Emissions	687	291	99	50	1,006
Mobile Sources					
On-Road Vehicles	605	664	4,363	32	53
Off-Road Mobile	83	253	525	52	16
Total Mobile Source Emissions	688	917	4,888	84	69
Total Stationary and Mobile Source Emissions	1,375	1,208	4,987	134	1,075

time before test, fuel level in the fuel tank, ambient temperature and relative humidity (during storage and testing), the driving schedules to be used, the method for determining the inertial load of the vehicle, and the emissions testing and calibration procedures. The driving load to be used is determined experimentally using coasting tests conducted from a high speed and a low speed (Adler, 1968a). The past, current and future emissions standards for California vehicles are shown in Table 1.3.1.1.

The exhaust emissions test is conducted by driving the vehicle on a dynamometer over a fixed speed versus time pattern, the Urban Dynamometer Driving Schedule (UDDS), which was developed to be representative of a typical morning commute in Los Angeles (Figure 1.3.1.1). The test is divided into three phases. A portion of the exhaust gas from each phase of the test is collected into an individual bag which is analyzed to determine the average emissions during the phase of the test.

Because of the method of emissions collection, the phases of the test are often

Table 1.3.1.1 California gasoline and diesel vehicle exhaust emission standards for passenger vehicles at 50,000 miles (CARB, 1991).

Vehicle Model Year	Grams/Mile by Pollutant		
	Total HC/NMOG	CO	NO _x
1966-69	275 ppm	1.5 %	None
1970	2.2	23	None
1971	2.2	23	4.0
1972 *	1.5 / 3.20	23 / 39	3.0 / 3.2
1973	3.2	39	3.0
1974	3.2	39	2.0
1975-76 **	0.90	9.0	2.0
1977-79	0.41	9.0	1.5
1980	0.41	9.0	1.0
1981 ***	0.41	3.4 / 7.0	1.0 / 0.7
1982-92 ****	0.41/0.390	7.0	0.4 / 0.7
1993	0.250	3.4	0.4
TLEV	0.125	3.4	0.4
LEV	0.075	3.4	0.2
ULEV	0.040	1.7	0.2
ZEV *****	0.0	0.0	0.0

* Switch to CVS-72 from 7 mode test.

** Switch to CVS-75 (UDDS) from CVS-72 test.

*** Option is for vehicles certified to 7-year/75,000 mile recall standard.

**** Switch to NMOG as opposed to total HC (HC/NMOG).

***** Does not include power generation emissions.

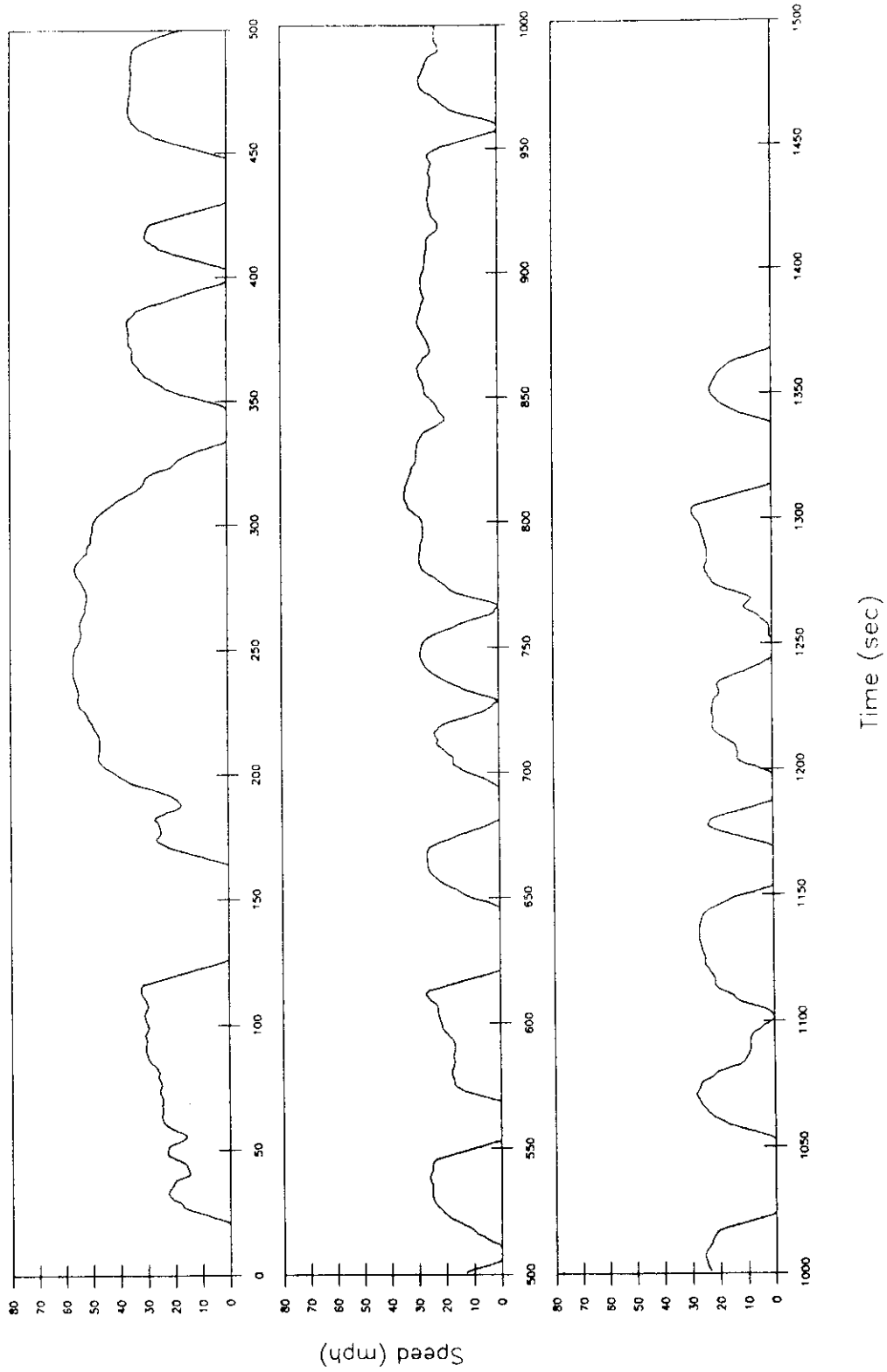


Figure 1.3.1.1.1 Speed versus time trace of the Urban Dynamometer Driving Schedule (UDDS).

referred to as "bags". The phases are as follows:

- Bag 1 - Cold start, 505 seconds
- Bag 2 - Hot running, 868 seconds
- Bag 3 - Warm start, 505 seconds

While driving the test pattern, emissions are collected during the first 505 seconds of the test pattern into bag 1 (this bag includes emissions during the "cold" start) and emissions from driving the remaining 868 seconds are collected into bag 2. At the completion of the pattern, the engine is shut off and the vehicle is allowed to rest for 10 minutes. At the end of the rest period, the emissions from driving the first 505 seconds of the test pattern again (including the emissions during the "hot" start) are collected into bag 3. After the completion of the bag 3 test, the engine is left at idle and the HFET is begun within the next few minutes (Figure 1.3.1.2).

1.3.1.1 Development of the Urban Dynamometer Driving Schedule

The UDDS was finalized by Kruse and Huls (1973) in 1973 after 10 years of research by several groups. It was developed from data collected on-road from six drivers who drove a combined urban and freeway route which started and ended near the old County Air Pollution Control Laboratory in downtown Los Angeles (Figure 1.3.1.1.1). Data collected from one of the six drivers was eliminated due to "obviously excessive throttle movement". The remaining five patterns were very similar and the pattern with the travel time closest to the average was chosen and named the "LA 4" driving pattern.

The LA 4 route was longer than the average trip length reported at that time (Kearn and Lamoureux, 1969), (12.0 versus 7.5 miles) so a shortened version of the LA 4 (the UDDS) was developed by deleting sections of the LA 4 pattern. The average speed on the UDDS was kept near the average of the LA 4 (19.6 versus 19.2 mph) and the maximum speed remained at 56 mph. Some of the acceleration and deceleration rates in the pattern exceeded the design rate of the dynamometers used at the time of development (3.3 mph s^{-1}). Where the pattern exceeded this rate, it was artificially reduced to 3.3 mph s^{-1} .

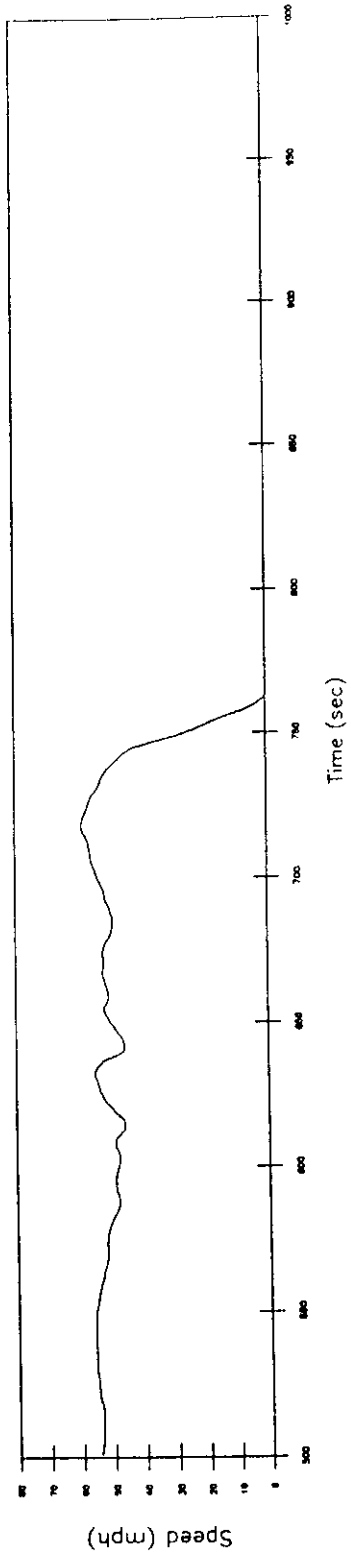
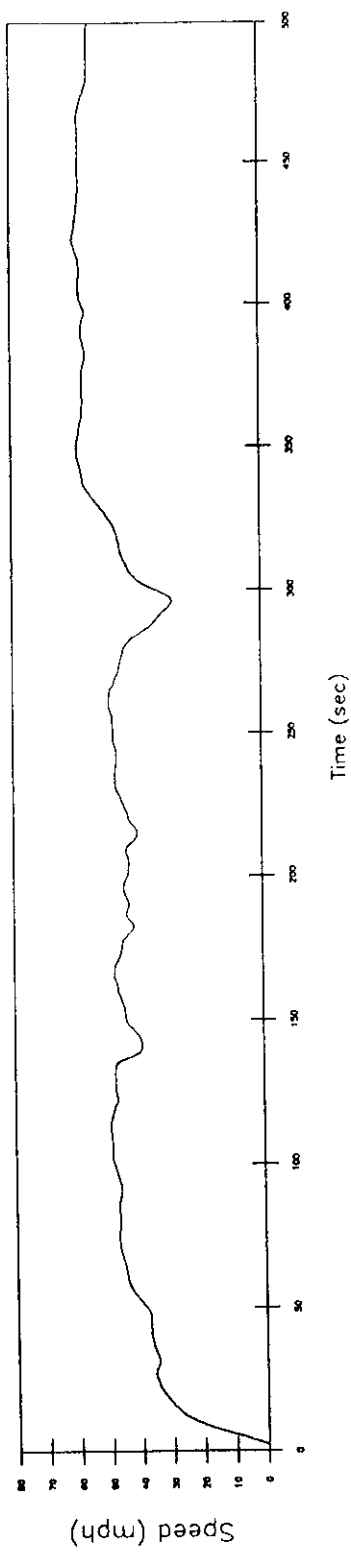


Figure 1.3.1.2 Speed versus time trace of the Highway Fuel Economy Test (HFET).

- 1 Start behind Country Air Pollution Laboratory.
- 2 Right on Fifth.
- 3 Right on San Pedro.
- 4 Left on Third St.
- 5 Up ramp to Harbor Fy. South.
- 6 Exit Harbor Fy. at Exposition.
- 7 Follow Exposition to Western.
- 8 Right on Western.
- 9 Right on Olympic.
- 10 Left on Santee.
- 11 Right on Ninth.
- 12 Left on San Pedro.
- 13 End just beyond intersection San Pedro and Fifth Street.

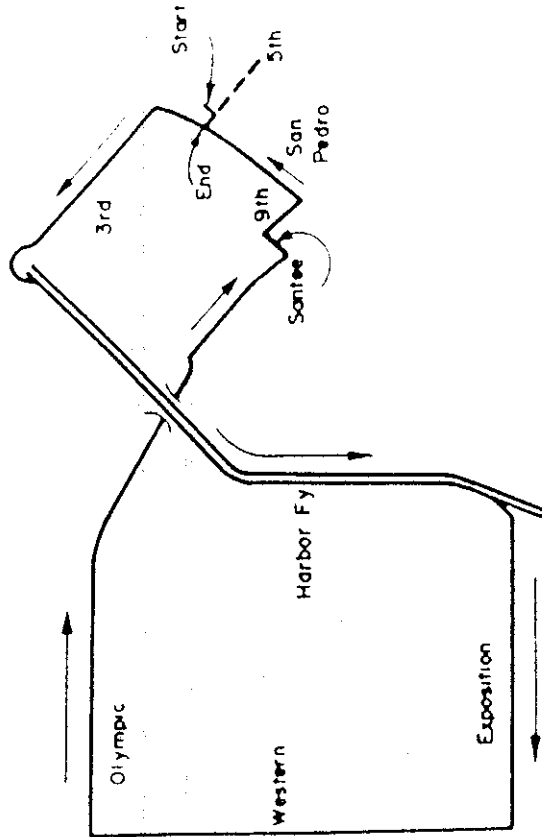


Figure 1.3.1.1.1 The LA 4 on-road driving route.

Five vehicles of varying inertial weights were used for 19 emissions tests on both the LA 4 and UDDS driving patterns to determine if the emissions from the UDDS were representative of emissions from the LA 4. Statistical analysis of the emissions data for HC, CO and carbon dioxide (CO₂) indicated the emissions from the UDDS were representative of the LA 4. For unknown reasons, an emissions comparison of NO_x for the LA 4 and the UDDS was not reported to have been performed.

1.3.2 The ARB's Emissions Factor Model, EMFAC

The motor vehicle emissions inventory process used by the ARB is shown in Figure 1.3.2.1. Emissions rate data for the model come from emissions tests of approximately 2000 randomly selected vehicles using the FTP and I/M 240 tests conducted during the year by the ARB. Emissions rate data also come from new vehicle certification (FTP) tests. The model CALIMFAC (Sierra Research, 1991) is used to determine base emissions rates from the FTP and I/M test data. The model E7EWT estimates the vehicle population, vehicle miles traveled (VMT) and trip fractions from data on vehicle sales and populations as well as mileage accrual rates. The data from CALIMFAC and E7EWT are input to EMFAC along with data on evaporative emissions and corrections for operating temperature, variability in speed, etc., and the model outputs composite emissions factors and technology group fractions. These are input to the BURDEN model along with daily VMT data, speed distributions and registration data to obtain fleet daily emissions (the mobile source emissions inventory). The outputs are divided by vehicle class, technology type, process and pollutant.

1.4 Sources of Under-Estimation in Mobile Source Emissions Inventories

There is beginning to be a consensus that the mobile source emissions inventory process is flawed and under-estimates both ROG and CO emissions. All three versions of the Federal Clean Air Act prior to the 1990 Amendments focused exclusively on reductions of ROG to reduce tropospheric ozone because based on the input emissions inventories, air pollution models predicted control of ROG to be the most effective

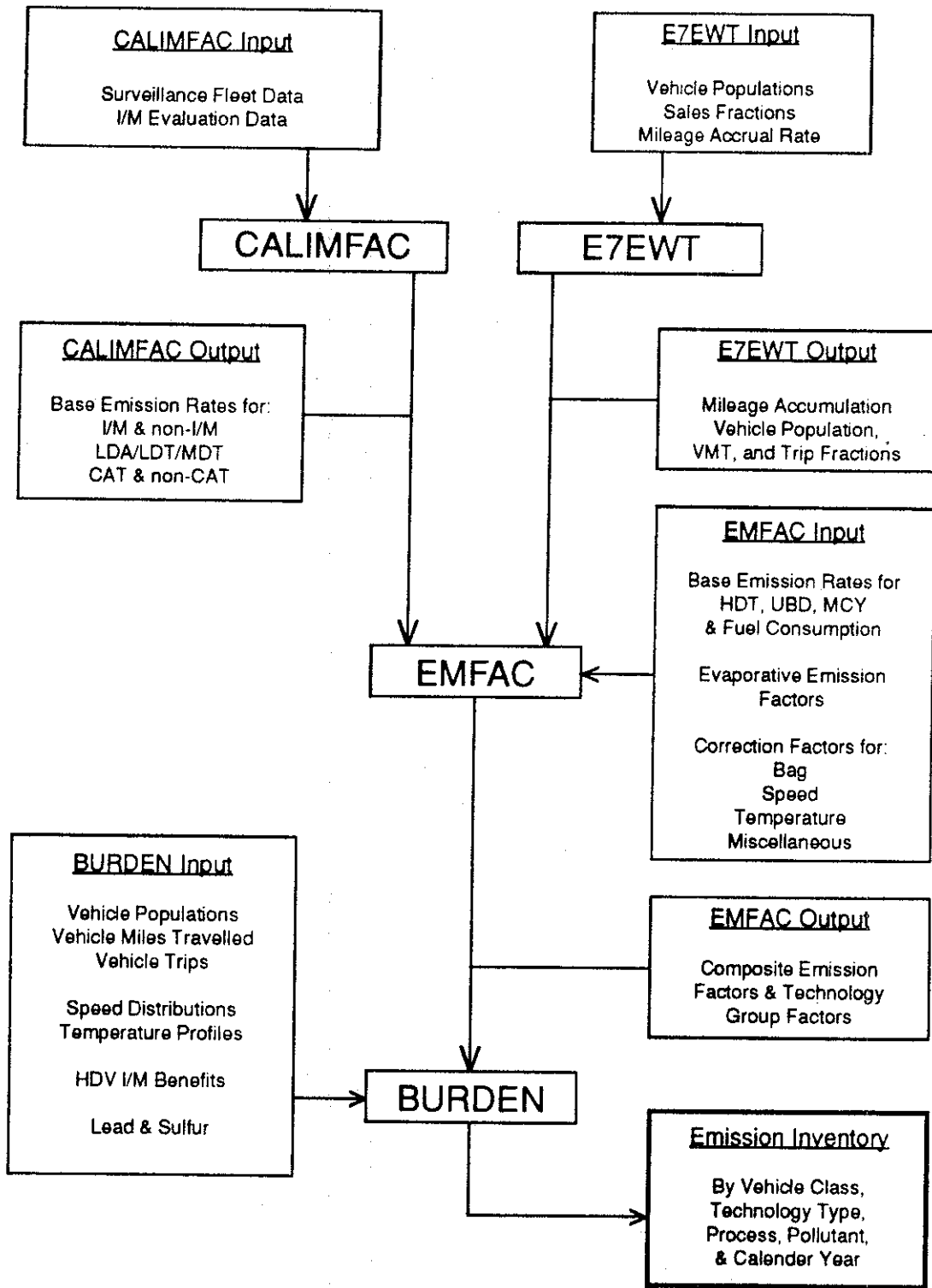


Figure 1.3.2.1 ARB's motor vehicle emissions inventory process (Horie, 1992).

strategy. However, despite major expenditures to control both stationary and mobile sources of ROG emissions, ozone levels in most urban areas have not been reduced as much as anticipated. In 1987 60 areas exceeded the National Ambient Air Quality Standard for ozone but by 1990, 98 areas failed to meet the NAAQS. Currently, it is being realized by regulatory agencies that the control strategy approach which has been used for over 20 years in all states but California, reductions in ROG alone will not achieve the ozone NAAQS in cities violating these standards without also developing regulations focusing on the control of NO_x (National Research Council, 1991). In California, a dual strategy of ROG and NO_x control has led to an approximately 30% reduction in peak ozone levels in the SoCAB over the past 15 years, and a dramatic reduction in first stage episodes, despite a more than doubling in VMT. Nevertheless, the SoCAB continues to experience the most serious ozone problem in the nation.

As mentioned previously errors in the emissions inventories could lead to incorrect control strategies. Beginning in the late 1980's new evidence began to appear based on several different types of specialized studies of on-road vehicular emissions that there are errors in the mobile source emissions inventories. As part of the 1987 Southern California Air Quality Study (SCAQS), (Lawson, 1990), Ingalls et al. (1989; 1989) conducted a study in the Van Nuys tunnel which yielded CO and ROG emission rates approximately factors of three and four higher, respectively, than those expected based on automotive emissions models (Table 1.4.1). Moreover, the CO/NO_x and ROG/NO_x ratios measured by Ingalls were also higher than expected, by similar factors, whereas the absolute NO_x emission rates measured in the tunnel were close to those predicted by the emissions models.

Pierson et al. (1990; 1992) reviewed the results of the SCAQS tunnel study and compared those results with other on-road vehicle emission data to determine whether the Van Nuys tunnel study results were reasonable in terms of previous experience. Their major conclusions were that: (1) on-road CO and ROG emissions higher than expected have been reported before, (2) on-road CO and ROG emissions consistent with the tunnel study have been reported before, and (3) on-road CO/NO_x and ROG/NO_x emission-rate

Table 1.4.1 Comparison of emissions rates measured in the tunnel study and emission factors calculated from EMFAC7C (Ingalls, 1989).

Pollutant	Tunnel Study (g/mile)	Ratio of Tunnel Study to the ARB EMFAC7C
HC	1.3 - 6.1	1.4 - 6.9
CO	18 - 44	1.1 - 3.6
NO _x	1.2 - 20	0.6 - 1.4

ratios higher than expected have been reported before. They suggested that these results indicate richer engine operation for on-road vehicles than predicted by emissions models or than observed in the in-use vehicle dynamometer tests which serve as model inputs. They also indicated that support for their suggestions and conclusions can be found in comparison of urban-air and emission-inventory HC/NO_x ratios.

Fujita and co-workers (1990; 1992a; 1992b; 1992c) and Main and Lurmann (1992) performed a "top-down" validation of the HC and CO emission inventories for the SoCAB by comparing speciation profiles for ROGs and ratios of CO/NO_x and ROG/NO_x derived from early-morning ambient measurements taken during the 1987 Southern California Air Quality Study with the corresponding ratios and speciation profiles derived from day specific, hourly, gridded emission inventories. They found the ratios of the ambient CO/NO_x and ROG/NO_x ratios to the inventory ratios to be 1.5 and 2 to 2.5 times higher respectively. If it is assumed the magnitude of the NO_x inventory is correct, this also suggests the magnitude of the emission inventories of CO and ROG in the SoCAB are low.

1.4.1 "Gross Emitters"

Additional evidence that in-use motor vehicle emissions of CO and ROG may be higher than emissions predicted by motor vehicle emissions models, comes from in-situ, spectroscopic, remote sensing experiments conducted by Stedman and co-workers (1991a;

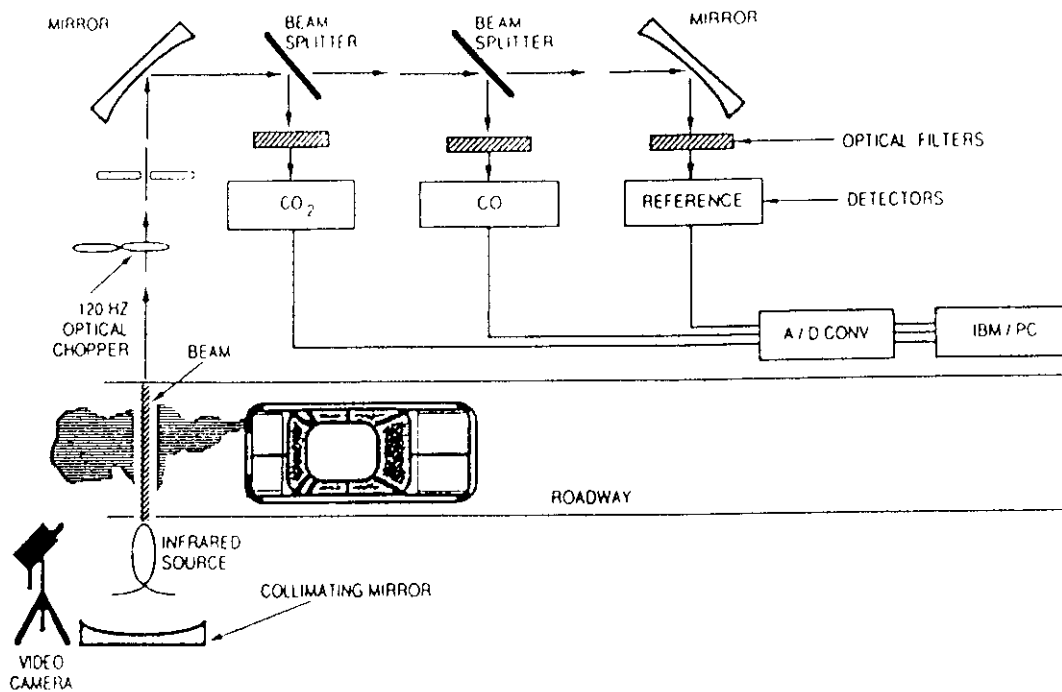


Figure 1.4.1.1 Schematic of General Motors instrumentation for roadside measurements of vehicle exhaust CO (Stephens and Cadle, 1991).

1991b) and by Stephens and Cadle (1991; 1992). A schematic diagram of the instrumentation used by Stephens and Cadle is shown in Figure 1.4.1.1. As reported by these authors, Lawson et al. (1990, 1992) in a summary paper, and Pollack (1992) roadside measurements of CO and exhaust hydrocarbons suggest that a minority of vehicles ($\approx 10\text{-}20\%$) tested in the SoCAB accounted for approximately half of total emissions (Figure 1.4.1.2). Lawson et al. also compared the roadside data set to the biennial Smog Check (inspection and maintenance) tests for the same vehicles and observed that CO and ROG from high emitters were much higher than when vehicles received their routine inspection. Stephens and Cadle analyzed the fraction of emissions of CO as a function of vehicle model year (Figure 1.4.1.3). They found 50% of all passenger car CO was emitted by the highest-emitting 8% of vehicles and on the average,

these vehicles were 12 years old and emit 90 g mi^{-1} . They also found vehicles over 15 years old accounted for greater than one-fourth of the measured CO while only comprising 7% of the fleet. They also compared the emissions rates of the vehicles to their model year (Figure 1.4.1.4). Emissions rates begin to increase shortly after the mandated 5 year warranty period of the emissions control system. Stephens and Cadle found if all passenger vehicles had emission rates similar to new vehicles, emissions of CO would be reduced by about 86%.

The causes for the high emissions rates observed included tampering with emissions control devices, mis-fueling (use of leaded gasoline in vehicles with three-way catalysts causing deactivation of the catalyst) and aging of the control system. Problems also come from the failure of inspection and maintenance programs to detect super-emitters due to the nature of the test used and because of limitations associated with the fact that the inspection and maintenance system in California is decentralized. Currently, these problems are being addressed and the inspection and maintenance program in California is being revised (Sommerville, 1993; CARB 1992).

1.4.2 Rich Open Loop Operation

A brief chronology of vehicle emissions control technology is listed in Table 1.4.2.1. Early emissions control systems in the 1970's consisted of oxidation catalysts for control of CO and HC, and then moved to dual-bed catalysts for control of CO, HC and NO_x (Figure 1.4.2.1a and b). The lowering of emissions standards over time forced vehicle manufacturers to switch in the early 1980's to three-way catalysts (Figure 1.4.2.1c). The chemistry of CO and HC oxidation and the reduction of NO_x on the surface of a three way catalyst is shown in Figure 1.4.2.2. Along with the conversion to three-way catalysts, on-board computers (or electronic engine controllers, EEC's) were installed for engine control, as well as exhaust gas oxygen (EGO) sensors and the exclusive use of fuel injectors as opposed to carburetors. These new systems not only provided for lower exhaust emissions but increased fuel economy and power output (Adler, 1985a). A schematic of the ignition and fuel metering control system for a

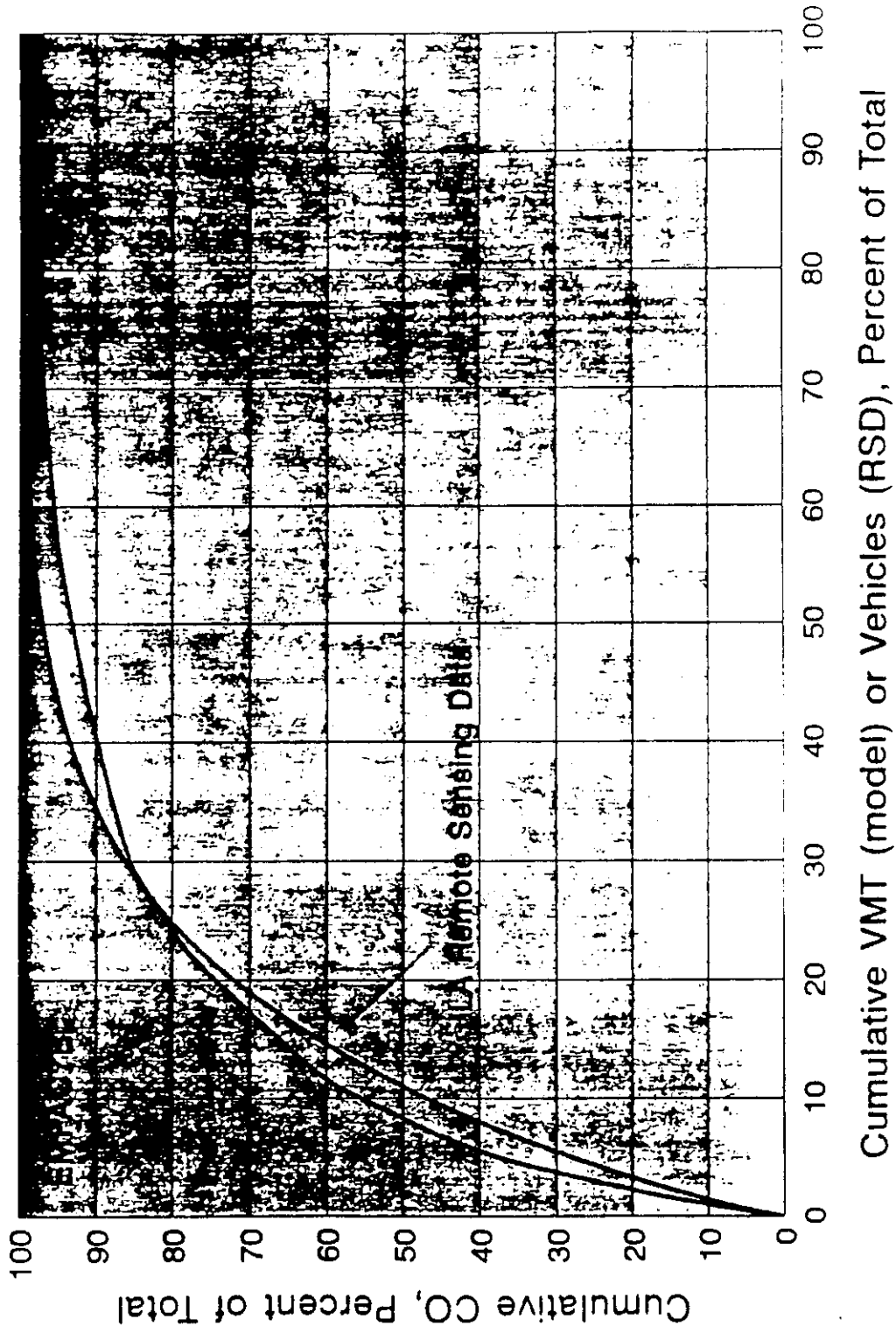


Figure 1.4.1.2 Cumulative VMT versus cumulative CO emissions for Los Angeles remote sensing data and EMFAC7E model predictions (Pollack, 1992).

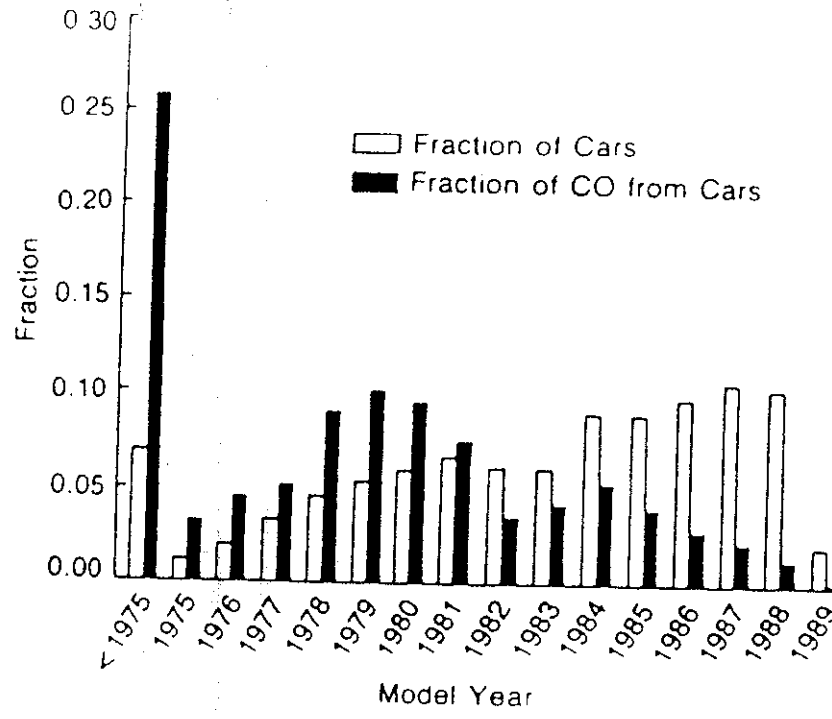


Figure 1.4.1.3 Fraction of cars and CO emissions by model year (Stephens and Cadle, 1991).

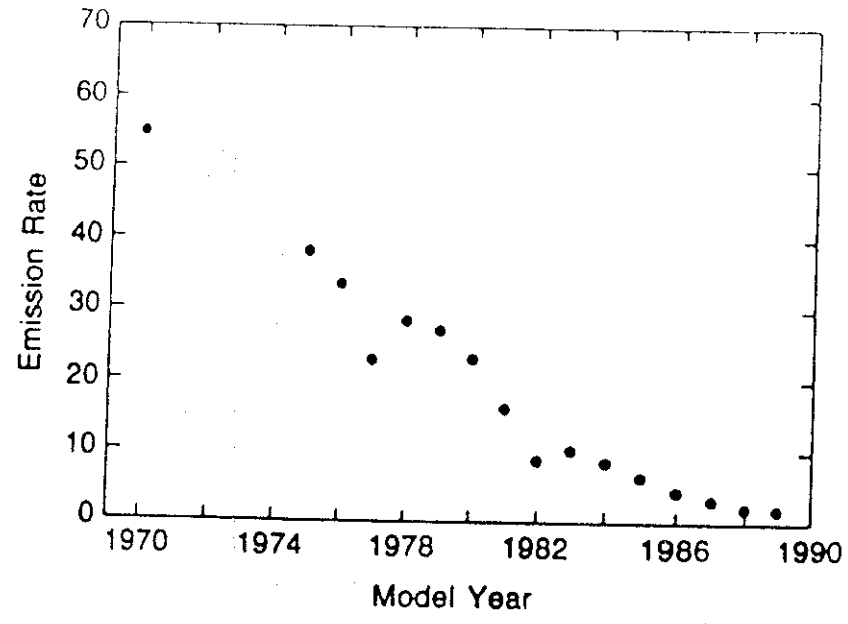


Figure 1.4.1.4 Mean emissions rates of passenger cars by model year (Stephens and Cadle, 1991).

Table 1.4.2.1 Chronology of vehicle emissions control technology in California.

Year	Control
1963	Positive Crankcase Ventilation
1966	HC/CO Control - Oxidation Catalysts
1970	Evaporative Controls
1971	Exhaust Gas Recirculation
1975	NO _x Control - Dual bed Catalysts
1981	Three Way Catalysts & Electronic Engine Controllers
1984	I&M Program
1985	On-Board Diagnostics

modern production vehicle, as well as the other related emissions control components including the evaporative emissions control system, are shown in Figure 1.4.2.3.

The switch to computerized engine control systems was required due to the narrow window of air-to-fuel ratio in which the catalyst is efficient for CO, HC and NO_x (Lies, 1989) as shown in Figure 1.4.2.4a and b. The EEC (shown in the bottom right corner of Figure 1.4.2.3) uses information from the EGO sensor and other sensors related to changes in driving conditions and air flow to the engine (the air flow sensor, air temperature sensor, throttle position sensor, etc.) to determine the amount of fuel required relative to the engine air charge volume to keep the engine running at stoichiometry (Figure 1.4.2.5). This type of system, where the exhaust gas composition is monitored and used to continuously adjust the mixture of air and fuel delivered to the engine is referred to as "closed loop" control (DIN 19 226), (Alder, 1986a). The operating cycle rate of the EEC is higher than the rate of cylinder firing of the engine allowing the air-to-fuel ratio of each combustion to be evaluated and the quantity of fuel delivered to the engine to be adjusted for the next cylinder to be fired.

The output voltage of the EGO sensor is used to determine if the engine is operating in the stoichiometric "window". The sensor exhibits a voltage jump at exactly the stoichiometric ratio. The EGO sensor uses a ceramic material which is conductive for oxygen ions starting at approximately 300°C and therefore does not provide any

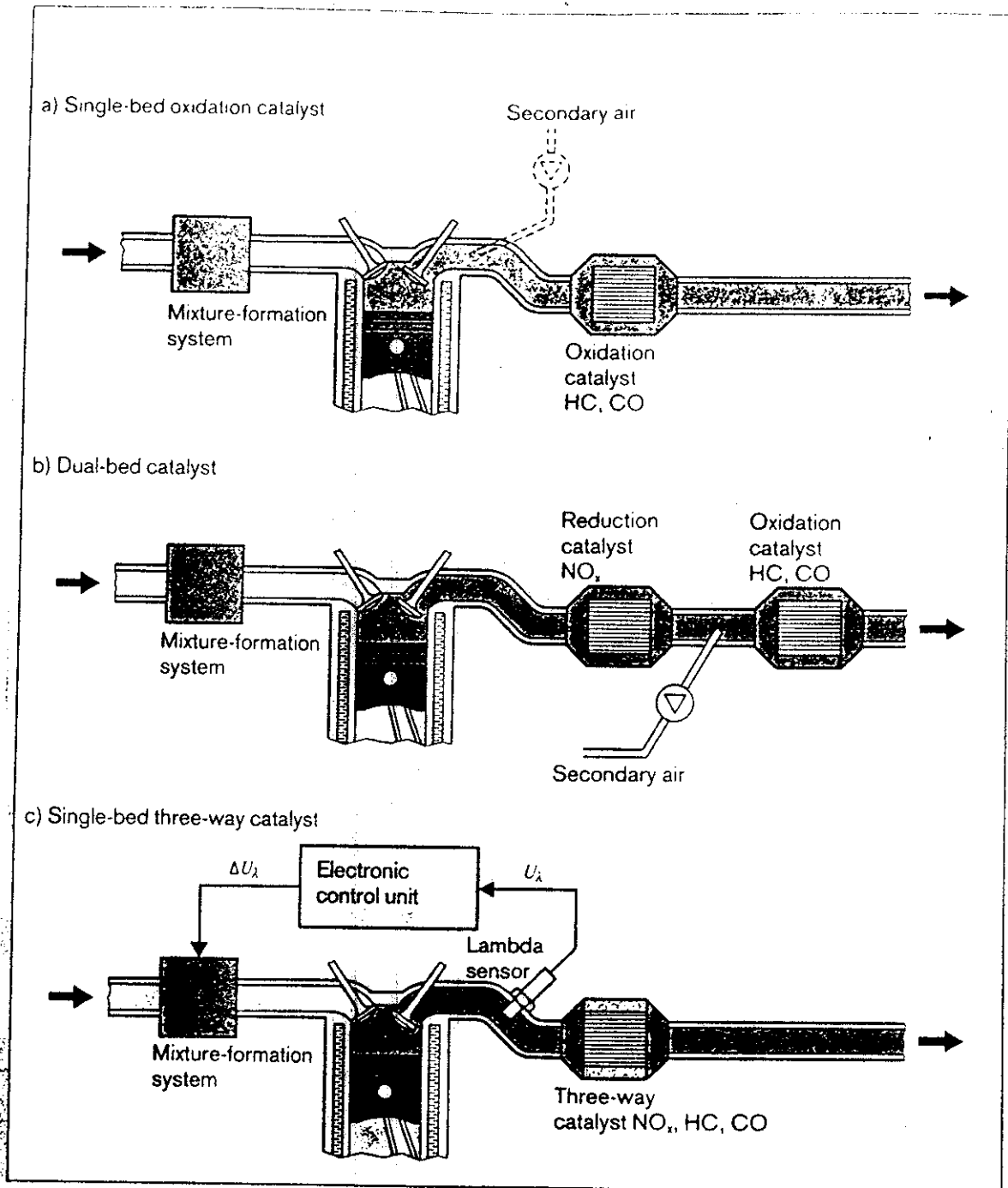


Figure 1.4.2.1 Emissions control system types: a. oxidation catalyst; b. dual-bed catalyst; and, c. three-way catalyst (Alder, 1985b).

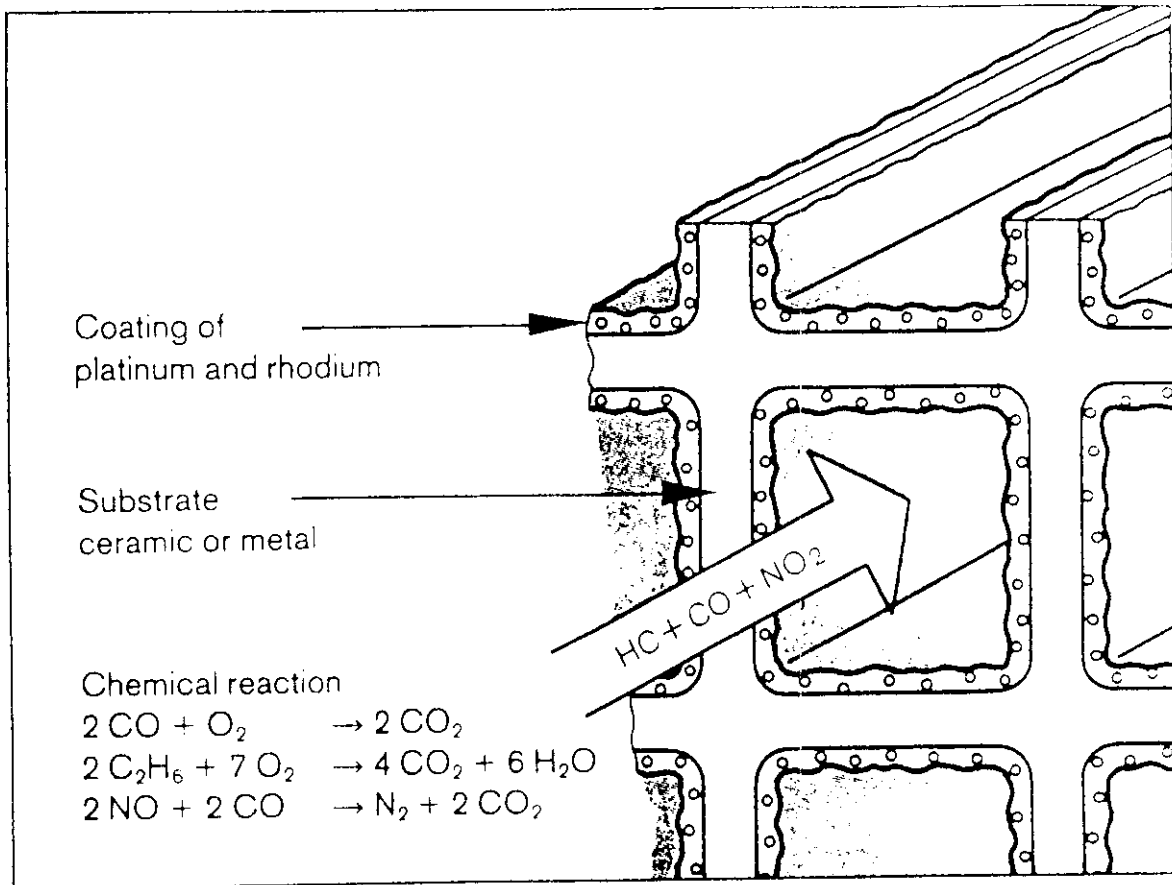


Figure 1.4.2.2 Chemistry of oxidation of CO and HC and reduction of NO_x on catalyst surface (Alder, 1985b).

information about the air to fuel ratio during start until the sensor is heated by the exhaust gas (Alder, 1985a). For this reason, some manufacturers are presently using heated EGO sensors (HEGO's) because they heat up faster and allow for the on-board computer to operate closed loop sooner after start (thereby reducing emissions during start).

Although closed loop operation produces the lowest emissions, there are conditions under which the manufacturer wants to command the vehicle to run off stoichiometry. Examples of rich operation include during start to facilitate the engine warming up and during passing (high acceleration) or high load conditions (as from grades or towing) where extra power is desired. Lean open loop operation is used to increase fuel economy

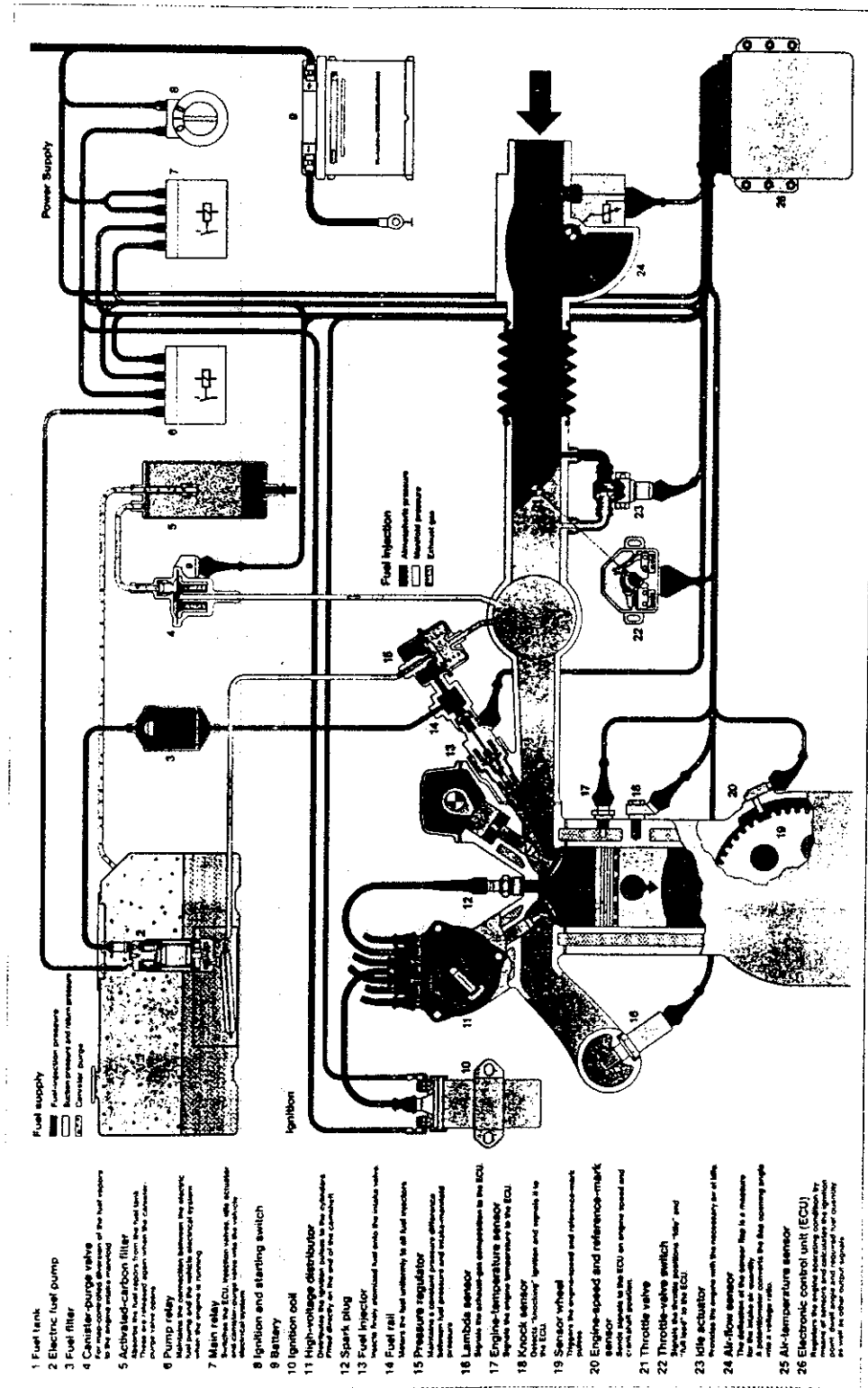


Figure 1.4.2.3 Ignition and fuel metering control system of a modern production vehicle (Alder, 1986b).

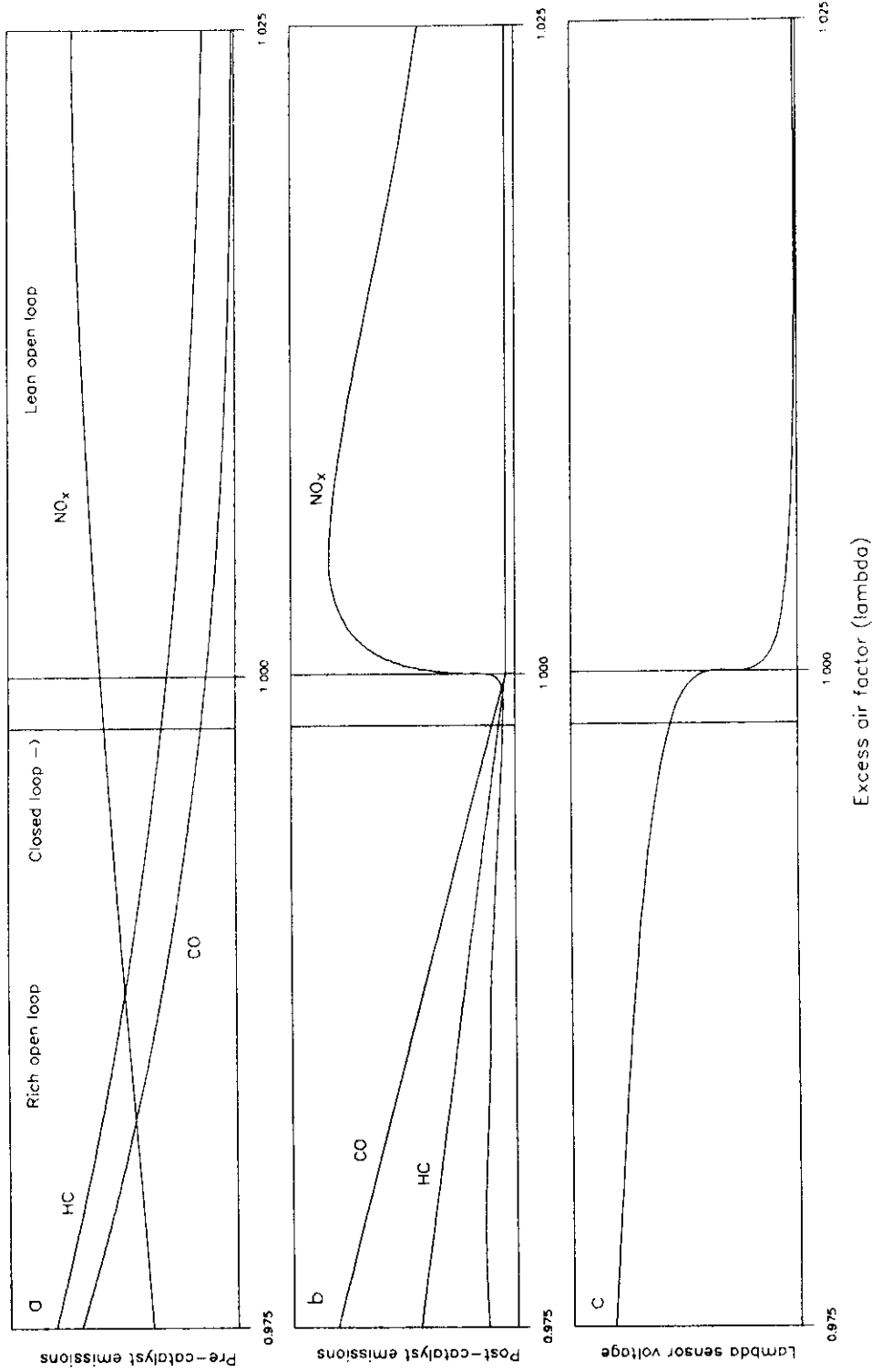


Figure 1.4.2.4 Pre-catalyst (a) and post-catalyst (b) relative emissions rates of CO, HC and NO_x as a function of air/fuel ratio (c), (Lies, 1989).

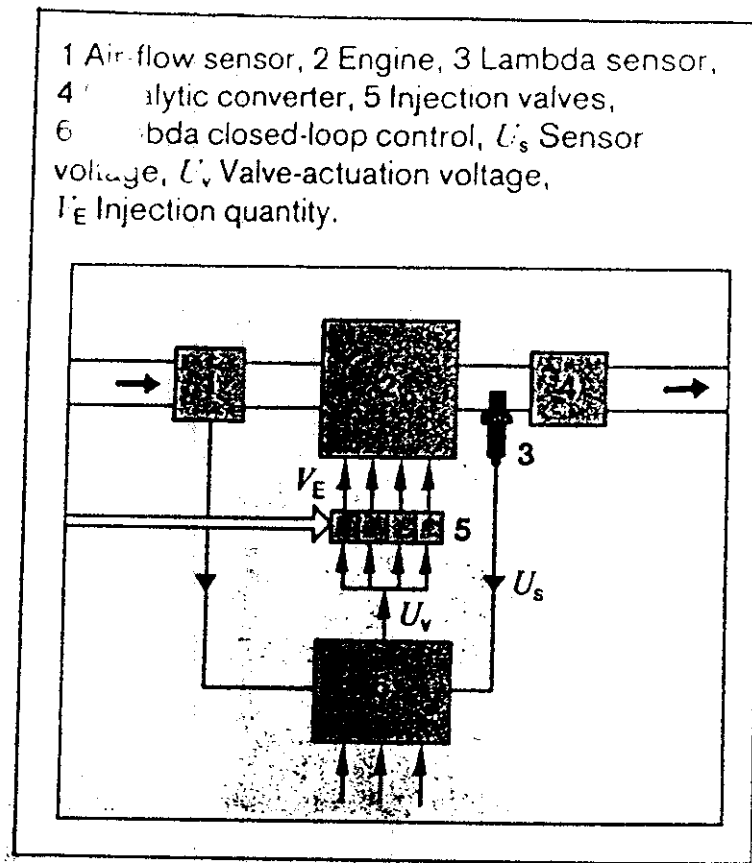


Figure 1.4.2.5 Schematic diagram of lambda closed-loop operation (1985b).

by lowering the quantity of fuel delivered to the engine during coasting. Commanding the vehicle to operate rich or lean is referred to as open loop operation because the quantity of fuel delivered to the engine is determined by an input to the EEC other than the exhaust gas air-to-fuel ratio. Non-heated EGOs may also cause the engine to operate open-loop because of cooling during idling which prevents the sensors from operating. (General Motors observed this to occur in at least one of their vehicles (Groblicki, 1992)).

The EEC in the vehicle uses a computer program which is the framework for decision making (the "strategy") and a set of look-up tables which contains the values of various set-points at which changes occur (the "calibration") to determine engine control. When the vehicle manufacturer is designing the strategy and calibration of the vehicle,

they are bounded by three parameters: obtaining the highest fuel economy; obtaining low enough emissions to pass the emissions certification test; and, allowing for enough power for the vehicle to be able to safely pass other vehicles and to handle conditions of increased load (Figure 1.4.2.6). The manufacturer can calibrate the vehicle to remain closed loop during the FTP (except during starts) to obtain the best combination of fuel economy and emissions, but also calibrate the vehicle so when driving in "off-cycle" conditions, the vehicle can operate open loop.

An example of a condition which could be used is the limitation of the maximum rate of acceleration in the FTP to 3.3 mph s^{-1} . The manufacturer could calibrate the vehicle to remain closed loop if the rate of acceleration or deceleration is less than or equal to 3.3 mph s^{-1} , but open loop if above this rate. Another example would be using the vehicle speed to determine open or closed loop. If the speed is less than 56.7 mph (the maximum in the FTP), the vehicle must remain closed loop. However, if the vehicle speed is greater than 56.7 mph, the EEC could allow the vehicle to operate open loop.

The California Air Resources Board (ARB) conducted experiments on modal acceleration testing to address concerns that the UDDS fails to adequately characterize on-road acceleration episodes and their associated emissions (Drachand, 1991). These data confirm that individual acceleration episodes greater than the maximum rate of acceleration in the FTP can result in emissions considerably greater than those of the FTP, or any of the other commonly used emissions test cycles. They stated they believe these high rates of emissions may be due to open loop operation. Revision of the FTP to include these events is mandated in the 1990 Clean Air Act Amendments. Section 208(c) added subsection (h) to section 206 on FTP modifications:

"Within 18 months after the enactment of the Clean Air Act Amendments of 1990, the Administrator shall review and revise as necessary the regulations under subsection (a) and (b) of this section regarding the testing of motor vehicles and motor vehicle engines to insure that vehicles are tested under circumstances which reflect the actual current driving conditions under which motor vehicles are used, including conditions relating to fuel, temperature, acceleration, and altitude."

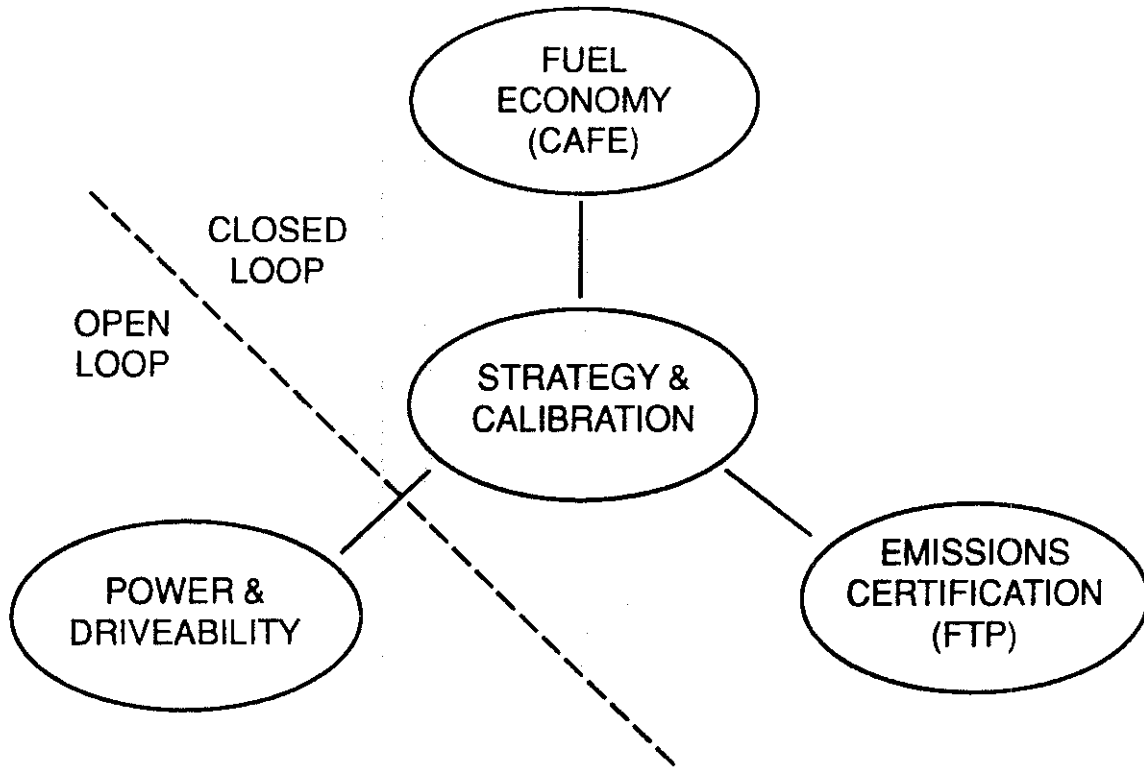


Figure 1.4.2.6 Limiting factors in the development of a vehicle strategy and calibration.

Presently, the US EPA is working in conjunction with the ARB to evaluate possible revisions to the FTP (US EPA, 1993). They are using data collected from chase car (Austin, 1992) and instrumented vehicle (DeFries, 1992) studies to determine the differences between actual driving conditions and the FTP (Markey, 1993a and b; German, 1993). They are proposing to add another test phase ("bag 4") to the FTP to represent changes in driving patterns since the FTP was developed. Three methods for the development of the drive cycles are under investigation, but of the candidates for bag 4 have not yet been determined. There is also debate whether the new test section should only include high emissions events which would be weighted separately, or when combined with emissions from the other three bags will be representative of actual

conditions (Carlock, 1993).

1.5 Objectives

The primary objective of this research was to collect on-road vehicle operating parameter data for a single vehicle driven in the SoCAB to compare to currently used vehicle certification testing conditions. Dynamometer emissions tests were conducted for the currently used certification test patterns (the UDDS and the HFET driving schedule) and three new patterns (freeway, urban and aggressive driving) developed from the on-road data to be representative of the current on-road driving conditions observed in this study for the SoCAB. Conditions which were of interest included comparing the current on-road driving to the conditions of certification tests; comparing modeled on-road emission rates to certification test emission rates; studying the operation of the on-board computer under varying conditions to determine the effects of the on-board computer on the magnitude of emissions; and evaluating changes in the certification testing methods which may improve the estimation of on-road emissions.

To conduct a comparison of on-road emissions to dynamometer based certification conditions, two vehicle emissions estimating models were developed. The models estimate on-road emissions as a function of acceleration and speed or engine load and speed. The emissions data collected on the dynamometer for the UDDS, HFET and the three new UCLA driving patterns were used to determine which modeling methodology estimated exhaust emissions more accurately, and to evaluate the accuracy of the models compared to the actual measured emissions during the tests. The vehicle emissions models were then used to estimate emissions from the on-road driving pattern data to compare current on-road emissions rates to those predicted by certification tests.

2.0 - EXPERIMENTAL

2.1 Hardware Description

2.1.1 Test Vehicle

The test vehicle was a new 1991 Flexible Fueled (FFV) Ford Taurus (VIN# 1FACP50U9MG200743) provided by the South Coast Air Quality Management District (SCAQMD) and is shown in Figure 2.1.1.1. The Taurus was one of 50 purchased by SCAQMD which were converted to operate on both unleaded gasoline (G100) and fuel methanol (M85, 85% methanol and 15% unleaded gasoline) or mixture of both fuels. The test vehicle had a 3.0L V-6 engine, fuel injection, a 4-speed automatic overdrive transmission, air conditioning and speed control. Operation of the vehicle with G100 fuel (gasoline) is expected to be equivalent to a similarly equipped non-flexible fuel Taurus (Smith, 1991). During all on-road experiments the vehicle was operated using a commercial source of 87 octane G100 fuel.

The vehicle was equipped with a California emissions control system. The major components of the emissions control system include the electronic engine controller (EEC), a single-bed three-way catalyst and a heated exhaust gas oxygen (HEGO) sensor. The catalyst was connected to the exhaust pipe downstream of the connection of the left and right exhaust header pipes. The HEGO sensor for the emissions control system was attached to the exhaust pipe at the joining of the exhaust header pipes (just upstream of the catalyst).

2.1.2 Vehicle Instrumentation and Data Collection System

The vehicle instrumentation is shown in Figure 2.1.2.1. The hardware consisted of a special ruggedized PC-based data acquisition and control computer developed by Ford, referred to as a Research Console (RCON), a 80368 microprocessor-based laptop computer, a Horiba air/fuel meter, an accelerometer transducer and three thermocouples.

The RCON is part of a proprietary vehicle data acquisition system (VDAS) used by engineers at Ford in the development of EEC strategies and calibrations as well as for



Figure 2.1.1.1 1991 FFV Ford Taurus test vehicle.

testing of other vehicle systems and on-road data collection for product development. The RCON was used during the experiments with special VDAS software to directly access the signals in the EEC during vehicle operation for recording.

The RCON is an industrialized 80386DX/20MHz-based IBM PC compatible computer operating on MS-DOS with a solid state hard disk (a battery backed-up RAM disk) to avoid potential problems from operation of a rotating hard disk in the vehicle. To aid with ease in connection of the RCON to the EEC, the EEC was removed from the stock placement under the front right dashboard and a special extension cable developed by Ford was used to connect the EEC to the bus connection for the EEC through the firewall under the dashboard. The EEC was then mounted under the passenger's side front seat and the RCON was placed behind the seat for connection to the EEC as shown in Figures 2.1.2.2 and 2.1.2.3. The RCON was interfaced to the EEC through a proprietary interface board, buffer box, cable and special Vehicle Data Acquisition System (VDAS) software developed by Ford. The RCON also allowed for collection of up to 12

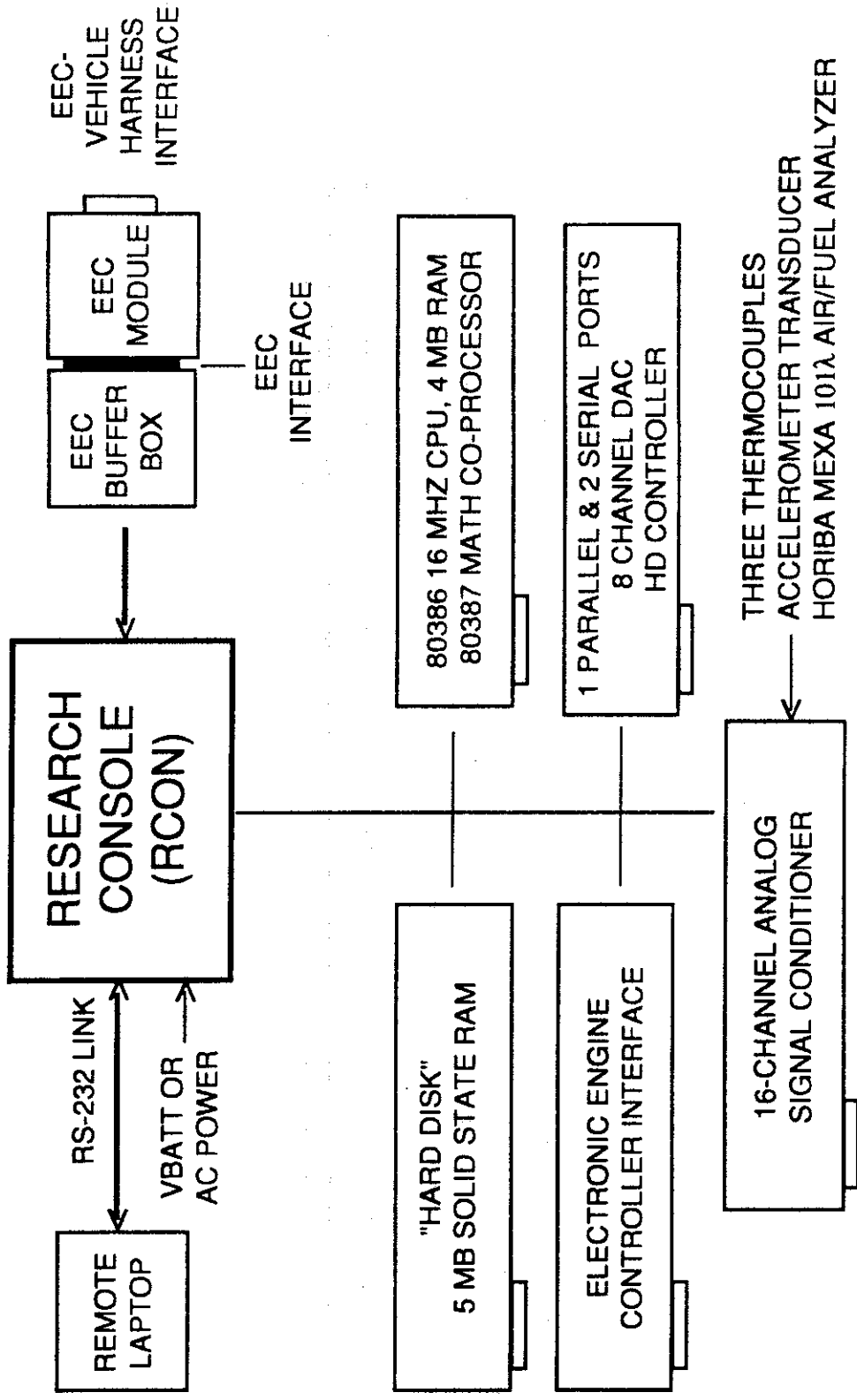


Figure 2.1.2.1 Vehicle data collection system.

analog signals and four thermocouple signals through an analog signal input conditioning module.

The VDAS software which was run on the RCON was controlled by an 80386SX/16MHz microprocessor-based laptop computer which was used as a keyboard and monitor for the RCON through the use of PC-Anywhere host-remote software. The PC-Anywhere software allowed for the control of the RCON (the remote in this case) by the laptop computer (the host) via a special cable from serial port to serial port. The hard disk in the laptop computer was also used to archive the experimental data (for transfer to a desk-top PC) which was uploaded from the hard disk of the RCON to the laptop by using the PC-Anywhere ASEND command. During the experiments, the laptop computer was held by the passenger or placed on the passenger's side front seat (Figure 2.1.2.4).

The VDAS software allowed for collection of a user-defined number of EEC signals and additional signals input through the analog signal input conditioning module. The software also allowed for the user to define the sample rate and a trigger for data collection, including setting the computer to automatically begin collecting data when the ignition is turned on in order to collect data during starts. For all of the experiments, an external push button trigger was connected to allow the driver to start the data collection at any time without having to look at the laptop keyboard to start the system.

The factory HEGO sensor is a simple oxygen sensor which exhibits a low voltage in an oxygen free atmosphere and a large voltage in the presence of oxygen (Figure 1.4.2.4c), therefore only qualitative information about the air/fuel ratio can be determined from this signal. For this reason, a laboratory grade air-to-fuel ratio (AFR) analyzer (Horiba Model MEXA-101 λ) was installed in the trunk of the vehicle (Figure 2.1.2.5) for accurate determination of the air-to-fuel ratio. The AFR sensor was installed in the same area of the exhaust pipe as the factory sensor but due to space limitations, the sensor was mounted in a manner in which the sensor pointed down under the vehicle. The sensor installed in the catalyst is shown in Figure 2.1.2.6. The AFR analyzer was interfaced to the RCON through the analog signal input conditioning module.

Factory thermocouples were used to determine the air charge temperature to the

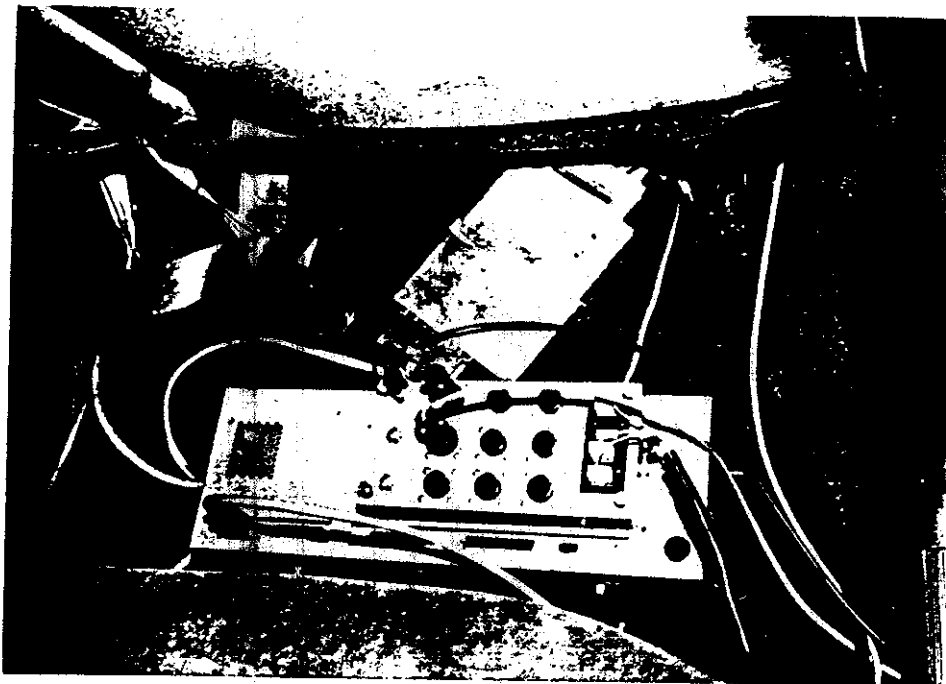


Figure 2.1.2.2 RCON connected to EEC behind passenger side front seat (top view).



Figure 2.1.2.3 RCON connected to EEC behind passenger side front seat (side view).

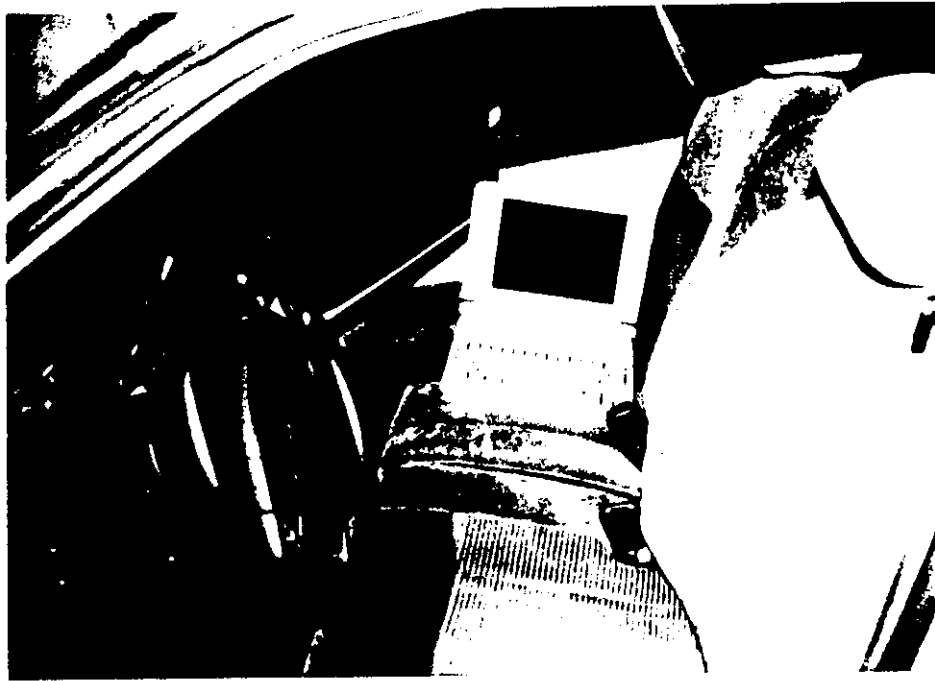


Figure 2.1.2.4 Remote laptop computer on passenger side front seat.

engine and the coolant temperature and were accessed through the EEC. Three additional thermocouples were added to the vehicle and interfaced to the RCON through the analog signal conditioning module. One thermocouple was attached under the front bumper to measure the ambient temperature and the other two thermocouples were attached to the exhaust system, the first directly before the catalyst to measure the catalyst feed-gas temperature and the second in the middle of the catalyst bed (see Figure 2.1.2.5). The mid-bed thermocouple was installed using a special procedure developed by Ford to prevent blockage of the catalyst matrix by broken catalyst substrate (Gutteridge, 1991).

To allow for the determination of the efficiency of the catalyst, two sampling ports were added to the exhaust system. They were 1/4" diameter stainless steel tubing welded to the exhaust system just prior to and after the catalyst. By examining the pollutant concentrations before and after the catalyst, combined with data on the catalyst temperature, the temperature at which the catalyst begins to work could be determined as

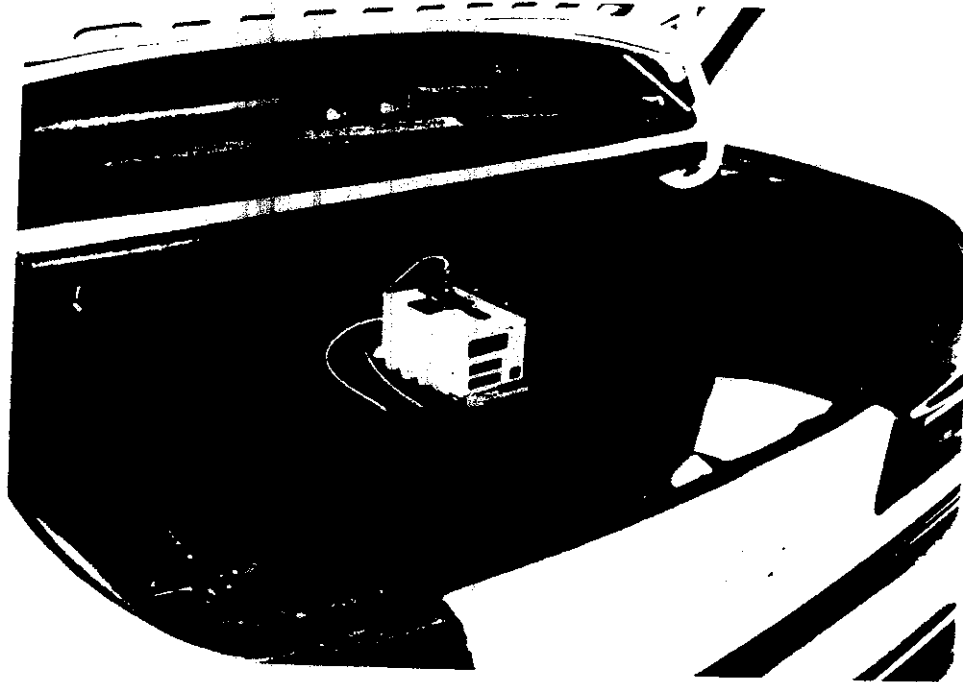


Figure 2.1.2.5 Placement of horiba air-to-fuel ratio analyzer and accelerometer transducer in trunk of test vehicle.



Figure 2.1.2.6 Placement of horiba AFR sensor and pre- and mid-bed catalyst thermocouples.

Table 2.2.1 Measured vehicle/engine operating parameters.

Engine RPM	Speed
Air conditioning operation	Brake operation
Open loop operation	Calculated load
Gear	Mass air flow through intake
Engine coolant temperature	Throttle position
Air charge temperature	Vehicle stock air/fuel sensor calculated lambda
Fuel injector pulse width	Supplementary air/fuel sensor measured lambda
Percent methanol	Ambient air temperature
Mid-bed catalyst temperature	Pre-catalyst exhaust gas temperature
Acceleration	

well. A marmon flange was welded to the end of the tailpipe to allow for connection to the dynamometer exhaust sampling system.

2.2 Data Collection Procedures

A list of the 20 vehicle and engine operating parameters monitored by the system is shown in Table 2.2.1. The signals were sampled at a rate of 10 Hz, and each signal was recorded at 1 second intervals as the average of the 10 Hz samples. Random access memory (RAM) for storage of data during the experiments was limited to 250,000 bits. After the RAM was full, the system would have to stop collecting data for approximately four seconds to write the data to the solid state hard disk, and then data collection would begin again. With a sample rate of 20 samples per second, and each being stored as an eight bit word, a total of 1562 seconds of data could be collected before the data would need to be written to a file on the hard disk. The RCON was programmed to collect 1500 seconds of data and then write the data to the hard disk. 1500 seconds was chosen because it allowed for easy calculation of the number of disk writes which occurred during a fixed period of time.

In addition to the vehicle and engine operating parameters recorded on-line, a manual log was used to record trip characteristic data such as route, direction and weather. Approximately every 300 seconds, and when special events such as accidents,

train crossings, hills, or presence of police vehicles occurred, a location, description and sample number were recorded verbally on a tape recorder. These data were later transcribed and used as a reference during data analysis to evaluate the cause of any unusual data.

2.3 On-Road Experiments

2.3.1 Start, Idle and Cool Down

Data were collected during 28 starts to determine the duration of open loop operation during start and to determine which vehicle operating parameter(s) are used by the EEC to determine the end of this operation. The condition of the start experiments ranged from cold to hot starts, in varying ambient temperature conditions. The conditions of the experiments are described in the Results and Discussion section. At the beginning of each test, the key was turned to the on position for 10 seconds before cranking the engine.

The test vehicle was driven after one of the start experiments (a cold start) for approximately 15 minutes in urban traffic (in Westwood) to aid in warming-up the vehicle. The vehicle was then parked in the shade and data were collected for the vehicle while idling in parking gear for 1500 seconds. Data were also collected while switching the air conditioning on and off during an idle 60 second intervals to determine the load induced by the air condition compressor. Immediately after the idling experiment, the vehicle was turned off and a new set of 1500 seconds of data was collected for the vehicle to study the rate of cooling of the engine and the catalyst after shut down.

2.3.2 Acceleration and Deceleration

In order to determine the operating envelope of the vehicle, acceleration and deceleration experiments were conducted on a level road in the Mojave desert with the air conditioning and all electrical devices turned off with the exception of the RCON. Vehicle operating data were collected during wide open throttle accelerations to 80 miles per hour (mph) from 0 mph and at 10 mph increments in starting speed up to an

acceleration from 70 to 80 mph. Deceleration tests were conducted in a similar manner by braking as hard as could safely be achieved to 0 mph from 80 mph and at 10 mph decrements in starting speed down to a deceleration from 10 to 0 mph. The natural rate of deceleration of the vehicle was determined by performing a coasting deceleration from 80 mph to the idle speed of the vehicle (≈ 18 mph).

2.3.3 Effects of Variation in Load

To determine the effects of increased and decreased load on vehicle and engine operating parameters, including open loop operation, experiments were conducted by driving up and down a 5 mile long, 6% grade on Interstate 5 from Fort Tejon to the town of Grapevine. The test consisted of driving a 7 mile section of the freeway (1 mile prior to the grade, 5 miles of grade, and 1 mile after the grade) while maintaining a constant speed of 65 mph. The experiment was repeated using the vehicle speed control to aid in differentiation between driver behavior and engine control on the frequency of rich open loop operation.

2.3.4 Repeated Freeway Route

The 405 freeway, from Wilshire Boulevard was driven in both directions repeatedly from 5:00 am to 8:00 pm to determine the effect of time of departure and direction of travel on time of travel and on frequency of open loop operation. This section of freeway is a major north/south thoroughfare between West Los Angeles and the San Fernando Valley. The experiment consisted of 28 northbound and 28 southbound trips over the approximately 10 mile long route which included a hill.

All trips were driven by one of two researchers who were instructed to drive in a "conservative" manner to determine the minimum conditions for the route. To drive as conservatively as possible, the drivers were instructed to move immediately to the center lane after beginning the test. When an even number of lanes were available, the driver kept the vehicle in the center left lane. The test vehicle was maintained with the speed of the vehicle it was following and the driver was not allowed to pass or change lanes.

Table 2.3.5.1 On-road freeway and urban driving matrix routes.

Freeway routes:

1. I-5 (S) at Calgrove to 710 (S), end at Long Beach.
2. 101 (E) at Topanga Canyon, end at 60.
3. I-5 (S) at Calgrove to 405 (S), end at 110.
4. 405 (N) at Lake Forest, end at 110.
5. 110 (N) at Seaside, end at Glenarm.
6. I-5 (N) at Lake Forest, end at 10.
7. 60 (W) at Country Ville to 10 (W), end at PCH.
8. 91 (S) at 60, end at 110.

Urban routes:

1. Supleveda (S) at Hwy 118 to PCH (S), end at Orange County Line.
 2. Roscoe (E) at Topanga Canyon to Coldwater (S) to Santa Monica (E) to Vermont (S), end at PCH.
 3. Wilshire (E) at PCH to Grand (S) to Washington (E) to Whittier (E).
 4. Hwy 42 (E) at Vista Del Mar, end at San Antonio.
 5. Atlantic (N) at Ocean to Los Robles (N), end at Hwy 210.
 6. Harbor (N) at Hwy 55 to Fullerton (N), end at Hwy 60.
 7. Beach (N) at PCH to Rosecrans (W), end at Vista Del Mar.
 8. Torrance (E) at PCH to Crenshaw (S) to Carson (E) to Santa Fe (S) to Wardlow (E) to Atlantic (N) to Carson (E) to Lincoln, end at Tustin.
-

2.3.5 Conservative Driving Freeway and Urban Route Matrix

A matrix of freeway and urban routes were driven in the morning and evening rush hours to examine driving patterns and their effect on vehicle and engine operating parameters including open loop operation.

The freeway routes were chosen based on vehicle densities and vehicle miles traveled on the highways in the SoCAB from both California Department of Transportation (1990) and SCAG data (1985; 1989). Information about urban routes comes from SCAG data. Each of the selected routes listed in Table 2.3.5.1 was driven

towards downtown (in the direction listed in Table 2.3.5.1) for the morning tests and in the opposite direction for the evening tests. The spatial distributions of the route matrices are shown in Figure 2.3.5.1 for the freeway routes and Figure 2.3.5.2 for the urban routes.

Data from the repeated freeway test were used to determine the effect of time of departure and direction of travel on time of travel in order to select the starting time for the driving route matrix experiments. The average time of travel for pilot studies driven on several of the matrix routes was 90 minutes. The times of peak traffic in the repeated freeway test occurred at 8:00 am and 5:15 pm. To ensure operation in peak traffic, and based on the estimated time of travel of 90 minutes, the start times for the morning and evening experiments were chosen to be 7:15 am and 4:30 pm respectively.

Data collection for the freeway routes began at the beginning of the on-ramp and for urban routes when entering the intersection of the cross streets. Data collection was ended at the beginning of the off ramps for the freeway routes and when exiting the intersection of the cross streets for the urban routes. All routes were again driven by one of two researchers who were instructed to drive in the "conservative" manner described for the repeated freeway experiment.

2.3.6 Aggressive Driving Freeway and Urban Route Matrix

In the freeway and urban route matrix the driver remained in the center lane during the entire route and therefore the driving was not as "aggressive" as the normal behavior for most drivers who change lanes in an attempt to reduce driving time. The driving could also be considered less aggressive because the speed of the test vehicle was determined by the speed of the vehicle ahead of it. Acceleration rates were expected to be lower than the vehicle being followed because the test vehicle driver took time to perceive and respond to the change in speed of the vehicle being followed.

Because the matrix of freeway and urban routes were driven in this constrained manner, two freeway routes (1 and 6) and two urban routes (4 and 7) from the driving matrix listed in Table 2.3.5.1 were driven again in an "aggressive driver" mode. During these experiments, the driver was allowed to make lane choice and passing decisions and

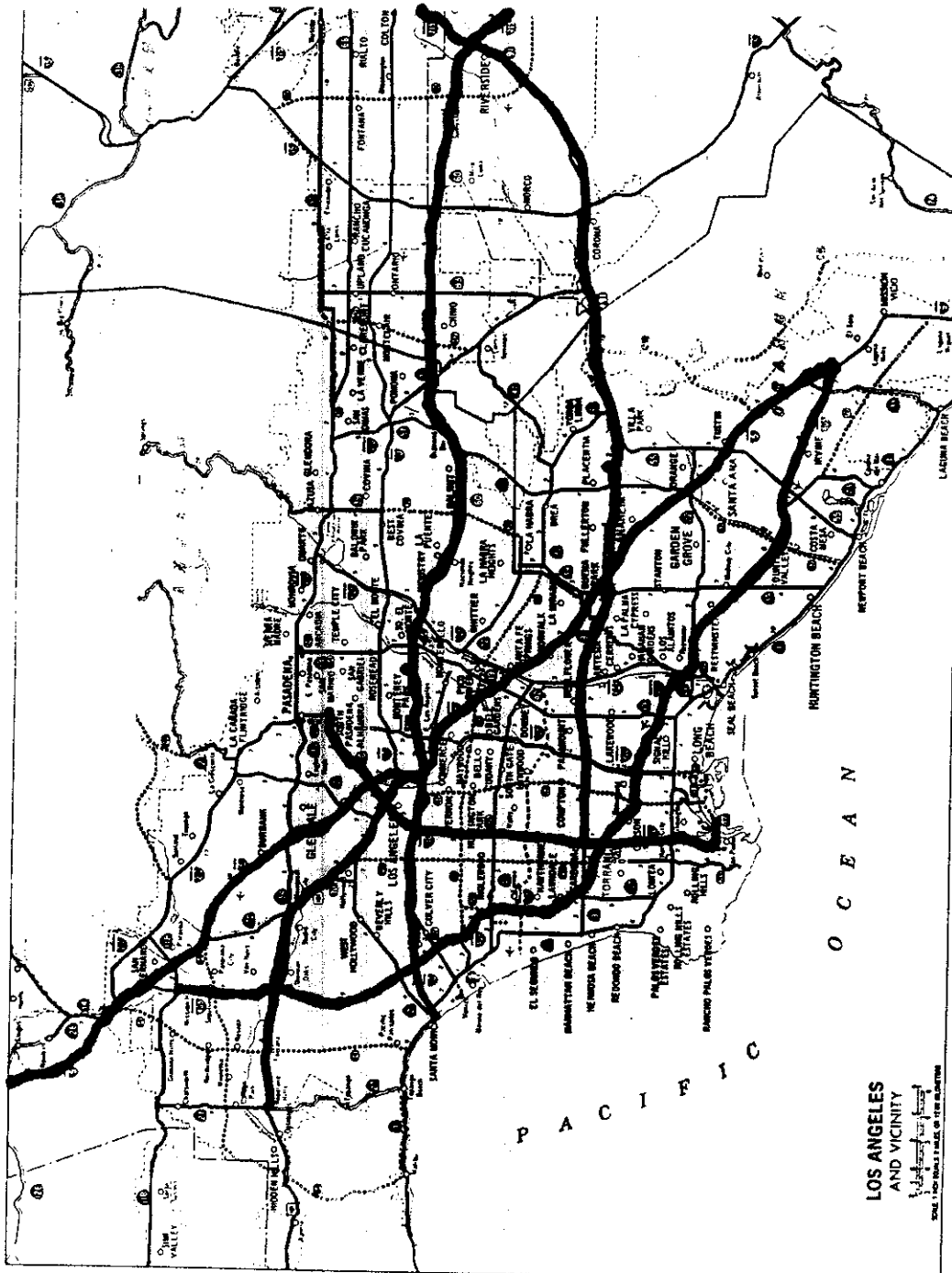


Figure 2.3.5.1 On-road freeway route matrix.

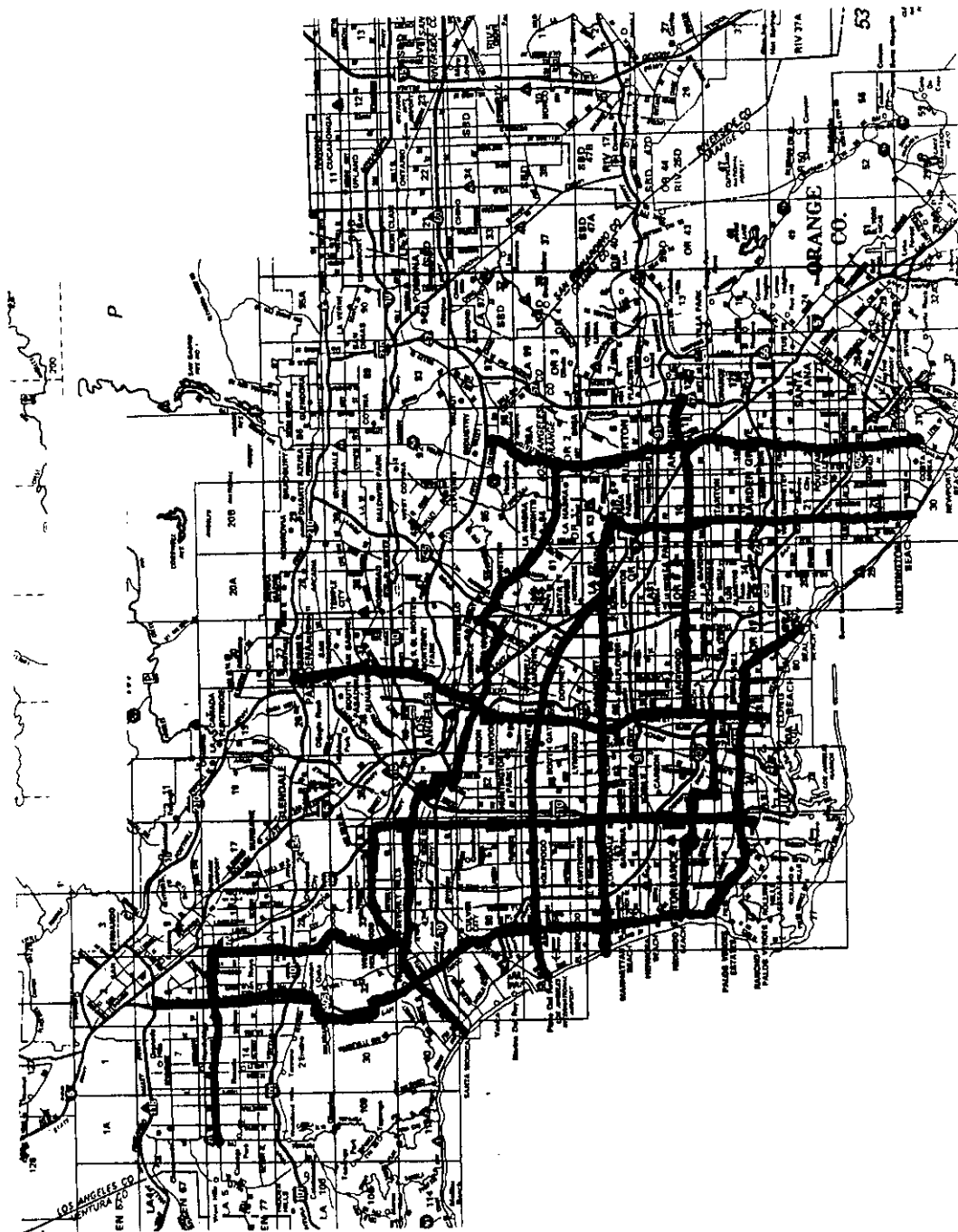


Figure 2.3.5.2 On-road urban route matrix.

was instructed to drive as fast as possible while still driving safely. The routes were driven on the same days of the week as employed previously to eliminate possible day-of-the-week influences.

2.4 Data Analysis Software

The vehicle data acquisition system (VDAS) software developed by Ford consists of several tools for analysis of data as well as its' data collection tools. A component of the software system is GVDAS (Graphical Vehicle Data Acquisition System), which allows for plotting and tabular review of the data. The on-road data were collected and written to files in binary to save disk space. Another component of the software is the program V5CVT (Version 5 of the conversion utility) which allows for the data to be converted to ASCII for further analysis.

In addition to the VDAS programs, several programs were written in Fortran 77 for the Microsoft Fortran Compiler (V 5.0) to aid in data analysis. An automated experiment log (LOG.FOR) was written to prompt the driver at the beginning of an experiment for beginning and ending points, start and completion times, date, initial and final mileage, subjective information about wind and rain, and unusual traffic incidents, and who the driver and instruments operators were (the source code is given in Appendix A.1). From the entered information, the program calculated the time of travel, distance traveled, and average speed for comparison to the data collected by the RCON. The output of the log program was an ASCII file with the extension of .OBD.

The flow chart for the analysis of the data from an on-road trip is shown in Figure 2.4.1. The analysis begins by converting the raw data files (*.DRW) to ASCII (*.AEU) with the program V5CVT. Because each of the files was limited to 1500 seconds each, the data set for most experiments consisted of 2 to 5 data files. Each file after the first data file was edited to remove the header from the file which describes the location of the variables in the file and then the data files were concatenated to create a single data file. During the writing of the 1500 second data files to disk, four seconds of data were not collected, therefore the concatenated data file, was edited and between each data file,

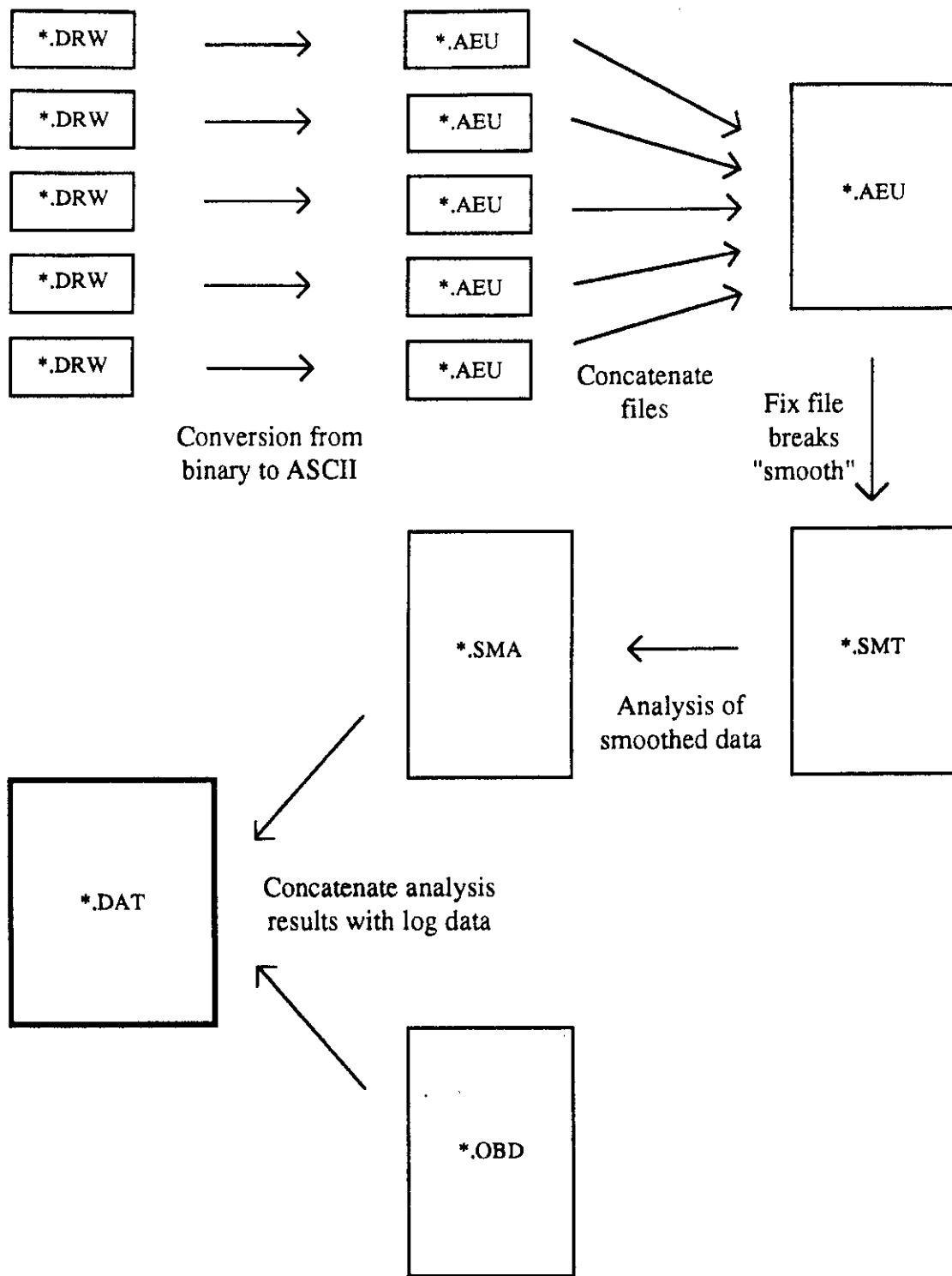


Figure 2.4.1 Flow chart for analysis of on-road VDAS data.

three seconds of data were added by linearly approximating the data from the end of one data file to the beginning of the next data file. The "smoothed" data files were saved with the extension of .SMT. If the variable in the data file was a binary variable (a flag), the first two seconds of the approximation were one state and the last two seconds were assigned to the other state.

The analysis of the data files was performed by the program ANLYS50C.FOR. The program source code is given in Appendix A.1.1 and is written in Fortran 77 for the Microsoft Fortran Compiler (version 5.0). For each of the experimental smoothed data files, a "control" file was created which contained the names of the input and output files to be used in the analysis. The use of control files allowed for the unattended analysis of the data and for changes to be made to the analysis while still retaining the original test conditions for future reference. The output of the analysis program was an ASCII file with the extension of .SMA (smoothed analysis). This file was concatenated with the log file (*.OBD) and the new file was named *.DAT.

A sample analysis sheet from the program is shown in Figures 2.4.2, 2.4.3 and 2.4.4. At the top of the sheet is the information from the automated data log. Following the log information are analyses of the trip characteristics, an analysis of the individual vehicle operating parameters recorded, a modal analysis using acceleration and speed based modes, a modal analysis using load and speed based modes, and an analysis of open loop operation.

The trip characteristics analysis includes the time of travel, distance traveled (calculated from the instantaneous one second speed measurements), average speed, maximum speed, maximum rate of acceleration, maximum rate of deceleration, and fuel economy (calculated from the sum of the fuel flow pulses of the fuel injectors and the distance traveled). The vehicle operating parameter analysis included the average, maximum and minimum measurements for each of the parameters. It also includes a calculation of the percent time braking and the percent time with the air conditioning compressor operating. The compressor operates when either the air conditioning or the defroster are turned on. The cooling is used intermittently when the defroster is turned

U-4E-WE-22

This is summary file: EXPT_022.OBD

Date: 230492

Route ID = Hwy 42 at Vista del Mar, Rosecrans to Parks.
Direction = East to West.

Beginning data file: grid_207.drw
Ending data file: grid_211.drw

Starting time at: 1630 HHMM
Ending time at: 1817 HHMM
Initial milage: 8232.9 miles
Final milage: 8262.0 miles

Total time traveled: 107 minutes
Total distance traveled: 29.1 miles
At an average speed of: 16.3 miles/hour

Driver: MICHAEL
Computer/Instruments Operator: MICHAEL

General conditions for driving and comments

Wind Class: Calm
Rain Class: Clear
Traffic Class: Accident in the contiguous lane

Calculated data from recorded data files:

Time of travel = 107.63 minutes.
Distance traveled = 29.03 miles.
Average velocity = 16.19 MPH.
Maximum velocity = 54.74 MPH.
Maximum Acceleration = 7.49 MPH s⁻¹.
Maximum Deceleration = -7.31 MPH s⁻¹.
Fuel economy = 18.64 mpg.

Figure 2.4.2 The first page of the data analysis output from the program ANLYS50C.FOR.

Velocity and acceleration modal analysis:

Mode	Number of Occurrences	Percent of Occurrences	Percent time	Average time
Start	0.	.00	.00	.00
Stopped	95.	6.31	35.67	24.24
Cruise	304.	20.19	8.55	1.82
Coast	143.	9.50	3.65	1.65
Hard Accl	2.	.13	.09	3.00
Med Accl	67.	4.45	2.15	2.07
Light Accl	345.	22.91	24.02	4.50
Hard Decl	107.	7.10	3.10	1.87
Med Decl	221.	14.67	16.99	4.96
Light Decl	222.	14.74	5.78	1.68
Totals	1506.	100.00	100.00	
Average distance between stops:		.31 miles.		

Vehicle operating parameter analysis:

Parameter	Average	Maximum	Minimum
Throttle Position	36.61	611.09	.00
RPM	1122.94	3954.00	648.75
Load	.24	.75	.07
Vehicle A/F	1.00	2.00	.83
Horiba A/F	1.00	1.70	.86
Percent MeOH	.01	.01	.00
Accelerometer	-.09	.28	-.56
Gear	2.15	4.00	1.00
Ambient Temp	85.92	97.63	71.83
Air Charge Temp	116.10	152.00	88.00
Eng Coolant Temp	209.60	218.00	194.00
Exhaust Gas Temp	751.29	1235.25	515.44
Catalyst Temp	988.14	1337.68	717.45
Percent time braking:	58.11		
Percent time with A/C on:	.00		

Load based modal analysis:

Mode	Percent of time
1. Open loop (rich & lean)	.20
2. High load	1.63
3. Medium high load	9.17
4. Medium low load	11.07
5. Low load	77.93
6. Hot Start	.00
7. Cold Start	.00
Total	100.00

Figure 2.4.3 The second page of the data analysis output from the program ANLYS50C.FOR.

Open loop and GM enrichment operation analysis:

Start was NOT present.

Percent time RICH open loop: .0929%.

Percent time LEAN open loop: .1084%.

Occurrences of GM enrichment mode:

Percent	Number	Total Sec
1.905	123.	6457.

Open loop occurrences: 3

Occurrences (seconds, accel/decel, rich/lean, mode, velocity, accel)

7	D	L	mode = MD	vel = 51.90	accl = -.41
4	A	R	mode = HA	vel = 23.07	accl = 3.56
2	A	R	mode = HA	vel = 36.74	accl = 3.43

Figure 2.4.4 The third page of the data analysis output from the program ANLYS50C.FOR.

on to aid in removal of moisture from the passenger compartment air by condensing the moisture on the surface of the air conditioning heat exchange core (the evaporator) which drips off and is bled out of the passenger compartment.

The acceleration and speed based modal analysis contains ten modes as shown in Figure 2.4.3 (page 2 of the output). The program calculates the number of occurrences in each mode, the percent of total occurrences for each mode, the percent time in each mode and the average time in each mode when the mode occurred. The load and speed based modes are also shown in Figure 2.4.3. For this analysis, only the percent time in each of the seven modes was calculated.

The analysis of open loop operation is shown in Figure 2.4.4 (page three of the output). The analysis determines if a start was present (the vehicle operates open loop during starts), the percent time in rich open loop operation, the percent time in lean open loop operation, compares the Taurus to a General Motors (GM) vehicle (see Chapter 3 - Results and Discussion for a description), and determines the total number of open loop events. For each individual open loop event, the program also provides the duration of the open loop event, whether it was during an acceleration or deceleration, whether the vehicle was operating lean or rich, the acceleration and speed based mode of operation when the event occurred, and the speed and acceleration when the event occurred.

2.5 Dynamometer Emissions Tests

2.5.1 Development of Dynamometer Driving Schedules

There is a need to develop new driving schedules which are more representative of current on-road driving conditions. Two dynamometer driving schedules were developed from the on-road freeway and urban conservative driving pattern data described earlier. An additional driving pattern was developed to collect emissions data at high rates of acceleration. The freeway and urban driving schedules were developed using the same techniques as were used in the development of the FTP (Kruse and Huls, 1973), but the patterns were developed to be representative of the averages of the freeway and urban data collected on-road. The driving schedules were compared for travel distance, speed,

Table 2.5.1.1 Comparison of the UCLA Freeway and Urban Driving Schedules to the average of the on-road data.

Route Number	Travel Time	Travel Dist	Avg. Vel	Max Vel	Max Accel	Max Decel	Fuel Econ	Open Loop	Open Loop	Avg Dist Per Stop
Dir, Expt#	min	miles	MPH	MPH	MPH s-1	MPH s-1	MPG	Rich %	Lean %	miles
FTP	22.9	7.27	20.3	55.96	5.08	4.26	22.9	0.00	0.00	0.45
Freeway										
7-EW-3	97.18	59.11	36.50	72.89	4.50	-6.73	32.3	0.03	0.93	3.11
Dyno Pattern	23.35	12.96	33.34	66.79	4.50	-6.73	28.4	0.14	0.64	2.16
Urban										
3-EW-42	104.28	35.99	20.71	49.31	7.10	-8.74	22.8	0.02	0.02	0.44
Dyno Pattern	23.35	7.69	19.77	49.31	7.10	-7.37	21.9	0.07	0.07	0.37

maximum speed, maximum acceleration and deceleration rates, fuel economy, percent time in rich and lean open loop operation, and average distance per stop. A comparison of the driving schedule statistics to the average on-road data is shown in Table 2.5.1.1.

The on-road driving pattern which was used as the basis for the UCLA freeway dynamometer driving schedule (UFDDS) is shown in Figures 2.5.1.1a, b, c, d. The sections which were deleted to create the driving schedule are shown marked out. The speed versus time trace of the UFDDS is shown in Figure 2.5.1.2.

The on-road driving pattern which was used as the basis for the UCLA urban dynamometer driving schedule (UUDDS) is shown in Figures 2.5.1.3a, b, c, d, e. The sections which were deleted to create the driving schedule are shown marked out. The speed versus time trace of the UUDDS is shown in Figure 2.5.1.4.

The UCLA acceleration dynamometer driving schedule was developed from parts of the ARB acceleration driving schedules (Figure 2.5.1.5) and adding other acceleration peaks which varied from 2 to 6 mph s^{-1} , ranging from speeds of 0 to 60 mph. The UCLA acceleration driving schedule is shown in Figure 2.5.1.5.

2.5.2 Dynamometer Emissions Measurements

The test vehicle was driven to Ford Motor Company's Scientific Research

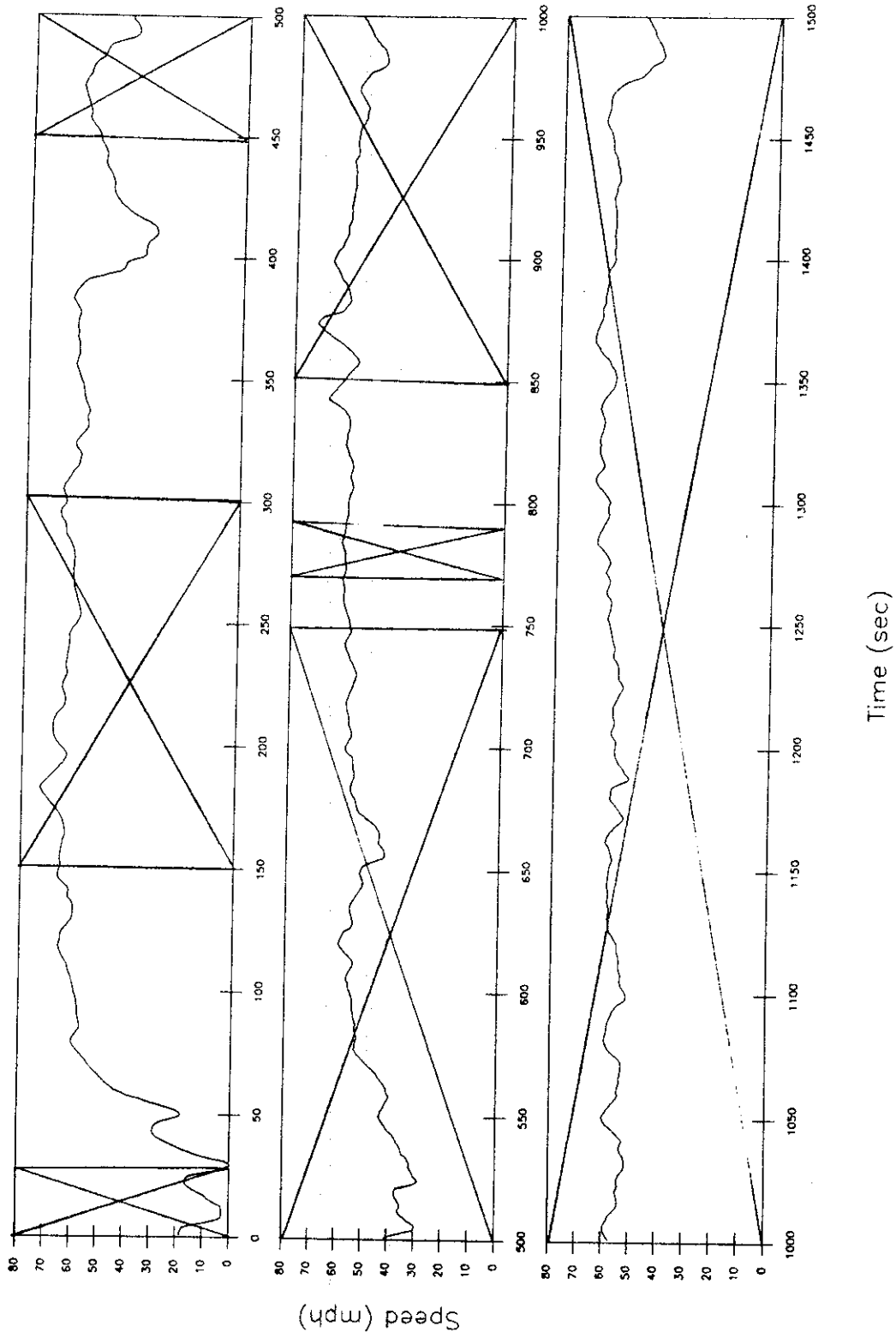


Figure 2.5.1.1a On-road freeway driving pattern used as basis for UCLA Freeway Dynamometer Driving Schedule continued (deleted sections shown marked out).

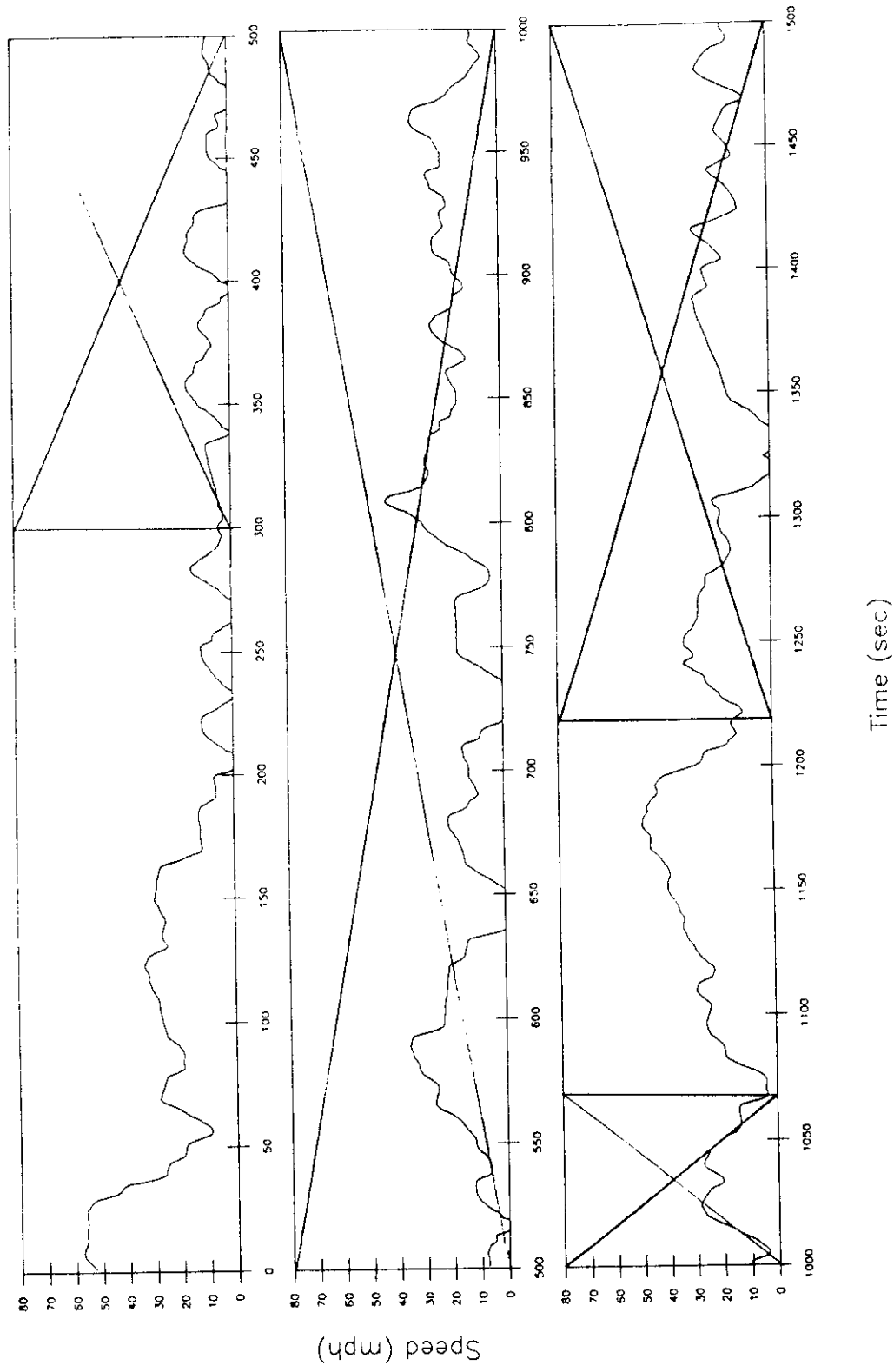


Figure 2.5.1.1b On-road freeway driving pattern used as basis for UCLA Freeway Dynamometer Driving Schedule continued (deleted sections shown marked out).

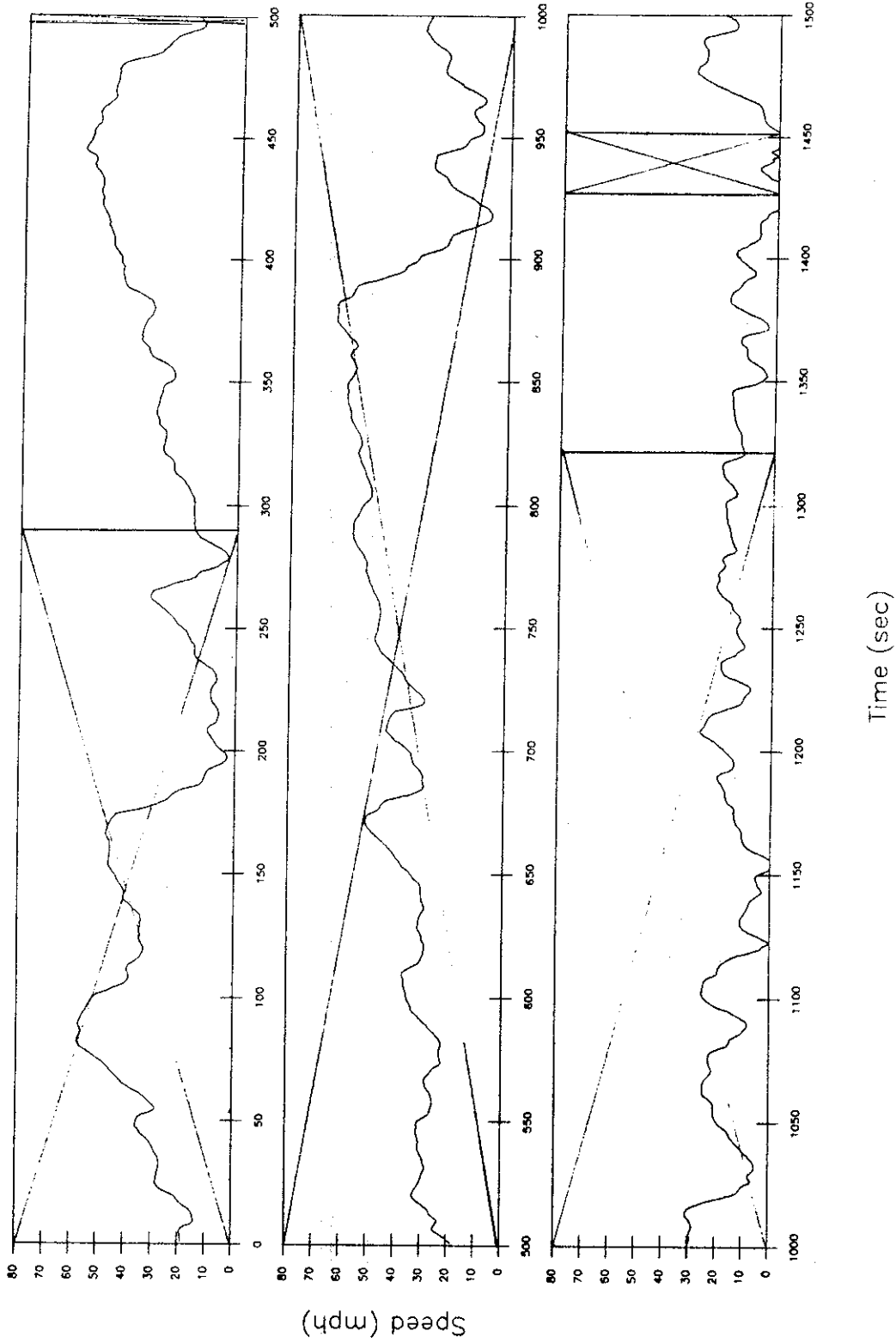


Figure 2.5.1.1c On-road freeway driving pattern used as basis for UCLA Freeway Dynamometer Driving Schedule continued (deleted sections shown marked out).

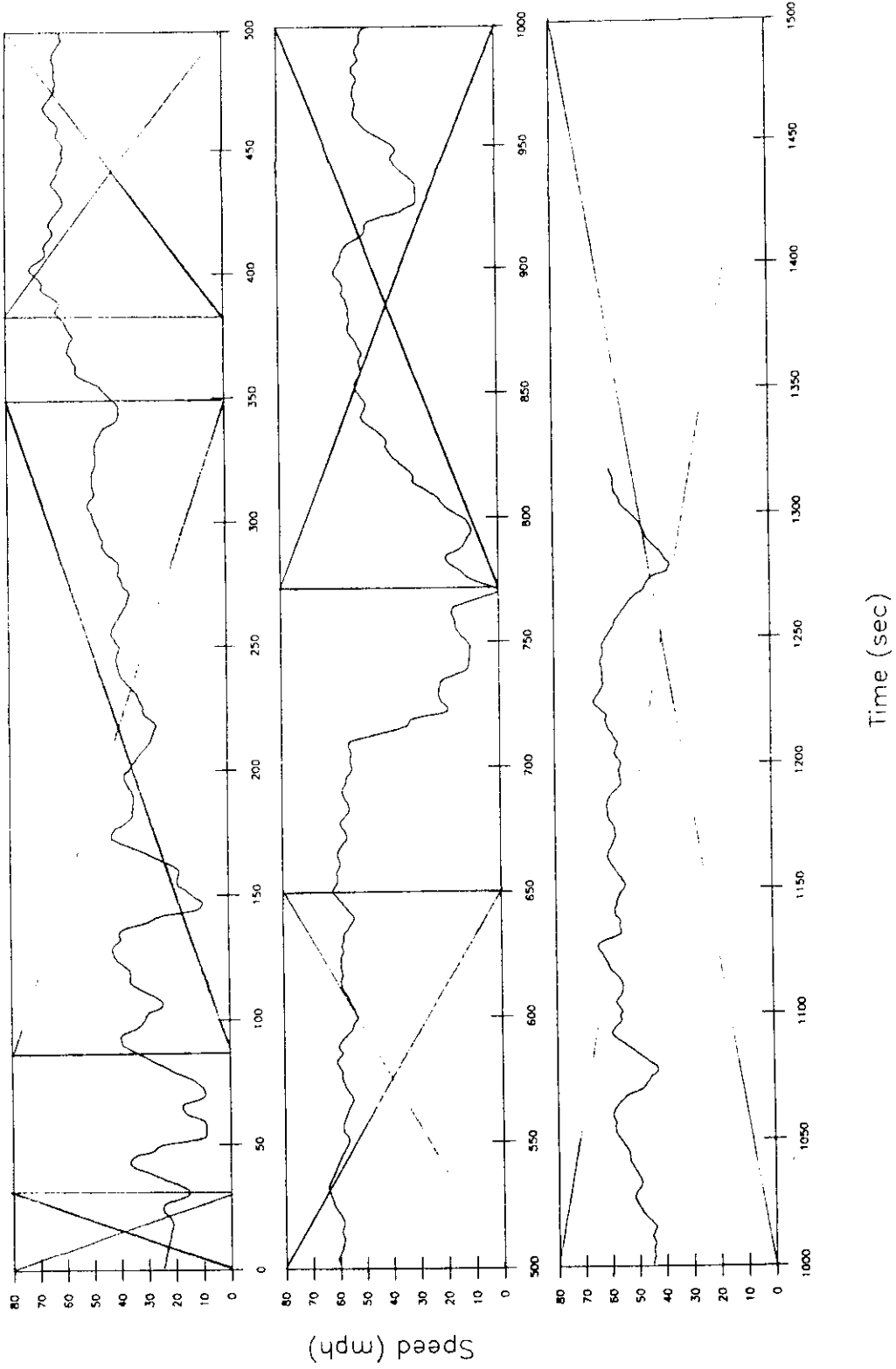


Figure 2.5.1.1d On-road freeway driving pattern used as basis for UCLA Freeway Dynamometer Driving Schedule continued (deleted sections shown marked out).

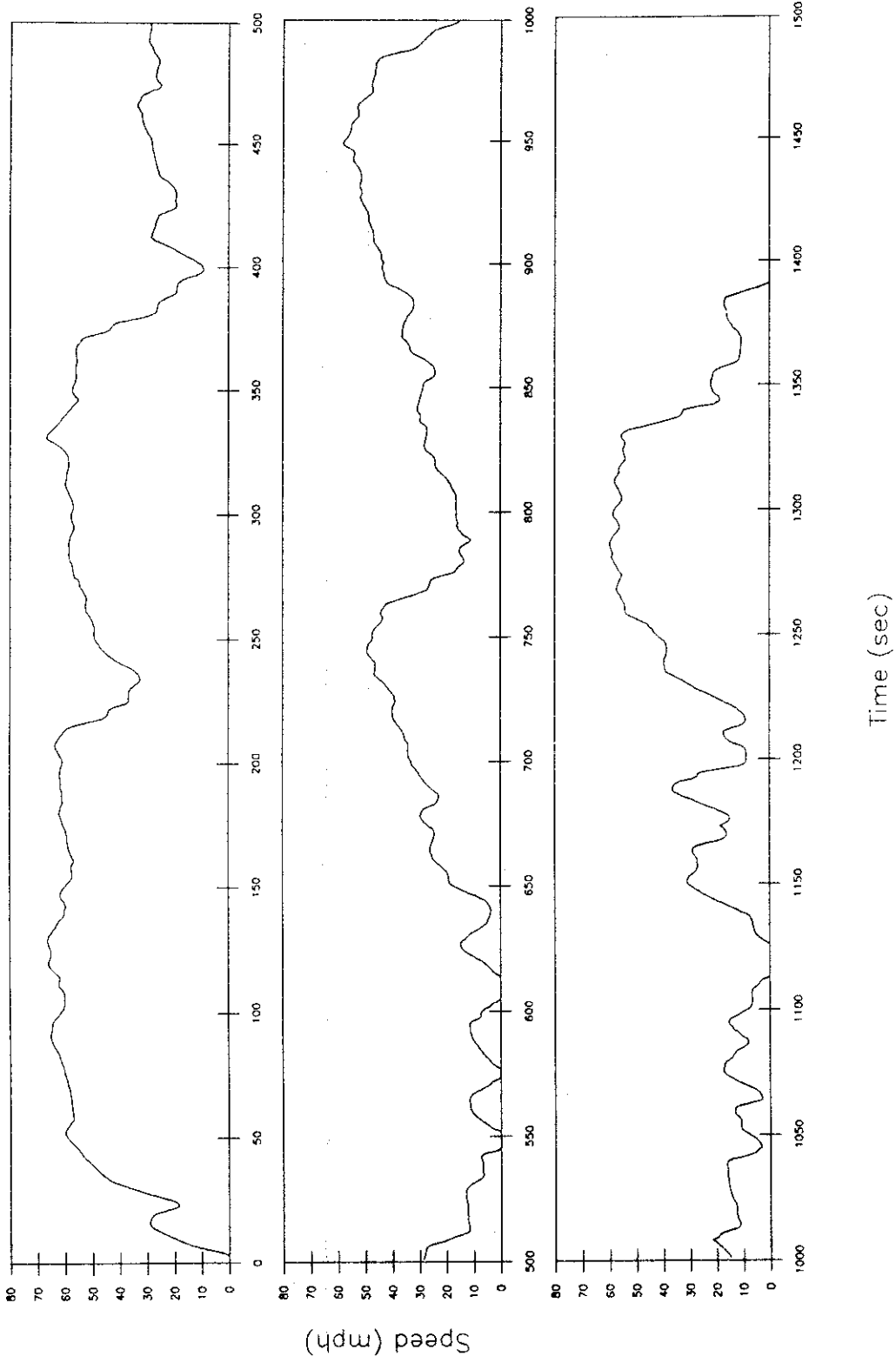


Figure 2.5.1.2 Time versus speed trace of the UCLA Freeway Dynamometer Driving Schedule.

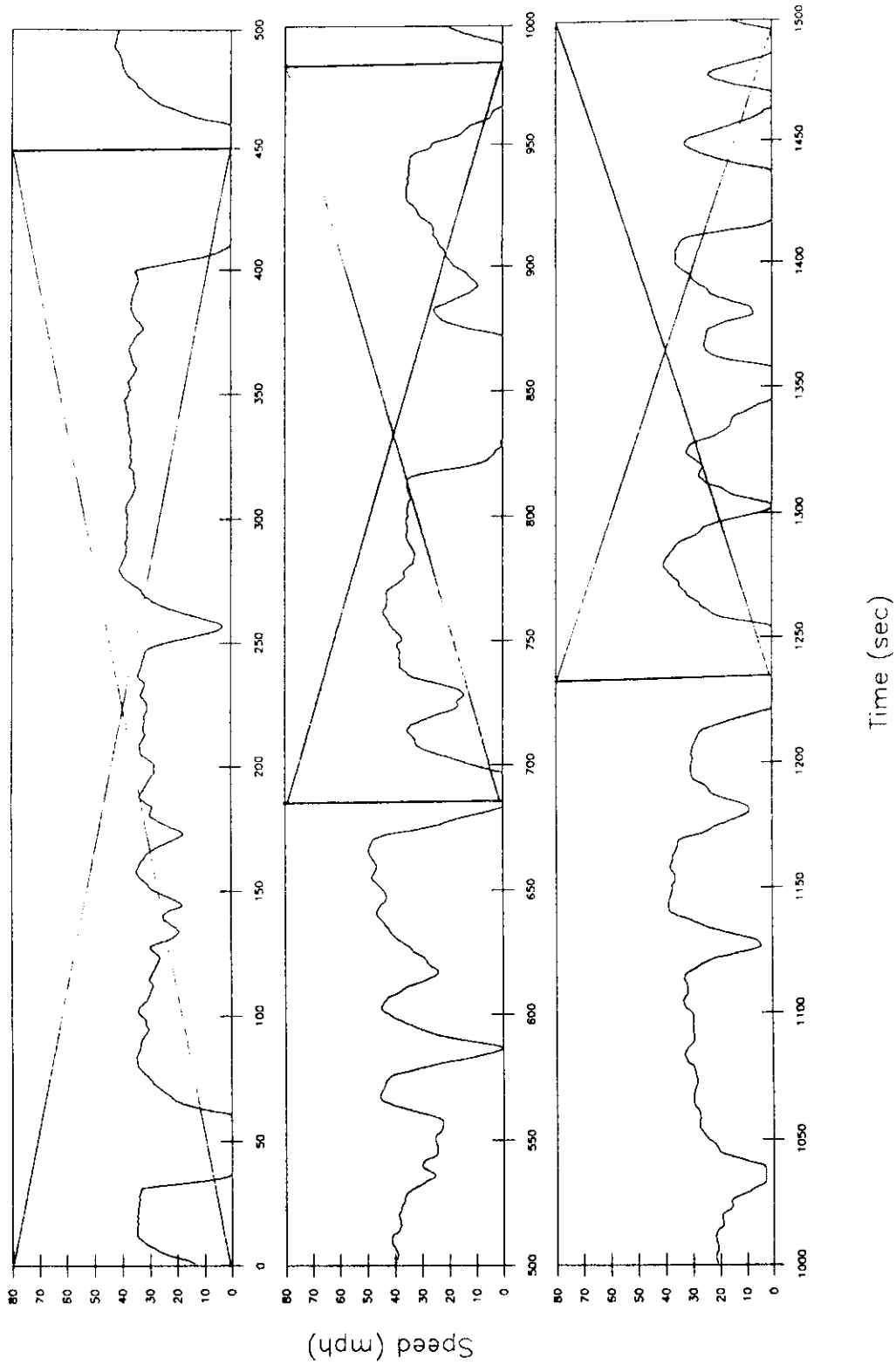


Figure 2.5.1.3a On-road urban driving pattern used as basis for UCLA Urban Dynamometer Driving Schedule continued (deleted sections shown marked out).

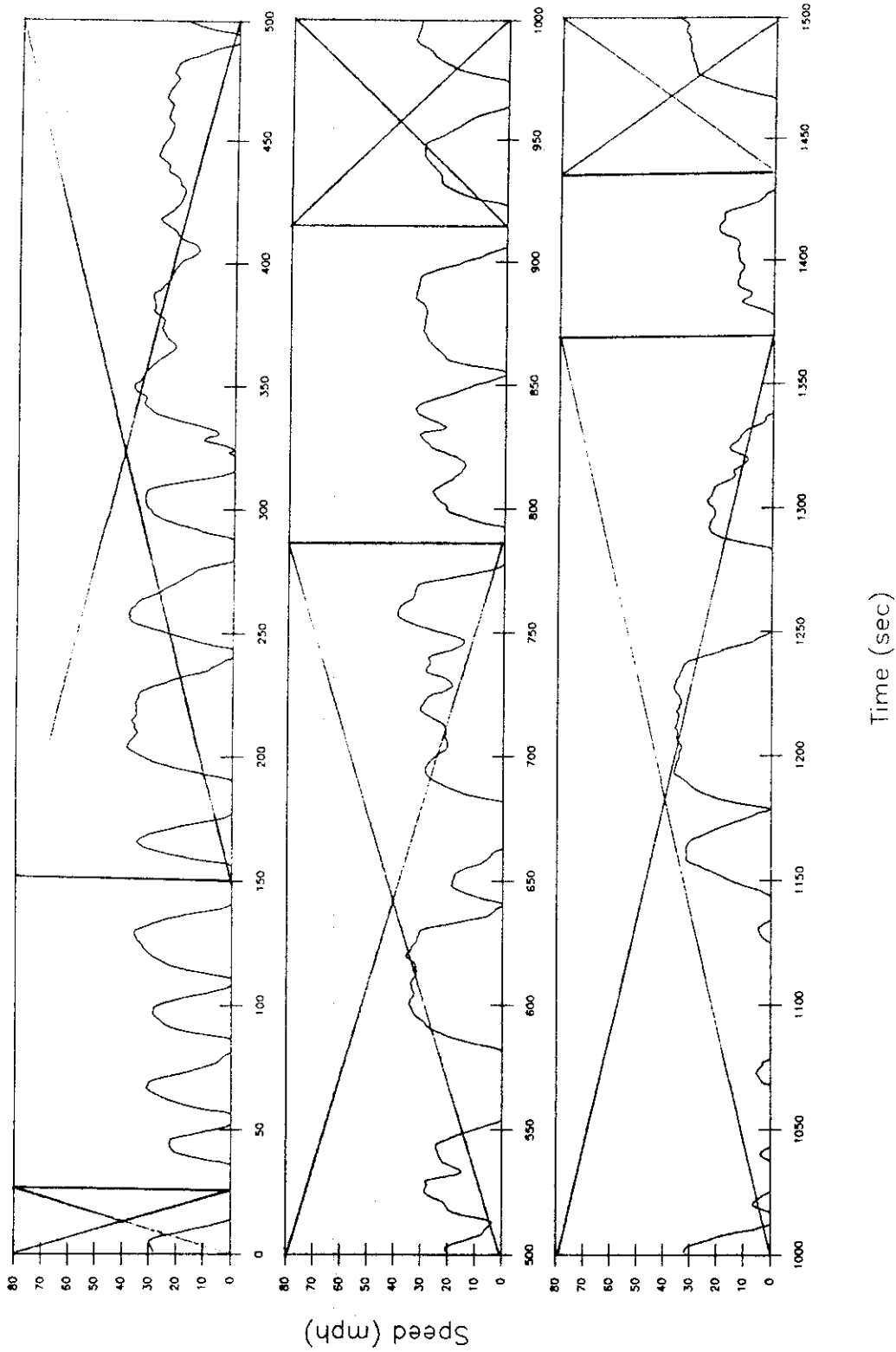


Figure 2.5.1.3b On-road urban driving pattern used as basis for UCLA Urban Dynamometer Driving Schedule continued (deleted sections shown marked out).

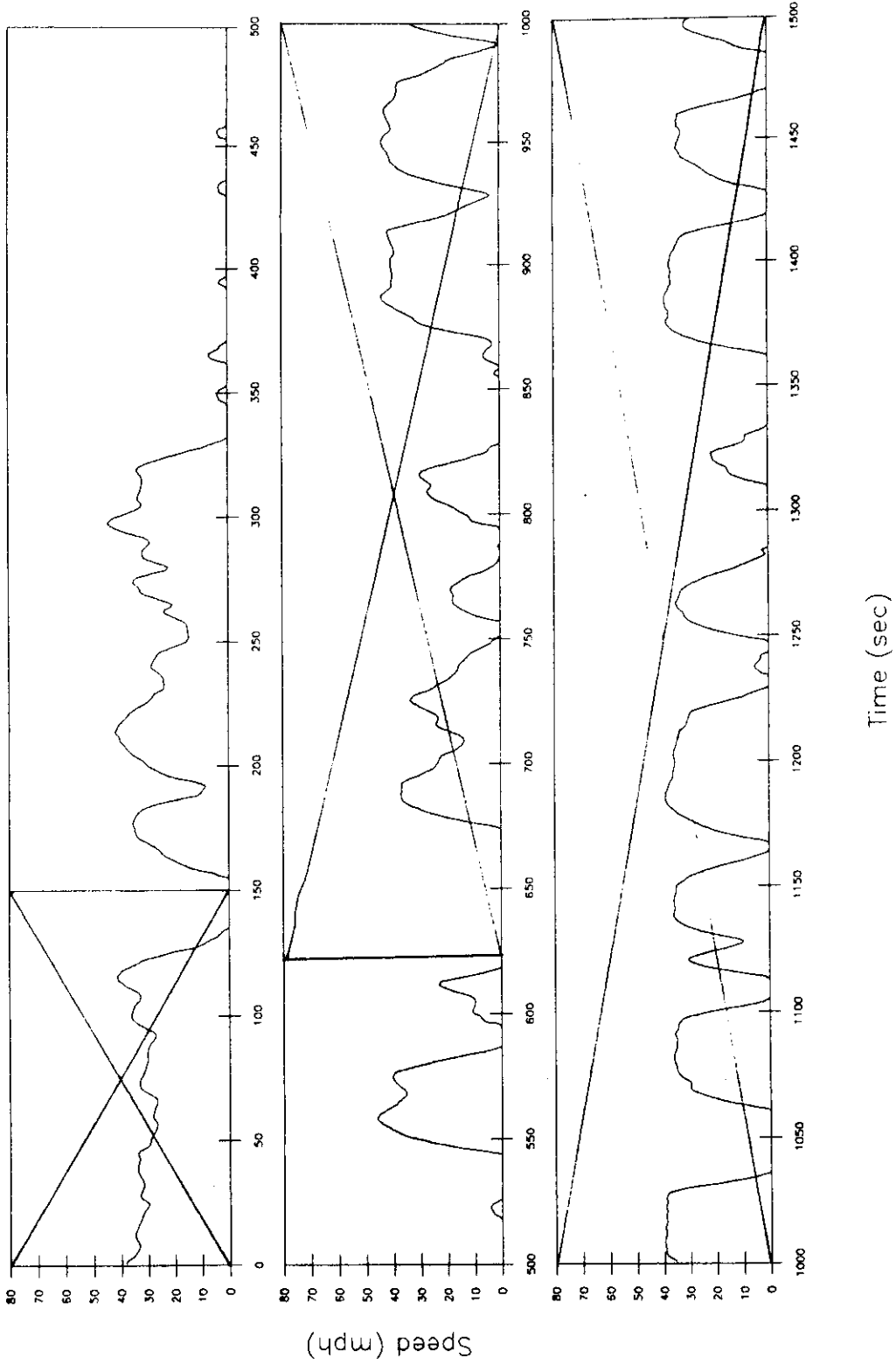


Figure 2.5.1.3c On-road urban driving pattern used as basis for UCLA Urban Dynamometer Driving Schedule continued (deleted sections shown marked out).

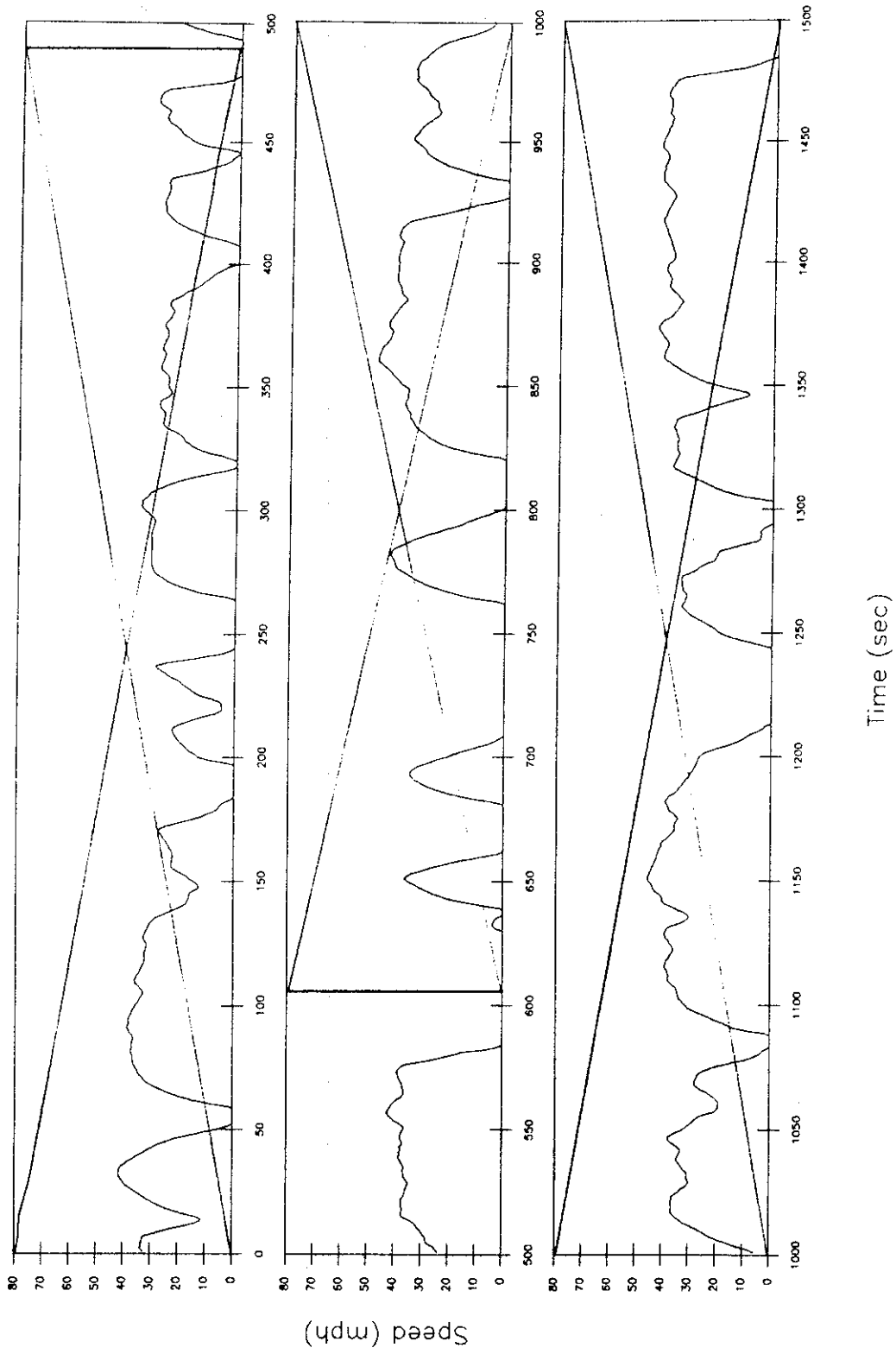


Figure 2.5.1.3d On-road urban driving pattern used as basis for UCLA Urban Dynamometer Driving Schedule continued (deleted sections shown marked out).

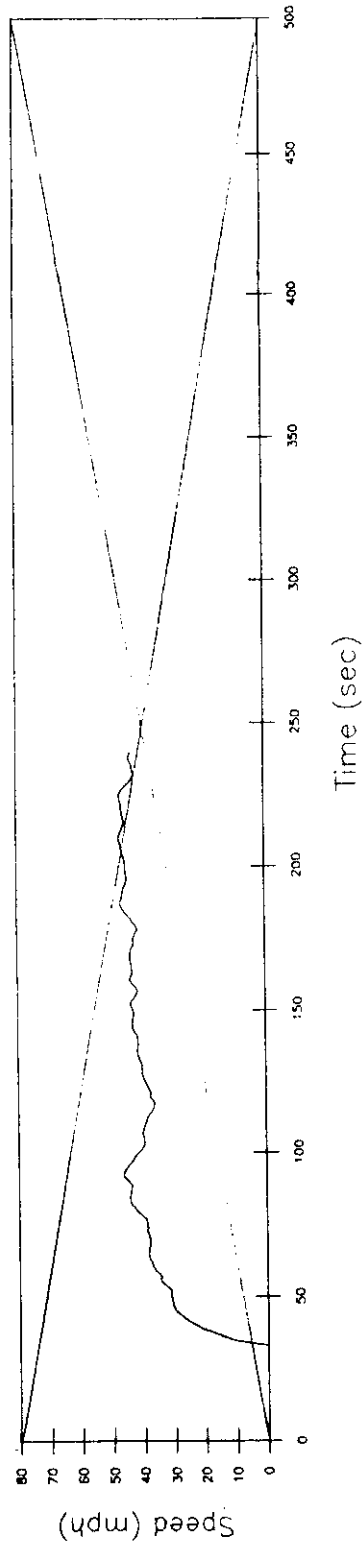


Figure 2.5.1.3e On-road urban driving pattern used as basis for UCLA Urban Dynamometer Driving Schedule continued (deleted sections shown marked out).

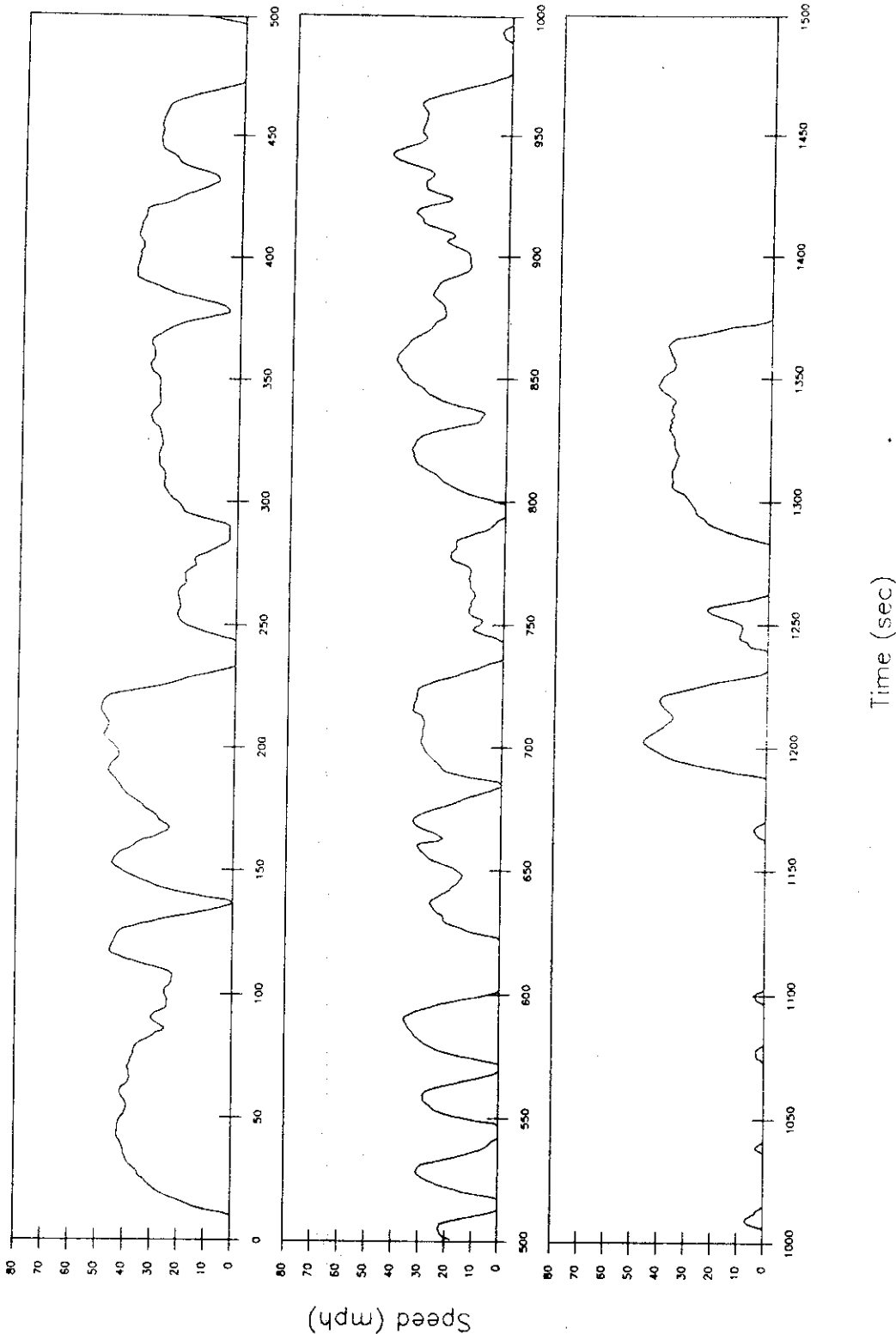


Figure 2.5.1.4 Time versus speed trace of the UCLA Urban Dynamometer Driving Schedule.

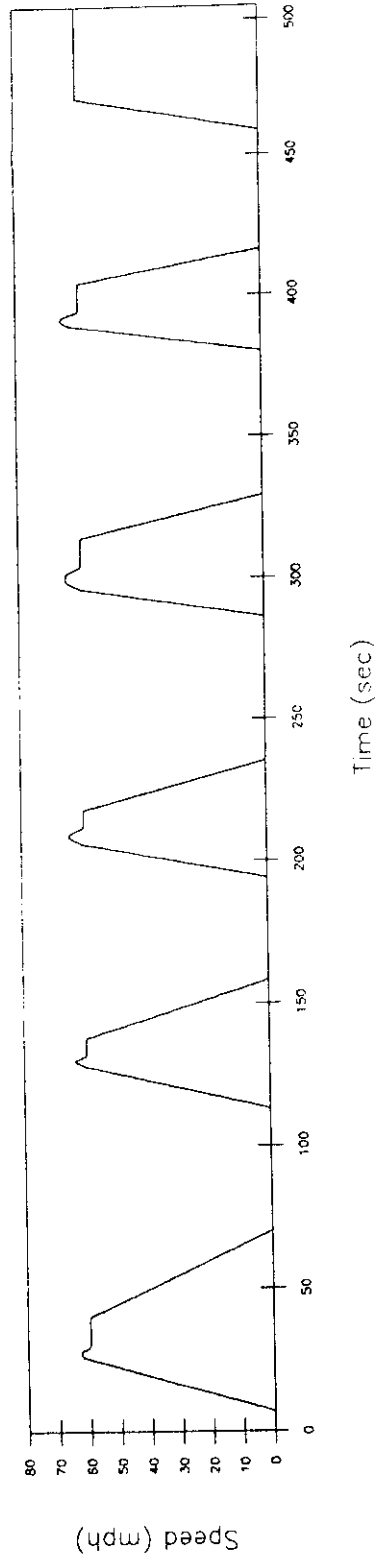
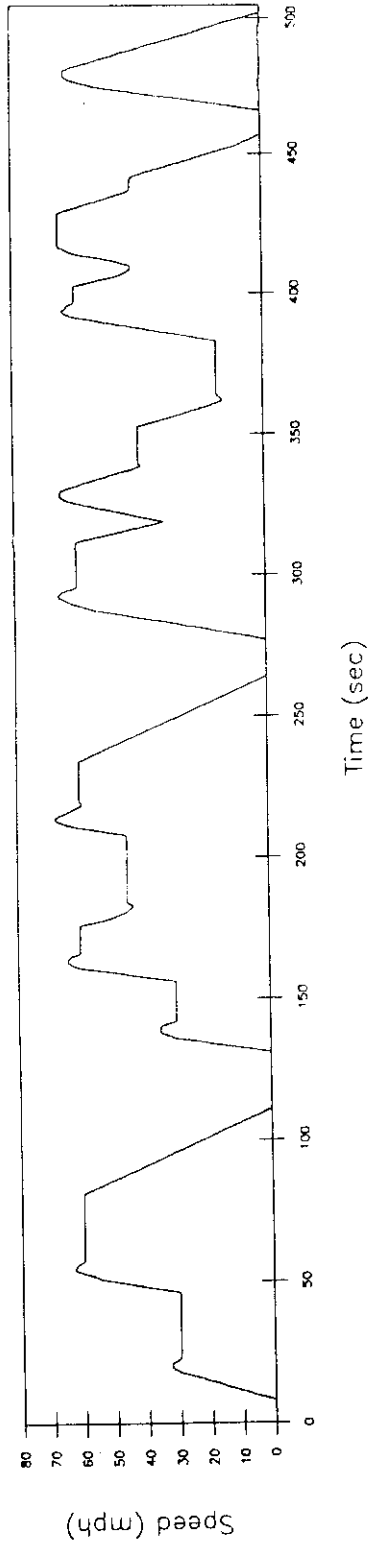


Figure 2.5.1.5 Time versus speed trace of the ARB Acceleration Dynamometer Driving Schedules (Long, 1992a).

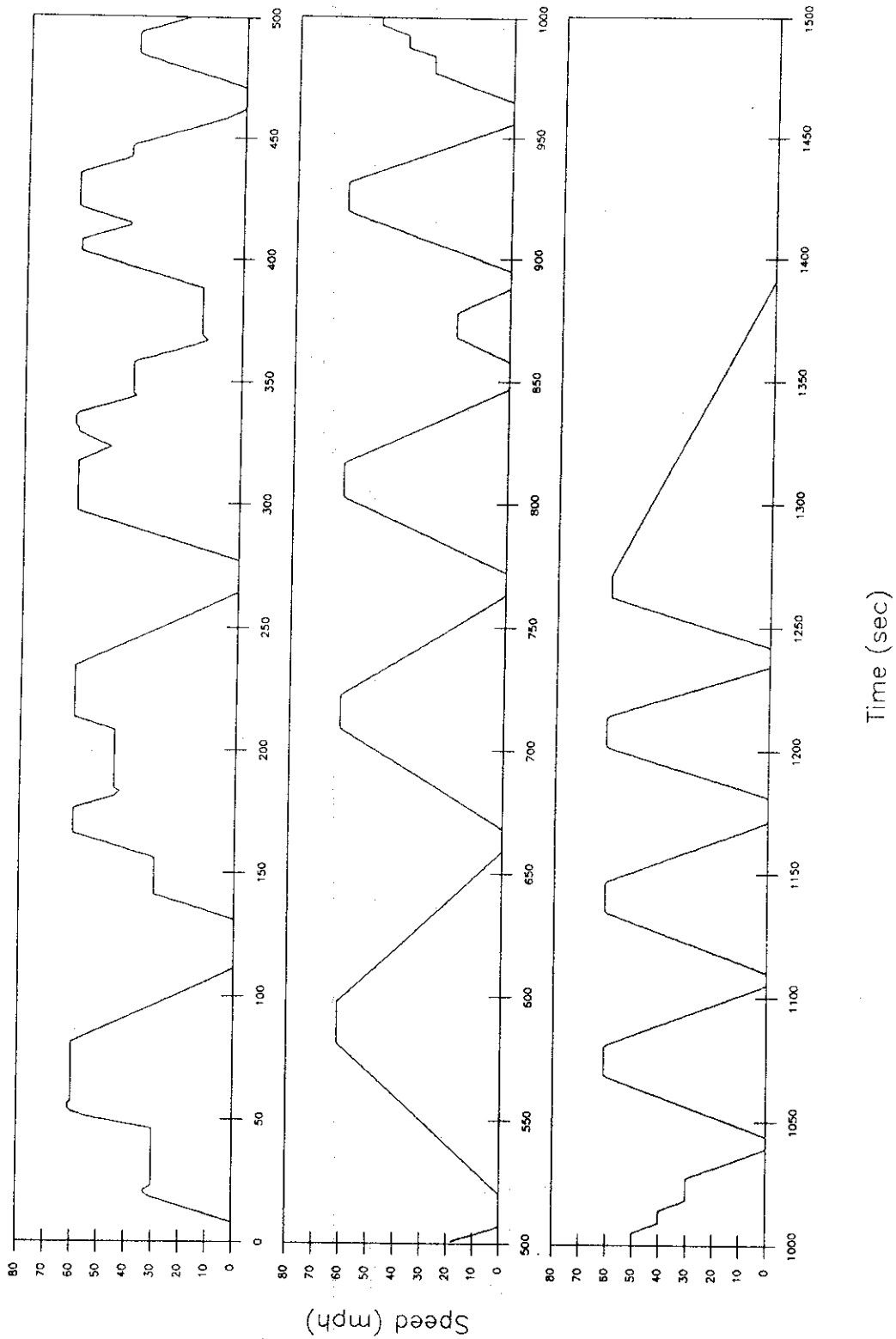


Figure 2.5.1.6 Time versus speed trace of the UCLA Acceleration Dynamometer Driving Schedule.

Laboratories for emissions testing. Emissions tests were conducted with the test vehicle for three FTP experiments driven in the three prescribed phases (cold start, hot running, and warm start) with each complete FTP followed by an HFET, and the UCLA freeway, urban and acceleration cycles each driven in the same three phases and same rest conditions between tests as the FTP. The fuel used for the test was indoline.

The tailpipe emissions were analyzed in three ways: collection of the emissions into 4 bags (by section of the test - cold start, hot running, warm start, and HFET) for later analysis by Horiba instruments for CO, HC, NO_x and CO₂; measurement of the emissions at 1 Hz intervals for the same four components; and measurement of 20 compounds or classes of compounds at 3 second intervals by a Matteson FTIR. The 1 Hz emissions measurements were also conducted for pre-catalyst emissions to determine catalyst efficiency.

The tests were conducted as follows:

1. The vehicle was stored at 75°F for > 12 hours.
2. The electric dynamometer rolls were turned on for 20 minutes to allow them to warm up.
3. The frictional loss of the rolls was calibrated and then the vehicle load was set.
4. FTIR backgrounds were taken and the FTIR was calibrated.
5. The zeros and spans for each scale of the Horiba analyzers were set by the automated Horiba analyzer system.
6. The drive wheels of the vehicle were lifted off of the ground and the vehicle was pushed onto the dynamometer cell and the drive wheels were placed on the rolls.
7. The electric dynamometer was run slightly to center the vehicle.
8. The tire pressure was set to 45 psi (normal is 36 psi).
9. The vehicle was strapped down by the tow hooks.
10. The auxiliary cooling fan was placed in front of the vehicle, the hood was opened and the fan was turned on.
11. The exhaust sampling pipe was attached to the tailpipe and the pre-catalyst sampling pipe was attached.
12. The computer and FTIR were setup to begin the test.
13. The driver got in the vehicle and prepared to begin the test.
14. The driver pressed the start button on the driving trace display and started the engine. Both the Horiba instruments and the FTIR began sampling but recording of the samples began when CO₂ was first detected to synchronize the measurements with the driving schedule.
15. The driving schedule was followed for phases 1 and 2 (cold start and hot running) and then the engine was shut off, the cooling fan in front of the vehicle was

- turned off and the hood was closed.
16. During the 10 minute rest period, the analyzer condensation traps were drained.
 17. At the end of the 10 minute rest period, the driver pressed the start button to begin phase 3 (warm start) and started the engine.
 18. The driving schedule was followed for phase 3 and then after idling for approximately 1 minute, driving of the HFET driving schedule was begun.
 19. At the end of the HFET, the engine was shut off and the vehicle was moved back to the storage area.

Note: For the UCLA driving schedules, the tests were ended after phase 3 and no HFET test was conducted.

2.6 On-Road Emissions Modeling

Presently, modeling of vehicle emissions are performed by models such as EMFAC (ARB) or MOBILE (US EPA) using emissions rate data from FTP experiments. The emissions rates from the three bags of the test are assigned fixed proportions of time (weighted) as shown in Equation 2.6.1 to calculate the weighted vehicle emissions.

$$\frac{(\text{Bag 1} \times 0.43) + \text{Bag 2} + (\text{Bag 3} \times 0.57)}{2.0} \quad \text{Eq. 2.6.1}$$

The weighted emissions rates are then adjusted for variations in speed by speed correction factors. The latest revision of the speed correction factors from the ARB with the data points they were derived from for EMFAC7F are shown in Figures 2.6.1 through 2.6.6 (CARB, 1993b). As can be seen in the figure, the speed correction factors assume there is a direct relationship between speed and emissions.

Vehicle emissions are related to speed because the emissions of the vehicle are a function of the load on the engine which is in part a function of speed. However, speed is not the only factor which contributes to vehicle load. The total load on the vehicle is the sum of the loads induced by driving (friction (L_f) and aerodynamic drag (L_{ad})), acceleration (L_{ac}) and changes in grade (L_g) as shown in Equation 2.6.2:

$$\text{Engine load} = L_f + L_{ad} + L_{ac} + L_g \quad \text{Eq. 2.6.2}$$

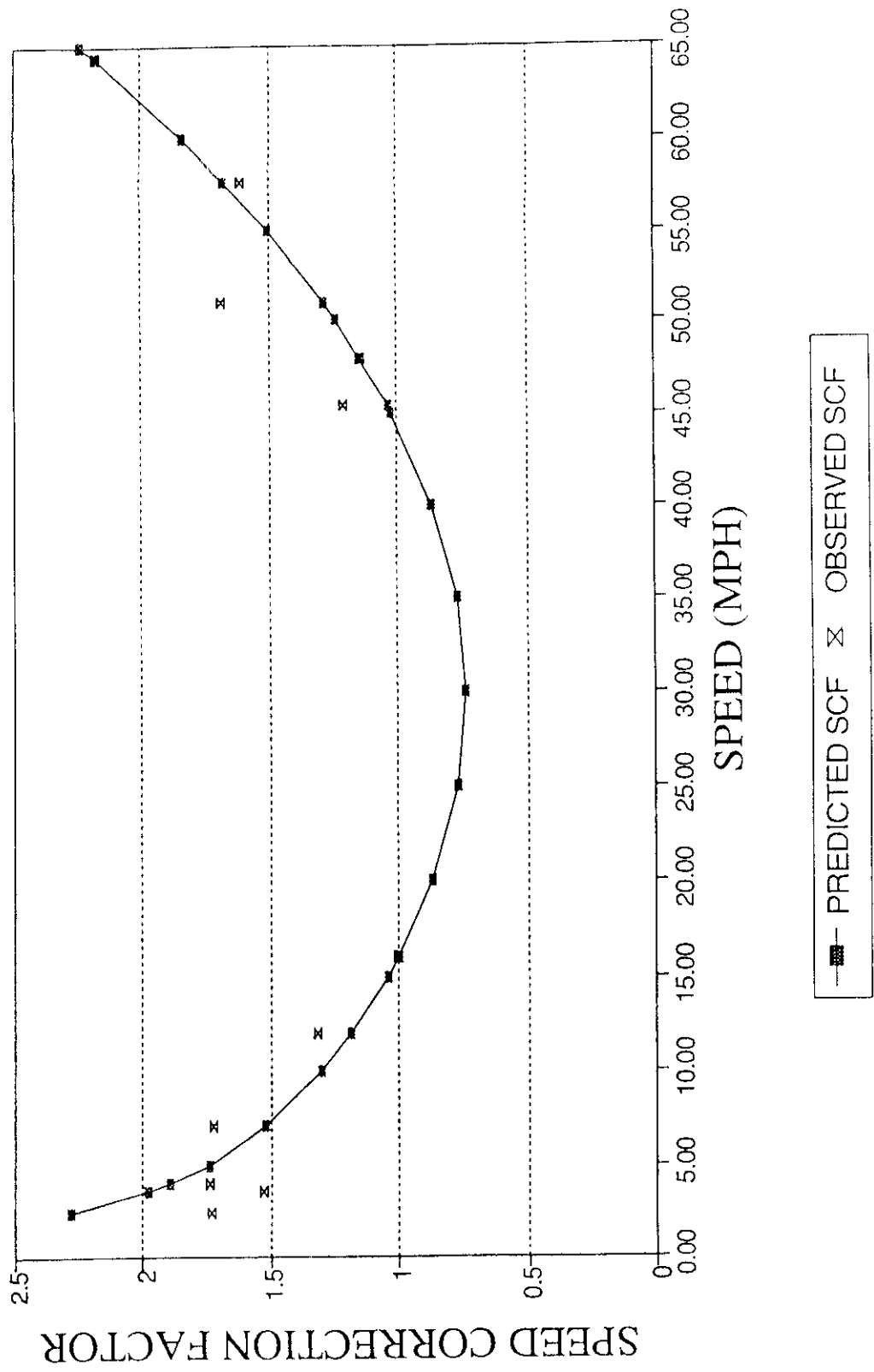


Figure 2.6.1 Predicted versus actual HC speed correction factors for carbureted and throttle-body fuel injected vehicles.

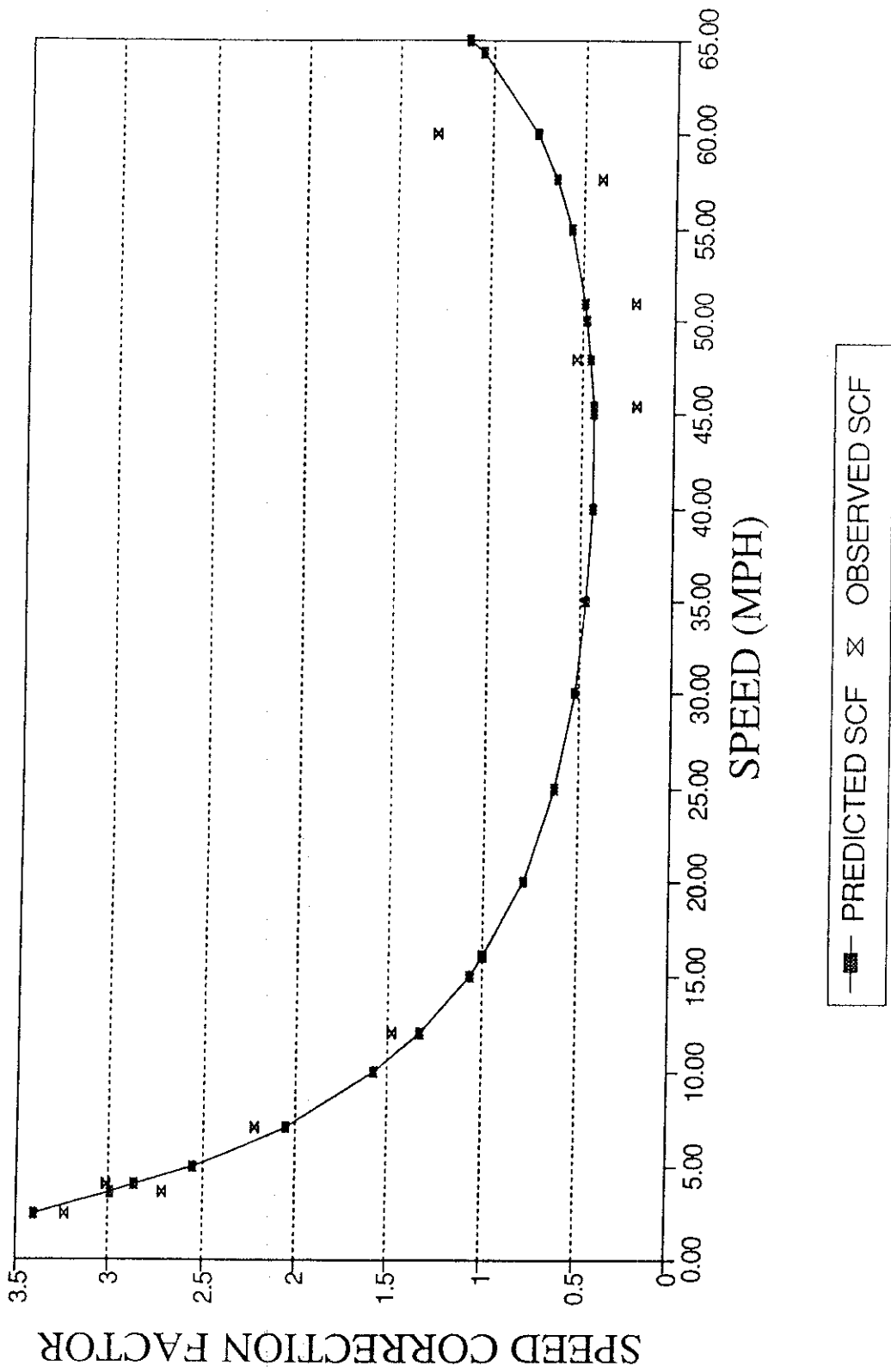


Figure 2.6.2 Predicted versus actual HC speed correction factors for multi-point fuel injected vehicles.

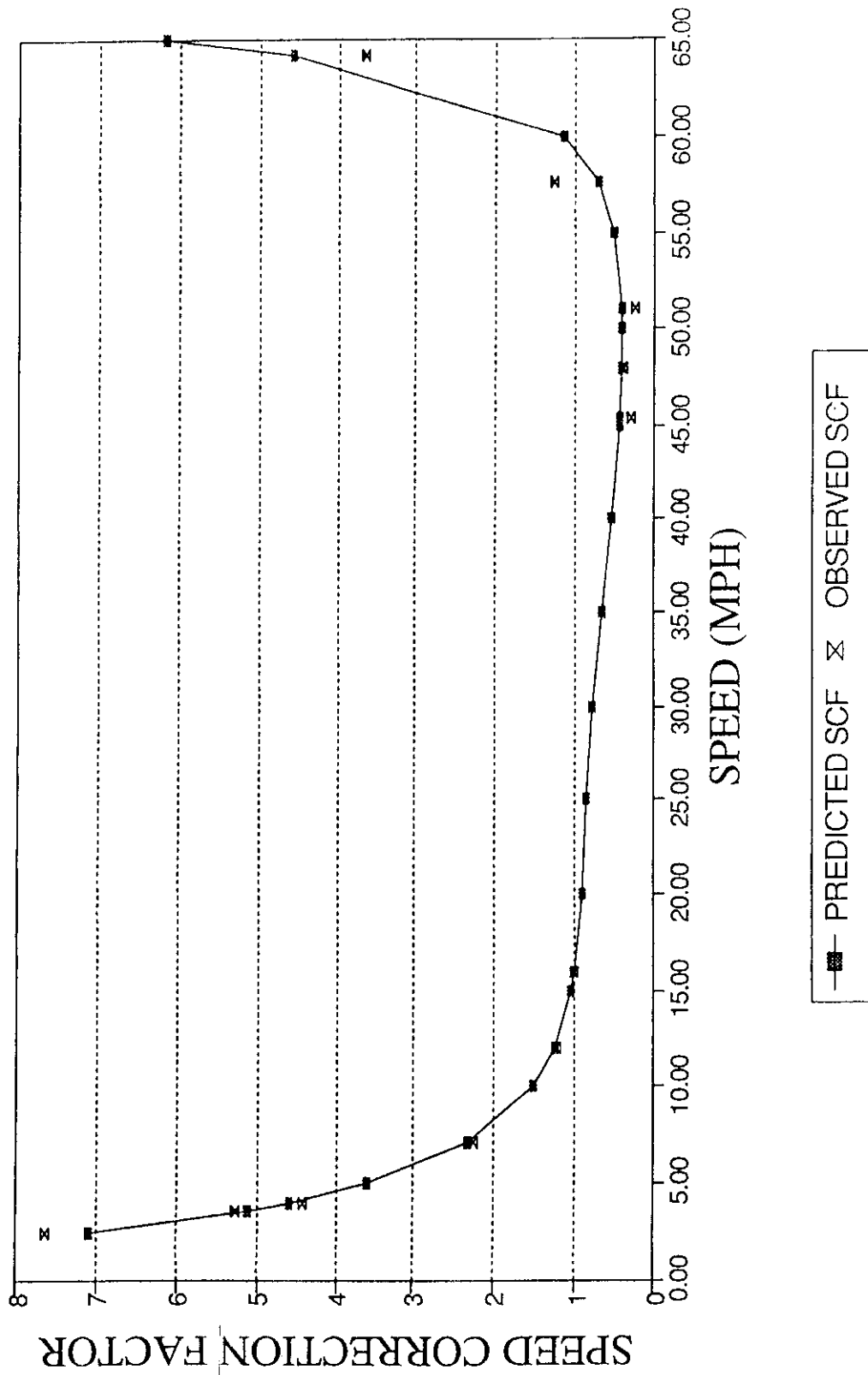


Figure 2.6.3 Predicted versus actual CO speed correction factors for carbureted and throttle-body fuel injected vehicles.

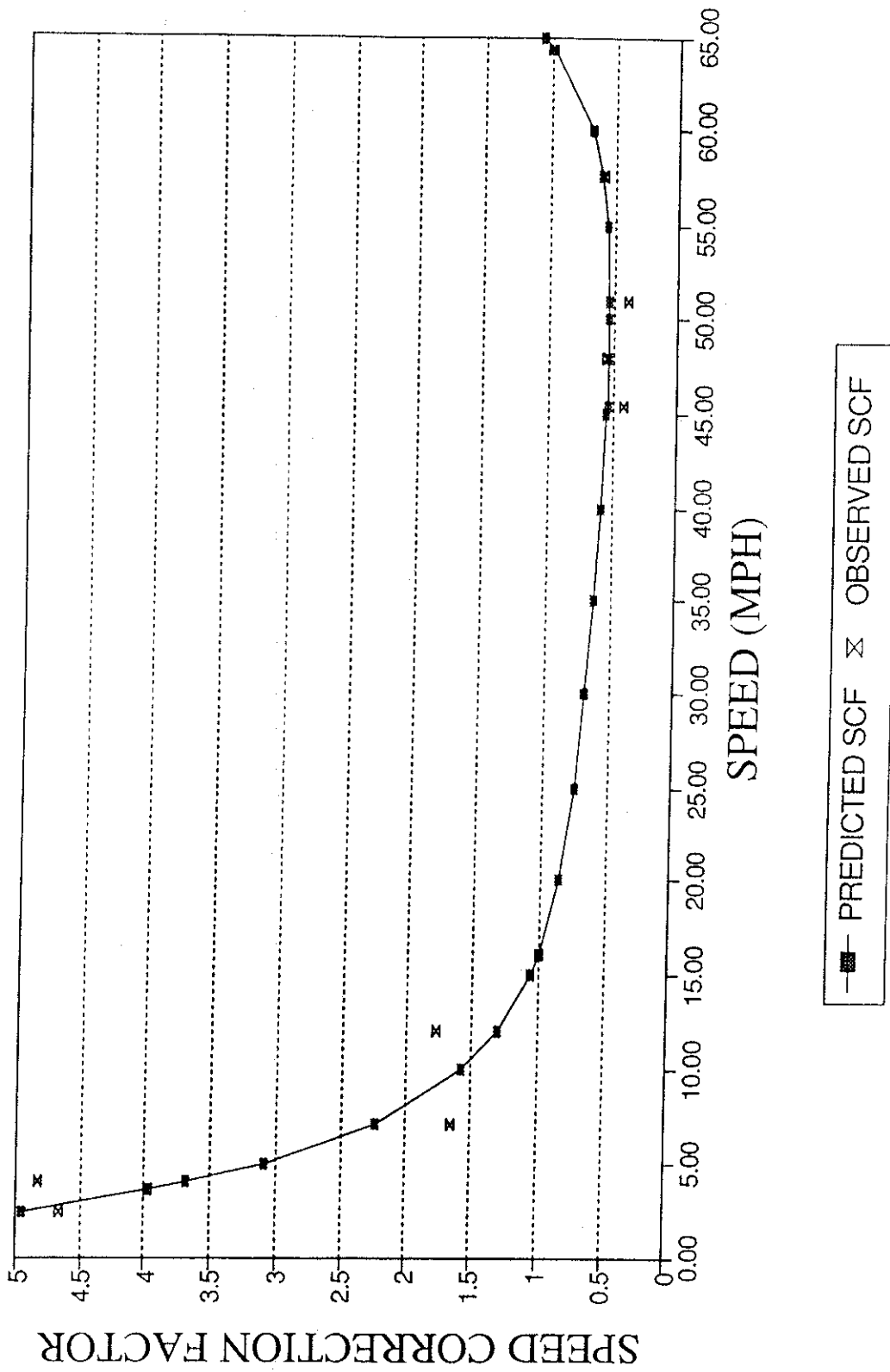


Figure 2.6.4 Predicted versus actual CO speed correction factors for multi-point fuel injected vehicles.

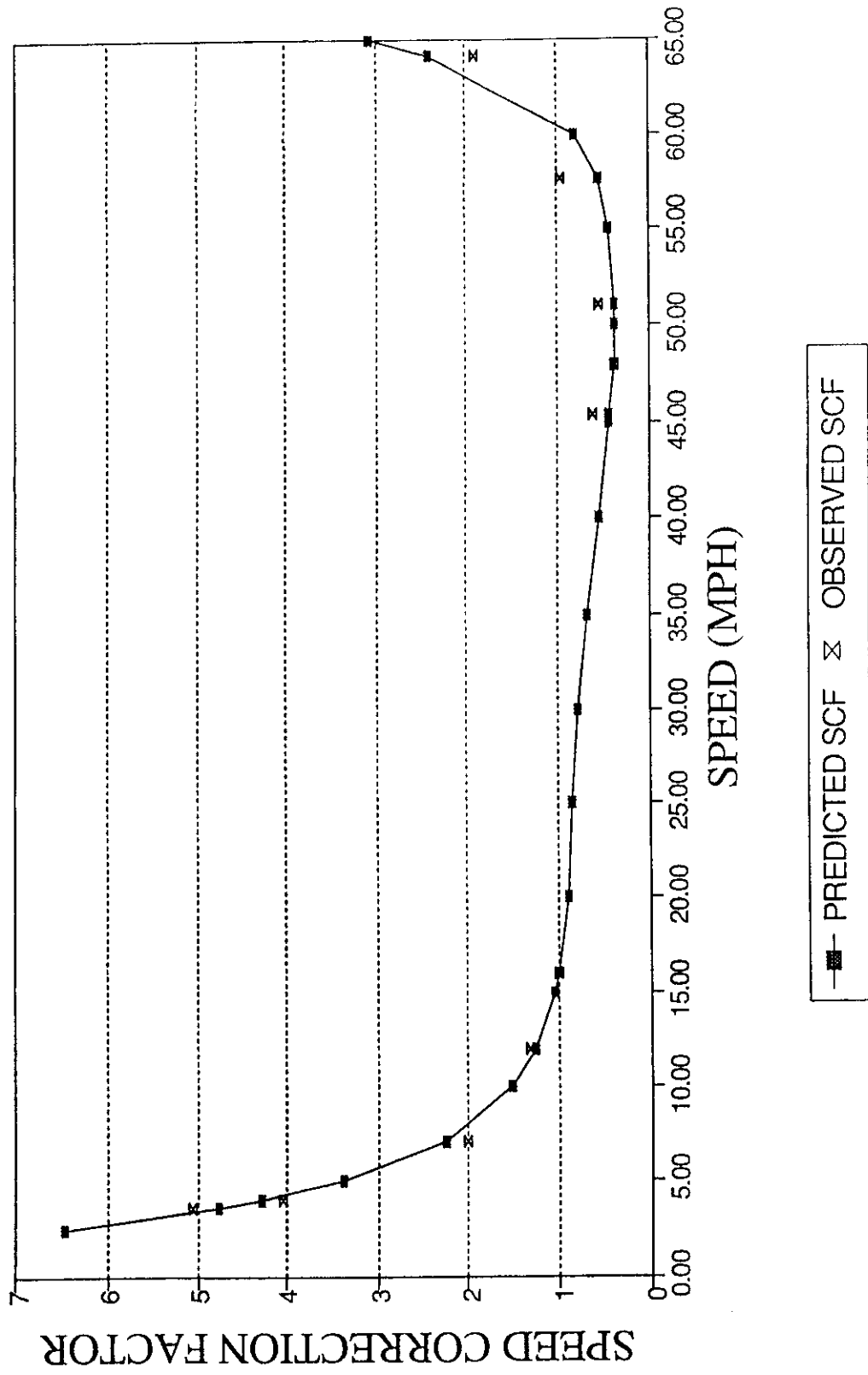


Figure 2.6.5 Predicted versus actual NO_x speed correction factors for carbureted and throttle-body fuel injected vehicles.

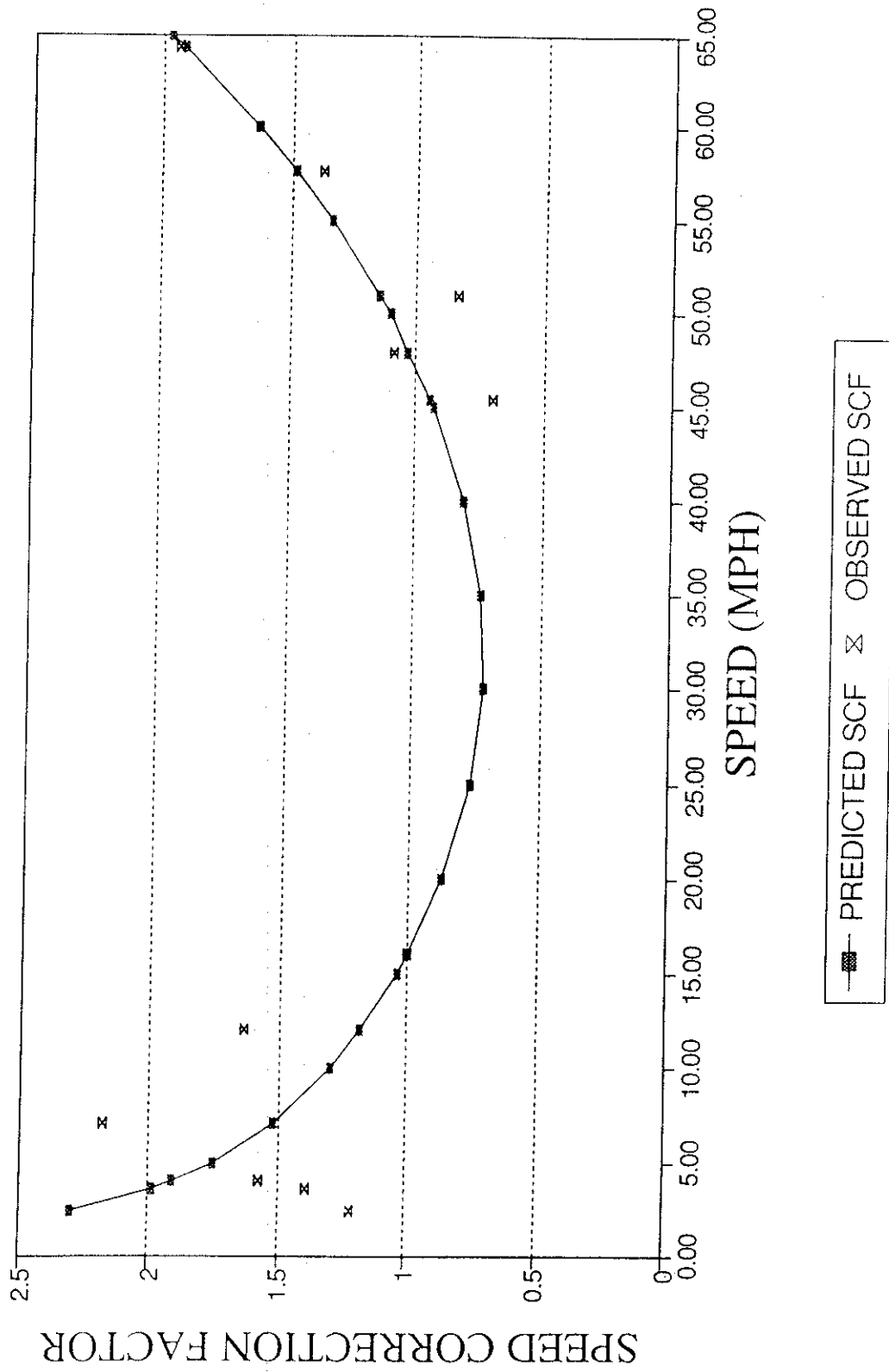


Figure 2.6.6 Predicted versus actual NO_x speed correction factors for multi-point fuel injected vehicles.

Loads from friction and acceleration are functions of speed and are accounted for during the test by adding a mechanical load to the rolls during the FTP test equal to the load of the vehicle. Loads from acceleration are included but only to accelerations or decelerations of 3.3 mph s^{-1} and are smaller at speeds above approximately 30 mph. Loads from grades are not included in the FTP, but modern dynamometers have the capability of simulating varying loads corresponding to the grades. Exclusion of higher rates of acceleration (above 3.3 mph s^{-1}) and grades from the FTP and, in turn, the calculation of vehicle emissions factors for use in modeling the mobile source emissions may be leading to errors in the on-road vehicle exhaust emissions estimates calculated by these models.

As mentioned earlier, efforts by the regulatory agencies to develop a test pattern which is "more representative" of current on-road driving conditions continues, with the goal of increasing the representativeness of the emissions estimates from certification tests. However, a single pattern of reasonable length cannot represent all of the driving conditions observed on-road and will only be an interim solution. The ARB's plans in the long term, (2 to 7 years), to develop a new emissions test and modeling methodology which will be based on modal emissions (Effa, 1992). This change to a modal emissions model will overcome the present limitation of reliance on a single, fixed test pattern to predict the emissions from the entire fleet. This type of model will allow for the modeling of any driving pattern for which vehicle dynamics data can be obtained (either through on-road data collection or from transportation models). A transportation model of this type (which predicts vehicle dynamics and driving pattern data) is presently being developed by Barth and co-workers at UCR (Barth et al., 1993). Because this model not only predicts driving patterns, but where they occur, it would allow flexibility in studying the effects of transportation control measures on the spatial distribution of vehicle exhaust emissions.

In the present study, modeling programs were developed which model vehicle emissions as a function of mode of operation. The first version of the model uses acceleration and speed based modes to estimate emissions, the UCLA Acceleration- and

Speed-Based Vehicle Emission (ASBVE) Model (development and definition of the specific modes are described in the results section). There is a significant limitation to modeling the vehicle's emissions as a function of these modes because the emissions measurements obtained from the dynamometer do not include the effects of load such as those caused by grades and load added to the vehicle. For this reason, the second version of the model estimates emissions based on the load on the engine calculated by the EEC and the vehicle speed, the UCLA Load- and Speed-Based Vehicle Emission (LSBVE) Model.

To model on-road vehicle emissions with either type of modes, three programs were necessary. The first program reads in emissions data collected on a dynamometer (described in the next section) and "bins" the emissions by mode. (An example of a mode bin would be acceleration between 0 and 3 mph s^{-1} and speed between 0 and 15 mph). Each mode based bin contains the average emission rate of HC, CO and NO_x for the vehicle while operating in the specific mode. The second program averages the emissions data from each of the individual dynamometer emissions experiments into a single summary file weighted by the number of measurements in each bin for each test. The last program reads in on-road data and the "binned" emissions data generated by the first program and estimates the on-road emissions from the given on-road data. A flow chart for the three models required to conduct the modeling (the binning program, the averaging program, and the emissions estimating program) are shown in Figure 2.6.7.

The relative accuracy of the models was evaluated by modeling the emissions from the driving schedules driven on a dynamometer and comparing the calculated emissions to the measured emissions. After testing, the models were used to estimate the emissions from the test vehicle for all of the on-road routes. The estimated emissions rates from the on-road routes were compared to the emissions rates obtained from the FTP and the UCLA driving schedules to determine their relative representativeness of on-road emissions rates.

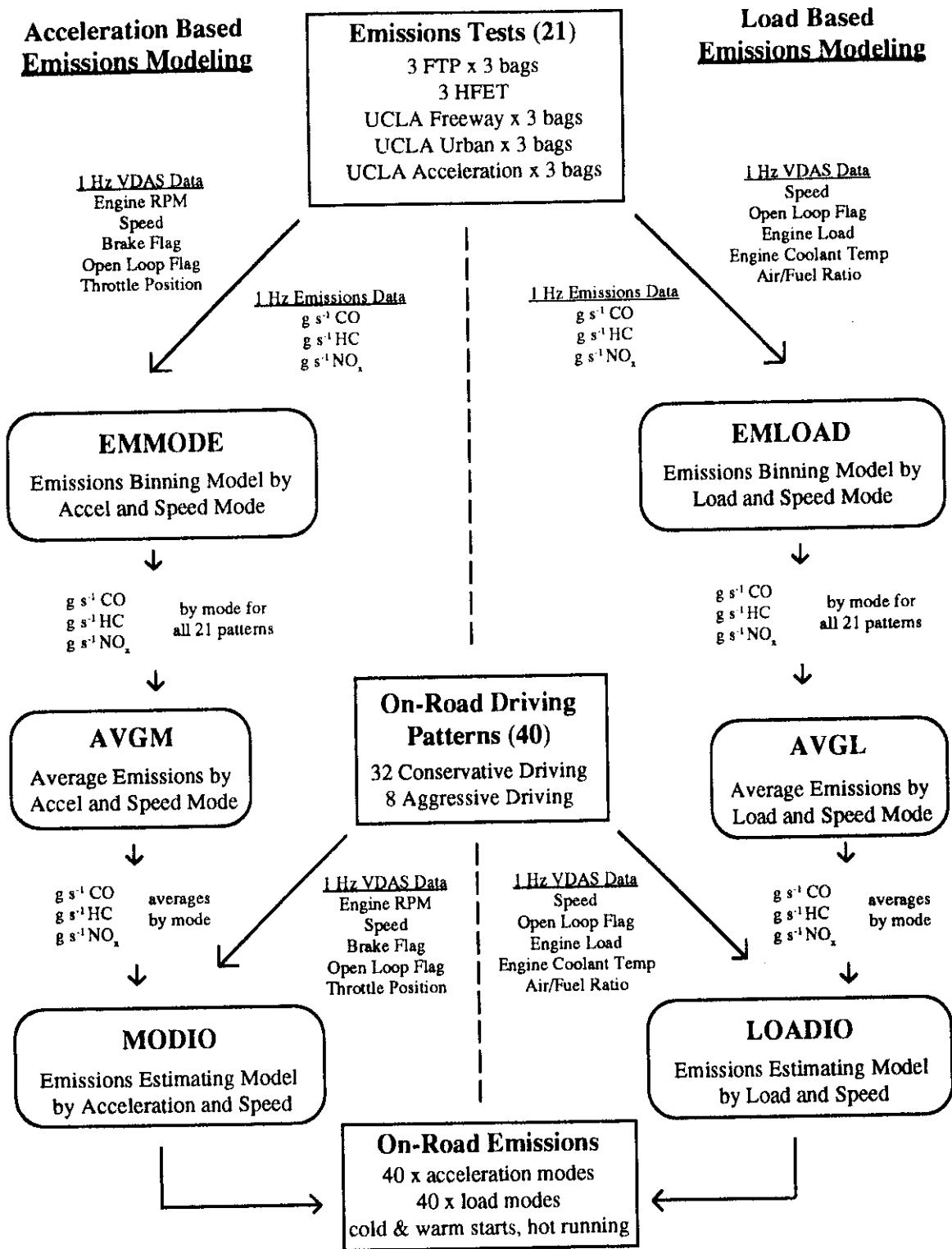


Figure 2.6.7 Flow diagram of the emissions modeling process.

2.6.1 Development of Emissions Binning Models

The source code for the ASBVE binning model (EMMODE.FOR) is listed in Appendix A.2.1. The source code for the LSBVE binning model (EMLOAD.FOR) is listed in Appendix A.2.4. The bin definitions for both of the mode types are listed in Table 2.6.1.1. There are acceleration and load bins which are not truly modes (eg. start and open loop operation), but are important modes relative to emissions.

Emissions from each of the dynamometer emissions tests (a total of 21 individual tests) conducted at FMCSRL on the vehicle were analyzed to determine emissions as a function of mode and the frequency of each mode for both acceleration and load based modes for HC, CO and NO_x. The modal emissions from each of the 21 dynamometer tests were weighted by their frequency of occurrence and averaged by acceleration or load "bins" (eg. cruise between 20 and 30 mph) using the programs AVGM.FOR and AVGL.FOR to obtain a modal emissions "inventory" for estimating the on-road emissions (the source codes for these programs are given in Appendices A.2.2 and A.2.5). The output sheets of emissions for each of the three pollutants for the ASBVE model are shown in Figure 2.6.1.1 and for the LSBVE are shown in Figure 2.6.1.2. Emissions were estimated for bins in which no emissions data were collected by fitting curves to the emissions data from the same acceleration or load bins at other speed bins and are shown in bold in the emissions results.

2.6.2 Development of Emissions Estimating Models.

The formulation of the model emissions estimation model is given in Equation 2.6.2.1.

$$\text{Vehicle Emissions (g mi}^{-1}\text{)} = \frac{\sum_t E_{m,v}}{\sum_t (vs \div 3600)} \quad \text{Eq. 2.6.2.1}$$

WHERE:

- t = One second time interval of measurements
- m = acceleration or load based mode
- v = vehicle speed (mph)
- E = emissions rate (g s⁻¹) for mode "m" and "v"

Table 2.6.1.1 Acceleration and load based modes.

"Acceleration" Bins	"Load" Bins	Speed Bins
Stopped	Cold Start	$0 \leq v_s < 10$ mph
Start	Hot Start	$10 \leq v_s < 20$ mph
Coast	Rich Open Loop	$20 \leq v_s < 30$ mph
Cruise	Lean Open Loop	$30 \leq v_s < 40$ mph
Light Acceleration	High Load	$40 \leq v_s < 50$ mph
Medium Acceleration	Medium Load	$50 \leq v_s < 60$ mph
Hard Acceleration	Low Load	$60 \leq v_s < 70$ mph
Light Deceleration		$v_s \leq 70$ mph
Medium Deceleration		
Hard Deceleration		

The model estimates the emissions of HC, CO and NO_x for a set of VDAS data using the binned emissions data described in Section 2.6.1 which is generated from the program EMMODE.FOR or EMLOAD.FOR. The emissions rates in grams per second are converted in the model to grams per mile at the end of the modeling to grams per mile by dividing the total grams emitted by the distance traveled. The distance traveled is calculated from the sum of distances calculated from the instantaneous velocities. The source code for the ASBVE and LSBVE emissions estimating programs (MODEIO.FOR and LOADIO.FOR) are listed in Appendices A.2.3 and A.2.6.

2.6.3 Validation of the Models

The accuracy of the models to predict emissions was determined by modeling the emissions from each set of dynamometer emissions test pattern VDAS data. The emissions from a total of 21 patterns were modeled. These included 3 FTP experiments with 3 bags each, three UCLA patterns (freeway, urban and acceleration) with 3 bags each and three HFET experiments.

Emissions results from the bags which were collected were compared to the results from the 1 Hz emissions data which comprised each bag and differences between the

AVG MASS EMISSIONS BY SPEED AND ACCEL CALCULATIONS

Emissions data files list: FILES.MBF
 Emissions output data file: MODEAVG.MBN

HC Mass Emissions by Mode (g/sec):

Mode	0-10	10-20	20-30	30-40	40-50	50-60	60-70	70+
Stopped	.0009							
Start	.0112	.0364	.0627	.0696	.0660	.0682	.0666	.0666
Coast	.0003	.0004	.0002	.0008	.0001	.0008	.0008	.0008
Cruise	.0004	.0004	.0007	.0007	.0005	.0010	.0020	.0030
Light Accel	.0007	.0012	.0013	.0013	.0011	.0030	.0052	.0077
Med Accel	.0009	.0018	.0047	.0075	.0103	.0131	.0159	.0187
Hard Accel	.0373	.0373	.0373	.0373	.0373	.0373	.0373	.0373
Light Decel	.0004	.0009	.0011	.0006	.0005	.0019	.0046	.0074
Med Decel	.0003	.0007	.0005	.0005	.0005	.0007	.0009	.0011
Hard Decel	.0003	.0005	.0007	.0009	.0011	.0013	.0015	.0017

CO Mass Emissions by Mode (g/sec):

Mode	0-10	10-20	20-30	30-40	40-50	50-60	60-70	70+
Stopped	.0029							
Start	.0619	.3334	.3521	.0968	.1872	.1120	.1800	.1800
Coast	.0016	.0037	.0017	.0036	.0001	.0037	.0037	.0037
Cruise	.0029	.0052	.0043	.0036	.0029	.0184	.0538	.0892
Light Accel	.0041	.0128	.0097	.0093	.0166	.2038	.2343	.2648
Med Accel	.0043	.0152	.0465	.0676	.0887	.1098	.1309	.1520
Hard Accel	3.1670							
Light Decel	.0061	.0030	.0057	.0041	.0054	.1293	.1282	.1293
Med Decel	.0028	.0074	.0058	.0037	.0037	.0098	.0159	.0220
Hard Decel	.0020	.0029	.0038	.0047	.0056	.0065	.0074	.0083

NOx Mass Emissions by Mode (g/sec):

Mode	0-10	10-20	20-30	30-40	40-50	50-60	60-70	70+
Stopped	.0002							
Start	.0005	.0035	.0057	.0045	.0020	.0018	.0057	.0057
Coast	.0000	.0000	.0002	.0000	.0001	.0002	.0002	.0002
Cruise	.0001	.0001	.0005	.0015	.0020	.0048	.0073	.0098
Light Accel	.0002	.0007	.0015	.0037	.0056	.0129	.0157	.0185
Med Accel	.0007	.0041	.0297	.0442	.0587	.0732	.0877	.1022
Hard Accel	.1059	.1059	.1059	.1059	.1059	.1059	.1059	.1059
Light Decel	.0001	.0002	.0005	.0007	.0016	.0056	.0017	.0056
Med Decel	.0000	.0001	.0003	.0004	.0005	.0012	.0019	.0026
Hard Decel	.0000	.0000	.0001	.0001	.0002	.0002	.0002	.0003

BOLD = Estimated emissions.

Figure 2.6.1.1 ASBVE model binned emissions for CO, HC and NO_x.

AVG MASS EMISSIONS BY SPEED AND LOAD CALCULATIONS

Emissions data files list: FILES.LBF
 Emissions output data file: LOADAVG.LBN

HC Mass Emissions by Load (g/sec):

Load	0-10	10-20	20-30	30-40	40-50	50-60	60-70	70+
Cold Start :	.0136	.0393	.0667	.0696	.0660	.0682	.0666	.0666
Hot Start :	.0017	.0133	.0213	.0346	.0346	.0346	.0346	.0346
Rich OL :	.0373							
Lean OL :	.0007	.0007	.0007	.0007	.0006	.0007	.0008	.0009
High Load :	.0326	.0207	.0088	.0036	.0029	.0055	.0081	.0107
Medium Load:	.0016	.0018	.0019	.0014	.0011	.0035	.0042	.0057
Low Load :	.0007	.0006	.0007	.0006	.0005	.0008	.0026	.0044

CO Mass Emissions by Load (g/sec):

Load	0-10	10-20	20-30	30-40	40-50	50-60	60-70	70+
Cold Start :	.0729	.3465	.3279	.0968	.1872	.1120	.1800	.1800
Hot Start :	.0189	.2290	.5986	.5986	.5986	.5986	.5986	.5986
Rich OL :	3.1670							
Lean OL :	.0057	.0057	.0057	.0057	.0035	.0057	.0079	.0101
High Load :	.2262	.1393	.0524	.0312	.0747	.4974	.9201	1.3428
Medium Load:	.0060	.0180	.0153	.0107	.0095	.1785	.1748	.1785
Low Load :	.0030	.0073	.0052	.0035	.0032	.0238	.0755	.1272

NOx Mass Emissions by Load (g/sec):

Load	0-10	10-20	20-30	30-40	40-50	50-60	60-70	70+
Cold Start :	.0006	.0039	.0062	.0045	.0020	.0018	.0045	.0045
Hot Start :	.0000	.0009	.0002	.0009	.0009	.0009	.0009	.0009
Rich OL :	.1059							
Lean OL :	.0005	.0004	.0003	.0002	.0001	.0000	.0001	.0001
High Load :	.0508	.0331	.0154	.0133	.0176	.0287	.0364	.0441
Medium Load:	.0011	.0013	.0023	.0031	.0040	.0108	.0124	.0140
Low Load :	.0001	.0002	.0005	.0012	.0017	.0043	.0074	.0104

BOLD = Estimated emissions.

Figure 2.6.1.2 LSBVE model binned emissions for CO, HC and NO_x.

emissions for each method were found (these results are discussed in Section 3.3.1). For this reason, the emissions from the models were compared to the emissions from the 1 Hz data and not the bag results. The program EMOUT.FOR (Appendix A.2.7) was written to extract the 1 Hz emissions data and calculate the average emissions in a manner similar to the FTP.

2.6.4 Modeling of On-Road Emissions

The modeling of emissions from the on-road driving patterns was conducted with both the ASBVE and the LSBVE models. The on-road data were collected by driving to the beginning of the route from UCLA and therefore none of the patterns included any starts. Because of this, none of the modeled on-road emissions results could be compared to the FTP overall estimates, only to the bag 2 (hot running) emissions results or the HFET results.

To allow for comparison to the bag 1 (cold start) and bag 3 (warm start) sections of the FTP and the overall weighted results, the modeling of emissions from the on-road patterns needed to be modified to include cold and warm starts and also needed to be modified to make the driving patterns the same duration (505 seconds) as the FTP. This was accomplished by modeling the emissions from the on-road driving patterns by adding a start (cold or warm) to the beginning of each on-road pattern. Because many of the patterns started at the outskirts of Los Angeles, the beginning or end of the data sets may have contained more free-flowing traffic than the rest of the data set. For this reason, the shortening of the pattern was arranged so the data which was used for the remainder of the 505 seconds (after the cold start) was selected from the middle of the data for each trip. The starts which were added were from the first 52 seconds of bag 1 and the first 16 seconds of bag 3 sections of the FTP. The durations of the two starts were chosen to include all of the open loop operation during the start plus the first second of closed loop operation. Including one second of closed loop operation allowed the emissions estimating programs to differentiate between open loop operation caused by start and by other causes. This is important because the emissions during the different forms of open

loop are different.

The procedure for the modeling was to first concatenate the start and on-road data files together. The modeling began by reading the number (seconds) of data in the data file to determine where the middle of the data file was. The model began by analyzing the data from the start, and then moved to the middle of the data file minus half of the remaining 505 seconds for the remainder of modeling.

Modeling was then conducted using both versions of the emissions estimating model for 32 conservative driving data sets (8 freeway and 8 urban) and 8 aggressive driving data sets (4 freeway and 4 urban) for the full patterns with no starts (equivalent to the HFET or bag 2 of the FTP), cold start limited to 505 seconds (equivalent to bag 1 of the FTP) and warm start limited to 505 seconds (equivalent to bag 3 of the FTP) for a total of 240 modeling runs. The results for each type of modeling (bag 1, 2, or 3) were compared to the equivalent bag of the FTP or to the HFET (for the freeway routes instead of bag 2 of the FTP) and were also compared by weighting the three data types in the same manner as the FTP and comparing the overall emissions rates. The results were similarly compared to the results from emissions tests for the UCLA freeway and urban driving patterns.

3.0 - RESULTS AND DISCUSSION

3.1 Limitations on the Scope of the Study

It is important to emphasize that due to the use of a single research vehicle there were limitations on the scope of this study. For example, the effects of several variables of interest for vehicle operating parameters could not be assessed. These included model year, age and/or accumulated miles on the vehicle, vehicle type (car, truck, van, etc.), physical characteristics (weight, load, drag, etc.), engine type (number and configuration of cylinders, displacement, power, etc.), transmission type (manual or automatic, number of gears, overdrive, 2 or 4 wheel drive), fuel delivery system (carbureted or fuel injected), catalyst technology (type, number present, proximity to engine, age, conditioning), and engine control technology (computer hardware and software for engine control). Notwithstanding these limitations, the results reported in the following sections provide important indicators of actual in-use vehicle behavior for contemporary driving patterns in a large metropolitan area, and the ways in which such behavior differs from mandated certification procedures, such as the FTP.

3.2 On-Road Experiments

3.2.1 Vehicle Operating Parameters During Start, Idle and Shut Down.

3.2.1.1 Starts

Data were collected for 28 starts of the test vehicle. The engine coolant temperature during the starts ranged from 66 to 216°F and the ambient temperature ranged from 64 to 96°F. Data were also collected during a start which occurred at an ambient temperature of 19°F in Gallup New Mexico during a cross country trip returning the vehicle from the Ford Laboratory. An example of the open loop flag, engine coolant temperature and catalyst temperature during a start at an ambient temperature of 72°F is shown in Figure 3.2.1.1.1. During the start, the duration of open loop operation was 51 seconds (the figure shows 61 seconds because 10 seconds of data were collected during

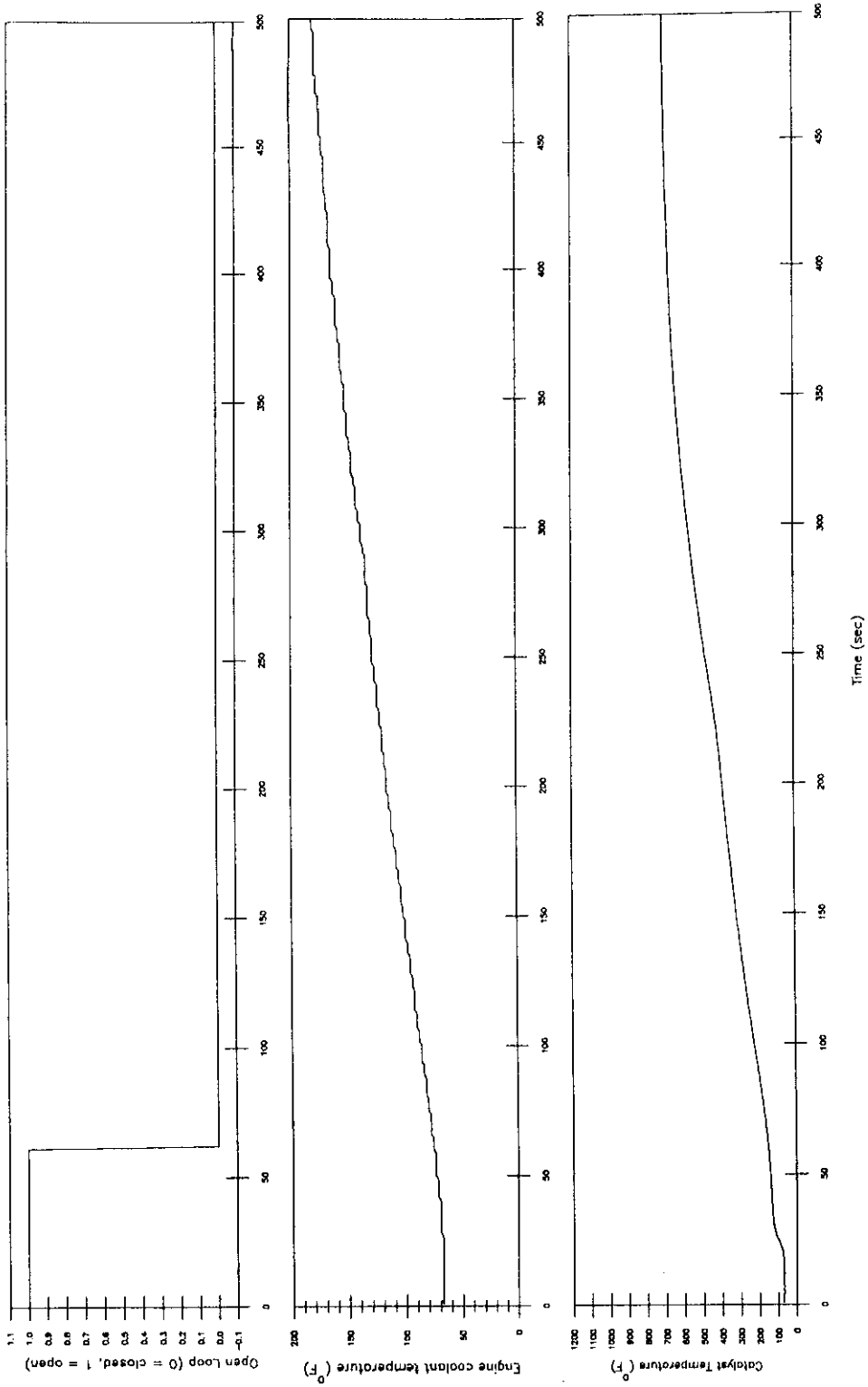


Figure 3.2.1.1.1 Open loop flag, engine coolant temperature and catalyst temperature during a cold start at an ambient temperature of 72°F.

the experiments before starting the engine), the engine coolant temperature rose from 68 to 200°F in 600 seconds, and the catalyst temperature rose from ambient temperature to approximately 700°F in 450 seconds and then leveled off.

For all of the experiments except the 19°F start, the duration of open loop operation during start fell into two categories, 16 seconds or 51 seconds. For the start at 19°F, the duration of cold start was 211 seconds. A plot of the vehicle speed, open loop flag and lambda is shown in Figure 3.2.1.1.2 and a plot of the engine coolant temperature, ambient temperature and catalyst temperature during this start is shown in Figure 3.2.1.1.3. The duration of open loop operation was plotted as a function of engine coolant temperature, catalyst temperature, ambient temperature and air charge temperature to the engine at the time of start (Figures 3.2.1.1.4, 3.2.1.1.5, 3.2.1.1.6 and 3.2.1.1.7 respectively) to determine if there was a relationship. As can be seen from the figures, there is no direct relationship between any of the four temperatures and the duration of open loop operation after start. There is no factory thermocouple used for ambient temperature or catalyst temperature to provide information to the EEC and therefore they would not be expected to be related to the duration of open loop operation.

Because the duration of open loop operation during start was only one of two lengths (16 or 51 seconds) and it is not related to any of the above parameters at start, the duration must be dependent on a operating parameter which is measured at a fixed period after start. To determine if this parameter was the engine coolant temperature, the engine coolant temperature at 15 seconds after start (when the vehicle was observed to go closed loop in some experiments) was plotted versus the duration of open loop (Figure 3.2.1.1.8). The same plot for a time after start of 51 seconds is shown in Figure 3.2.1.1.9 for all of the starts including the start at 19°F. The two plots show there is a relationship between the engine coolant temperature and the duration of open loop operation. If the temperature of the engine coolant reaches $\approx 140^\circ\text{F}$ by 15 seconds, the engine goes closed loop, otherwise the engine remains open loop until 51 seconds and checks the engine coolant temperature again. Because there was only data for one "very" cold start, it is not possible to determine if or when the EEC checked the engine coolant temperature

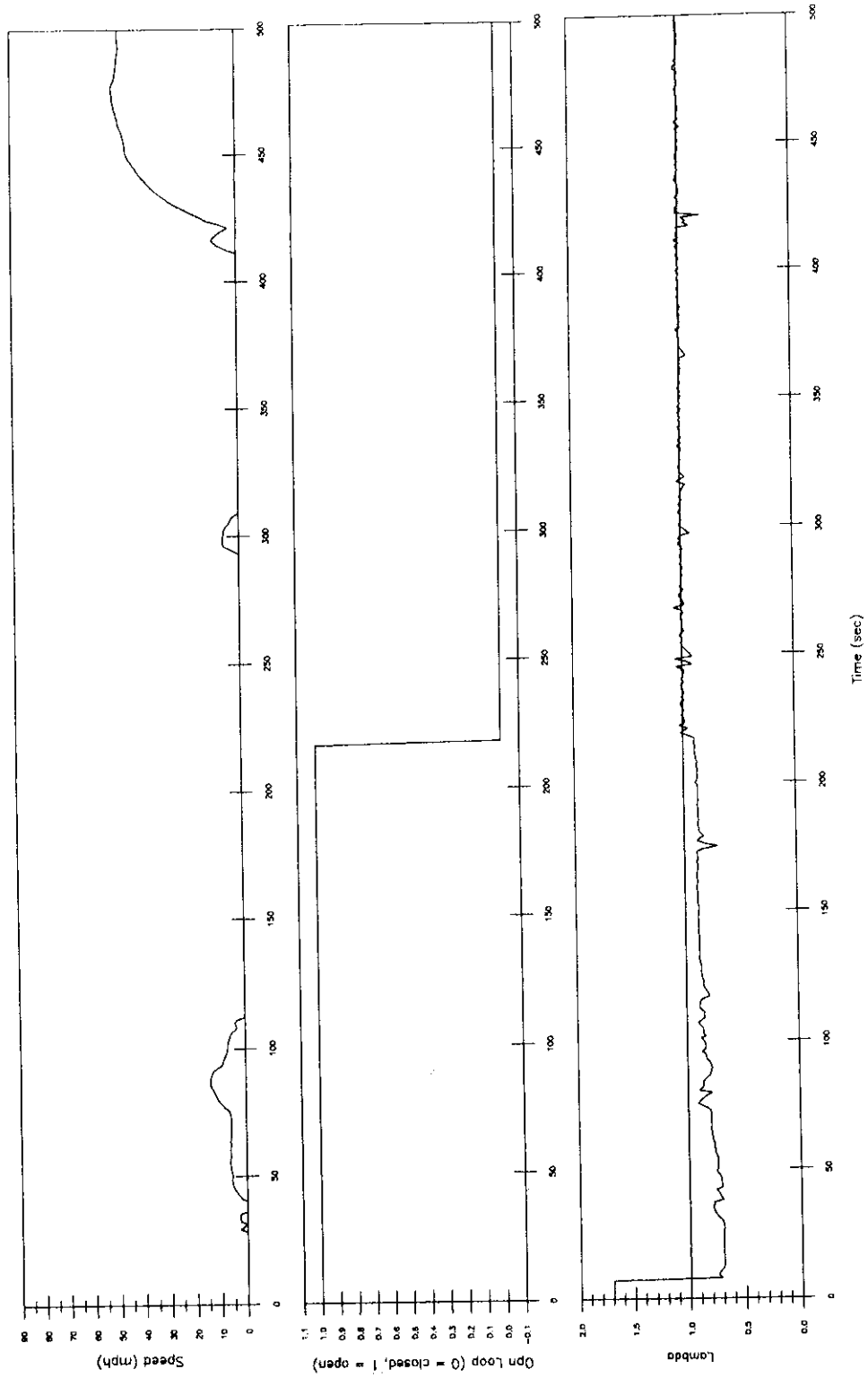


Figure 3.2.1.1.2 Vehicle speed, open loop flag, and lambda during cold start at an ambient temperature of 19°F.

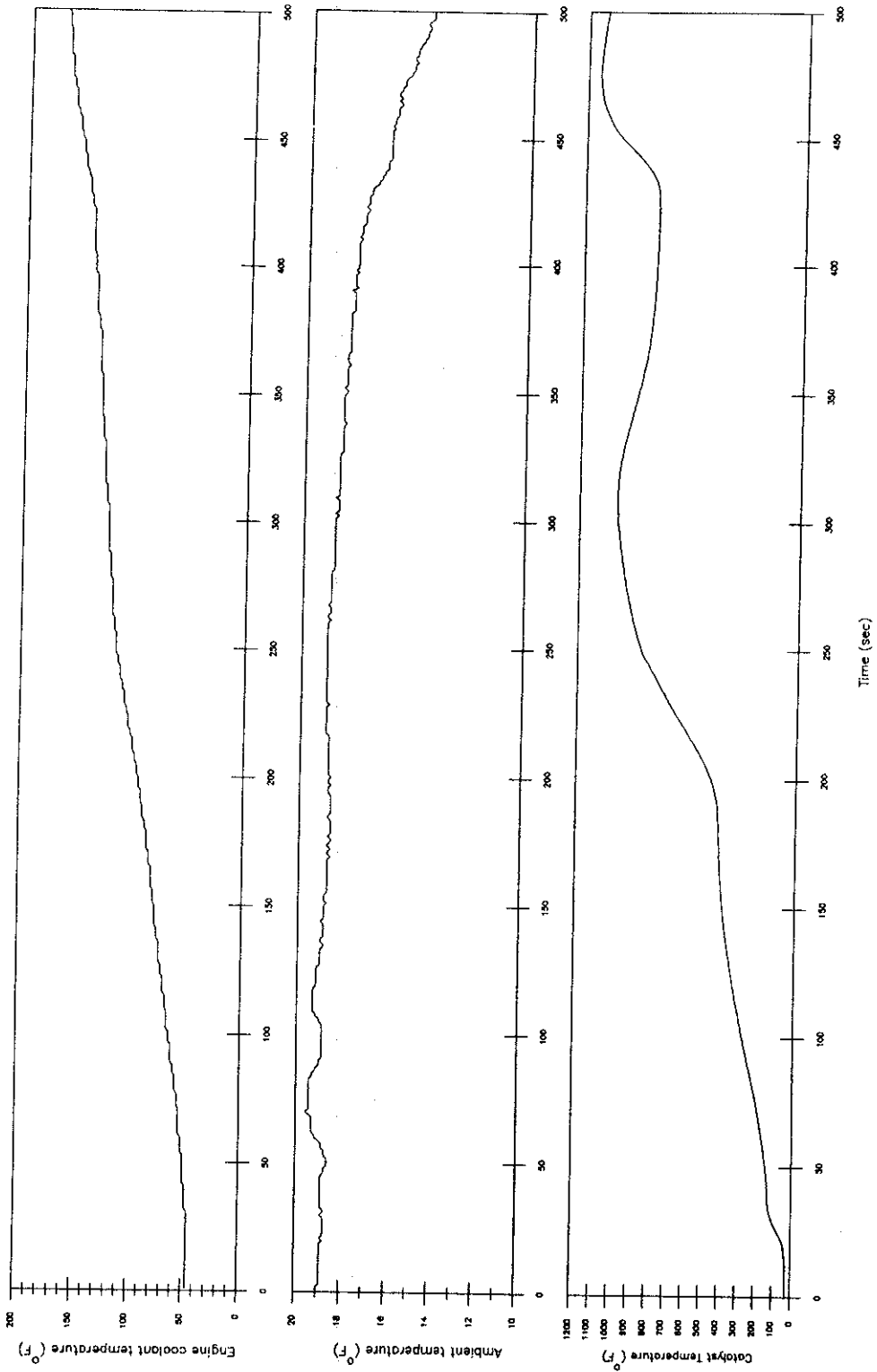


Figure 3.2.1.1.3.3 Engine coolant temperature, ambient temperature and catalyst temperature during cold start at an ambient temperature of 19°F.

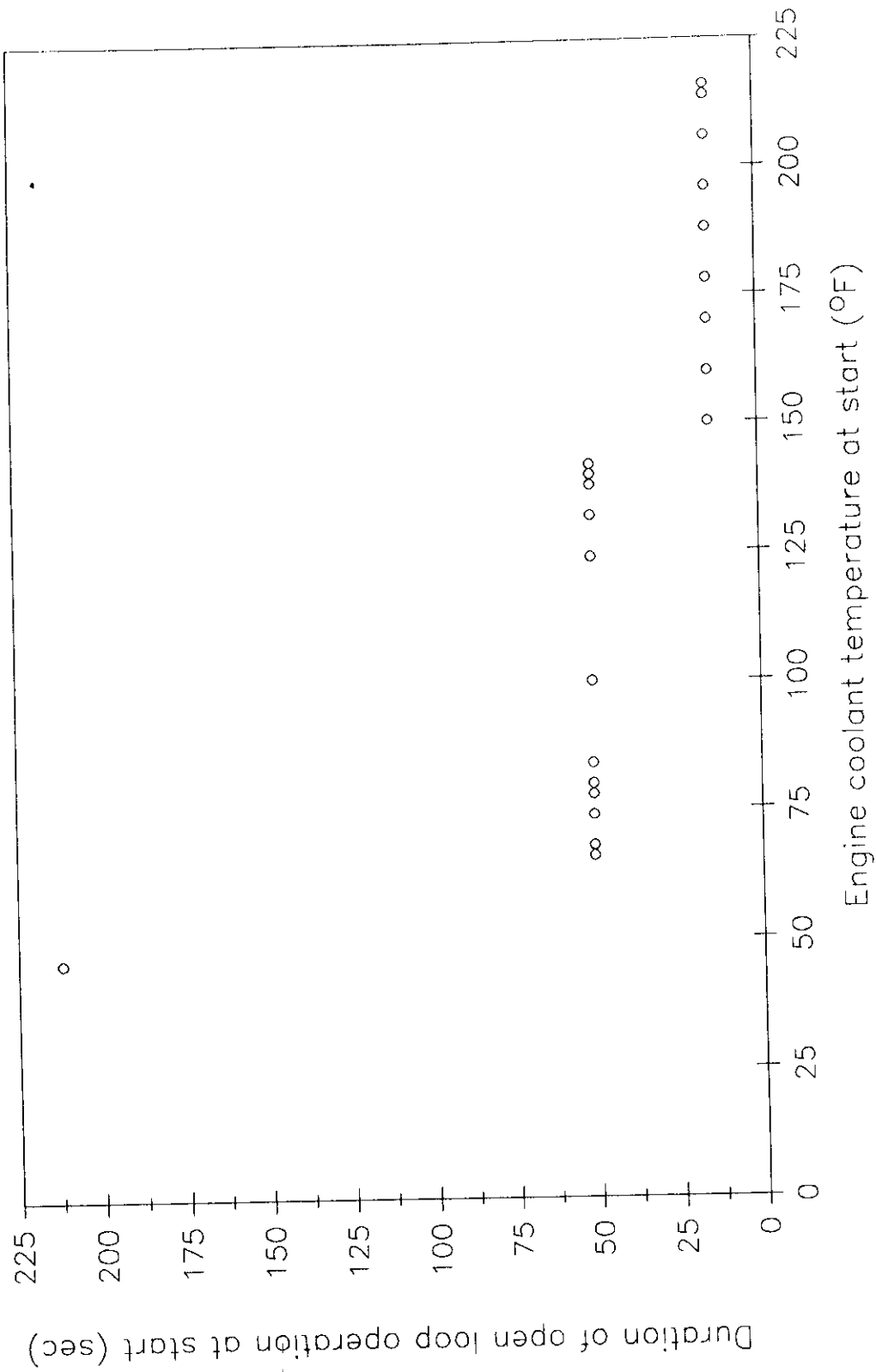


Figure 3.2.1.1.4 Duration of open loop operation as a function of engine coolant temperature at start.

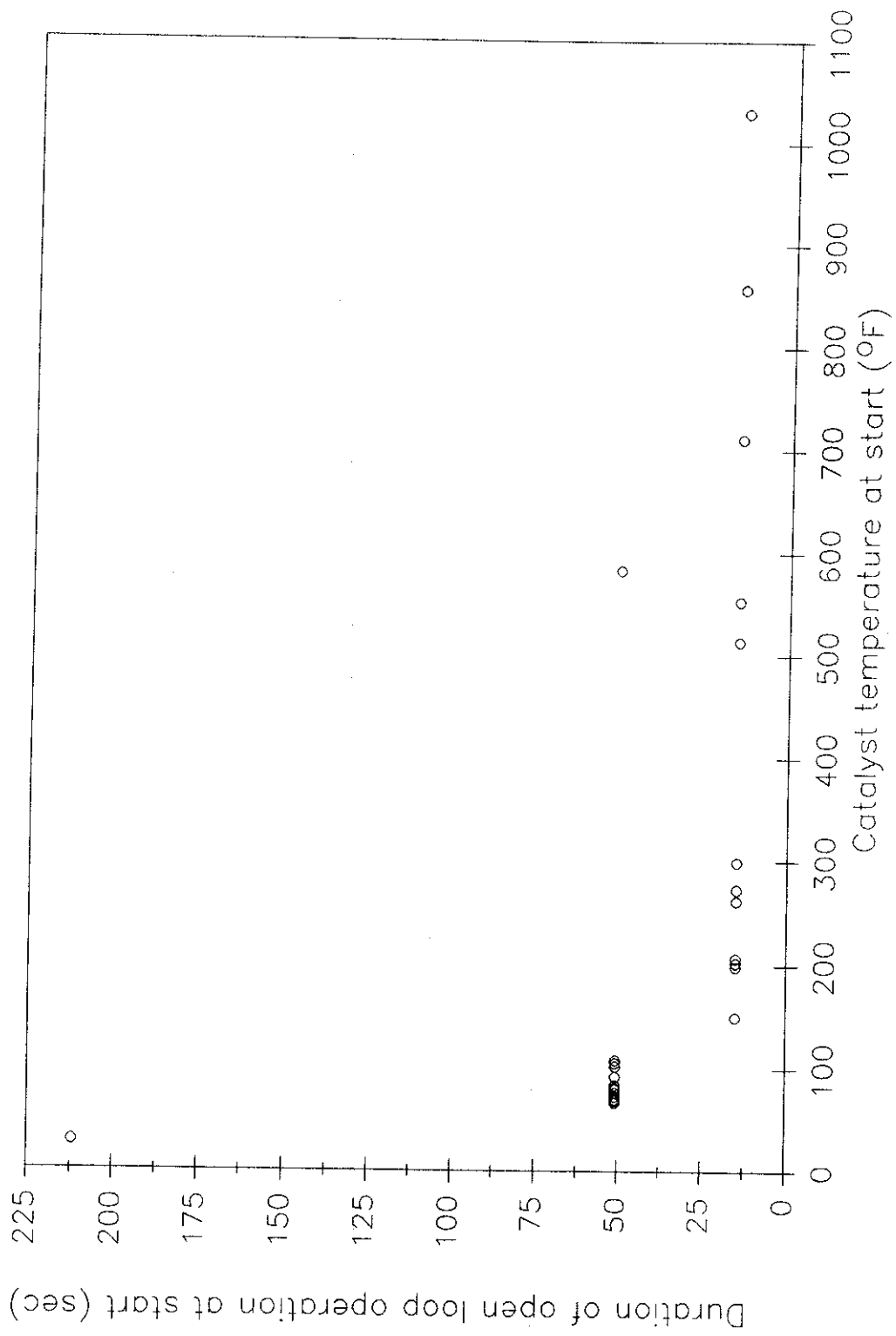


Figure 3.2.1.1.5 Duration of open loop operation as a function of catalyst temperature at start.

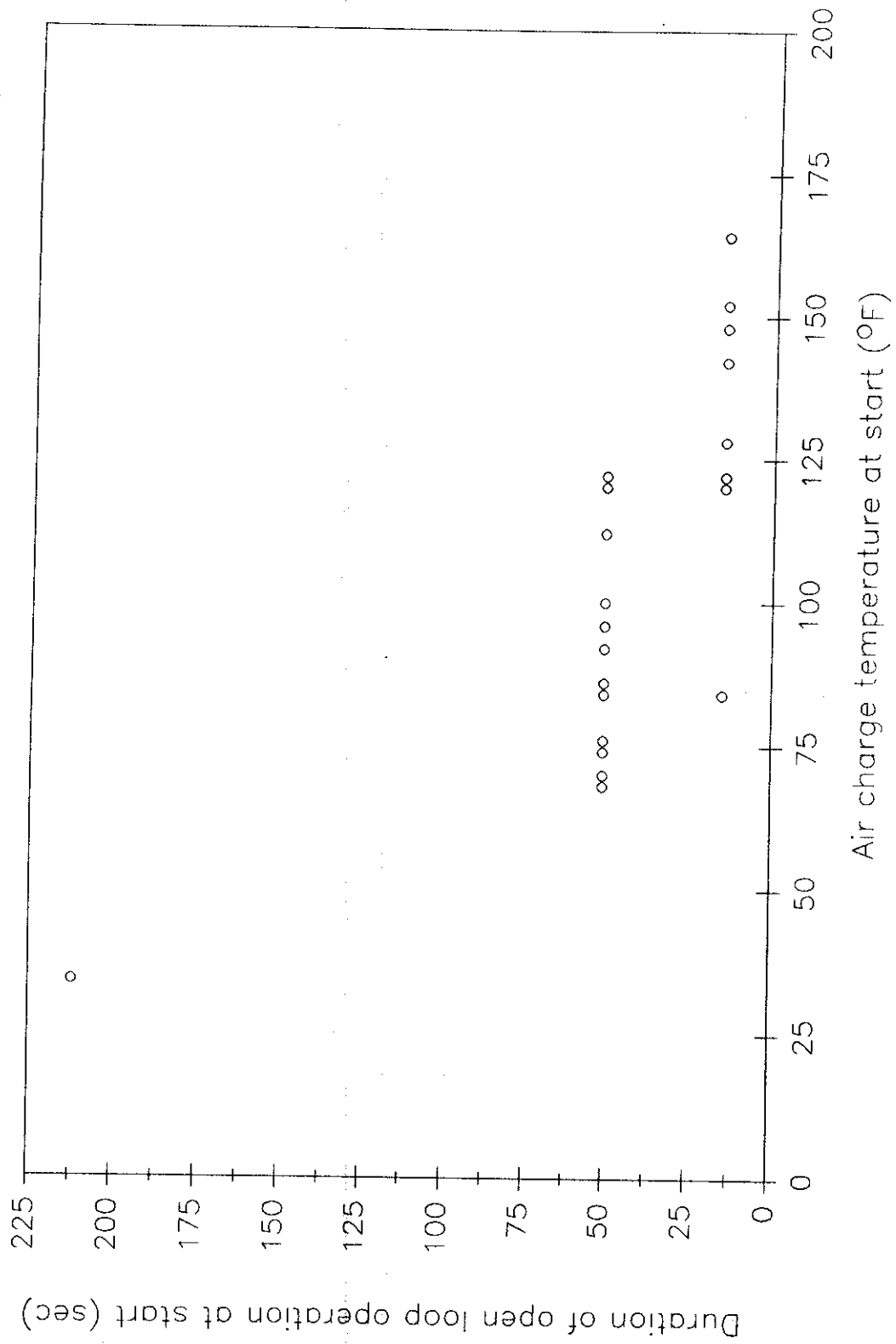


Figure 3.2.1.1.7 Duration of open loop operation as a function of engine air charge temperature at start.

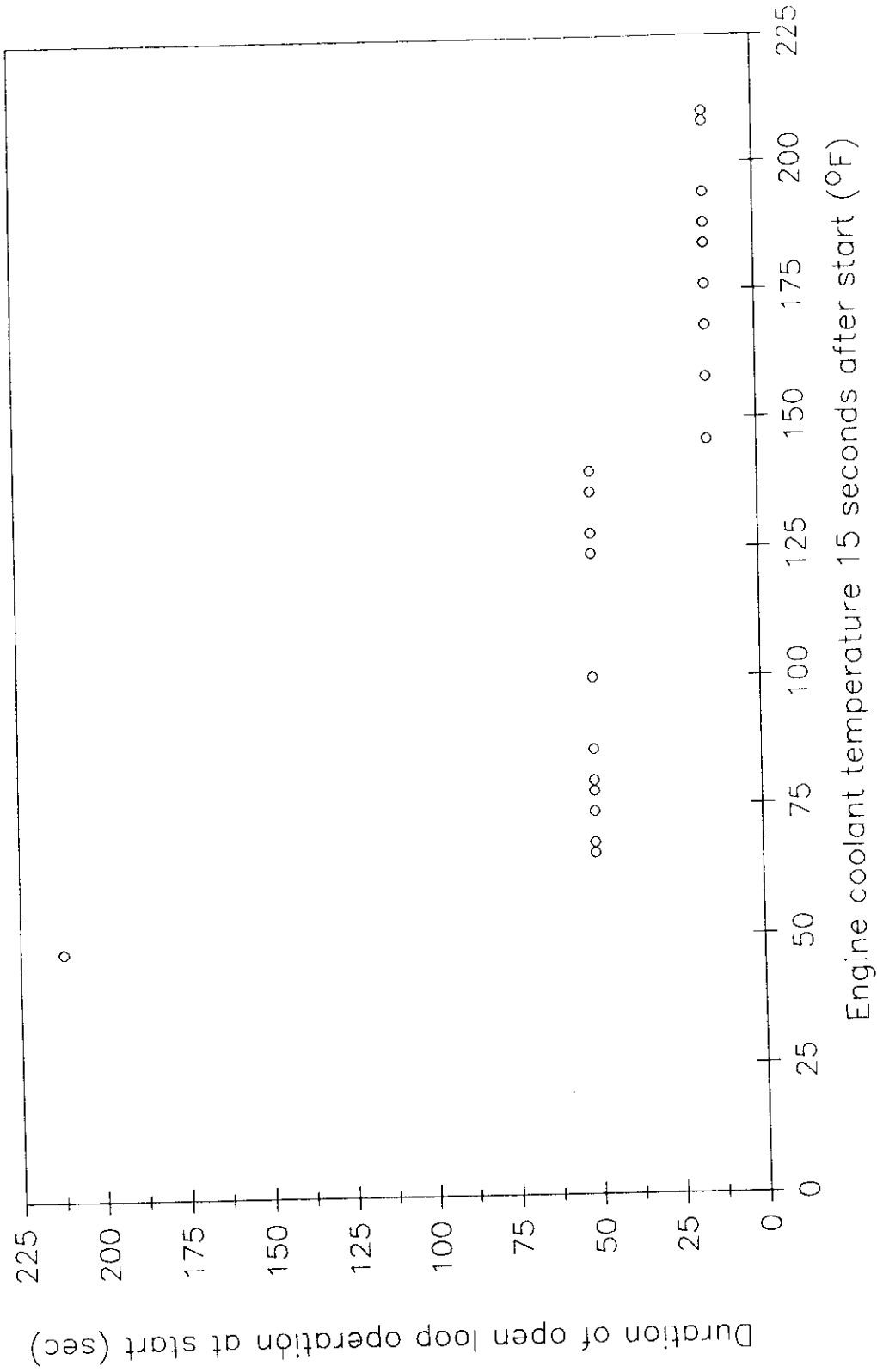


Figure 3.2.1.1.8 Duration of open loop operation as a function of engine coolant temperature 15 seconds after start.

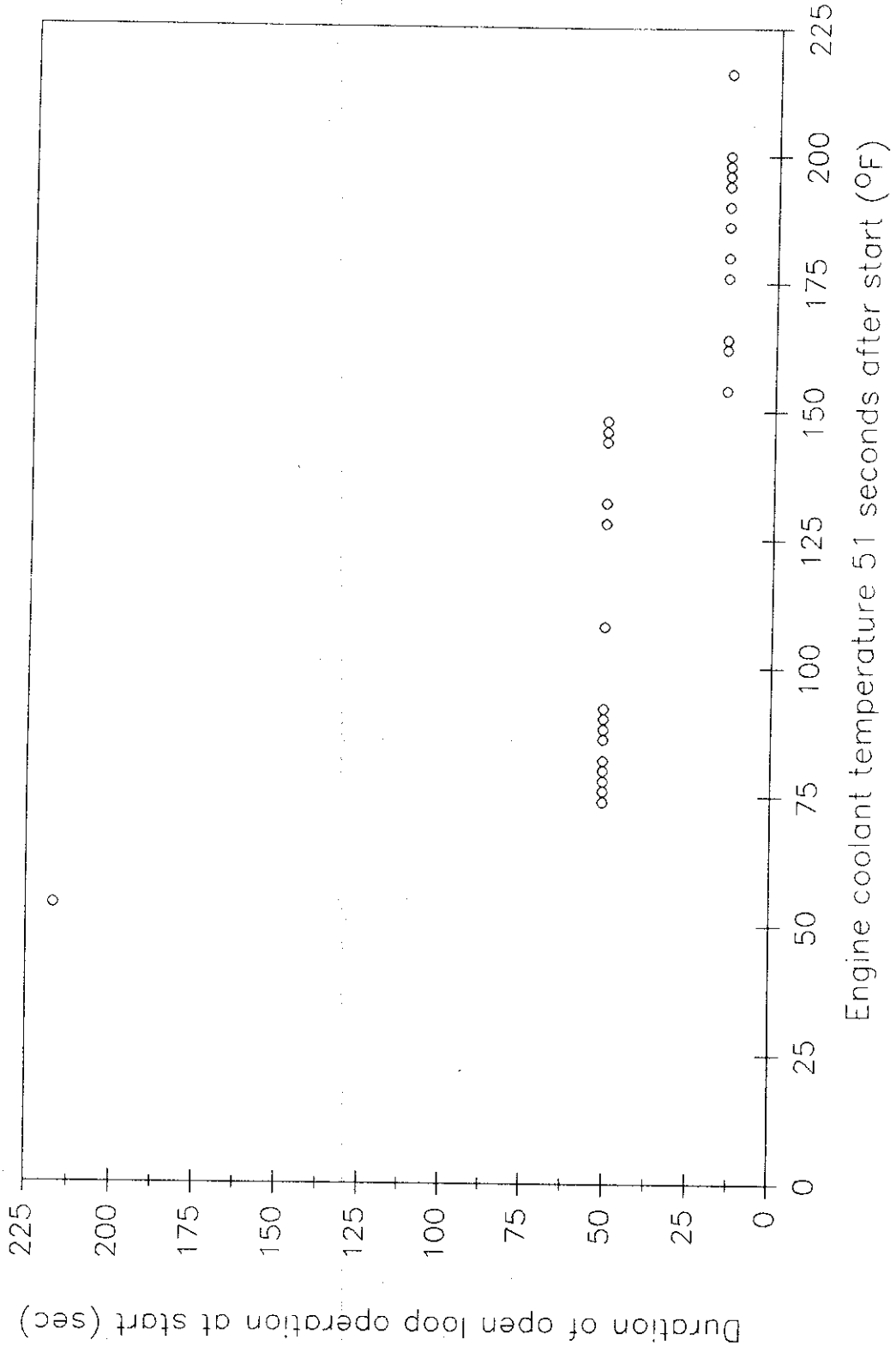


Figure 3.2.1.1.9 Duration of open loop operation as a function of engine coolant temperature 51 seconds after start.

between 51 and 211 seconds. For the start at 19°F at 15 seconds after start, the engine coolant temperature was 46°F and the catalyst temperature was also 46°F, and at 51 seconds the engine coolant temperature was 52°F and the catalyst temperature was 155°F. When the control system went closed loop at 211 seconds the engine coolant temperature was still only 102°F but the catalyst temperature was 550°F which is above the light-off temperature for the catalyst (see section 3.3.5).

3.2.1.2 Idle

The engine load, engine coolant temperature and the catalyst temperature during a 1500 second idle after driving the vehicle for 25 minutes to warm up the engine and catalyst is shown in Figure 3.2.1.2.1. The catalyst cooled down from approximately 800°F when the idle period started after driving, to a constant temperature of 690°F. The engine load and the engine coolant temperature varied with a period of approximately 100 seconds. The change in load was attributed to the engine fan coming on and off during the idle period and this caused the engine coolant temperature variation between 206 and 214°F in a sinusoidal manner. The engine load was grouped into high load and low load and linear regression lines were plotted through each group (Figure 3.2.1.2.1). The average difference between the two regression lines (0.0053 units or 0.71% of maximum observed load (0.75)) was equal to the load induced by the engine cooling fan. Figure 3.2.1.2.2. shows the result of switching the air conditioning on and off during an idle to determine the load induced by the air conditioning compressor. The average difference between the two regression lines was 0.034 units or 4.5% of maximum observed load.

3.2.1.3 Cool Down

The engine coolant temperature, exhaust gas temperature and the catalyst temperature after engine shut down are presented in Figure 3.2.1.3.1. During the first 150 seconds of the cool down period, the engine coolant temperature rose from 214°F to 220°F due to the fan not operating after the vehicle was shut off. The temperature remained constant at 220°F for approximately 600 seconds and then it fell approximately

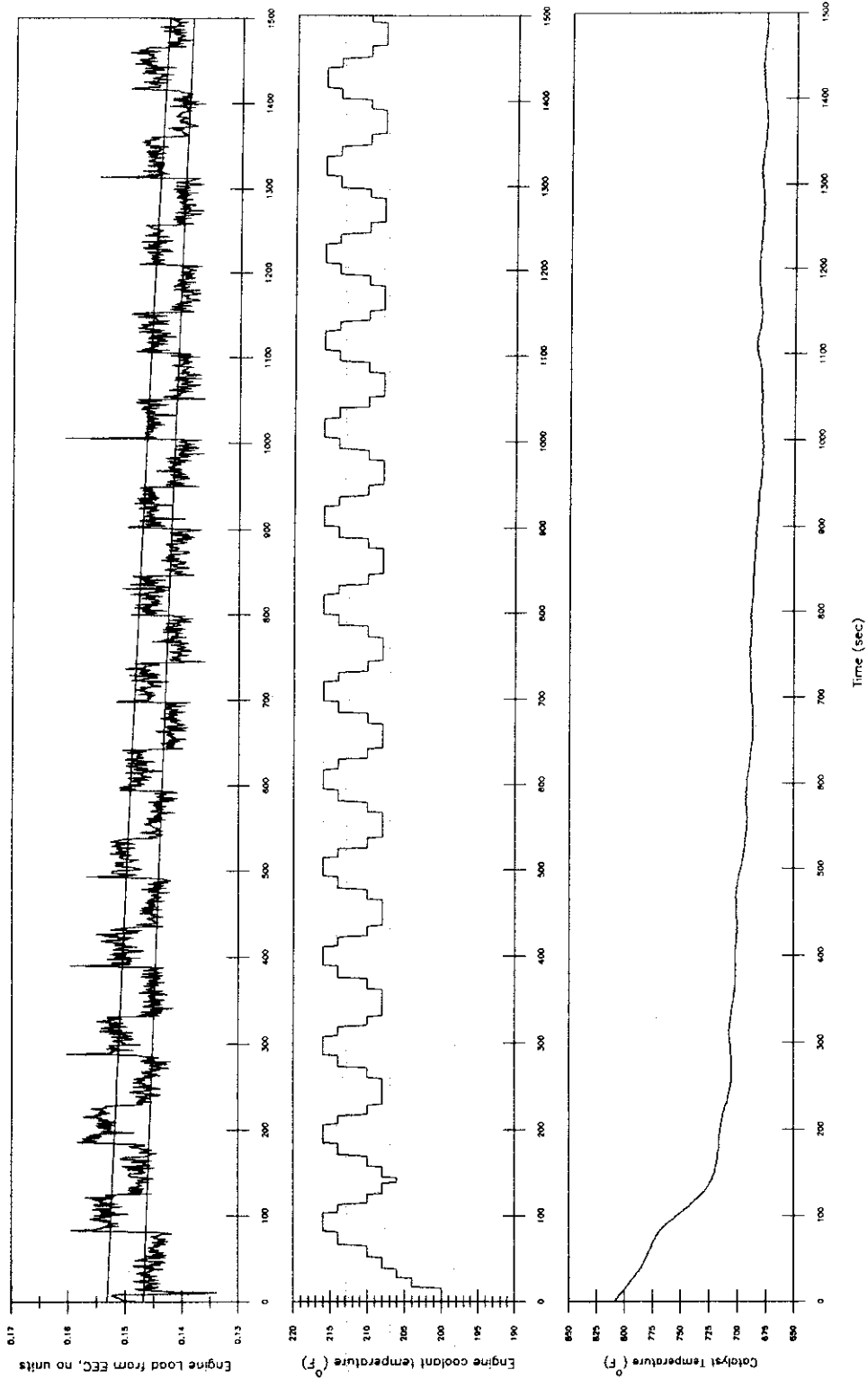


Figure 3.2.1.2.1 Engine load, engine coolant temperature, and catalyst temperature during 1500 second idle.

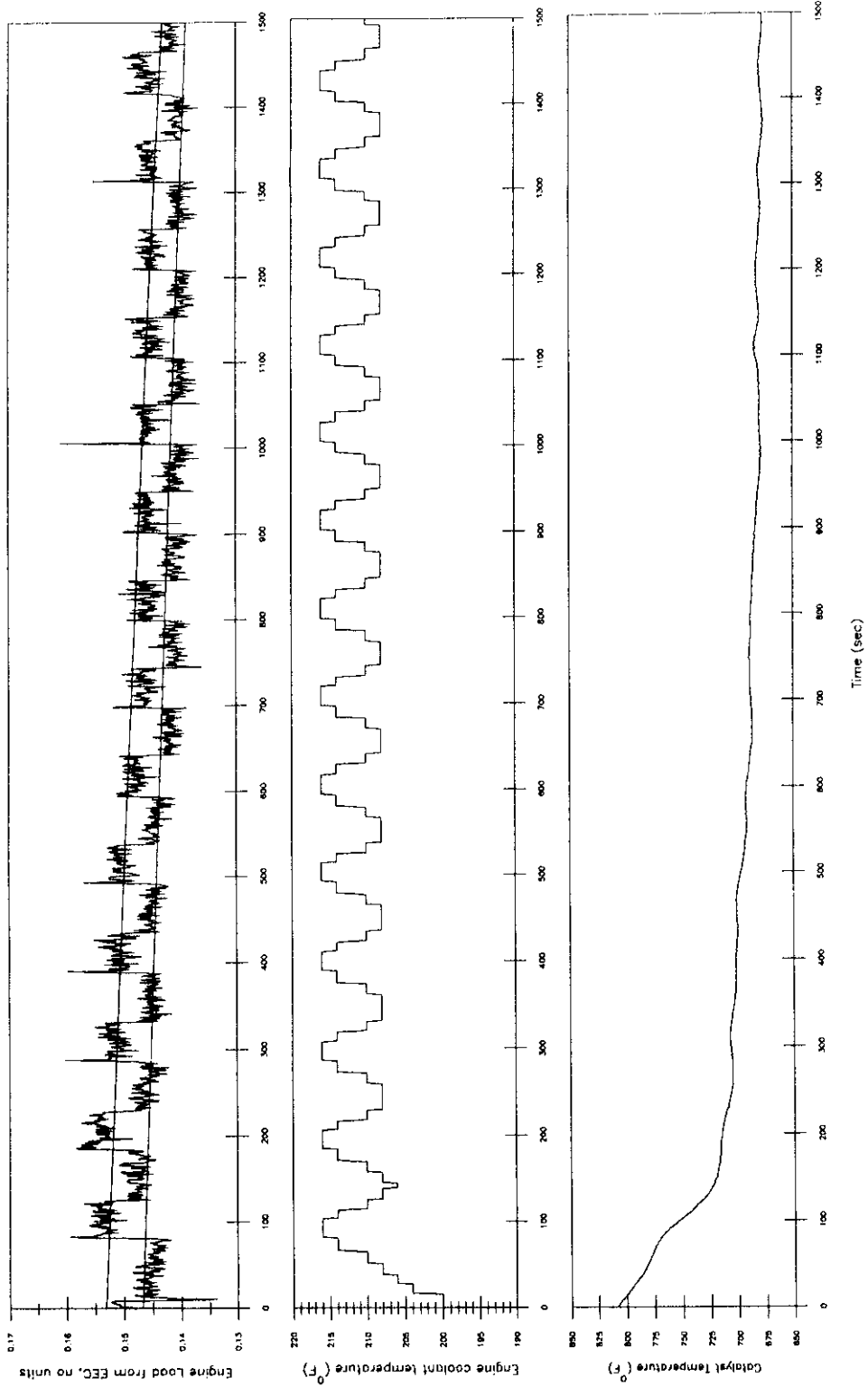


Figure 3.2.1.2.2 Engine load, engine coolant temperature, and air conditioning flag during 360 second idle.

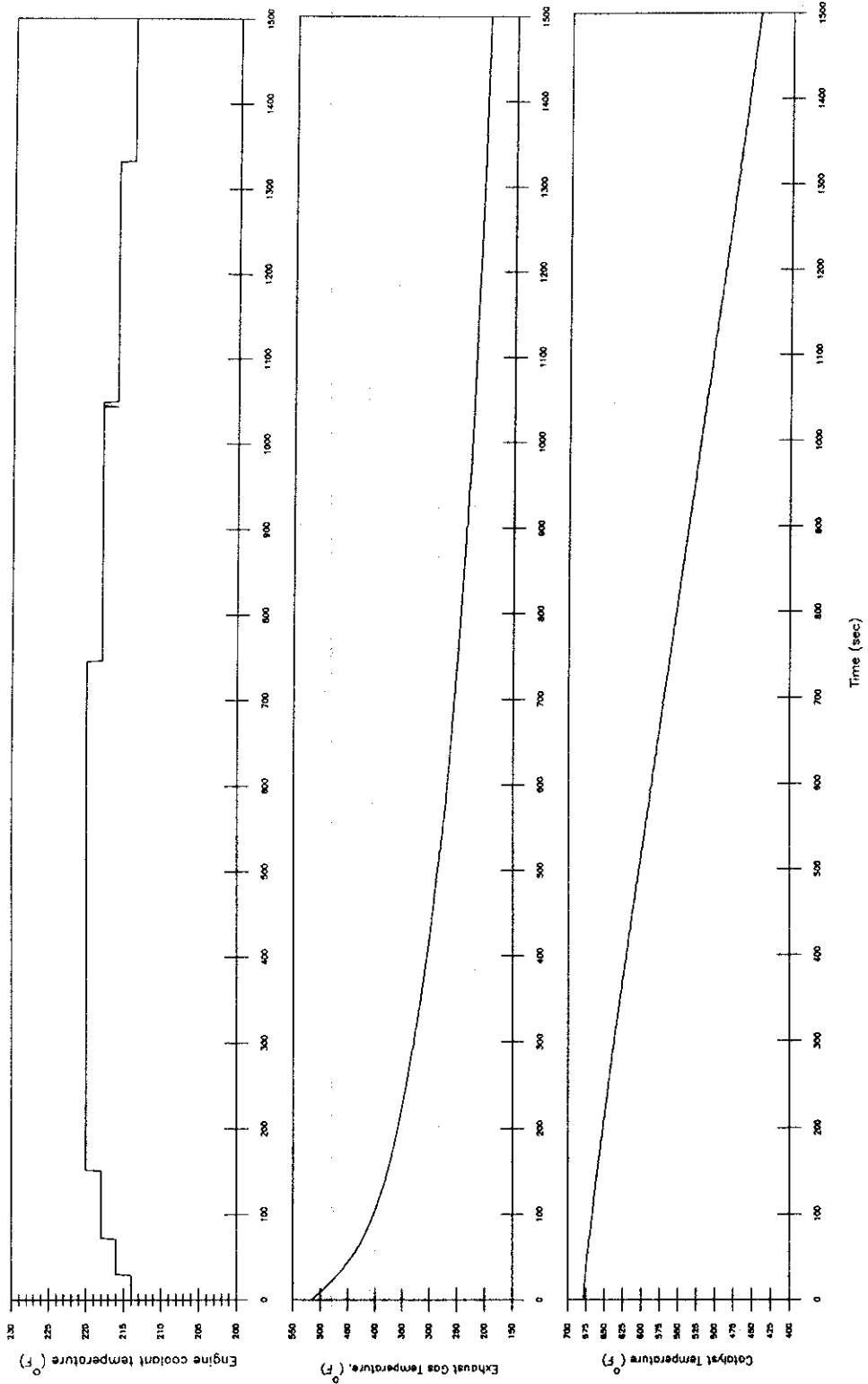


Figure 3.2.1.3.1 Engine coolant temperature, exhaust gas temperature, and catalyst temperature for first 1500 seconds after engine shut down.

linearly back down to 214°F by the end of the 1500 second test. At the beginning of the of the cool down period, the catalyst temperature was 678°F and fell at an approximately linear rate (16°F per 100 seconds) to 439°F after 1500 seconds which is near the light off temperature of the catalyst.

3.2.2 Maximum Operating Envelope

The trace of the vehicle speed, braking flag and open loop flag are shown in Figure 3.2.2.1 for the acceleration/deceleration experiments. The portions of the trace which correspond to the individual accelerations and decelerations were removed and treated as individual experiments for further analysis. In all, a total of 19 experimental traces were analyzed and the results are tabulated in Table 3.2.2.1. The one second speed and acceleration data from the combined individual experiments are shown in Figure 3.2.2.2. The maximum rates of acceleration were achieved starting from a stop and the maximum of three tests was 8.7 mph s⁻¹. This compares to a maximum acceleration rate in the Urban Dynamometer Driving Schedule of 3.3 mph s⁻¹. Between 40 and 60 mph the acceleration rate was fairly constant, as was the case for the 65 to 80 mph range. These plateaus were a function of the vehicle coming to an approximately constant acceleration rate in a particular gear (2nd or 3rd respectively) in which the vehicle was operating. Figure 3.2.2.3 shows the speed, acceleration and gear during one of the 0-80 mph accelerations.

Deceleration rates were constant from 80 mph to approximately 20 mph at a maximum rate of 15.9 mph s⁻¹. These may not be the absolute deceleration capabilities of the vehicle because it was not equipped with anti-lock brakes and therefore the maximum deceleration rate was limited by the operator to avoid loss of control of the vehicle. Thus, the deceleration rates measured represent the greatest rate of deceleration which the operator believed could safely be maintained without the braking system locking. From 20 to 0 mph, the rate of deceleration decreased approximately linearly to zero with a slope of -0.8.

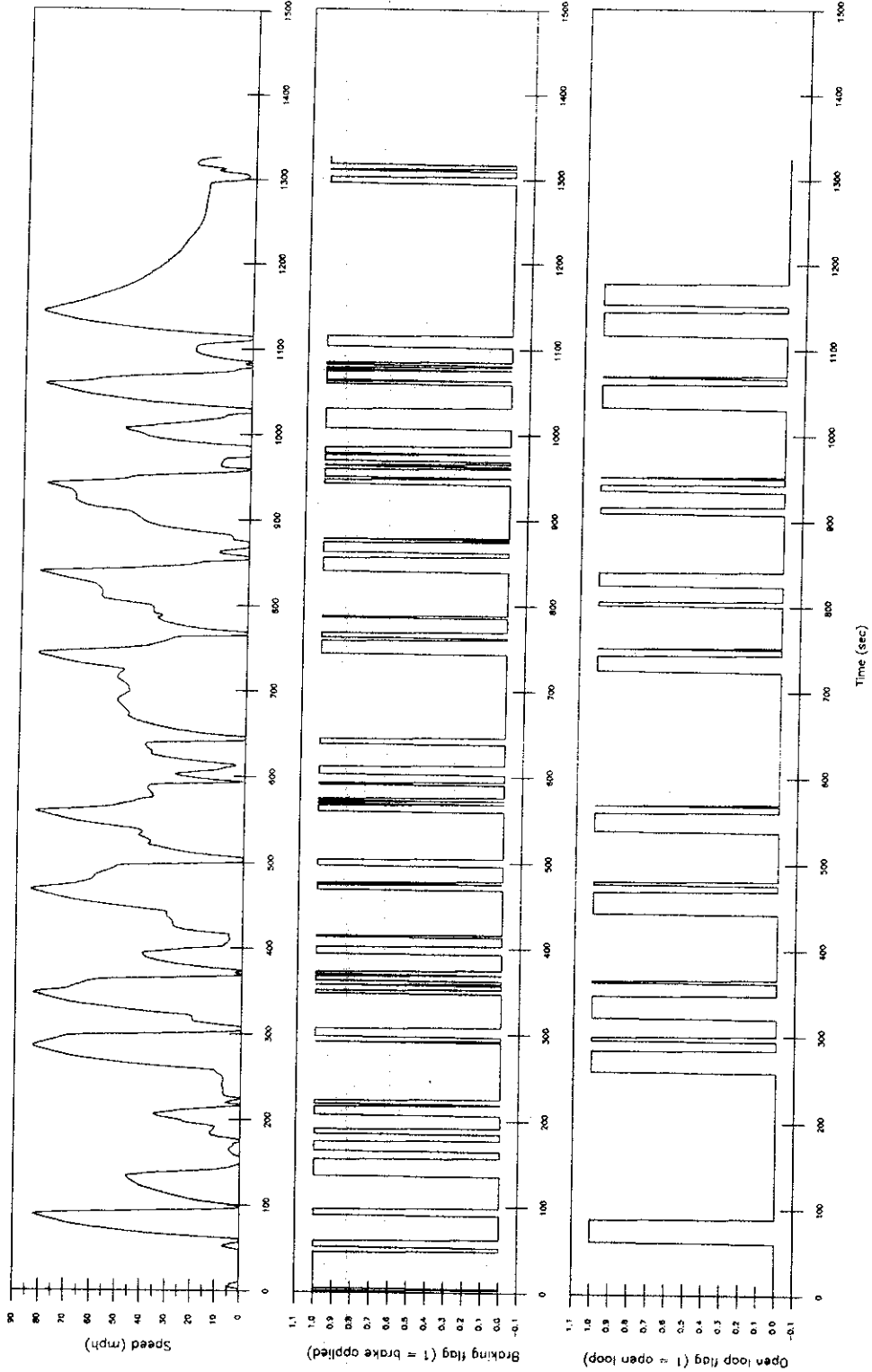


Figure 3.2.2.1 Speed, braking flag, and open loop flag during acceleration, deceleration, and coasting experiment.

Table 3.2.2.1 Acceleration/deceleration/coasting experiments results.

Test	Time	Dist	Avg Speed	Fuel Econ
V ₀ -V _f (MPH)	sec	miles	mph	mpg
Acceleration				
0-80	29	0.402	51.69	6.51
0-80	29	0.402	51.75	6.49
0-80	28	0.384	51.20	6.46
10-80	26	0.373	53.70	6.57
20-80	25	0.378	56.65	6.70
30-80	25	0.391	58.71	7.47
40-80	24	0.391	61.26	8.09
50-80	17	0.300	67.49	7.56
60-80	15	0.277	71.21	9.44
70-80	10	0.189	75.49	10.01
Coast				
80-20	153	1.497	35.47	109.01
Deceleration				
10-0	5	0.006	5.46	15.05
20-0	7	0.021	12.64	33.93
30-0	6	0.019	13.67	28.04
40-0	7	0.034	20.64	39.84
50-0	7	0.039	23.34	62.09
60-0	9	0.075	33.82	127.24
70-0	9	0.067	30.33	138.26
80-0	10	0.100	39.95	62.29

3.2.2.1 Comparison to the FTP

The measured maximum operating envelope of the test vehicle from Figure 3.2.2.2 was compared to the corresponding one second data for the FTP from the Federal Register in Figure 3.2.2.1.1. Although the size of the envelope can change with different vehicles, the plot shows the Urban Dynamometer Driving Schedule (UDDS) used in the FTP does not take into account the higher acceleration and deceleration rates which the Ford Taurus was capable of on-road. This was due to artificial limits placed on the UDDS by limitations of the dynamometers used when the UDDS was developed. Although the UDDS captures a substantial amount of in-use vehicle operation, the vehicle

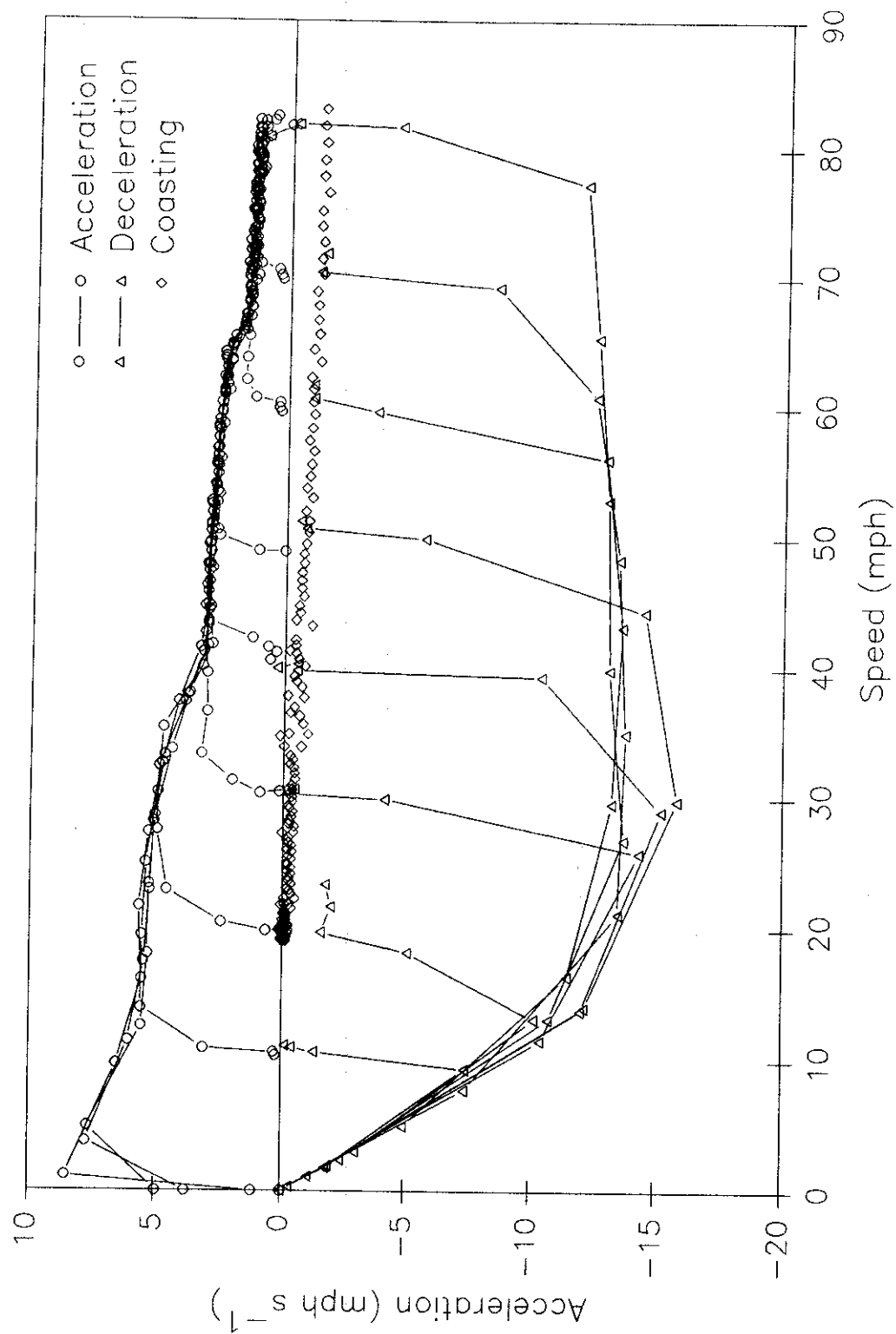


Figure 3.2.2.2 One second and acceleration data from the acceleration/deceleration/coasting experiments.

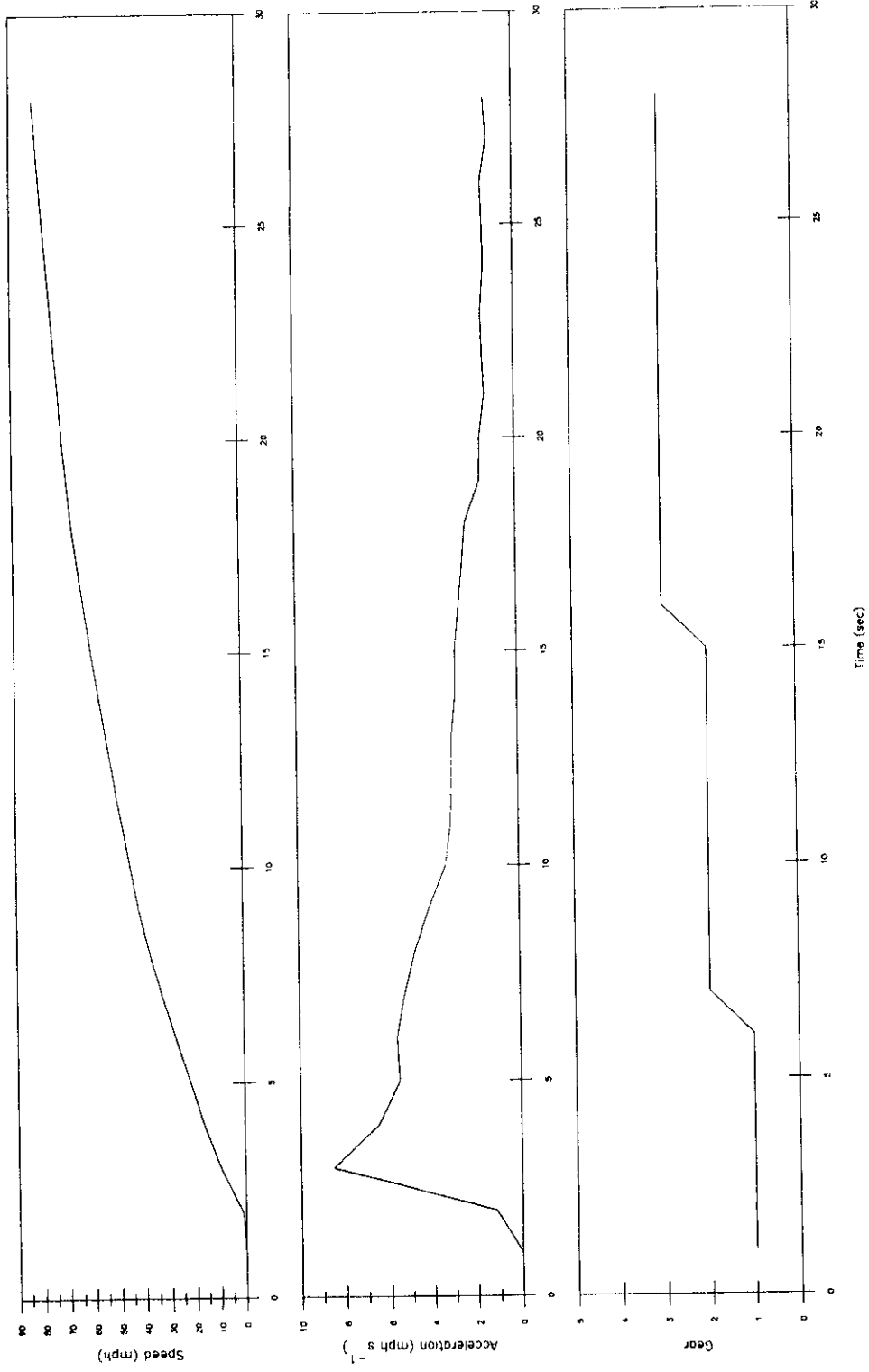


Figure 3.2.2.3 Speed, acceleration and gear during a 0 to 80 mph acceleration experiment.

is capable of operating outside the conditions found in the UDDS.

3.2.3 Development of Modes of Operation

Data from the acceleration experiments were used to define acceleration- and speed-based driving modes which were used for comparison of different driving patterns and for modeling of vehicle emissions. The ten modes of operation used in the modal analysis were: hard, medium and light accelerations and decelerations, start, coast, idle, and cruise.

The acceleration modes were determined by plotting a regression line through the one second data from the three 0 to 80 mph acceleration tests (Figure 3.2.3.1). The area below the regression line was divided into two sections corresponding to low and medium accelerations. Hard accelerations were defined as occurring any time the vehicle was operating wide open throttle.

Deceleration rates were divided into hard and light by dividing the area into two sections (Figure 3.2.3.2). From 0 to 20 mph, hard decelerations were defined as below the line shown with a slope of -0.4 which is half of the slope of the regression line shown through the data points from 0 to 20 mph. From 20 to 80 mph, hard decelerations were defined as below the horizontal line at a deceleration of 8 mph s^{-1} (approximately half the maximum deceleration rate).

To determine the difference between a light deceleration, a cruise and a coast, the data from the coasting experiment were plotted with a regression line in Figure 3.2.3.3. The slope of the line is approximately 0.03. To allow for small variations caused by driving in traffic, the window to be considered a cruise was set at 10 times the slope from the experiment (0.3 mph s^{-1}) with the condition that the throttle was applied, otherwise it was considered a coast. The definition of a light deceleration was a deceleration greater than 0.3 mph s^{-1} with no application of the brakes.

3.2.4 Effect of Variations in Load

A summary of the experiments conducted driving up and down a five mile long

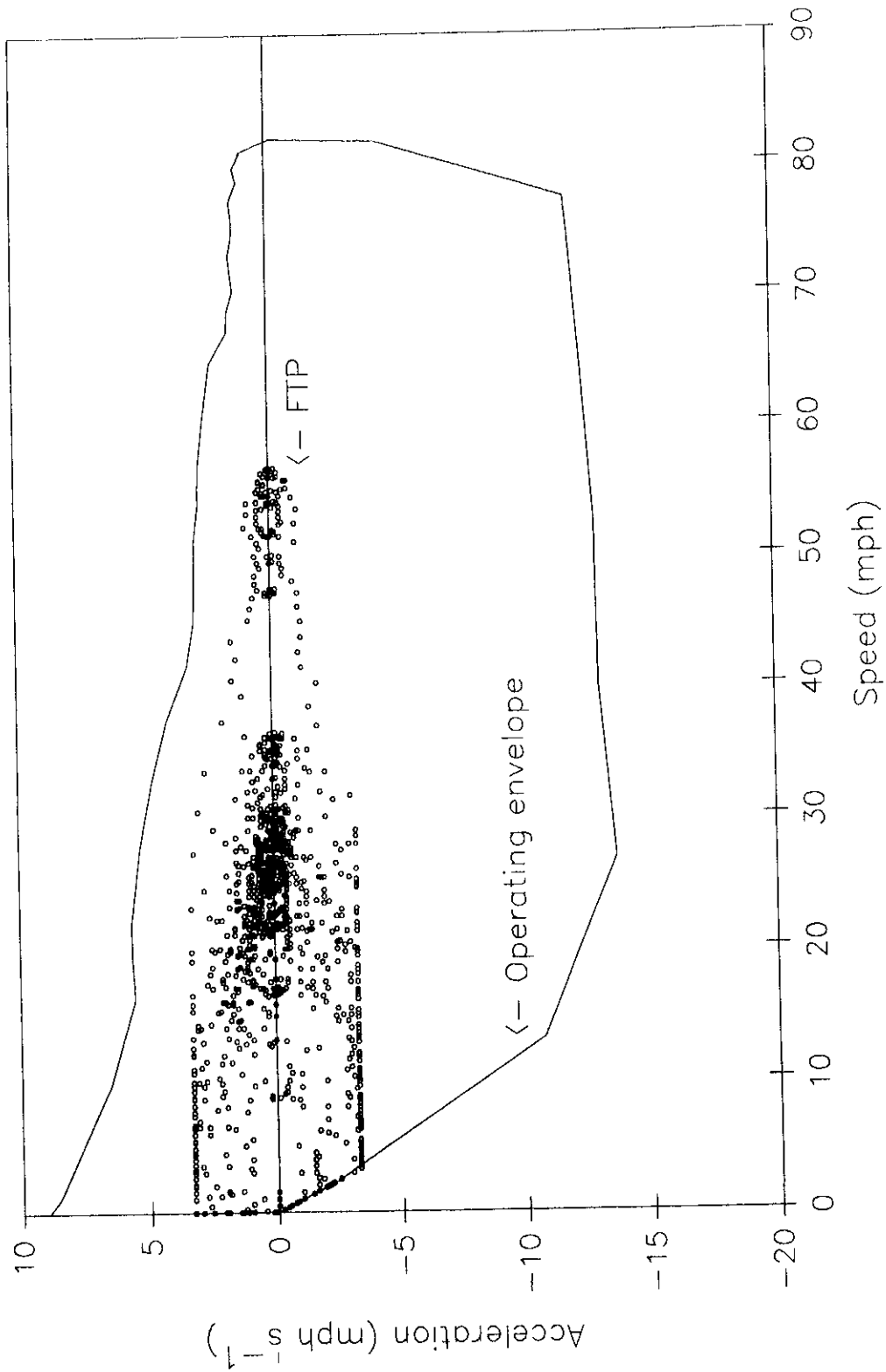


Figure 3.2.2.1.1 One second FTP data points and operating envelope.

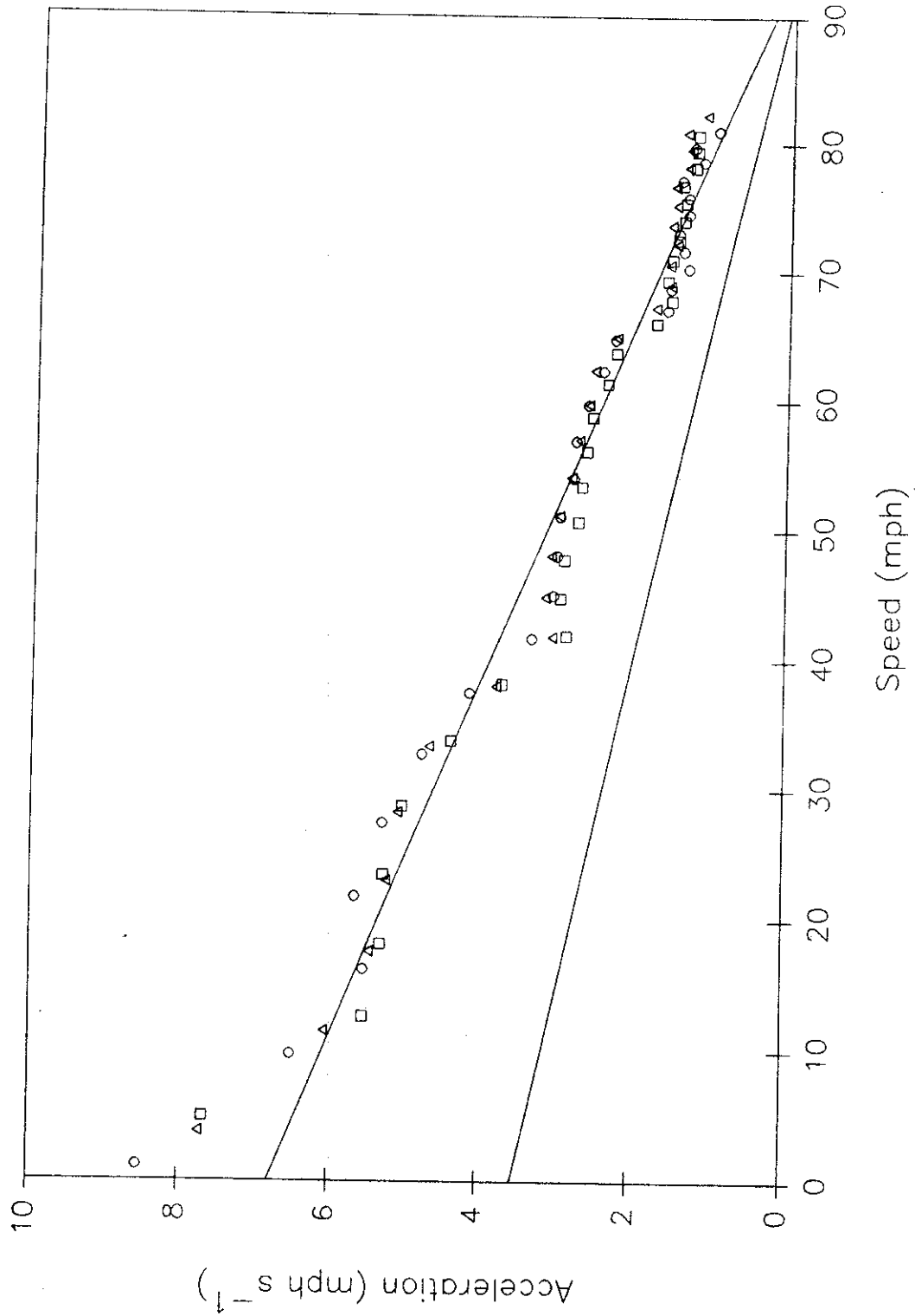


Figure 3.2.3.1 Acceleration as a function of speed showing divisions used to define light and medium accelerations.

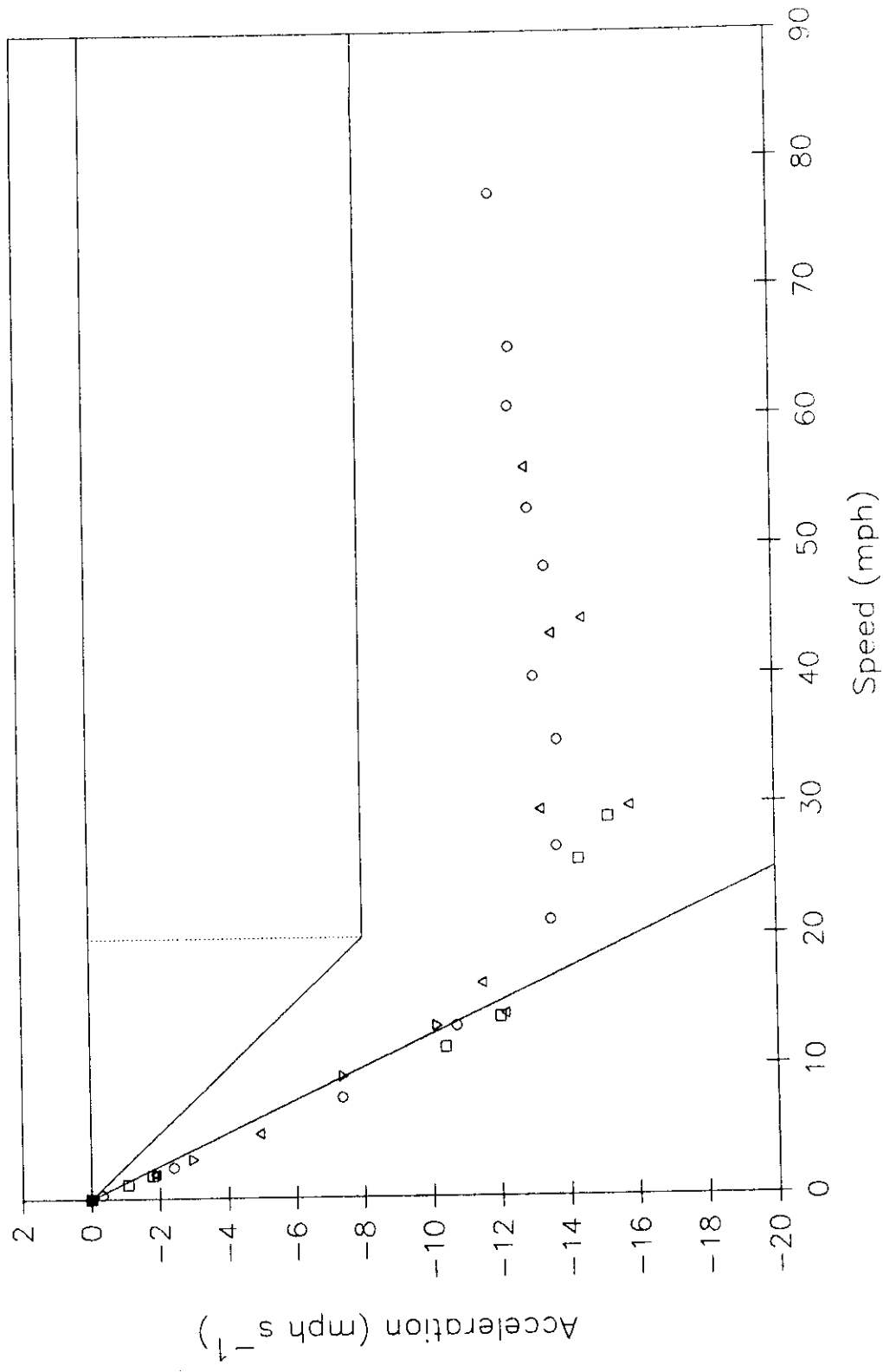


Figure 3.2.3.2 Deceleration as a function of speed showing divisions used to define hard and medium decelerations.

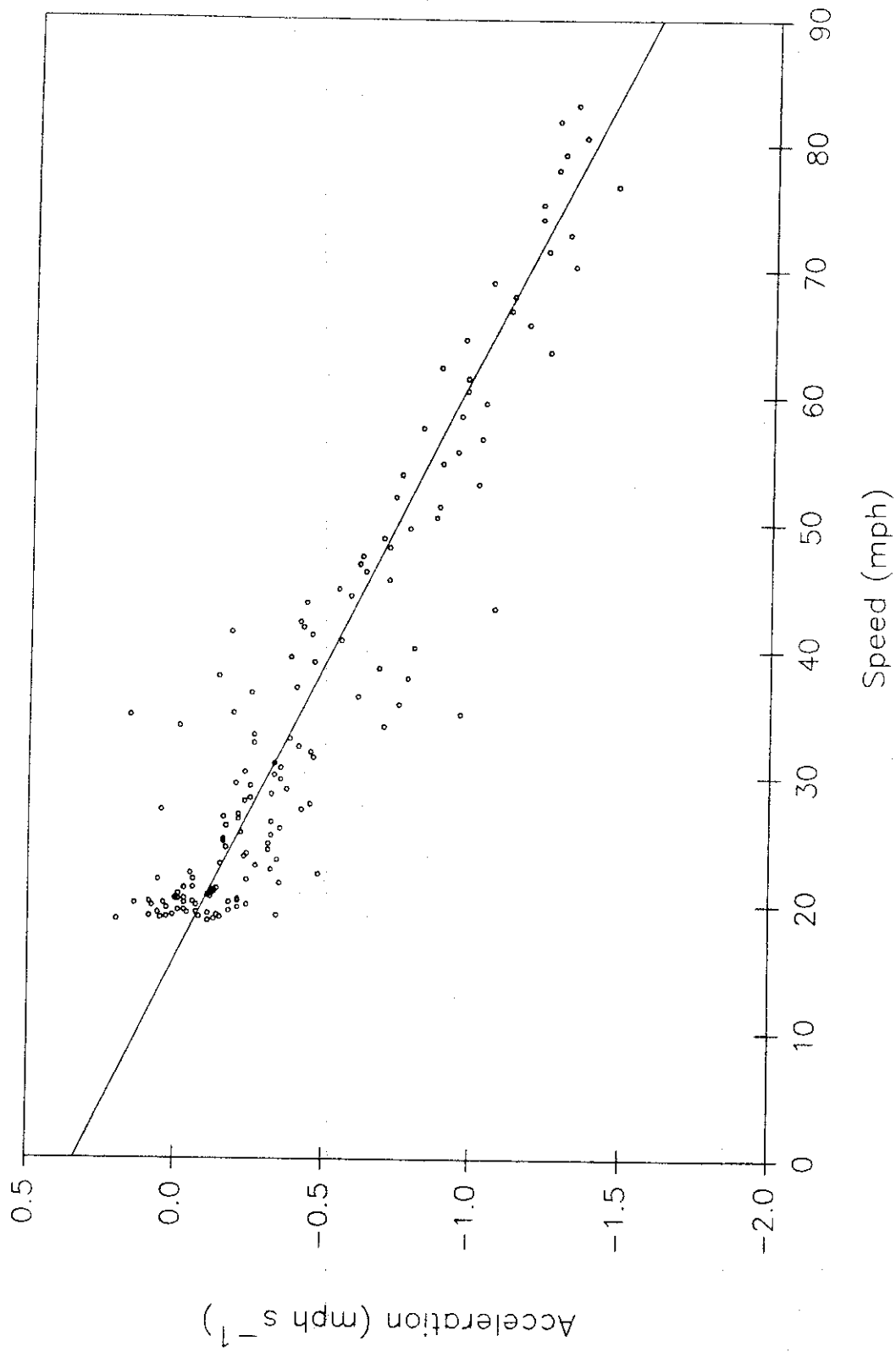


Figure 3.2.3.3 Deceleration as a function of speed from coasting experiment used to determine natural rate of deceleration.

6% grade are presented in Table 3.2.4.1. The fourth experiments, both up- and down-hill, were conducted with the cruise control set to 65 mph. The results show the vehicle cruise control only kept the average speed at 60 mph, but it did not allow any rich open loop operation while driving up hill compared to an average frequency of 3% of the time without the use of the cruise control. The experiments without the use of the cruise control did not appear to be driven in a more aggressive manner because the maximum rate of acceleration for these experiments was approximately the same as for with the use of the cruise control. There may be a portion of the EEC which does not allow for rich open loop operation with the use of the cruise control.

For the downhill trip (Figures 3.2.4.1 and 3.2.4.2), the vehicle coasted down the grade with no application of the throttle but occasional application of the brake (between 70 and 340 seconds, before and after driving on the level terrain at the beginning and end of the grade). When the vehicle was coasting, the vehicle operated lean open loop which closed the fuel injectors. It is believed the reason for this lean open loop operation is to increase fuel economy. At the bottom of the coasting portion, the throttle was applied and the vehicle went into closed loop operation again and began delivering fuel to the engine at stoichiometry.

For the uphill trip (Figures 3.2.4.3 and 3.2.4.4), the load increased close to the maximum when the grade began (at approximately 80 seconds) and except for some deviations, remained at high load for the entire uphill trip to the level terrain. There were six occurrences of rich open loop operation, with the longest occurrence lasting 10 seconds.

Both the downhill and uphill experiments were repeated with the cruise control set of 65 mph. For the downhill experiments, the cruise control would not remain on because the vehicle would coast faster than the set speed of 65 mph and therefore no coasting data with the cruise control on was obtained. For the uphill experiment, the cruise control increased the throttle position as the load increased, and then began to increase and decrease the throttle position in a cyclical manner (shown in Figure 3.2.4.5) from 340 to 530 (arbitrary units) through seven cycles and the speed of the vehicle also

Table 3.2.4.1 Summary of up- and down-hill grade experiments results with and without the use of cruise control.

Trip Number	Travel Time minutes	Distance Traveled miles	Average Speed mph	Maximum Speed mph	Maximum Acceleration mph s-1	Fuel Economy mpg	% Open Loop Rich	% Open Loop Lean
Uphill								
1	7.28	7.49	61.81	68.11	0.84	18.03	3.21	0.00
2	7.20	7.49	62.53	69.06	0.74	17.76	4.87	0.00
3	7.10	7.49	63.42	68.30	0.77	17.52	1.18	0.00
Average	7.19	7.49	62.59	68.49	0.78	17.77	3.09	0.00
4- w/CC	7.43	7.48	60.55	65.46	0.76	17.79	0.00	0.00
Downhill								
1	7.07	7.44	63.30	68.09	0.98	206.83	0.00	68.56
2	6.97	7.44	64.19	66.75	0.82	191.90	0.00	66.67
3	6.95	7.44	64.36	70.04	1.01	190.80	0.00	65.87
Average	7.00	7.44	63.95	68.29	0.94	196.51	0.00	67.03
4 - w/CC	6.82	7.41	65.35	70.19	0.71	212.91	0.00	66.67

varied in the same manner from 60 to 64 mph. After the seven cycles, the throttle position remained at a fixed setting of 412 and the speed of the vehicle decreased to 53 mph and then increased again after the end of the grade. The load and the fuel injector pulse width (Figure 3.2.4.6) also varied slightly during the cycles of throttle position and speed and then remained fixed at 0.64 and 3200, respectively, during the remainder of the grade. The most significant finding of the experiment is that during the entire experiment the vehicle remained closed loop. This implies the vehicle has the ability to operate at high loads (the maximum was 0.70) and not operate open loop.

3.2.5 Repeated Freeway Experiment

During the repeated freeway experiment, the 405 freeway was driven back and forth from Wilshire boulevard to Victory boulevard from 5:00 to 20:00. As can be seen from Table 3.2.5.1 and Figure 3.2.5.1, the two longest times of travel in the morning were 25 and 31 minutes and occurred south bound when departing at 7:53 and 8:32 am. The average time when maximum time of travel occurred (8:12.5) was rounded to 8:00

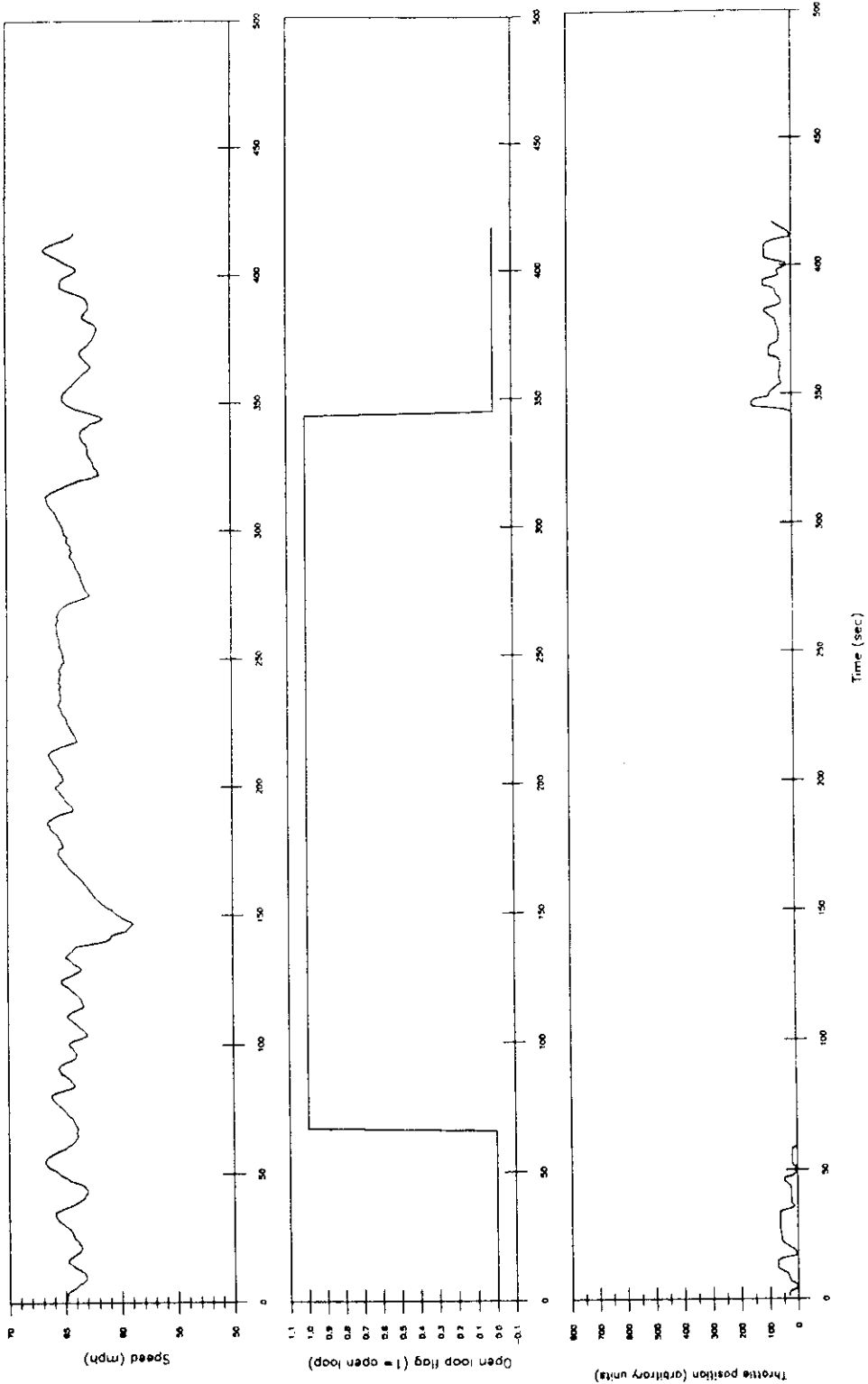


Figure 3.2.4.1 Speed, open loop flag, and throttle position during downhill trip on 5 mile 6% grade.

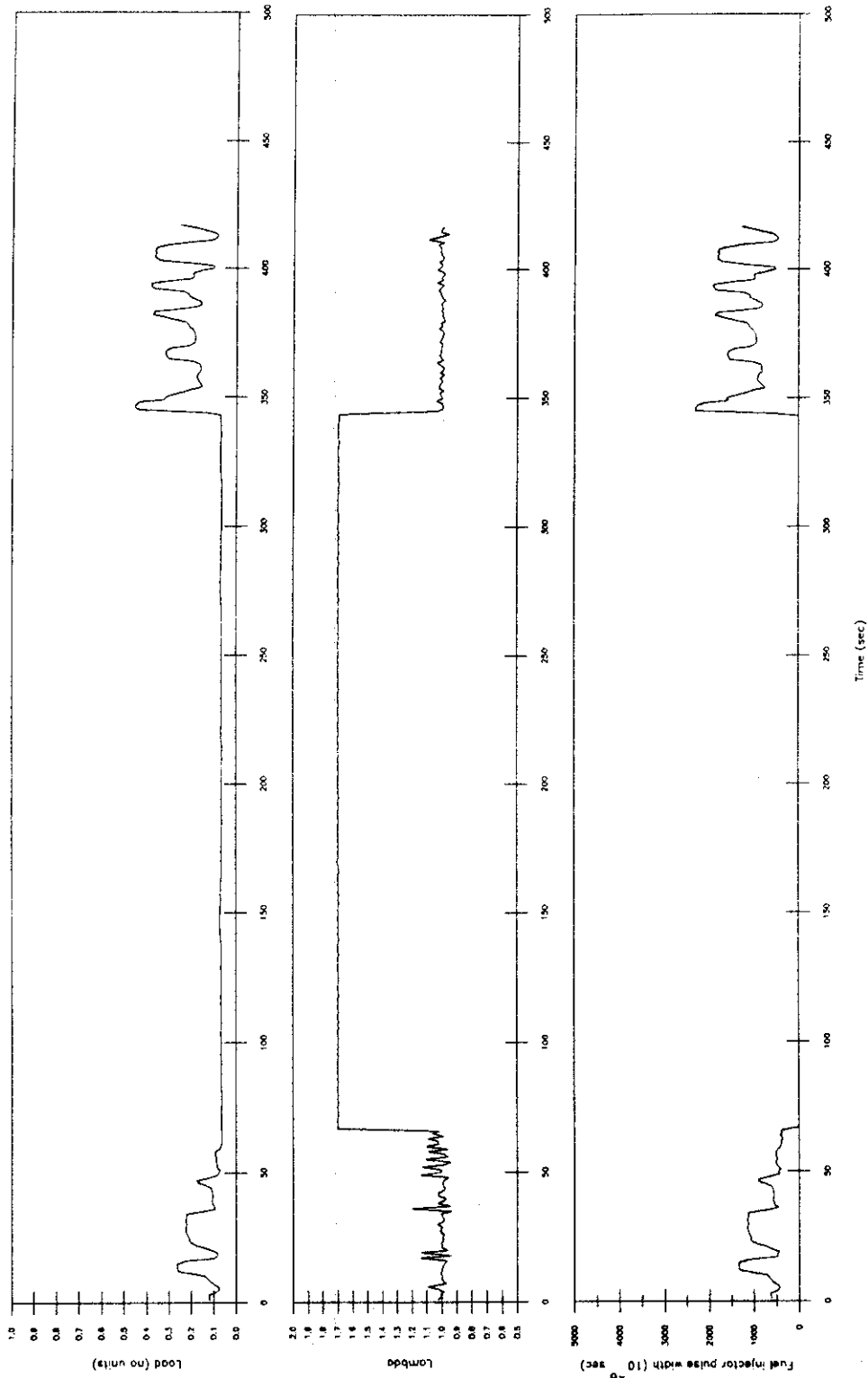


Figure 3.2.4.2 Load, lambda, and fuel injector pulse width during downhill trip on 5 mile 6% grade.

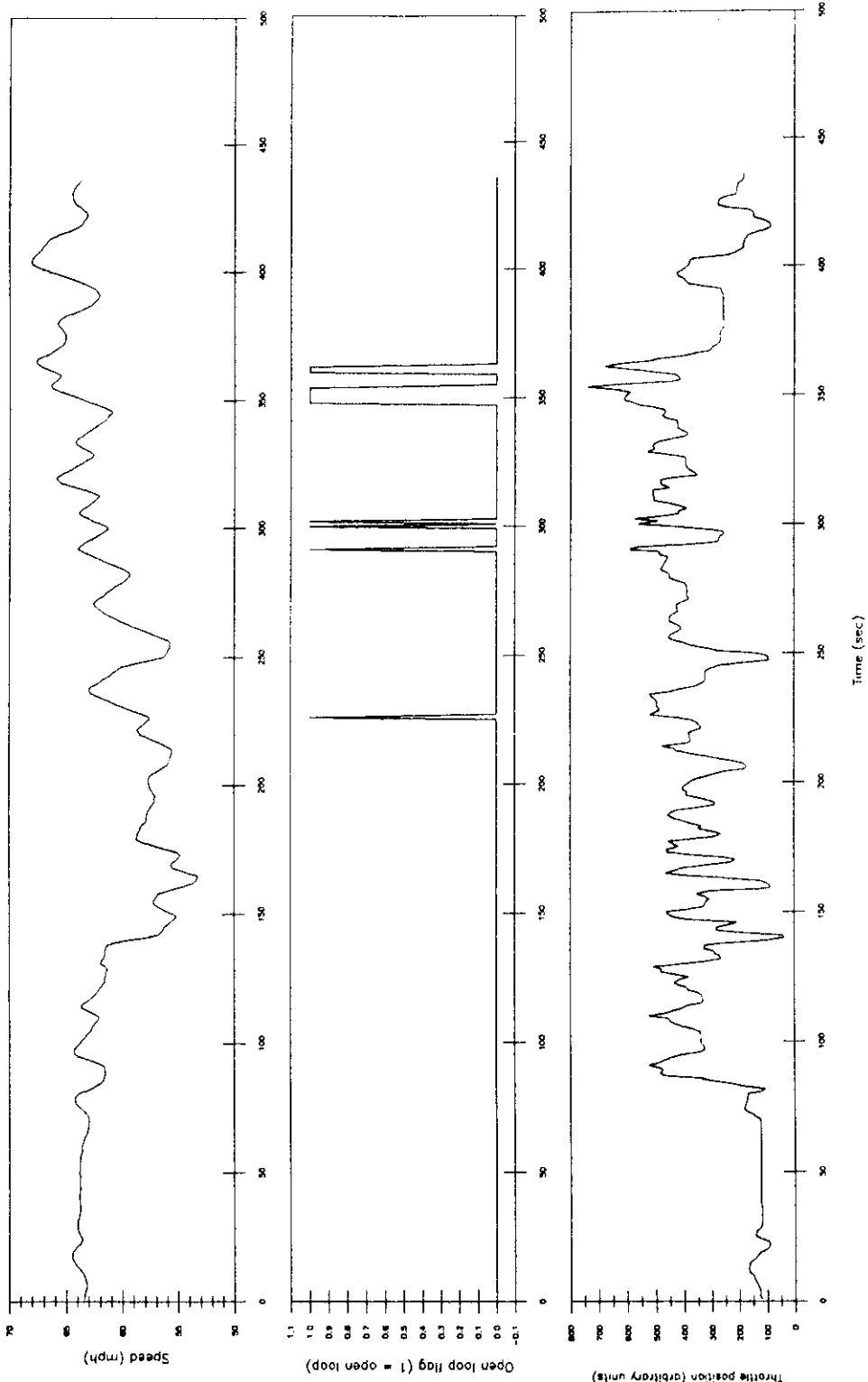


Figure 3.2.4.3 Speed, open loop flag, and throttle position during uphill trip on 5 mile 6% grade.

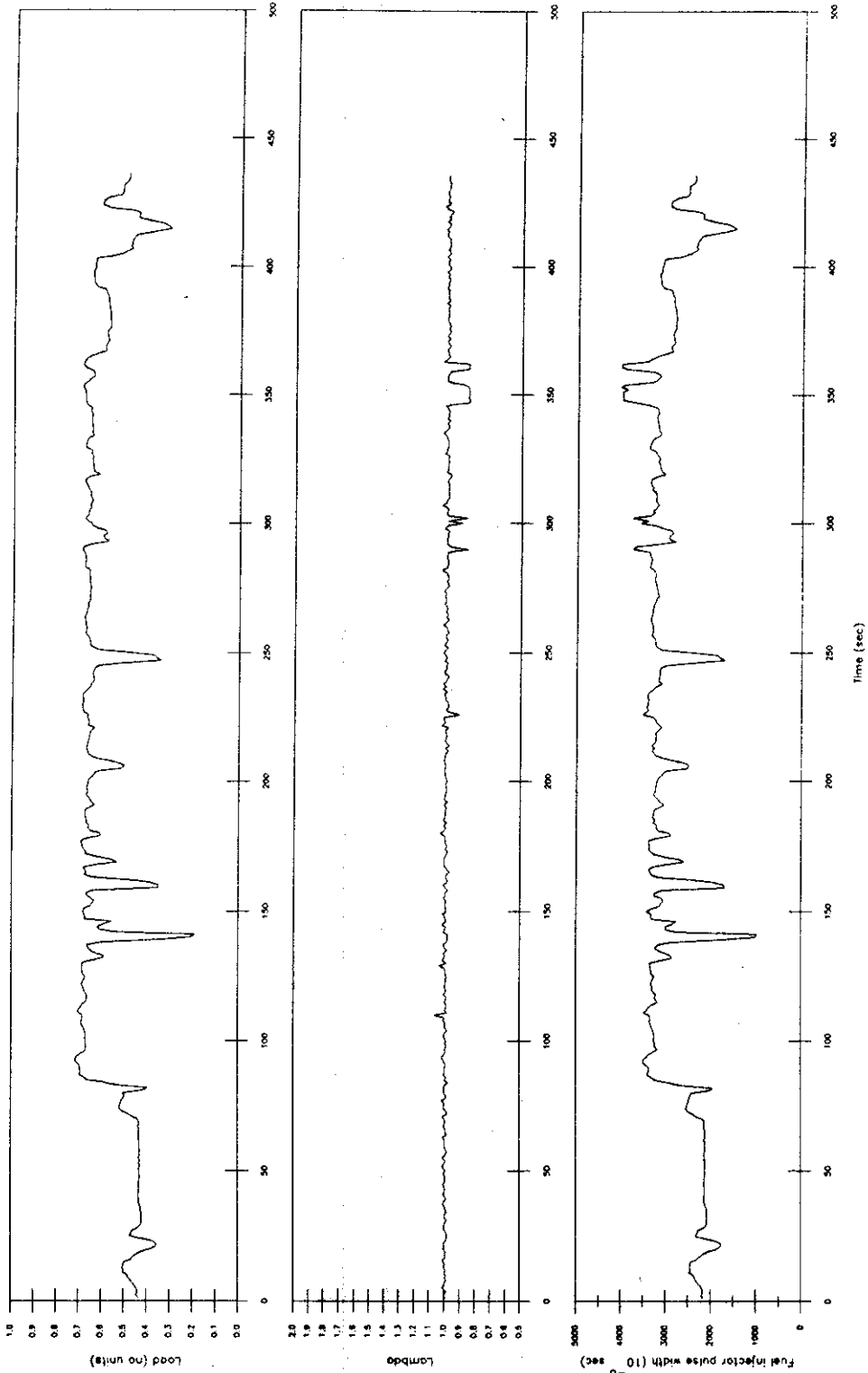


Figure 3.2.4.4 Load, lambda, and fuel injector pulse width during uphill trip on 5 mile 6% grade.

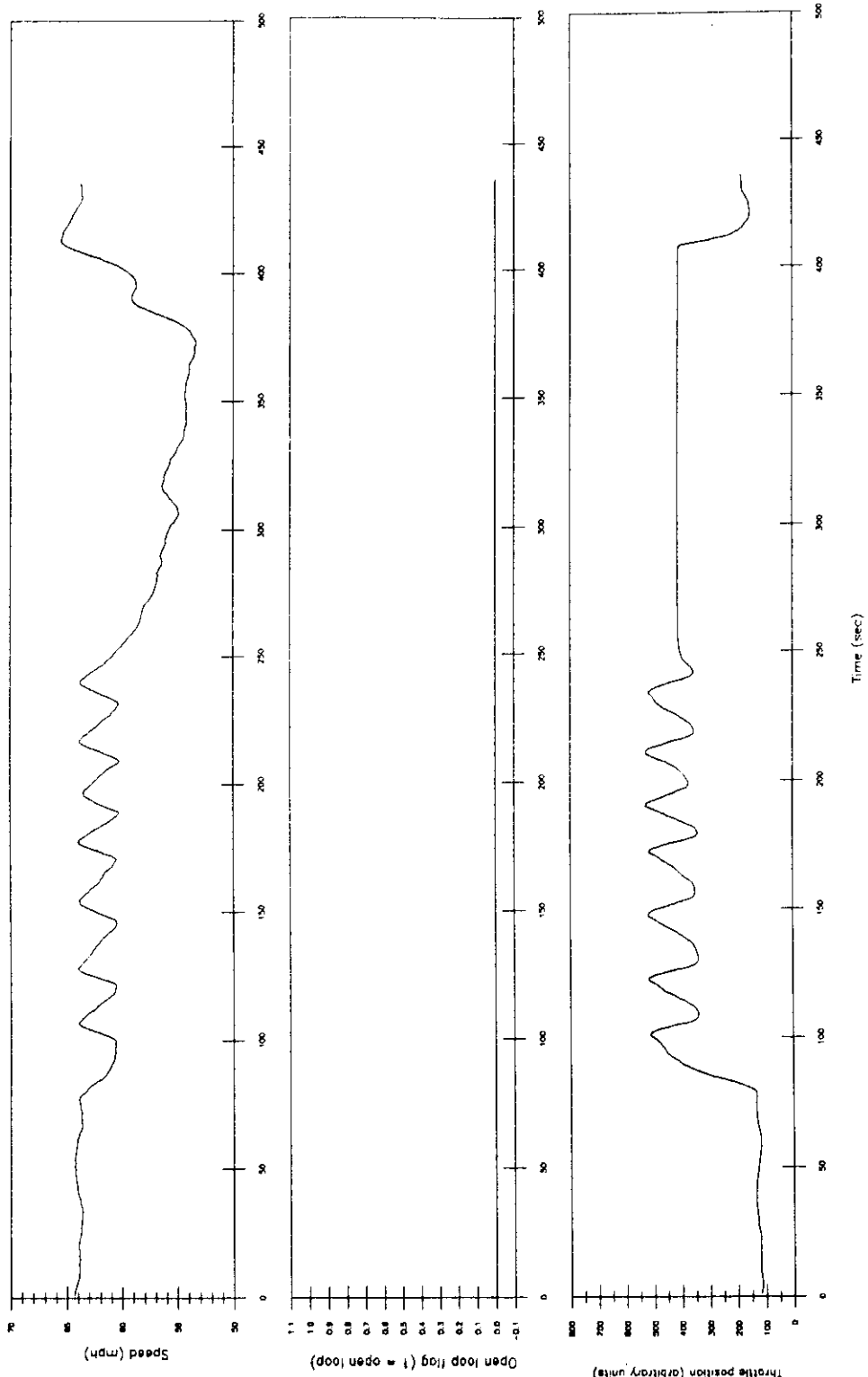


Figure 3.2.4.5 Speed, open loop flag, and throttle position during uphill trip on 5 mile 6% grade with cruise control set at 65 mph.

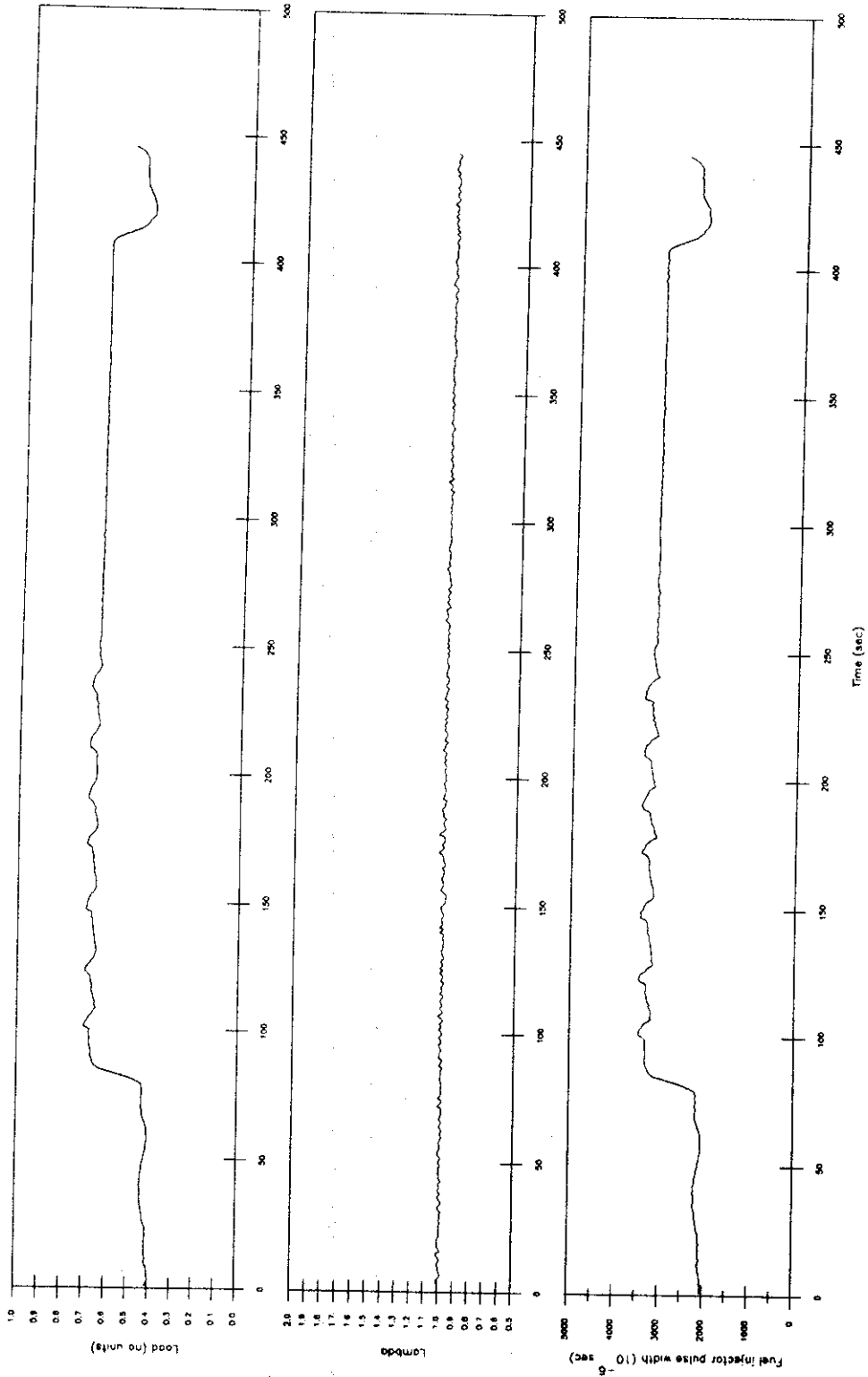


Figure 3.2.4.6 Load, lambda, and fuel injector pulse width during uphill trip on 5 mile 6% grade with cruise control set at 65 mph.

because the shape of the peak appeared weighted to earlier time of departure. In the evening, the longest times of travel were both 21 minutes in the north bound direction with departure times of 4:52 and 5:27 pm. The average time when maximum time of travel occurred (5:08.5) was rounded to 5:15 because the shape of the peak appeared approximately normally distributed. As mentioned in the Experimental section, these data were used to determine the time of departure for the conservative and aggressive driving matrices. The expected increase in travel time during rush hour south bound (towards the down town area) in the morning and north bound (away from down town) in the evening was observed.

Fuel economy as a function of average speed and direction of travel for these runs is also shown in Figure 3.2.5.1. The average fuel economy for the north bound trips was 30.7 mpg and in the south bound direction was 39.0 mpg. The difference in fuel economy with direction of travel occurred because the ending point in the north bound direction (Victory Blvd.) was at a higher elevation than the starting point (Wilshire Blvd.) and therefore more energy was required for travel in this direction of travel as opposed to south bound. In both directions, the fuel economy was better at higher average speeds than lower average speeds, although the frequency of open loop operation was higher at higher average speeds. In both directions the fuel economies were higher than predicted by the FTP (23.1 mpg) but were split above and below the predicted fuel economy of the HFET (37.5 mph).

3.2.6 Comparison of Conservative Driving to the FTP

Tables 3.2.6.1, 3.2.6.2 and Figure 3.2.6.1 show comparisons of the freeway, urban, and combined freeway and urban on-road matrix data with the FTP as a function of vehicle operating parameter. On-road data for conservative driving were collected for 68,019 seconds on freeway routes and 94,954 seconds for urban routes for a total of 162,973 seconds of data. Data for the HFET are also included in the tables. The combined freeway and urban results are the average/maximum/minimum of the freeway and urban data weighted 1:1 because the distribution of vehicle miles traveled (VMT)

Table 3.2.5.1 Repeated freeway experiment driving parameter summary.

Depart Hourly Time	Time of Travel Minute	Distance Traveled Miles	Average Speed mph	Maximum Speed mph	Maximum Accel mph e-1	Fuel Econ mpg	% Time GM Enrich	% Open Loop Rich	% Open Loop Lean	Number Of Stops
South										
5:29 AM	10.05	9.75	58.32	71.58	6.62	42.89	5.150	0.000	8.804	0
5:51 AM	10.73	9.86	55.21	65.30	7.01	42.38	4.821	0.467	5.754	0
6:14 AM	14.20	9.76	41.30	67.23	7.36	36.43	3.408	0.353	2.468	0
6:40 AM	20.42	9.77	28.73	63.13	6.94	29.49	0.980	0.000	2.124	6
7:13 AM	23.67	9.77	24.77	65.11	8.19	30.92	1.128	0.141	1.480	5
7:53 AM	24.82	9.76	23.62	76.04	7.66	28.60	1.680	0.000	1.613	8
8:32 AM	30.55	9.75	19.16	61.82	5.05	25.33	0.546	0.000	0.109	16
9:22 AM	19.38	9.76	30.25	65.79	5.19	33.21	2.065	0.000	1.291	1
10:00 AM	14.00	9.76	41.86	65.67	6.65	38.48	1.907	0.000	0.477	0
10:38 AM	11.37	9.72	51.41	66.66	4.91	38.73	4.405	0.734	1.615	0
11:04 AM	10.77	9.76	54.46	69.08	3.02	42.30	4.186	0.930	3.721	0
11:31 AM	10.67	9.76	54.98	70.40	5.90	40.17	3.912	0.313	4.069	0
11:55 AM	10.47	9.76	56.01	69.95	3.46	41.63	3.828	0.478	6.539	0
12:20 PM	10.80	9.75	54.27	63.83	5.70	42.86	3.246	0.155	4.637	0
12:59 PM	10.63	9.76	55.15	66.30	4.34	39.54	6.907	0.471	3.925	0
1:22 PM	10.18	9.76	57.58	68.28	3.88	39.17	5.738	0.656	2.623	0
1:48 PM	10.35	9.75	56.62	65.82	2.85	42.03	5.161	0.645	3.710	0
2:13 PM	10.35	9.75	56.63	64.89	2.64	41.64	5.968	0.484	4.032	0
2:45 PM	10.73	9.75	54.58	63.71	2.69	40.13	7.154	0.622	5.599	0
3:35 PM	10.67	9.75	54.91	63.19	2.88	42.48	3.286	0.000	3.443	0
4:05 PM	10.53	9.74	55.58	62.54	2.10	44.02	1.585	0.000	4.120	0
4:40 PM	10.30	9.75	56.90	65.03	2.69	42.48	1.945	0.000	6.969	0
5:14 PM	10.75	9.76	54.56	64.52	2.75	42.50	3.106	0.000	9.317	0
5:56 PM	10.08	9.74	58.08	70.55	2.44	39.63	8.940	0.331	4.636	0
6:36 PM	9.77	9.75	60.00	67.08	2.77	40.03	4.615	0.000	4.957	0
7:02 PM	9.88	9.75	59.29	71.49	2.99	41.45	2.872	0.000	6.926	0
7:30 PM	10.77	9.86	55.06	66.08	2.30	43.74	3.721	0.000	7.132	0
Avg/Max	13.22	9.76	49.23	76.04	8.19	38.97	3.787	0.251	4.151	1.33
North										
5:19 AM	9.43	9.72	61.92	71.02	2.75	29.29	9.204	0.000	8.496	0
5:40 AM	9.88	9.68	58.88	71.38	2.97	30.39	3.209	0.000	5.068	0
6:03 AM	9.27	9.68	62.76	71.45	3.15	29.10	10.270	0.000	10.450	0
6:29 AM	9.35	9.68	62.23	68.41	3.06	30.43	6.607	0.357	8.214	0
7:02 AM	9.65	9.67	60.23	70.94	3.37	31.01	8.824	0.346	10.380	0
7:41 AM	9.97	9.69	58.41	67.94	3.10	32.62	5.360	0.000	4.858	0
8:20 AM	9.68	9.67	60.02	68.11	3.11	32.06	5.862	0.000	9.850	0
9:02 AM	9.83	9.68	59.14	68.93	2.91	32.62	9.168	0.000	11.540	0
9:45 AM	10.00	9.67	58.14	68.32	2.58	34.06	4.174	0.000	11.520	0
10:27 AM	10.37	9.68	56.13	67.09	2.05	31.71	6.441	0.000	6.280	0
10:54 AM	9.88	9.68	58.85	70.96	2.48	30.82	7.601	0.338	6.419	0
11:18 AM	10.22	9.68	56.95	67.48	3.57	32.16	4.575	0.980	7.843	0
11:42 AM	10.18	9.66	57.03	67.83	2.04	31.96	4.426	1.311	6.230	0
12:08 PM	10.02	9.68	58.06	68.16	2.98	31.89	5.333	0.500	4.167	0
12:31 PM	10.18	9.68	57.11	73.09	3.22	32.39	4.754	0.328	0.820	0
1:11 PM	9.95	9.68	58.48	69.70	2.55	32.81	3.859	0.168	3.859	0
1:36 PM	10.15	9.68	57.34	68.07	2.12	33.37	2.796	0.329	5.263	0
2:00 PM	10.53	9.68	55.20	68.76	2.78	32.44	2.536	0.792	2.536	0
2:26 PM	10.43	9.68	55.73	66.28	2.16	31.76	4.640	0.800	2.880	0
3:20 PM	14.27	9.68	40.78	62.84	3.43	29.99	2.105	0.000	2.105	0
3:47 PM	16.15	9.68	36.01	64.12	5.02	28.53	0.930	0.000	5.579	2
4:17 PM	20.63	9.69	28.19	58.75	5.83	26.74	1.213	0.000	0.000	7
4:52 PM	20.83	9.68	27.91	57.78	5.23	25.46	0.801	0.000	0.000	5
5:27 PM	21.27	9.68	27.33	54.73	5.04	24.36	1.569	0.000	0.000	5
6:07 PM	17.15	9.68	33.89	61.25	3.54	27.84	0.778	0.000	0.486	0
6:48 PM	11.95	9.68	48.68	68.21	3.03	30.53	5.028	0.000	0.419	0
7:13 PM	9.75	9.68	59.66	67.81	3.36	32.09	6.678	0.000	9.589	0
Avg/Max	11.89	9.68	52.41	73.09	5.83	30.68	4.768	0.231	5.365	0.70
All Avg/Max	12.55	9.72	50.82	76.04	8.19	34.83	4.278	0.241	4.758	1.02

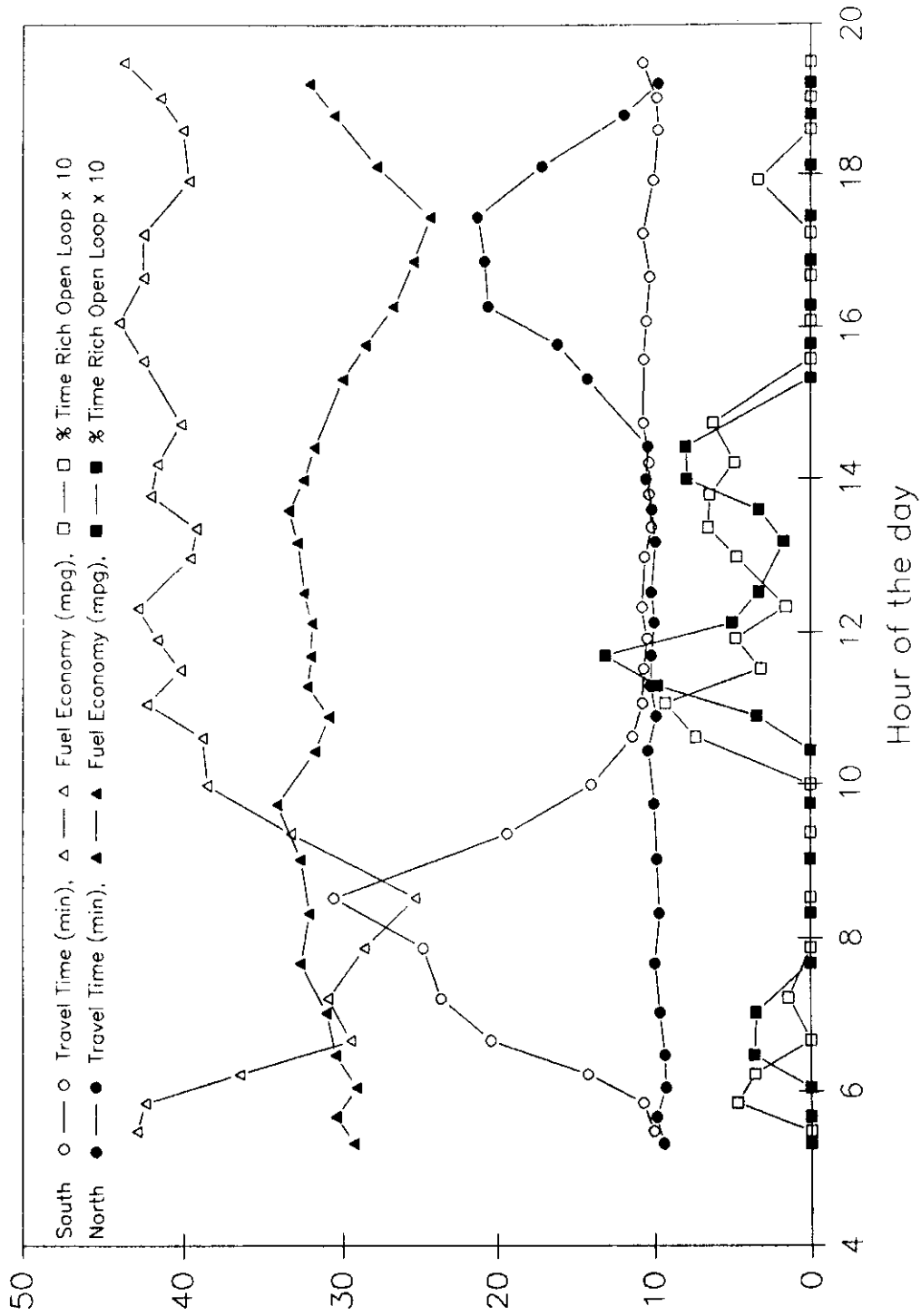


Figure 3.2.5.1 Time of travel, percent time open loop and fuel economy for repeated freeway experiment by direction of travel.

Table 3.2.6.1 Driving parameter data for the FTP and the HFET.

Dynamometer Experiment and Bag Number	Travel	Travel	Avg.	Max	Max	Max	Fuel	GM	Open	Open	Open	Avg Dist
	Time	Dist	Speed	Speed	Accel	Decel	Econ	Enrich	Loop	Loop	Loop	Per Stop
	min	miles	mph	mph	mph s ⁻¹	mph s ⁻¹	mpg	%	%	Rich %	Lean %	miles
FTP Experiment 1, bag 1	8.43	3.51	25.05	55.96	5.08	3.93	22.13	0.99	0.00	0.00	0.00	0.70
FTP Experiment 2, bag 1	8.43	3.51	25.06	55.92	4.49	3.97	22.10	0.00	0.00	0.00	0.00	0.70
FTP Experiment 3, bag 1	8.43	3.51	25.02	55.49	4.75	3.78	22.40	0.59	0.00	0.00	0.00	0.70
FTP Bag 1, average	8.43	3.51	25.04	55.79	4.77	3.89	22.21	0.53	0.00	0.00	0.00	0.70
FTP Experiment 1, bag 2	14.47	3.77	15.64	33.56	4.46	3.80	22.01	0.79	0.00	0.00	0.00	0.27
FTP Experiment 2, bag 2	14.47	3.76	15.62	33.44	4.58	3.94	21.73	0.00	0.00	0.00	0.00	0.27
FTP Experiment 3, bag 2	14.47	3.76	15.61	33.74	4.69	4.26	21.96	0.59	0.00	0.00	0.00	0.27
FTP Bag 2, average	14.47	3.76	15.62	33.58	4.58	4.00	21.90	0.46	0.00	0.00	0.00	0.27
FTP Experiment 1, bag 3	8.43	3.50	24.96	55.68	4.88	4.11	25.71	0.40	0.00	0.00	0.00	0.58
FTP Experiment 2, bag 3	8.43	3.50	24.93	55.54	4.81	4.01	24.98	0.00	0.00	0.00	0.00	0.58
FTP Experiment 3, bag 3	8.43	3.50	24.94	55.47	4.57	3.85	25.06	0.40	0.00	0.00	0.00	0.58
FTP Bag 3, average	8.43	3.50	24.94	55.56	4.75	3.99	25.25	0.26	0.00	0.00	0.00	0.58
FTP all bags, average	10.44	3.59	21.87	48.31	4.70	3.96	23.12	0.42	0.00	0.00	0.00	0.52
HFET 1	14.10	9.98	42.53	58.42	3.31	3.16	37.65	0.00	0.00	0.00	0.00	9.98
HFET 2	14.42	9.98	41.58	58.25	4.55	3.38	37.18	0.00	0.00	0.00	0.00	9.98
HFET 3	14.00	9.98	42.84	58.32	3.55	3.29	37.71	0.00	0.00	0.00	0.00	9.98
HFET average	14.17	9.98	42.32	58.33	3.80	3.28	37.51	0.00	0.00	0.00	0.00	9.98

between freeway and urban routes are approximately equal in the SoCAB (SCAG, 1985).

The data show significant differences between the freeway and urban experiments. The average (36.5 versus 22.1 mph) and maximum (73.9 versus 61.2 mph) speed, fuel economy (34.0 versus 23.2 mpg) and average distance per stop (4.99 versus 0.63 mi) were greater for the freeway experiments. The maximum rates of acceleration (5.84 versus 7.98 mph s⁻¹) and deceleration (9.43 versus 10.46 mph s⁻¹) were greater for the urban experiments.

Results from equal weighting of the on-road freeway and urban routes driven in the SoCAB in this study were higher than the FTP for average speed (29.3 versus 20.7 mph), maximum speed (73.9 versus 56.6 mph), maximum rate of acceleration (8.0 versus 3.3 mph s⁻¹), maximum rate of deceleration (10.5 versus 3.3 mph s⁻¹), fuel economy (28.6 versus 23.1 mpg), and a greater average distance per stop (2.8 versus 0.46 miles). The maximum acceleration rate measured by the RCON during three FTP experiments on the dynamometer was 5.08 mph s⁻¹. Although this was higher than the acceleration rate specified in the UDDS (3.3 mph s⁻¹), it was well within the allowable instantaneous

Table 3.2.6.2 Driving parameter data for on-road conservative driving experiments.

Route	Depart	Travel	Travel	Avg.	Max	Max	Max	Fuel	GM	Open	Open	Avg Dst
Number	Time	Time	Dist	Speed	Speed	Accel	Decel	Econ	Enrich	Loop	Loop	Per Stop
Dir, Expt#	hr:min	min	miles	mph	mph	mph s-1	mph s-1	mpg	%	Rich %	Lean %	miles
Freeway Routes												
1-NS-36	7:30	59.97	49.83	49.87	71.58	4.46	5.06	42.7	1.28	0.00000	2.31	16.61
1-SN-37	16:30	62.13	49.72	48.03	73.76	3.33	4.62	35.7	0.86	0.00000	1.64	24.86
2-NS-40	7:30	47.68	28.05	35.30	66.37	5.84	8.13	35.9	0.91	0.00000	1.43	3.51
2-SN-41	16:30	60.25	27.97	27.86	62.95	5.23	5.70	28.0	0.89	0.00000	0.83	1.47
3-NS-38	7:30	74.23	41.74	33.75	67.12	5.04	6.64	36.7	1.08	0.00000	2.04	1.35
3-SN-39	16:30	83.07	41.71	30.14	69.09	4.95	5.71	27.8	1.16	0.00000	0.78	2.09
4-SN-17	7:30	49.20	37.09	45.25	71.72	5.07	5.65	36.4	0.34	0.00000	0.75	3.71
4-NS-18	16:30	61.83	36.81	35.73	68.81	5.36	7.16	32.7	0.16	0.00000	0.16	2.63
5-SN-25	7:30	49.73	27.27	32.91	62.91	3.92	5.29	32.0	0.30	0.00000	0.30	1.95
5-NS-26	16:30	41.27	27.19	39.55	68.99	5.67	5.25	37.1	0.24	0.00000	0.85	2.47
6-SN-29	7:30	79.30	39.57	29.94	73.87	4.97	4.93	31.4	0.29	0.00000	0.15	1.98
6-NS-30	16:30	80.53	39.41	29.37	64.81	4.08	6.77	31.2	0.17	0.00000	0.04	2.07
7-EW-2	7:30	97.18	59.11	36.50	72.89	4.50	6.73	32.3	1.05	0.03431	0.93	3.11
7-WE-3	16:30	98.80	58.31	35.42	65.68	4.57	9.43	34.2	0.29	0.01687	0.27	7.29
8-NS-13	7:30	78.12	56.72	43.58	70.78	5.39	4.76	37.9	0.00	0.00000	0.51	2.84
8-SN-14	16:30	110.42	57.27	31.12	68.78	5.72	7.60	31.2	0.17	0.00000	0.27	1.97
Freeway Averages		70.86	42.36	36.52	68.76	4.88	6.21	33.9	0.57	0.00320	0.83	4.99
Freeway Std. Dev.		20.22	11.60	6.88	3.56	0.70	1.36	3.9	0.44	0.00930	0.69	6.48
Freeway Maxima		110.42	59.11	49.87	73.87	5.84	9.43	42.7	1.28	0.03431	2.31	24.86
Freeway Minima		41.27	27.19	27.86	62.91	3.33	4.62	27.8	0.00	0.00000	0.04	1.35
Urban Routes												
1-NS-6	7:30	122.00	50.88	25.03	61.23	7.98	10.46	25.3	1.08	0.00000	0.31	0.89
1-SN-7	16:30	129.20	50.91	23.65	54.15	6.99	7.97	23.1	1.44	0.00000	0.00	0.71
2-EW-46	7:30	130.47	49.07	22.57	51.25	7.28	9.79	24.6	0.98	0.00000	0.00	0.58
2-WE-47	16:30	133.03	49.06	22.13	51.59	6.73	8.99	22.7	1.38	0.00000	0.00	0.61
3-EW-42	7:30	104.28	35.99	20.71	49.31	7.10	8.74	22.8	0.90	0.01599	0.02	0.44
3-WE-43	16:30	118.47	35.99	18.23	47.51	7.79	8.52	21.7	0.58	0.00000	0.00	0.36
4-WE-21	7:30	74.38	29.08	23.46	49.20	6.63	9.62	23.8	0.43	0.00000	0.00	0.59
4-EW-22	16:30	107.63	29.03	16.19	54.74	7.49	7.31	18.6	1.90	0.09292	0.11	0.31
5-SN-11	7:30	78.40	27.51	21.06	46.57	6.58	7.18	20.9	0.70	0.00000	0.00	0.51
5-NS-12	16:30	96.62	27.45	17.05	43.39	6.28	9.62	21.5	0.09	0.00000	0.00	0.33
6-NS-27	7:30	64.82	25.05	23.20	58.49	6.69	7.31	24.2	1.21	0.00000	0.00	0.70
6-SN-28	16:30	65.62	25.06	22.92	58.09	7.29	8.46	24.1	1.85	0.00000	0.00	0.63
7-SN-50	7:30	92.45	40.05	26.00	58.37	6.99	8.28	26.0	0.97	0.00000	0.04	1.03
7-NS-51	16:30	103.55	40.03	23.20	52.57	6.84	8.55	23.6	1.16	0.00000	0.00	0.77
8-EW-48	7:30	75.38	32.78	26.09	52.88	6.82	9.27	24.7	0.57	0.00000	0.00	0.80
8-WE-49	16:30	86.53	32.73	22.70	55.77	6.98	7.15	24.0	0.40	0.00000	0.02	0.76
Urban Averages:		98.93	36.29	22.14	52.82	7.03	8.58	23.2	0.98	0.00681	0.03	0.63
Urban Std. Dev.		23.33	9.38	2.90	4.91	0.45	1.02	1.8	0.51	0.02331	0.08	0.20
Urban Maxima		133.03	50.91	26.09	61.23	7.98	10.46	26.0	1.90	0.09292	0.31	1.03
Urban Minima		64.82	25.05	16.19	43.39	6.28	7.15	18.6	0.09	0.00000	0.00	0.31
Combined Averages:												
Combined Averages:		84.89	39.33	29.33	60.79	5.96	7.40	28.6	0.78	0.00500	0.43	2.81
Combined Std. Dev.		25.78	10.82	8.96	9.13	1.23	1.68	6.2	0.51	0.01755	0.63	5.02
Combined Maxima		133.03	59.11	49.87	73.87	7.98	10.46	42.7	1.90	0.09292	2.31	24.86
Combined Minima		41.27	25.05	16.19	43.39	3.33	4.62	18.6	0.00	0.00000	0.00	0.31

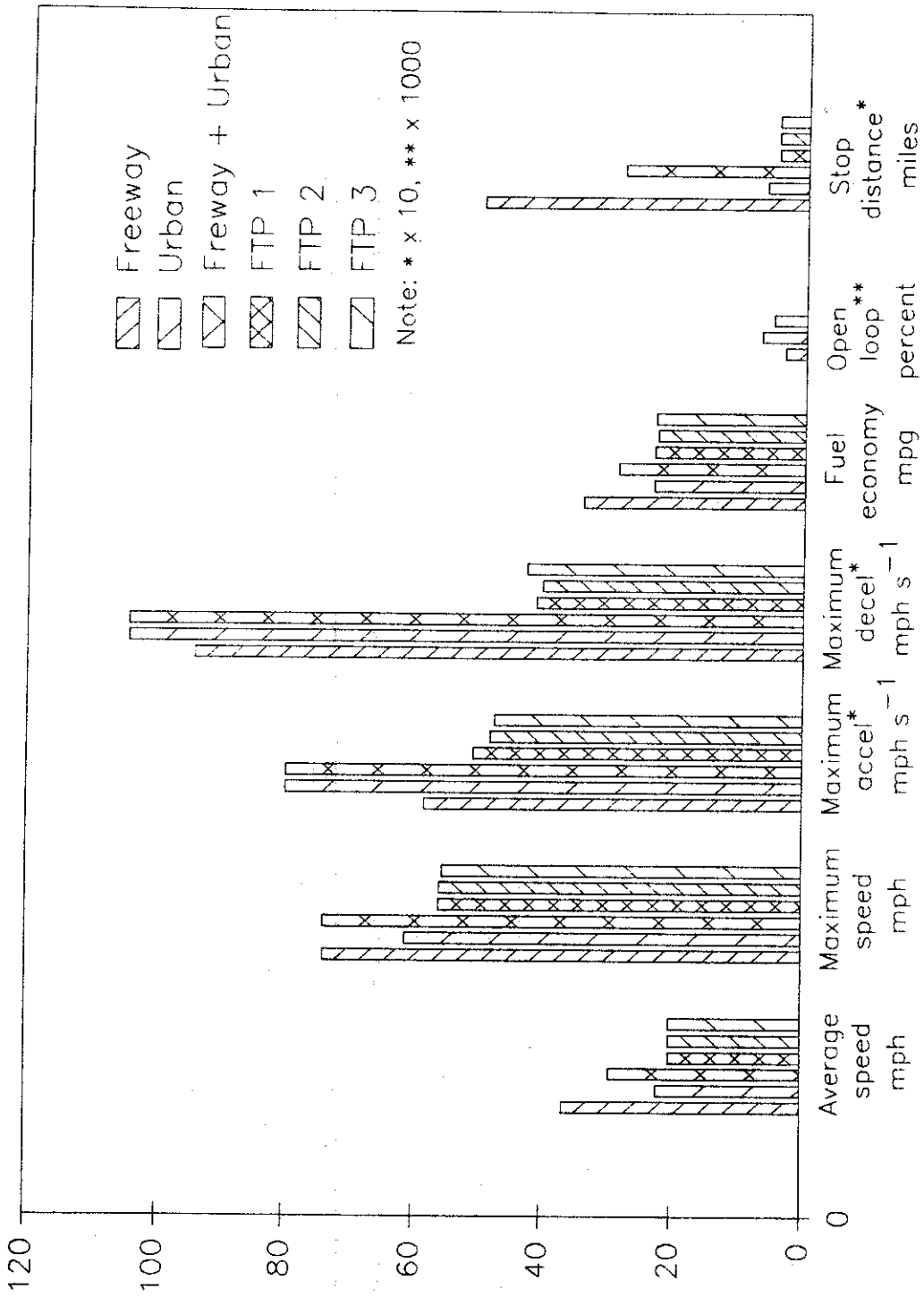


Figure 3.2.6.1 Comparison of the freeway, urban, and combined freeway and urban on-road matrix data with the FTP by vehicle operating parameter.

acceleration range for the FTP.

Comparison of the percent time spent in acceleration based modes for the average freeway and urban on-road data and the FTP reveal the FTP has more time at cruise (24.2 versus 18.5%), stopped (17.4 versus 12.7%), and in hard decelerations (3.1 versus 1.9%) than the on-road data (Tables 3.2.6.3, 3.2.6.4 and Figure 3.2.6.2). There is no coasting or hard acceleration in the FTP and compared to the average on-road conditions it under-represents medium accelerations (0.58 versus 1.03%).

The average time in the acceleration based modes when they occurred for the FTP and the conservatively driven on-road routes is presented in Tables 3.2.6.5 and 3.2.6.6. There were only small differences between the FTP and the average on-road routes, however there were a few significant differences between the urban and the freeway routes. The largest difference was between the time stopped for the freeway and urban routes (8.0 versus 21.9 seconds).

The percent time in the load based modes for the FTP and the on-road experiments is presented in Tables 3.2.6.7 and 3.2.6.8. The load based modes include open loop operation and therefore there were no occurrences for the FTP but there was 0.01% rich and 0.43% lean open loop operation on-road. The FTP contained only 0.26% time in high load mode versus 1.26% on-road. The percent time in medium high, medium low and low load modes for the FTP (21.7, 10.2, and 65.2%) showed a similar trend to the average of the freeway and urban on-road data (29.4, 11.3, and 57.6%). However, the freeway experiments had more time in medium high loads than urban experiments (45.2 versus 13.7%), slightly less time in medium low loads (6.9 versus 15.6%) and less time in low loads (45.8 versus 69.4%).

The average, maximum and minimum values for the FTP and HFET and the conservatively driven on-road data are shown in Tables 3.2.6.9 through 3.2.6.14. The maximum load observed for the FTP was 0.73 and for the HFET was 0.66 compared to 0.75 for both the on-road freeway and urban experiments, and the average load for the FTP and the HFET were close to the average on-road freeway and urban load (0.26 and 0.28 versus 0.26).

Table 3.2.6.3 Percent time in acceleration-based modes for the FTP and the HFET.

Dynamometer Experiment and Bag Number	Modes									
	Cold	At	Cruise	Coast	Hard	Med	Light	Hard	Med	Light
	Start	Stop			Accel	Accel	Accel	Decel	Decel	Decel
FTP Experiment 1, bag 1	9.50	15.45	23.96	0.00	0.00	0.40	25.15	3.17	13.66	8.71
FTP Experiment 2, bag 1	9.50	15.64	21.58	0.20	0.00	0.40	27.13	2.57	13.66	9.31
FTP Experiment 3, bag 1	9.70	15.64	25.35	0.00	0.00	0.59	25.15	2.18	15.25	6.14
FTP Bag1, average	9.57	15.58	23.63	0.07	0.00	0.46	25.81	2.64	14.19	8.05
FTP Experiment 1, bag 2	0.00	19.72	22.61	1.73	0.00	0.58	31.60	4.15	15.34	4.27
FTP Experiment 2, bag 2	0.00	19.49	25.49	1.38	0.00	0.46	30.57	4.15	15.80	2.65
FTP Experiment 3, bag 2	0.00	20.18	23.18	1.38	0.00	0.46	30.57	4.04	15.80	4.38
FTP Bag2, average	0.00	19.80	23.76	1.50	0.00	0.50	30.91	4.11	15.65	3.77
FTP Experiment 1, bag 3	2.77	16.44	25.35	0.79	0.00	0.99	28.91	2.97	14.06	7.72
FTP Experiment 2, bag 3	2.57	17.03	24.95	0.40	0.00	0.59	30.10	2.57	17.03	4.75
FTP Experiment 3, bag 3	2.77	17.03	25.54	0.20	0.00	0.79	28.71	2.18	17.03	5.74
FTP Bag 3, average	2.70	16.83	25.28	0.46	0.00	0.79	29.24	2.57	16.04	6.07
FTP all bags, average	4.09	17.40	24.22	0.68	0.00	0.58	28.65	3.11	15.29	5.96
HFET 1	0.00	10.06	55.03	0.12	0.00	0.00	20.24	0.47	5.33	8.76
HFET 2	0.00	12.15	55.44	0.00	0.00	0.12	17.71	0.35	5.44	8.80
HFET 3	0.00	9.42	55.07	0.00	0.00	0.00	20.86	0.24	6.32	8.10
HFET average	0.00	10.54	55.18	0.04	0.00	0.04	19.60	0.35	5.70	8.55

The maximum air/fuel ratio for the Horiba instrument (recorded as lambda - measured air/fuel divided by the theoretical stoichiometric air/fuel ratio) was either 0.70 or 1.71 for all on-road freeway experiments (there was lean open loop operation during all on-road freeway experiments). For the on-road urban experiments which contained lean open loop operation, the maximum was also 1.70 except for one case in which it was 1.61. It appears that a value of 1.70 is the maximum lean value of the sensor because during the downhill grade experiments when no fuel was supplied to the engine (the engine was only pumping air), the same maximum was observed. The same comparison for rich open loop operation was difficult due to the low frequency of rich open loop operation for conservative driving, however a better comparison is included in the discussion of the aggressive driving experiments. The maximum and minimum data from the stock air/fuel sensor are not meaningful because the sensor is designed only to give

Table 3.2.6.4 Percent time in acceleration-based modes for on-road conservative driving experiments.

Route Number	Depart Time	Modes									
		Cold	At	Cruise	Coast	Hard	Med	Light	Hard	Med	Light
Dir, Expt#	hr:min	Start	Stop			Accel	Accel	Accel	Decel	Decel	Decel
Freeway Routes											
1-NS-36	7:30	0.00	0.33	33.58	3.17	0.00	0.06	33.00	0.39	10.43	19.04
1-SN-37	16:30	0.00	0.78	32.09	4.05	0.00	0.00	33.16	0.11	9.12	20.69
2-NS-40	7:30	0.00	2.66	20.52	7.62	0.00	0.45	35.98	0.87	18.67	13.22
2-SN-41	16:30	0.00	3.62	16.57	9.32	0.00	0.44	35.39	1.60	22.16	10.87
3-NS-38	7:30	0.00	6.45	22.70	11.52	0.00	0.16	31.15	1.50	14.35	12.17
3-SN-39	16:30	0.00	2.17	18.74	5.34	0.00	0.38	37.73	1.18	22.14	12.32
4-SN-17	7:30	0.00	3.02	29.24	4.00	0.00	0.14	33.85	0.81	14.84	14.10
4-NS-18	16:30	0.00	2.00	22.84	5.58	0.00	0.32	36.91	1.13	19.87	11.35
5-SN-25	7:30	0.00	5.30	20.28	7.98	0.00	0.00	35.77	1.11	13.21	16.36
5-NS-26	16:30	0.00	2.79	25.74	5.74	0.04	0.48	33.66	1.21	13.45	16.89
6-SN-29	7:30	0.00	3.83	22.85	10.97	0.00	0.08	32.42	0.90	17.17	11.77
6-NS-30	16:30	0.00	2.32	16.77	10.33	0.00	0.04	38.85	1.20	18.61	11.88
7-EW-2	7:30	0.00	2.37	22.68	10.46	0.03	0.02	36.72	0.81	12.92	14.00
7-WE-3	16:30	0.00	1.13	27.82	8.00	0.02	0.03	31.94	0.22	13.68	17.16
8-NS-13	7:30	0.00	3.61	31.24	4.80	0.00	0.30	30.35	0.96	14.17	14.58
8-SN-14	16:30	0.00	3.02	21.33	8.94	0.00	0.24	34.09	1.25	19.97	11.16
Freeway Averages		0.00	2.84	24.06	7.36	0.01	0.20	34.44	0.95	15.92	14.22
Freeway Std. Dev.		0.00	1.56	5.35	2.73	0.01	0.18	2.44	0.42	3.97	3.00
Freeway Maxima		0.00	6.45	33.58	11.52	0.04	0.48	38.85	1.60	22.16	20.69
Freeway Minima		0.00	0.33	16.57	3.17	0.00	0.00	30.35	0.11	9.12	10.87
Urban Routes											
1-NS-6	7:30	0.00	23.57	12.13	4.44	0.00	1.52	29.18	2.01	16.97	10.18
1-SN-7	16:30	0.00	19.18	14.10	3.57	0.00	1.88	29.89	2.49	18.62	10.26
2-EW-46	7:30	0.00	15.94	14.81	4.02	0.00	2.41	31.54	3.07	18.88	9.31
2-WE-47	16:30	0.00	17.44	13.90	3.17	0.00	1.92	31.81	2.97	19.35	9.45
3-EW-42	7:30	0.00	22.49	12.93	4.20	0.02	2.37	28.48	3.31	16.11	10.09
3-WE-43	16:30	0.00	23.53	8.64	7.89	0.00	1.84	30.18	3.86	16.29	7.77
4-WE-21	7:30	0.00	20.17	13.90	4.06	0.00	1.48	33.46	3.32	13.29	10.35
4-EW-22	16:30	0.00	35.67	8.55	3.65	0.09	2.15	24.02	3.10	16.99	5.78
5-SN-11	7:30	0.00	22.69	11.82	2.51	0.00	2.21	30.45	3.59	16.46	10.27
5-NS-12	16:30	0.00	28.62	7.69	7.71	0.00	1.48	29.66	3.62	15.79	5.42
6-NS-27	7:30	0.00	27.13	16.00	2.21	0.00	1.85	27.44	2.60	14.15	8.62
6-SN-28	16:30	0.00	24.16	13.06	4.09	0.00	1.88	28.30	2.69	17.71	8.10
7-SN-50	7:30	0.00	16.41	16.64	2.36	0.00	1.30	32.26	1.97	19.26	9.81
7-NS-51	16:30	0.00	23.45	13.20	1.96	0.00	2.04	29.76	2.50	18.38	8.69
8-EW-48	7:30	0.00	19.48	16.72	1.39	0.00	1.77	32.13	2.57	15.57	10.37
8-WE-49	16:30	0.00	21.31	13.66	3.27	0.00	1.64	30.28	2.49	18.19	9.17
Urban Averages:		0.00	22.58	12.98	3.78	0.01	1.86	29.93	2.89	17.00	8.98
Urban Std. Dev.		0.00	4.97	2.73	1.81	0.02	0.32	2.25	0.56	1.78	1.55
Urban Maxima		0.00	35.67	16.72	7.89	0.09	2.41	33.46	3.86	19.35	10.37
Urban Minima		0.00	15.94	7.69	1.39	0.00	1.30	24.02	1.97	13.29	5.42
Combined Averages:											
Combined Averages:		0.00	12.71	18.52	5.57	0.01	1.03	32.18	1.92	16.46	11.60
Combined Std. Dev.		0.00	10.66	7.01	2.92	0.02	0.88	3.25	1.10	3.08	3.55
Combined Maxima		0.00	35.67	33.58	11.52	0.09	2.41	38.85	3.86	22.16	20.69
Combined Minima		0.00	0.33	7.69	1.39	0.00	0.00	24.02	0.11	9.12	5.42

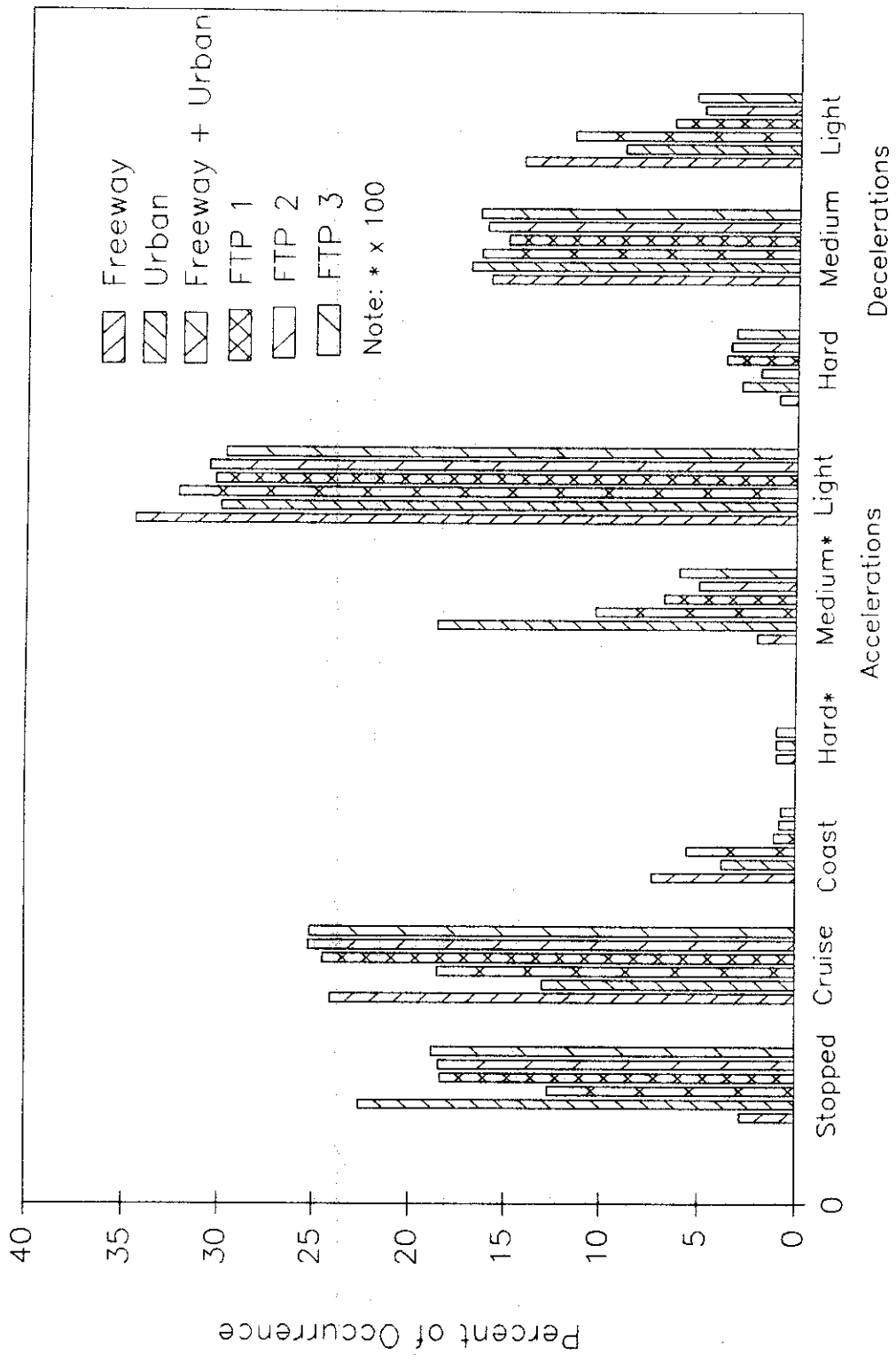


Figure 3.2.6.2 Comparison of on-road data to the FTP by percent time in acceleration based modes of operation.

Table 3.2.6.5 Average time in acceleration-based modes for the FTP and the HFET (seconds).

Dynamometer Experiment and Bag Number	Modes									
	Cold	At	Cruise	Coast	Hard	Med	Light	Hard	Med	Light
	Start	Stop			Accel	Accel	Accel	Decel	Decel	Decel
note: **** mode did not occur during driving of driving schedule										
FTP Experiment 1, bag 1	48.00	15.60	3.56	****	****	1.00	5.77	3.20	6.90	2.44
FTP Experiment 2, bag 1	48.00	15.80	2.72	1.00	****	1.00	5.27	2.60	7.67	2.14
FTP Experiment 3, bag 1	49.00	15.80	3.66	****	****	1.50	5.77	2.20	7.00	1.82
FTP Bag1, average	48.33	15.73	3.31	1.00	****	1.17	5.60	2.67	7.19	2.13
FTP Experiment 1, bag 2	****	12.21	2.76	1.67	****	1.25	6.09	2.12	4.43	1.37
FTP Experiment 2, bag 2	****	12.07	4.02	1.20	****	1.00	6.31	2.40	5.96	1.44
FTP Experiment 3, bag 2	****	12.50	3.72	1.00	****	1.00	6.31	2.19	4.42	1.73
FTP Bag2, average	****	12.26	3.50	1.29	****	1.08	6.24	2.24	4.94	1.51
FTP Experiment 1, bag 3	14.00	13.83	2.98	1.00	****	1.25	4.87	3.00	7.10	1.86
FTP Experiment 2, bag 3	13.00	14.33	3.23	1.00	****	1.00	4.90	2.60	7.17	1.71
FTP Experiment 3, bag 3	14.00	14.33	3.39	1.00	****	1.00	5.00	2.20	7.82	1.45
FTP Bag 3, average	13.67	14.16	3.20	1.00	****	1.08	4.92	2.60	7.36	1.67
FTP all bags, average	31.00	14.05	3.34	1.10	****	1.11	5.59	2.50	6.50	1.77
HFET 1	****	42.50	6.84	1.00	****	****	3.98	2.00	5.63	2.24
HFET 2	****	52.50	7.04	****	****	1.00	3.56	1.50	5.88	2.45
HFET 3	****	39.50	6.60	****	****	****	4.27	1.00	4.82	1.84
HFET average	****	44.83	6.83	1.00	****	1.00	3.94	1.50	5.44	2.18

qualitative data about the air/fuel ratio (only lean or rich data).

Comparison of the gear data shows the average gear for the on-road experiments to be slightly higher than the FTP (2.9 versus 2.5), and a large difference between freeway and urban driving (3.2 versus 2.6) with the freeway average close to the average gear for the HFET (3.6). The maximum gear for all on-road experiments was 4th but the maximum gear on in bag 2 of the FTP was only 3rd. The minimum gear for all data sets was 1st.

The ambient temperature was measured by a thermocouple located under the front bumper on the passenger side of the vehicle. During the FTP and the HFET, the engine cooling is provided by operating a 3 foot diameter fan directly in front of the vehicle. Because the thermocouple was out of the path of the cooling air and heat from the engine was not efficiently removed from under the bumper, the ambient air measurements for

Table 3.2.6.6 Average time in acceleration-based modes for on-road conservative driving experiments (seconds).

Route Number	Depart Time	Modes									
		Cold	At	Cruise	Coast	Hard	Med	Light	Hard	Med	Light
Dir, Expt#	hr:min	Start	Stop			Accel	Accel	Accel	Decel	Decel	Decel
note: **** mode did not occur during driving of on-road route											
Freeway Routes											
1-NS-36	7:30	****	4.00	2.67	1.73	****	1.00	4.02	2.80	4.21	3.00
1-SN-37	16:30	****	14.50	2.50	2.19	****	****	4.13	1.33	4.10	2.88
2-NS-40	7:30	****	9.50	2.11	1.74	****	1.86	4.79	2.08	4.08	2.35
2-SN-41	16:30	****	6.89	2.00	1.76	****	1.45	4.94	1.76	3.97	2.46
3-NS-38	7:30	****	9.26	2.57	2.53	****	1.40	4.29	1.72	3.57	2.81
3-SN-39	16:30	****	5.40	2.04	1.57	****	1.27	5.00	1.97	4.23	2.05
4-SN-17	7:30	****	8.90	2.74	1.90	****	1.33	4.50	1.71	5.62	2.81
4-NS-18	16:30	****	5.29	2.25	1.85	****	1.33	4.94	1.62	4.88	2.54
5-SN-25	7:30	****	11.29	1.95	2.11	****	****	5.08	1.57	4.28	2.44
5-NS-26	16:30	****	6.27	2.43	1.48	1.00	1.33	4.00	1.88	4.06	2.81
6-SN-29	7:30	****	9.10	2.55	2.51	****	1.33	4.51	1.48	4.42	2.69
6-NS-30	16:30	****	5.89	1.76	1.84	****	1.00	4.85	1.49	4.22	2.18
7-EW-2	7:30	****	7.26	2.36	2.23	2.00	1.00	5.05	1.42	4.14	2.59
7-WE-3	16:30	****	8.38	2.49	2.09	1.00	1.00	4.06	1.30	4.18	2.68
8-NS-13	7:30	****	8.45	3.05	1.74	****	2.00	4.60	1.73	5.11	2.55
8-SN-14	16:30	****	6.90	2.22	1.86	****	1.23	4.60	1.77	4.21	2.33
Freeway Averages		****	7.96	2.36	1.95	1.33	1.32	4.59	1.73	4.33	2.57
Freeway Std. Dev.		****	2.58	0.34	0.31	0.58	0.30	0.39	0.36	0.49	0.26
Freeway Maxima		****	14.50	3.05	2.53	2.00	2.00	5.08	2.80	5.62	3.00
Freeway Minima		****	4.00	1.76	1.48	1.00	1.00	4.00	1.30	3.57	2.05
Urban Routes											
1-NS-6	7:30	****	30.26	1.94	1.53	****	2.13	4.89	2.04	5.89	2.30
1-SN-7	16:30	****	20.65	1.99	1.42	****	2.09	4.53	2.05	5.29	2.09
2-EW-46	7:30	****	14.68	1.90	1.46	****	2.12	4.23	2.16	4.75	1.73
2-WE-47	16:30	****	17.19	1.79	1.32	****	1.91	4.52	2.17	4.78	1.69
3-EW-42	7:30	****	17.37	1.81	1.49	1.00	2.11	4.19	2.11	5.36	1.86
3-WE-43	16:30	****	16.72	1.57	1.68	****	1.98	4.43	1.93	4.09	1.75
4-WE-21	7:30	****	18.37	2.03	1.46	****	1.67	5.43	2.39	5.25	1.96
4-EW-22	16:30	****	24.24	1.82	1.65	3.00	2.07	4.50	1.87	4.96	1.68
5-SN-11	7:30	****	19.76	1.70	1.17	****	1.96	4.73	2.38	5.13	1.98
5-NS-12	16:30	****	19.75	1.52	1.54	****	1.76	4.79	1.93	4.05	1.55
6-NS-27	7:30	****	29.31	2.20	1.48	****	2.12	4.72	2.02	5.98	1.81
6-SN-28	16:30	****	23.77	1.91	1.36	****	2.00	4.55	2.16	4.74	1.72
7-SN-50	7:30	****	23.33	2.15	1.42	****	1.85	5.44	1.95	5.84	1.77
7-NS-51	16:30	****	28.02	1.93	1.20	****	2.15	5.11	2.12	5.68	1.68
8-EW-48	7:30	****	21.49	2.26	1.37	****	2.05	5.91	2.15	6.46	2.12
8-WE-49	16:30	****	25.72	1.74	1.38	****	1.89	4.87	2.30	5.86	1.66
Urban Averages:		****	21.91	1.89	1.43	2.00	1.99	4.80	2.11	5.26	1.83
Urban Std. Dev.		****	4.71	0.21	0.14	1.41	0.14	0.47	0.16	0.68	0.20
Urban Maxima		****	30.26	2.26	1.68	3.00	2.15	5.91	2.39	6.46	2.30
Urban Minima		****	14.68	1.52	1.17	1.00	1.67	4.19	1.87	4.05	1.55
Combined Averages:											
Combined Averages:		****	14.93	2.12	1.69	1.60	1.68	4.69	1.92	4.79	2.20
Combined Std. Dev.		****	8.02	0.36	0.35	0.89	0.41	0.44	0.33	0.75	0.44
Combined Maxima		****	30.26	3.05	2.53	3.00	2.15	5.91	2.80	6.46	3.00
Combined Minima		****	4.00	1.52	1.17	1.00	1.00	4.00	1.30	3.57	1.55

Table 3.2.6.7 Percent time in load-based modes for the FTP and the HFET.

Dynamometer Experiment and Bag Number	Modes							
	Open Loop		High	Medium	Medium	Low	Hot	Cold
	Rich	Lean	Load	High Load	Low Load	Load	Start	Start
FTP Experiment 1, bag 1	0.00	0.00	1.39	21.58	11.09	56.44	0.00	9.50
FTP Experiment 2, bag 1	0.00	0.00	1.39	21.58	11.29	56.24	0.00	9.50
FTP Experiment 3, bag 1	0.00	0.00	1.39	21.78	11.29	55.84	0.00	9.70
FTP Bag 1, average	0.00	0.00	1.39	21.65	11.22	56.17	0.00	9.57
FTP Experiment 1, bag 2	0.00	0.00	0.00	0.00	4.38	95.62	0.00	0.00
FTP Experiment 2, bag 2	0.00	0.00	0.00	0.00	4.61	95.39	0.00	0.00
FTP Experiment 3, bag 2	0.00	0.00	33.74	0.00	5.07	94.93	0.00	0.00
FTP Bag 2, average	0.00	0.00	11.25	0.00	4.69	95.31	0.00	0.00
FTP Experiment 1, bag 3	0.00	0.00	0.59	21.78	10.50	64.36	2.77	0.00
FTP Experiment 2, bag 3	0.00	0.00	0.20	21.58	10.10	65.54	2.57	0.00
FTP Experiment 3, bag 3	0.00	0.00	0.00	21.58	9.90	65.74	2.77	0.00
FTP Bag 3, average	0.00	0.00	0.26	21.65	10.17	65.21	2.70	0.00
FTP all bags, average	0.00	0.00	4.30	14.43	8.69	72.23	0.90	3.19
HFET 1	0.00	0.00	0.00	77.99	2.13	19.88	0.00	0.00
HFET 2	0.00	0.00	0.00	76.04	1.74	22.22	0.00	0.00
HFET 3	0.00	0.00	0.12	78.19	2.03	19.67	0.00	0.00
HFET average	0.00	0.00	0.04	77.41	1.97	20.59	0.00	0.00

the FTP and the HFET were higher than the actual ambient temperature. In the dynamometer cell, the ambient temperature and relative humidity are carefully controlled by a climate system which keeps the cell in the prescribed range for these tests and therefore the temperature in the cell had only slight deviations from the required temperature of 75°F. The effect of the cooling fan not providing ambient air over the thermocouple is apparent in the minimum ambient air measurements for the FTP and the HFET. The minimum temperatures (which occurred at the beginning of the tests) for bag 1 of the FTP were within the required range, but for the other two bags and the HFET, the minimum temperature was higher although the room temperature did not change.

On-road, the ambient temperature ranged from 40°F to 104°F with the freeway and urban averages of both 75°F, the same as the temperature specified in the FTP. The

Table 3.2.6.8 Percent time in load-based modes for on-road conservative driving experiments.

Route	Depart	Modes							
Number	Time	Open Loop		High	Medium	Medium	Low	Hot	Cold
Dir, Expt#	hr:min	Rich	Lean	Load	High Load	Low Load	Load	Start	Start
Freeway Routes									
1-NS-36	7:30	0.00	2.31	2.11	72.12	3.28	20.18	0.00	0.00
1-SN-37	16:30	0.00	1.64	1.37	74.11	4.48	18.41	0.00	0.00
2-NS-40	7:30	0.00	1.43	1.22	40.35	11.29	45.70	0.00	0.00
2-SN-41	16:30	0.00	0.83	1.33	28.47	7.55	61.82	0.00	0.00
3-NS-38	7:30	0.00	2.04	0.76	42.62	5.84	48.73	0.00	0.00
3-SN-39	16:30	0.00	0.78	0.94	25.95	13.31	59.02	0.00	0.00
4-SN-17	7:30	0.00	0.75	0.98	61.17	5.93	31.18	0.00	0.00
4-NS-18	16:30	0.00	0.16	0.78	41.98	9.41	47.67	0.00	0.00
5-SN-25	7:30	0.00	0.30	1.44	38.65	7.48	52.13	0.00	0.00
5-NS-26	16:30	0.00	0.85	1.37	54.63	6.30	36.85	0.00	0.00
6-SN-29	7:30	0.00	0.15	0.95	31.47	5.68	61.78	0.00	0.00
6-NS-30	16:30	0.00	0.04	1.18	28.13	7.43	63.22	0.00	0.00
7-EW-2	7:30	0.03	0.93	2.80	43.50	6.33	46.42	0.00	0.00
7-WE-3	16:30	0.02	0.27	1.65	41.89	5.99	50.18	0.00	0.00
8-NS-13	7:30	0.00	0.51	0.83	60.79	5.47	32.40	0.00	0.00
8-SN-14	16:30	0.00	0.27	0.88	36.55	5.07	57.23	0.00	0.00
Freeway Averages		0.00	0.83	1.29	45.15	6.93	45.81	0.00	0.00
Freeway Std. Dev.		0.01	0.69	0.54	15.17	2.54	14.31	0.00	0.00
Freeway Maxima		0.03	2.31	2.80	74.11	13.31	63.22	0.00	0.00
Freeway Minima		0.00	0.04	0.76	25.95	3.28	18.41	0.00	0.00
Urban Routes									
1-NS-6	7:30	0.00	0.31	2.95	23.80	13.13	59.80	0.00	0.00
1-SN-7	16:30	0.00	0.00	2.27	13.82	16.36	67.55	0.00	0.00
2-EW-46	7:30	0.00	0.00	0.79	11.59	14.76	72.86	0.00	0.00
2-WE-47	16:30	0.00	0.00	0.76	9.40	18.12	71.72	0.00	0.00
3-EW-42	7:30	0.02	0.02	0.77	7.35	16.53	75.32	0.00	0.00
3-WE-43	16:30	0.00	0.00	0.35	3.63	13.18	82.83	0.00	0.00
4-EW-21	7:30	0.00	0.00	0.58	15.78	18.71	64.93	0.00	0.00
4-WE-22	16:30	0.09	0.11	1.63	9.17	11.07	77.93	0.00	0.00
5-SN-11	7:30	0.00	0.00	1.11	6.53	20.54	71.83	0.00	0.00
5-NS-12	16:30	0.00	0.00	0.07	2.45	12.53	84.96	0.00	0.00
6-NS-27	7:30	0.00	0.00	2.26	21.32	14.30	62.11	0.00	0.00
6-SN-28	16:30	0.00	0.00	2.16	15.68	14.84	67.33	0.00	0.00
7-SN-50	7:30	0.00	0.04	1.39	22.38	16.07	60.13	0.00	0.00
7-NS-51	16:30	0.00	0.00	0.93	16.69	16.08	66.29	0.00	0.00
8-EW-48	7:30	0.00	0.00	1.30	27.40	16.96	54.33	0.00	0.00
8-WE-49	16:30	0.00	0.02	0.52	12.43	16.97	70.06	0.00	0.00
Urban Averages		0.01	0.03	1.24	13.71	15.63	69.37	0.00	0.00
Urban Std. Dev.		0.02	0.08	0.81	7.33	2.46	8.37	0.00	0.00
Urban Maxima		0.09	0.31	2.95	27.40	20.54	84.96	0.00	0.00
Urban Minima		0.00	0.00	0.07	2.45	11.07	54.33	0.00	0.00
Combined Averages									
Combined Averages		0.01	0.43	1.26	29.43	11.28	57.59	0.00	0.00
Combined Std. Dev.		0.02	0.63	0.68	19.81	5.06	16.62	0.00	0.00
Combined Maxima		0.09	2.31	2.95	74.11	20.54	84.96	0.00	0.00
Combined Minima		0.00	0.00	0.07	2.45	3.28	18.41	0.00	0.00

range of average ambient temperatures was from 52 to 96°F. It is important to note these ambient temperatures are only characteristic of the SoCAB and for the seasons in which these experiments were driven (winter, spring and summer).

The average engine coolant temperature for the FTP was 192°F and for the HFET was 212°F with the maximum temperature during the tests of 218°F. On-road the average engine coolant temperature was 205°F (203°F for freeway experiments and 207°F for urban experiments), slightly higher than the FTP. The maximum engine coolant temperatures for all of the on-road experiments was either 216 or 218°F except for the freeway experiment 7-EW for which the maximum on-road temperature was 204°F. For experiment 7-EW, the average ambient temperature was 52°F and the maximum ambient temperature was only 64°F, both the lowest recorded on-road. The low ambient temperature appears to be responsible for the cooler engine coolant temperature.

The catalyst temperature is an important factor in the conversion efficiency of all three classes of pollutants. Ford defines the "light-off" temperature of the catalyst as the temperature at which the catalyst conversion efficiency reaches 50% and the temperature at which this occurs for the catalyst in the test vehicle is 800°F (Jesion, 1993). The average catalyst temperature during the FTP was 895°F and for the HFET was 1037°F, both above the light-off temperature. For both the FTP and the HFET the maximum catalyst temperature was approximately 1100°F. For the on-road experiments the average catalyst temperature (1030°F) was higher than the average for the FTP but was close to the catalyst temperature of the HFET. The maximum catalyst temperature was 1031°F which is well below the maximum allowed catalyst temperature of approximately 1450°F.

The acceleration and speed data from the FTP are plotted in Figure 3.2.6.3 as a function of probability (z) of being within a 1 mph speed (x) and 1 mph s^{-1} acceleration (y) interval (the source code for the speed versus acceleration probability binning program VABINEW.FOR is given in Appendix A.1.2). The ridges at low speed from 0 to 15 mph represent accelerations and decelerations with little cruise at these speeds. There are two peaks, one which represents cruising between 20 and 40 mph and one between 45 and 55 mph. There is also a large amount of time spent at stop (18.3%).

Table 3.2.6.9 Average vehicle operating parameter data for the FTP and the HFET.

Dynamometer Experiment and Bag Number	Throttle		Load	Stock	Horiba	%	Vehicle	Gear	Amb	Air	Eng	Exh	Cat	%
	Position	RPM		A/F	A/F	MeOH	Accel		Temp	Charge	Coolant	Gas	Temp	Temp
FTP Experiment 1, bag 1	51.28	1326	0.30	0.98	****	0.00	0.02	2.66	79.18	78	153	749	836	36.56
FTP Experiment 1, bag 2	25.33	1134	0.22	0.99	****	0.00	0.02	2.25	93.20	100	211	732	928	39.29
FTP Experiment 1, bag 3	44.11	1320	0.26	0.98	****	0.01	0.02	2.67	95.03	115	211	742	922	37.35
note: **** sensor was not working														
FTP Experiment 2, bag 1	50.85	1323	0.31	1.00	0.98	0.01	0.02	2.66	80.64	78	156	750	836	36.96
FTP Experiment 2, bag 2	25.14	1135	0.23	1.00	1.00	0.01	0.02	2.25	93.30	101	211	733	927	40.55
FTP Experiment 2, bag 3	45.13	1322	0.27	0.98	1.00	0.02	0.02	2.66	94.41	117	211	748	926	39.33
FTP Experiment 3, bag 1	49.80	1324	0.30	0.99	0.98	0.01	0.02	2.67	81.07	79	156	748	831	37.94
FTP Experiment 3, bag 2	24.63	1128	0.22	1.00	1.00	0.01	0.02	2.25	92.14	101	211	732	925	40.21
FTP Experiment 3, bag 3	44.09	1320	0.26	0.98	1.00	0.01	0.02	2.66	94.35	116	211	749	926	36.17
Combined averages	40.04	1259	0.26	0.99	0.99	0.01	0.02	2.53	89.26	98	192	743	895	38.26
Combined std. dev.	11.58	95	0.04	0.01	0.01	0.01	0.00	0.21	6.79	16	28	8	46	1.63
Combined maxima	51.28	1326	0.31	1.00	1.00	0.02	0.02	2.67	95.03	117	211	750	928	40.55
Combined minima	24.63	1128	0.22	0.98	0.98	0.00	0.02	2.25	79.18	78	153	732	831	36.17
HFET 1	60.68	1514	0.28	0.99	****	0.01	0.02	3.58	103.68	125	212	849	1039	15.96
HFET 2	59.43	1492	0.28	0.99	1.00	0.02	0.02	3.52	103.75	125	212	844	1038	17.80
HFET 3	60.48	1521	0.28	0.99	1.00	0.02	0.02	3.60	101.87	125	212	851	1035	15.95
HFET average	60.20	1509	0.28	0.99	1.00	0.02	0.02	3.57	103.10	125	212	848	1037	16.57
HFET std. dev.	0.67	15	0.00	0.00	0.00	0.01	0.00	0.04	1.07	0	0	3	2	1.07
HFET maxima	60.68	1521	0.28	0.99	1.00	0.02	0.02	3.60	103.75	125	212	851	1039	17.80
HFET minima	59.43	1492	0.28	0.99	1.00	0.01	0.02	3.52	101.87	125	212	844	1035	15.95

By contrast, the on-road freeway data (Figure 3.2.6.4) show a more smoothed ridge than the FTP, corresponding to higher rates of acceleration and deceleration. The freeway routes had less time at stop (2.5%), a small equal probability "slow-and-go" peak of cruise between 5 and 35 mph and a large high-speed cruise peak from 50 to 70 mph. Only small differences were found between morning (Figure 3.2.6.5) and evening (Figure 3.2.6.6) freeway driving with a larger percent of time at stop in the mornings (3.1% versus 1.8%) and a slightly larger high-speed cruise peak.

The on-road urban data exhibited a larger percent of time at a stop (21.9%) than the FTP, higher rates of acceleration (at 5 mph acceleration rates were observed up to 7 or 8 mph s⁻¹) and a similar cruise peak from 25 to 45 mph with a maximum speed approximately equal to the FTP (Figure 3.2.6.7). The only difference between the morning (Figure 3.2.6.8) and evening data (Figure 3.2.6.9) for the urban routes was a slightly greater cruise peak from 25 to 45 mph for the morning data.

Table 3.2.6.10

Average vehicle operating parameter data for on-road conservative driving experiments.

Route	Depart	Throttle			Stock	Horiba	%	Vehicle		Amb	Air	Eng	Exh	Cat	%
Number	Time	Position	RPM	Load	A/F	A/F	MeOH	Accel	Gear	Temp	Charge	Coolant	Gas	Temp	Time
Dir, Expt#	hr:min							G's		deg F	Temp	Temp	Temp	deg F	Braking
Freeway Routes															
1-NS-36	7:30	62.85	1736	0.26	1.02	1.02	0.00	-0.02	3.71	75.65	87	199	863	1116	13.23
1-SN-37	16:30	77.90	1676	0.31	1.01	1.01	0.00	-0.01	3.74	95.76	109	205	909	1123	12.31
2-NS-40	7:30	48.62	1425	0.25	1.01	1.01	0.00	-0.02	3.35	73.02	92	202	813	1043	25.52
2-SN-41	16:30	49.00	1336	0.25	1.00	1.01	0.00	-0.01	2.84	88.66	116	208	797	1007	33.47
3-NS-38	7:30	43.01	1414	0.23	1.02	1.02	0.00	-0.02	2.99	76.85	104	204	766	991	29.50
3-SN-39	16:30	56.27	1391	0.27	1.00	1.01	0.00	-0.01	3.06	86.29	110	208	836	1042	29.39
4-SN-17	7:30	60.34	1669	0.28	1.00	1.01	0.00	-0.12	3.50	67.76	84	201	878	1098	20.53
4-NS-18	16:30	52.09	1476	0.27	1.00	1.00	0.00	-0.11	3.22	77.70	97	205	847	1053	26.68
5-SN-25	7:30	50.14	1399	0.27	1.00	1.00	0.00	-0.03	3.15	70.89	91	204	820	1033	20.84
5-NS-26	16:30	51.05	1519	0.26	1.01	1.01	0.00	-0.06	3.41	77.78	95	202	825	1057	21.49
6-SN-29	7:30	41.67	1363	0.25	1.00	1.00	0.02	-0.02	2.85	72.03	95	205	781	979	27.91
6-NS-30	16:30	42.33	1333	0.25	1.00	1.00	0.02	-0.05	2.97	75.23	100	207	788	955	26.59
7-EW-2	7:30	51.61	1486	0.28	1.00	1.01	0.05	-0.06	3.23	51.65	71	196	793	1004	18.97
7-WE-3	16:30	48.19	1395	0.26	1.00	1.00	0.06	-0.06	3.34	66.39	85	203	816	1015	19.05
8-NS-13	7:30	55.27	1605	0.27	1.00	1.00	0.00	-0.12	3.48	64.29	75	200	857	1079	20.88
8-SN-14	16:30	44.72	1382	0.25	1.00	1.00	0.00	-0.12	2.98	74.89	108	206	800	1000	29.57
Freeway Averages		52.19	1475	0.26	1.00	1.01	0.01	-0.05	3.24	74.68	95	203	824	1037	23.50
Freeway Std. Dev.		9.16	129	0.02	0.01	0.01	0.02	0.04	0.28	10.26	13	3	39	49	6.04
Freeway Maxima		77.90	1736	0.31	1.02	1.02	0.06	-0.01	3.74	95.76	116	208	909	1123	33.47
Freeway Minima		41.67	1333	0.23	1.00	1.00	0.00	-0.12	2.84	51.65	71	196	766	955	12.31
Urban Routes															
1-NS-6	7:30	44.69	1263	0.27	1.00	1.00	0.04	-0.04	2.74	55.84	75	203	818	1053	38.63
1-SN-7	16:30	47.55	1263	0.27	1.00	1.00	0.07	-0.01	2.69	64.65	88	207	827	1053	42.23
2-EW-46	7:30	42.44	1242	0.25	1.00	1.00	0.00	-0.10	2.65	72.65	99	208	796	1024	40.97
2-WE-47	16:30	46.81	1248	0.26	1.00	1.00	0.00	-0.18	2.62	85.59	112	210	805	1026	42.21
3-EW-42	7:30	40.78	1207	0.25	0.99	1.00	0.00	-0.01	2.50	78.17	107	209	795	1017	42.88
3-WE-43	16:30	33.74	1170	0.23	1.00	1.00	0.00	-0.02	2.36	85.36	115	210	768	990	44.91
4-WE-21	7:30	45.48	1269	0.27	1.00	1.00	0.00	-0.11	2.66	67.92	90	206	811	1032	36.99
4-EW-22	16:30	36.61	1123	0.24	1.00	1.00	0.01	-0.09	2.15	85.92	116	210	751	988	58.11
5-SN-11	7:30	45.95	1248	0.27	1.00	1.00	0.05	-0.11	2.52	65.43	92	208	826	1047	43.03
5-NS-12	16:30	28.29	1135	0.23	1.00	1.00	0.06	-0.13	2.25	74.77	105	208	744	953	50.85
6-NS-27	7:30	46.03	1225	0.27	1.00	1.00	0.00	-0.04	2.61	69.15	92	206	796	1035	44.54
6-SN-28	16:30	45.05	1234	0.26	1.00	1.00	0.02	-0.06	2.63	74.62	99	207	798	1041	46.81
7-SN-50	7:30	48.33	1285	0.27	1.00	1.00	0.00	-0.09	2.85	76.68	98	208	817	1038	39.30
7-NS-51	16:30	46.58	1251	0.26	1.00	1.00	0.00	-0.09	2.64	87.33	114	209	806	1035	44.76
8-EW-48	7:30	51.49	1287	0.29	1.00	1.00	0.00	-0.19	2.82	70.62	93	199	792	1018	37.78
8-WE-49	16:30	41.70	1232	0.26	1.00	1.00	0.00	-0.07	2.64	82.39	105	206	789	1010	42.62
Urban Averages		43.22	1230	0.26	1.00	1.00	0.02	-0.08	2.58	74.82	100	207	796	1022	43.54
Urban Std. Dev.		5.94	49	0.02	0.00	0.00	0.02	0.05	0.19	9.07	11	3	24	27	5.23
Urban Maxima		51.49	1287	0.29	1.00	1.00	0.07	-0.01	2.85	87.33	116	210	827	1053	58.11
Urban Minima		28.29	1123	0.23	0.99	1.00	0.00	-0.19	2.15	55.84	75	199	744	953	36.99
Combined Averages															
Combined Averages		47.71	1353	0.26	1.00	1.00	0.01	-0.07	2.91	74.75	98	205	810	1030	33.52
Combined Std. Dev.		8.86	157	0.02	0.01	0.01	0.02	0.05	0.41	9.52	12	4	35	39	11.60
Combined Maxima		77.90	1736	0.31	1.02	1.02	0.07	-0.01	3.74	95.76	116	210	909	1123	58.11
Combined Minima		28.29	1123	0.23	0.99	1.00	0.00	-0.19	2.15	51.65	71	196	744	953	12.31

Table 3.2.6.11 Maximum vehicle operating parameter data for the FTP and the HFET.

Dynamometer Experiment and Bag Number	Throttle			Stock	Horiba	%	Vehicle		Amb	Air	Eng	Exh	Cat
	Position	RPM	Load	A/F	A/F	MeOH	Accel	Gear	Temp	Charge	Coolant	Gas	Temp
							G's		deg F	Temp	Temp	Temp	deg F
FTP Experiment 1, bag 1	337.09	2369	0.73	1.12	****	0.00	0.03	4.00	84.90	80	208	1047	1098
FTP Experiment 1, bag 2	162.20	2045	0.52	1.06	****	0.01	0.03	3.00	96.71	112	216	857	1086
FTP Experiment 1, bag 3	329.09	2285	0.69	1.04	****	0.02	0.03	4.00	100.24	120	216	1021	1066
note: **** sensor was not operating													
FTP Experiment 2, bag 1	326.70	2362	0.73	1.13	1.09	0.01	0.03	4.00	85.95	80	210	1046	1096
FTP Experiment 2, bag 2	137.59	2028	0.49	1.05	1.05	0.02	0.03	3.00	96.97	114	216	859	1089
FTP Experiment 2, bag 3	280.50	2330	0.65	1.06	1.12	0.03	0.03	4.00	100.77	122	218	1028	1073
FTP Experiment 3, bag 1	287.30	2321	0.72	1.11	1.09	0.01	0.03	4.00	85.69	82	210	1026	1084
FTP Experiment 3, bag 2	140.80	2005	0.50	1.05	1.06	0.02	0.03	3.00	95.14	114	216	857	1085
FTP Experiment 3, bag 3	271.70	2337	0.65	1.05	1.07	0.02	0.03	4.00	98.94	122	218	1044	1080
Combined averages	252.55	2231	0.63	1.07	1.08	0.02	0.03	3.67	93.92	105	214	976	1084
Combined std. dev.	82.71	156	0.10	0.04	0.03	0.01	0.00	0.50	6.55	19	4	89	10
Combined maxima	337.09	2369	0.73	1.13	1.12	0.03	0.03	4.00	100.77	122	218	1047	1098
Combined minima	137.59	2005	0.49	1.04	1.05	0.00	0.03	3.00	84.90	80	208	857	1066
HFET 1	263.91	2277	0.61	1.05	****	0.01	0.04	4.00	108.60	130	218	979	1119
HFET 2	243.09	2241	0.59	1.04	1.11	0.02	0.03	4.00	108.99	132	218	979	1116
HFET 3	267.09	2015	0.66	1.05	1.06	0.02	0.03	4.00	107.69	132	218	980	1119
HFET average	258.03	2177	0.62	1.05	1.09	0.02	0.03	4.00	108.43	131	218	979	1118
HFET std. dev.	13.04	142	0.04	0.01	0.04	0.01	0.01	0.00	0.67	1	0	1	2
HFET maxima	267.09	2277	0.66	1.05	1.11	0.02	0.04	4.00	108.99	132	218	980	1119
HFET minima	243.09	2015	0.59	1.04	1.06	0.01	0.03	4.00	107.69	130	218	979	1116

The freeway and urban data were averaged with equal weighting to form a plot of the average percent time spent in each combination of acceleration and speed (Figure 3.2.6.10). The plot shows higher rates of acceleration at low speeds, an "urban" cruise peak and a "freeway" cruise peak. The maximum of the freeway cruise peak was at 59 mph, 2 mph faster than the maximum speed of the FTP.

The averaged freeway and urban data were then subtracted in three dimensions from the FTP probability surface. The resulting plot (Figure 3.2.6.11) reveals the areas in which the FTP over- and under-estimates the frequency of being at a particular speed and acceleration. The FTP overestimates the amount of time at stop by 6.2% and cruise between 25 and 40 mph and under-estimates accelerations from a stop and at higher speeds. The FTP also under-estimates all driving above 40 mph.

Table 3.2.6.12

Maximum vehicle operating parameter data for on-road conservative driving experiments.

Route	Depart	Throttle			Stock	Horiba	%	Vehicle		Amb	Air	Eng	Exh	Cat
Number	Time	Position	RPM	Load	A/F	A/F	MeOH	Accel	Gear	Temp	Charge	Coolant	Gas	Temp
Dir, Expt#	hr:min							G's		deg F	Temp	Temp	Temp	deg F
Freeway Routes														
1-NS-36	7:30	456	3164	0.73	2.00	1.70	0.00	0.21	4.00	81.34	112	216	1252	1344
1-SN-37	16:30	425	2739	0.70	2.00	1.70	0.00	0.18	4.00	103.38	160	216	1196	1314
2-NS-40	7:30	423	3453	0.71	2.00	1.71	0.00	0.26	4.00	77.38	138	216	1167	1283
2-SN-41	16:30	451	2965	0.71	2.00	1.70	0.00	0.28	4.00	95.79	152	216	1176	1276
3-NS-38	7:30	395	3474	0.73	2.00	1.70	0.00	0.22	4.00	88.71	148	218	1275	1380
3-SN-39	16:30	476	3179	0.69	2.00	1.70	0.00	0.22	4.00	99.72	140	218	1268	1348
4-SN-17	7:30	496	3312	0.74	2.00	1.70	0.00	0.13	4.00	74.34	144	216	1127	1231
4-NS-18	16:30	494	2705	0.73	2.00	1.70	0.00	0.17	4.00	84.90	126	218	1141	1218
5-SN-25	7:30	406	2793	0.72	2.00	1.70	0.00	0.17	4.00	76.59	118	216	1113	1201
5-NS-26	16:30	474	2975	0.73	2.00	1.70	0.00	0.22	4.00	86.48	134	216	1132	1257
6-SN-29	7:30	510	3389	0.74	2.00	1.70	0.02	0.21	4.00	79.63	124	218	1179	1284
6-NS-30	16:30	357	2605	0.72	1.93	1.70	0.02	0.17	4.00	83.32	134	216	1101	1230
7-EW-2	7:30	637	3383	0.75	2.00	1.70	0.06	0.17	4.00	63.73	102	204	1239	1333
7-WE-3	16:30	661	3495	0.73	2.00	1.70	0.07	0.17	4.00	73.29	114	216	1173	1238
8-NS-13	7:30	266	2557	0.70	2.00	1.70	0.00	0.15	4.00	70.11	92	216	1104	1232
8-SN-14	16:30	398	2491	0.70	2.00	1.70	0.00	0.15	4.00	87.00	150	218	1128	1213
Freeway Averages		458	3042	0.72	2.00	1.70	0.01	0.19	4.00	82.86	131	216	1173	1274
Freeway Std. Dev.		96	357	0.02	0.02	0.00	0.02	0.04	0.00	10.70	19	3	58	55
Freeway Maxima		661	3495	0.75	2.00	1.71	0.07	0.28	4.00	103.38	160	218	1275	1380
Freeway Minima		266	2491	0.69	1.93	1.70	0.00	0.13	4.00	63.73	92	204	1101	1201
Urban Routes														
1-NS-6	7:30	555	3136	0.74	2.00	1.70	0.05	0.33	4.00	74.21	122	216	1253	1330
1-SN-7	16:30	552	3443	0.75	1.12	1.12	0.08	0.32	4.00	75.27	144	218	1259	1325
2-EW-46	7:30	533	3283	0.72	1.10	1.13	0.00	0.39	4.00	80.82	122	218	1144	1203
2-WE-47	16:30	497	3538	0.71	1.09	1.11	0.00	0.29	4.00	103.64	130	218	1164	1260
3-EW-42	7:30	558	3759	0.72	1.59	1.70	0.00	0.34	4.00	89.11	148	218	1196	1288
3-WE-43	16:30	420	3368	0.72	1.09	1.13	0.00	0.31	4.00	94.35	134	218	1137	1210
4-WE-21	7:30	526	3302	0.74	1.08	1.12	0.00	0.17	4.00	75.27	150	218	1217	1316
4-EW-22	16:30	611	3954	0.75	2.00	1.70	0.01	0.28	4.00	97.63	152	218	1235	1338
5-SN-11	7:30	361	3246	0.72	1.09	1.14	0.06	0.20	4.00	75.53	136	216	1179	1240
5-NS-12	16:30	380	2808	0.72	1.08	1.21	0.07	0.16	4.00	86.87	142	218	1056	1108
6-NS-27	7:30	443	3760	0.73	1.09	1.14	0.00	0.28	4.00	74.61	114	218	1240	1420
6-SN-28	16:30	493	3553	0.74	1.10	1.23	0.03	0.31	4.00	83.71	128	218	1301	1432
7-SN-50	7:30	494	3474	0.73	1.54	1.61	0.00	0.23	4.00	89.63	154	218	1193	1289
7-NS-51	16:30	501	3455	0.71	1.07	1.10	0.00	0.27	4.00	104.00	152	218	1181	1274
8-EW-48	7:30	524	2836	0.73	1.10	1.10	0.00	0.33	4.00	76.06	126	216	1100	1190
8-WE-49	16:30	363	3268	0.70	1.63	1.70	0.00	0.24	4.00	99.33	164	218	1149	1214
Urban Averages		488	3386	0.73	1.30	1.31	0.02	0.28	4.00	86.25	139	218	1188	1277
Urban Std. Dev.		75	308	0.01	0.34	0.26	0.03	0.06	0.00	10.89	14	1	63	84
Urban Maxima		611	3954	0.75	2.00	1.70	0.08	0.39	4.00	104.00	164	218	1301	1432
Urban Minima		361	2808	0.70	1.07	1.10	0.00	0.16	4.00	74.21	114	216	1056	1108
Combined Averages														
Combined Averages		473	3214	0.72	1.65	1.50	0.01	0.24	4.00	84.55	135	217	1180	1276
Combined Std. Dev.		86	371	0.02	0.43	0.27	0.03	0.07	0.00	10.76	17	3	60	70
Combined Maxima		661	3954	0.75	2.00	1.71	0.08	0.39	4.00	104.00	164	218	1301	1432
Combined Minima		266	2491	0.69	1.07	1.10	0.00	0.13	4.00	63.73	92	204	1056	1108

Table 3.2.6.13 Minimum vehicle operating parameter data for the FTP and the HFET.

Dynamometer Experiment and Bag Number	Throttle			Stock	Horiba	%	Vehicle		Amb	Air	Eng	Exh	Cat
	Position	RPM	Load	A/F	A/F	MeOH	Accel	Gear	Temp	Charge	Coolant	Gas	Temp
							G's		deg F	Temp	Temp	Temp	deg F
FTP Experiment 1, bag 1	0.00	600	0.11	0.54	****	0.00	0.01	1.00	75.80	76	72	126	75
FTP Experiment 1, bag 2	1.00	679	0.12	0.93	****	0.00	0.01	1.00	85.03	80	204	615	872
FTP Experiment 1, bag 3	0.00	677	0.10	0.81	****	0.00	0.01	1.00	83.45	110	200	356	728
note:**** sensor was not operating													
FTP Experiment 2, bag 1	0.00	631	0.11	0.57	0.78	0.00	0.01	1.00	77.65	78	78	122	81
FTP Experiment 2, bag 2	1.00	670	0.12	0.93	0.90	0.01	0.01	1.00	85.95	80	204	617	868
FTP Experiment 2, bag 3	0.00	696	0.09	0.84	0.93	0.01	0.02	1.00	80.02	112	200	372	732
FTP Experiment 3, bag 1	0.00	612	0.11	0.55	0.76	0.00	0.01	1.00	78.84	78	78	112	80
FTP Experiment 3, bag 2	1.00	655	0.12	0.93	0.91	0.01	0.01	1.00	85.82	82	204	617	865
FTP Experiment 3, bag 3	0.00	695	0.10	0.83	0.93	0.01	0.01	1.00	84.77	110	200	367	733
Combined averages	0.33	657	0.11	0.77	0.87	0.00	0.01	1.00	81.93	90	160	367	559
Combined std. dev.	0.50	35	0.01	0.17	0.08	0.01	0.00	0.00	3.88	16	63	215	365
Combined maxima	1.00	696	0.12	0.93	0.93	0.01	0.02	1.00	85.95	112	204	617	872
Combined minima	0.00	600	0.09	0.54	0.76	0.00	0.01	1.00	75.80	76	72	112	75
HFET 1	0	671	0.08	0.89	****	0.01	0.01	1.00	97.24	118	206	618	909
HFET 2	0	665	0.08	0.89	0.95	0.01	0.01	1.00	97.50	118	206	621	901
HFET 3	0	661	0.08	0.87	0.95	0.01	0.01	1.00	95.66	118	206	621	903
HFET average	0.00	666	0.08	0.88	0.95	0.01	0.01	1.00	96.80	118	206	620	904
HFET std. dev.	0.00	5	0.00	0.01	0.00	0.00	0.00	0.00	1.00	0	0	1	4
HFET maxima	0.00	671	0.08	0.89	0.95	0.01	0.01	1.00	97.50	118	206	621	909
HFET minima	0.00	661	0.08	0.87	0.95	0.01	0.01	1.00	95.66	118	206	618	901

3.2.7 Comparison of Aggressive Driving to the FTP and Conservative Driving

Table 3.2.7.1 contains the on-road data from the aggressive driving experiments which are compared to the FTP and conservative driving experiments in Figure 3.2.7.1. Data were collected for the aggressive driving experiments for 16,163 seconds on freeway routes and 19,226 seconds on urban routes. It is important to note that during the aggressive driving experiments, the test vehicle was still passed by other vehicles indicating more aggressive driving behavior occurs on-road than in our experiments.

For aggressive driving, there was a greater percent of time spent in hard accelerations (0.74% versus 0.005% and 0.0% for the FTP), the maximum speed and maximum acceleration rate increased over conservative driving (80.3 versus 73.9 mph and 9.6 versus 8.0 mph s⁻¹) and average fuel economy decreased when driving aggressively

Table 3.2.6.14

Minimum vehicle operating parameter data for on-road conservative driving experiments.

Route Number	Depart Time	Throttle Position	RPM	Load	Stock A/F	Horiba A/F	% MeOH	Vehicle Accel	Gear	Amb Temp	Air Charge	Eng Coolant Temp	Exh Gas Temp	Cat Temp
Dir, Expt#	hr:min							G's		deg F	Temp	Temp	Temp	deg F
Freeway Routes														
1-NS-36	7:30	0.09	643	0.05	0.82	0.90	0.00	-0.28	1.00	66.79	78	190	599	864
1-SN-37	16:30	0.00	700	0.06	0.83	0.92	0.00	-0.26	1.00	86.35	100	196	603	825
2-NS-40	7:30	0.00	685	0.07	0.85	0.90	0.00	-0.42	1.00	70.50	82	190	570	747
2-SN-41	16:30	0.00	681	0.06	0.83	0.89	0.00	-0.32	1.00	82.92	100	194	574	667
3-NS-38	7:30	0.00	669	0.06	0.80	0.88	0.00	-0.37	1.00	65.99	74	190	513	714
3-SN-39	16:30	0.00	674	0.06	0.82	0.89	0.00	-0.31	1.00	74.08	82	194	579	802
4-SN-17	7:30	0.00	652	0.07	0.84	0.89	0.00	-0.42	1.00	64.79	72	194	550	749
4-NS-18	16:30	0.91	659	0.07	0.85	0.90	0.00	-0.48	1.00	74.48	82	196	636	843
5-SN-25	7:30	0.91	649	0.07	0.85	0.90	0.00	-0.31	1.00	65.59	74	194	605	817
5-NS-26	16:30	0.00	642	0.07	0.85	0.89	0.00	-0.33	1.00	72.36	80	190	602	880
6-SN-29	7:30	0.00	659	0.06	0.84	0.90	0.01	-0.29	1.00	68.91	76	194	529	734
6-NS-30	16:30	0.00	653	0.07	0.85	0.88	0.01	-0.41	1.00	70.77	78	194	578	767
7-EW-2	7:30	0.00	651	0.06	0.84	0.84	0.04	-0.39	1.00	39.46	48	186	497	592
7-WE-3	16:30	1.00	659	0.06	0.83	0.83	0.05	-0.53	1.00	60.40	70	194	583	805
8-NS-13	7:30	0.00	649	0.06	0.83	0.87	0.00	-0.39	1.00	59.20	66	190	628	855
8-SN-14	16:30	0.30	653	0.07	0.85	0.88	0.00	-0.52	1.00	69.04	76	194	556	748
Freeway Averages		0.20	661	0.06	0.84	0.89	0.01	-0.38	1.00	68.23	77	193	575	776
Freeway Std. Dev.		0.38	16	0.01	0.01	0.02	0.02	0.08	0.00	10.47	12	3	39	77
Freeway Maxima		1.00	700	0.07	0.85	0.92	0.05	-0.26	1.00	86.35	100	196	636	880
Freeway Minima		0.00	642	0.05	0.80	0.83	0.00	-0.53	1.00	39.46	48	186	497	592
Urban Routes														
1-NS-6	7:30	0.00	642	0.07	0.85	0.87	0.02	-0.57	1.00	44.18	64	190	550	730
1-SN-7	16:30	0.59	666	0.09	0.85	0.89	0.07	-0.41	1.00	58.26	70	194	584	670
2-EW-46	7:30	0.70	653	0.09	0.88	0.90	0.00	-0.44	1.00	67.72	82	194	572	781
2-WE-47	16:30	1.00	663	0.10	0.89	0.90	0.00	-0.52	1.00	75.67	90	194	587	828
3-EW-42	7:30	0.97	656	0.09	0.86	0.87	0.00	-0.48	1.00	72.23	90	196	559	729
3-WE-43	16:30	0.00	640	0.10	0.91	0.91	0.00	-0.45	1.00	76.99	94	196	595	841
4-WE-21	7:30	0.00	657	0.09	0.91	0.92	0.00	-0.64	1.00	63.20	74	194	522	696
4-EW-22	16:30	0.00	649	0.07	0.83	0.86	0.00	-0.56	1.00	71.83	88	194	515	717
5-SN-11	7:30	0.00	657	0.09	0.88	0.89	0.04	-0.52	1.00	62.13	78	194	616	695
5-NS-12	16:30	0.00	658	0.10	0.90	0.90	0.05	-0.64	1.00	70.11	86	194	523	722
6-NS-27	7:30	0.91	649	0.07	0.85	0.93	0.00	-0.41	1.00	66.12	78	190	601	774
6-SN-28	16:30	0.00	649	0.07	0.85	0.90	0.02	-0.52	1.00	69.97	88	190	616	725
7-SN-50	7:30	1.00	658	0.09	0.91	0.93	0.00	-0.52	1.00	73.02	88	196	525	668
7-NS-51	16:30	1.00	653	0.08	0.91	0.92	0.00	-0.57	1.00	78.18	96	198	546	660
8-EW-48	7:30	0.88	643	0.09	0.88	0.92	0.00	-0.49	1.00	67.58	82	190	485	633
8-WE-49	16:30	0.00	644	0.08	0.90	0.92	0.00	-0.46	1.00	75.80	90	194	579	642
Urban Averages		0.44	652	0.09	0.88	0.90	0.01	-0.51	1.00	68.31	84	194	561	719
Urban Std. Dev.		0.47	8	0.01	0.03	0.02	0.02	0.07	0.00	8.53	9	2	39	62
Urban Maxima		1.00	666	0.10	0.91	0.93	0.07	-0.41	1.00	78.18	96	198	616	841
Urban Minima		0.00	640	0.07	0.83	0.86	0.00	-0.64	1.00	44.18	64	190	485	633
Combined Averages														
Combined Averages		0.32	657	0.07	0.86	0.89	0.01	-0.44	1.00	68.27	81	193	568	747
Combined Std. Dev.		0.43	13	0.01	0.03	0.02	0.02	0.10	0.00	9.39	11	3	39	74
Combined Maxima		1.00	700	0.10	0.91	0.93	0.07	-0.26	1.00	86.35	100	198	636	880
Combined Minima		0.00	640	0.05	0.80	0.83	0.00	-0.64	1.00	39.46	48	186	485	592

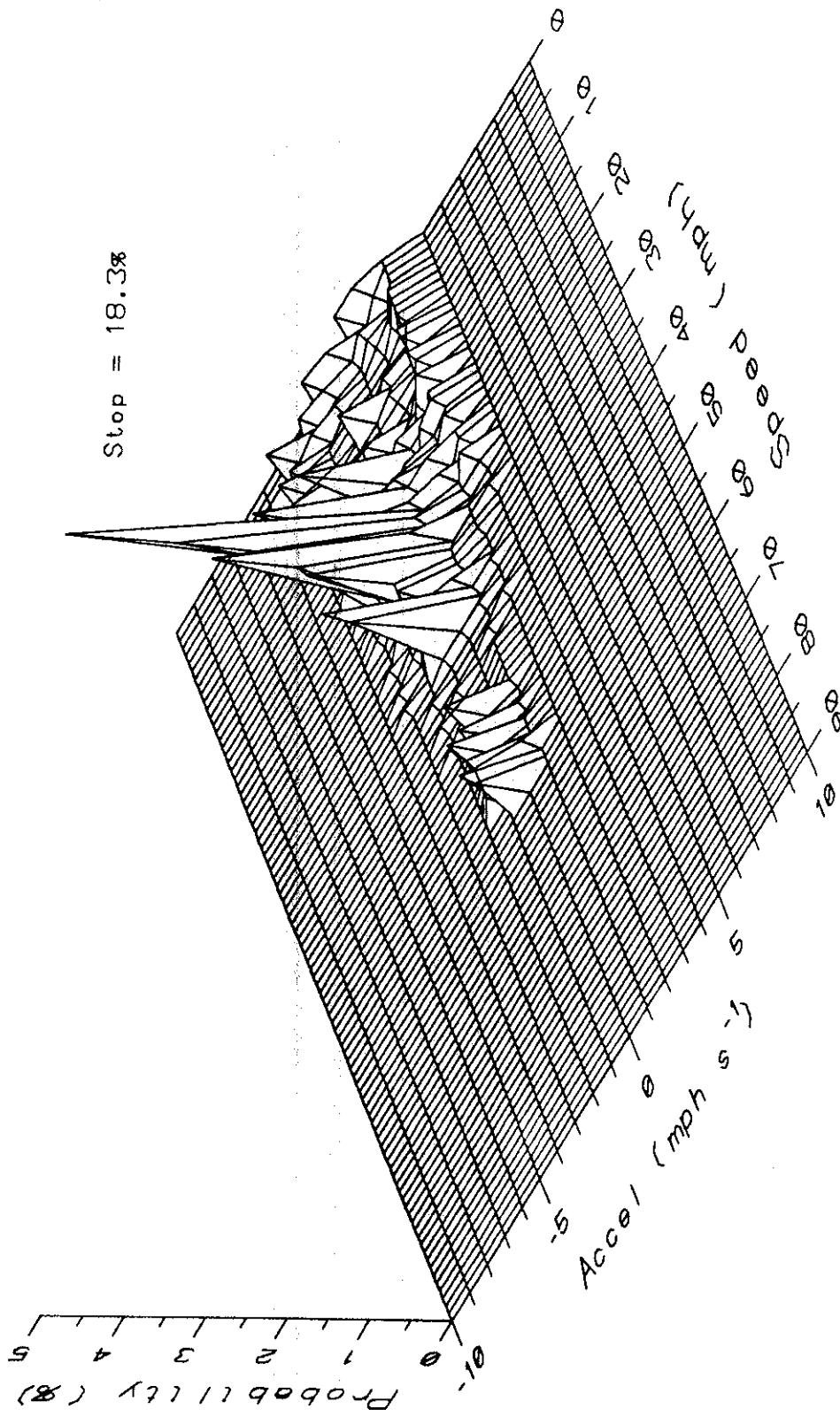


Figure 3.2.6.3 Probability plot of the UDDS, bags 1 and 2.

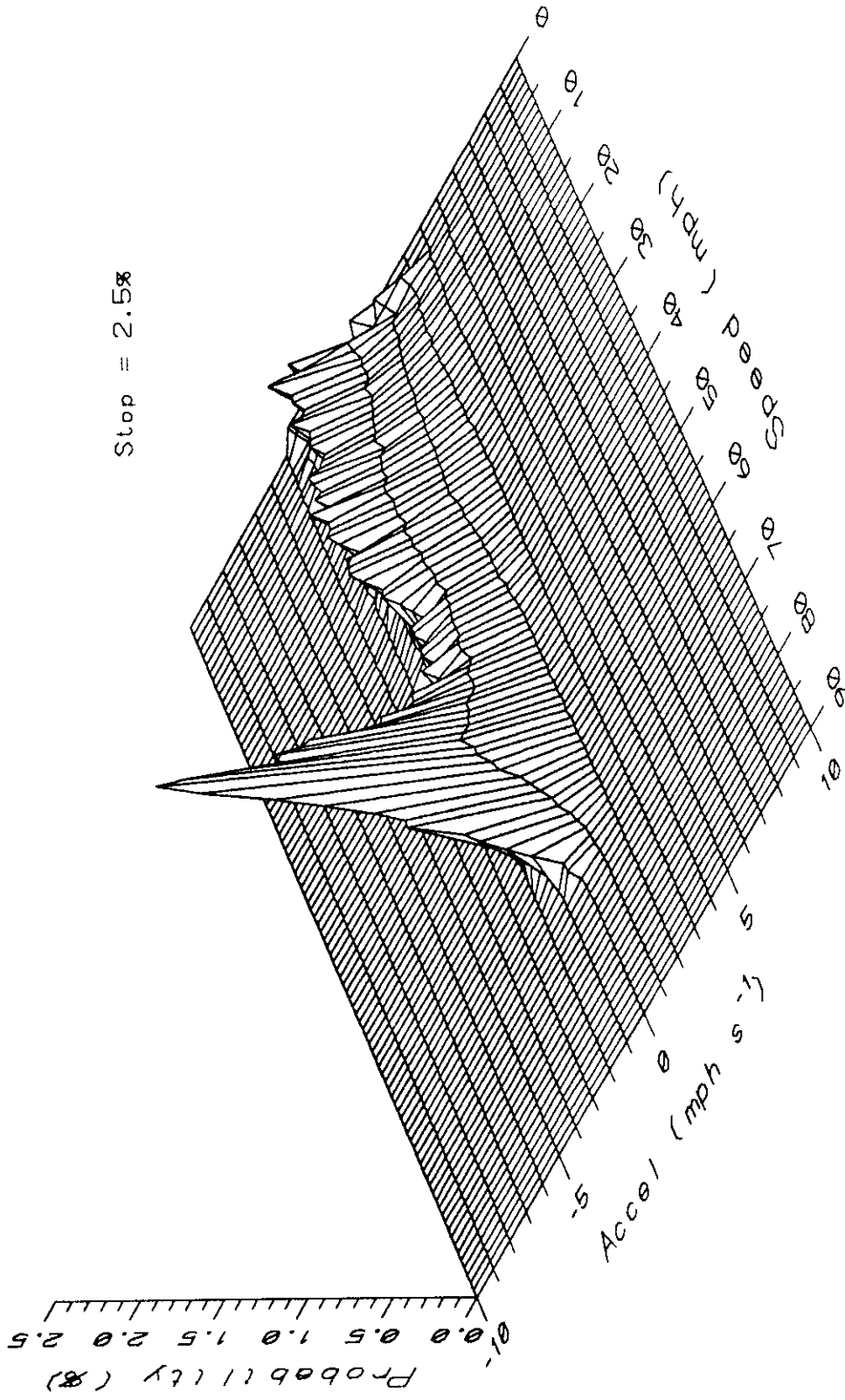


Figure 3.2.6.4 Probability plot of conservative freeway driving pattern data.

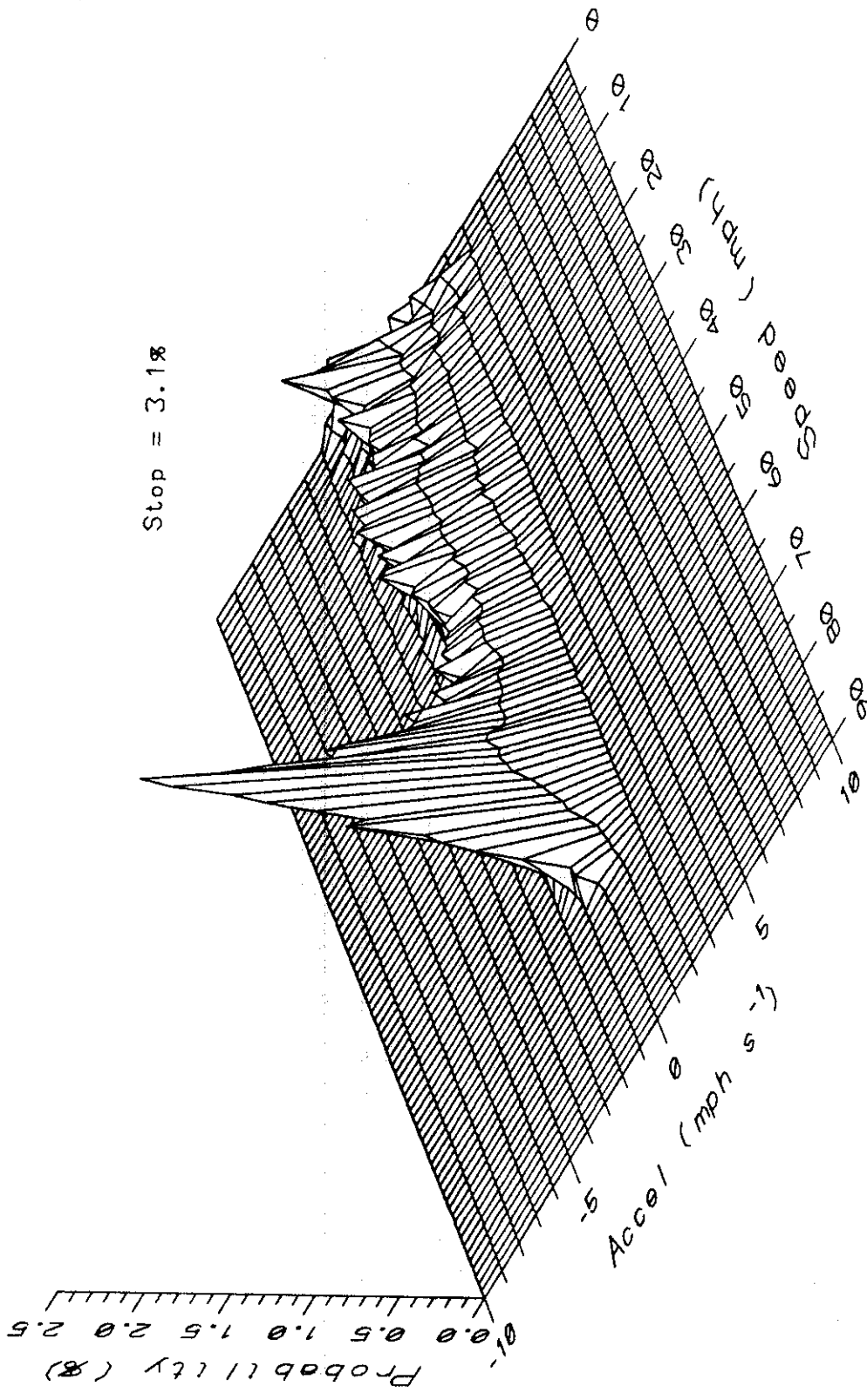


Figure 3.2.6.5 Probability plot of conservative morning freeway driving pattern data.

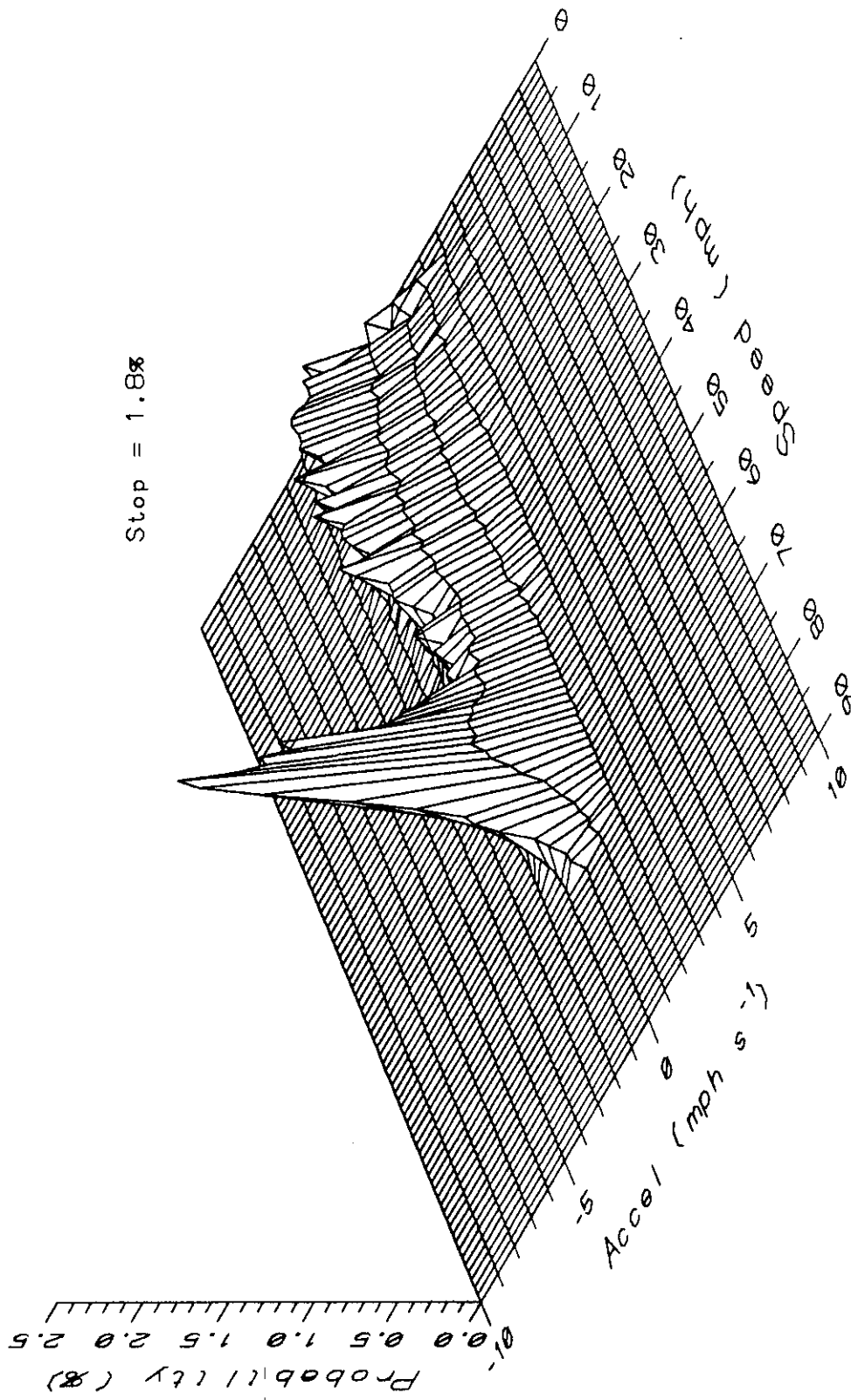


Figure 3.2.6.6 Probability plot of conservative evening freeway driving pattern data.

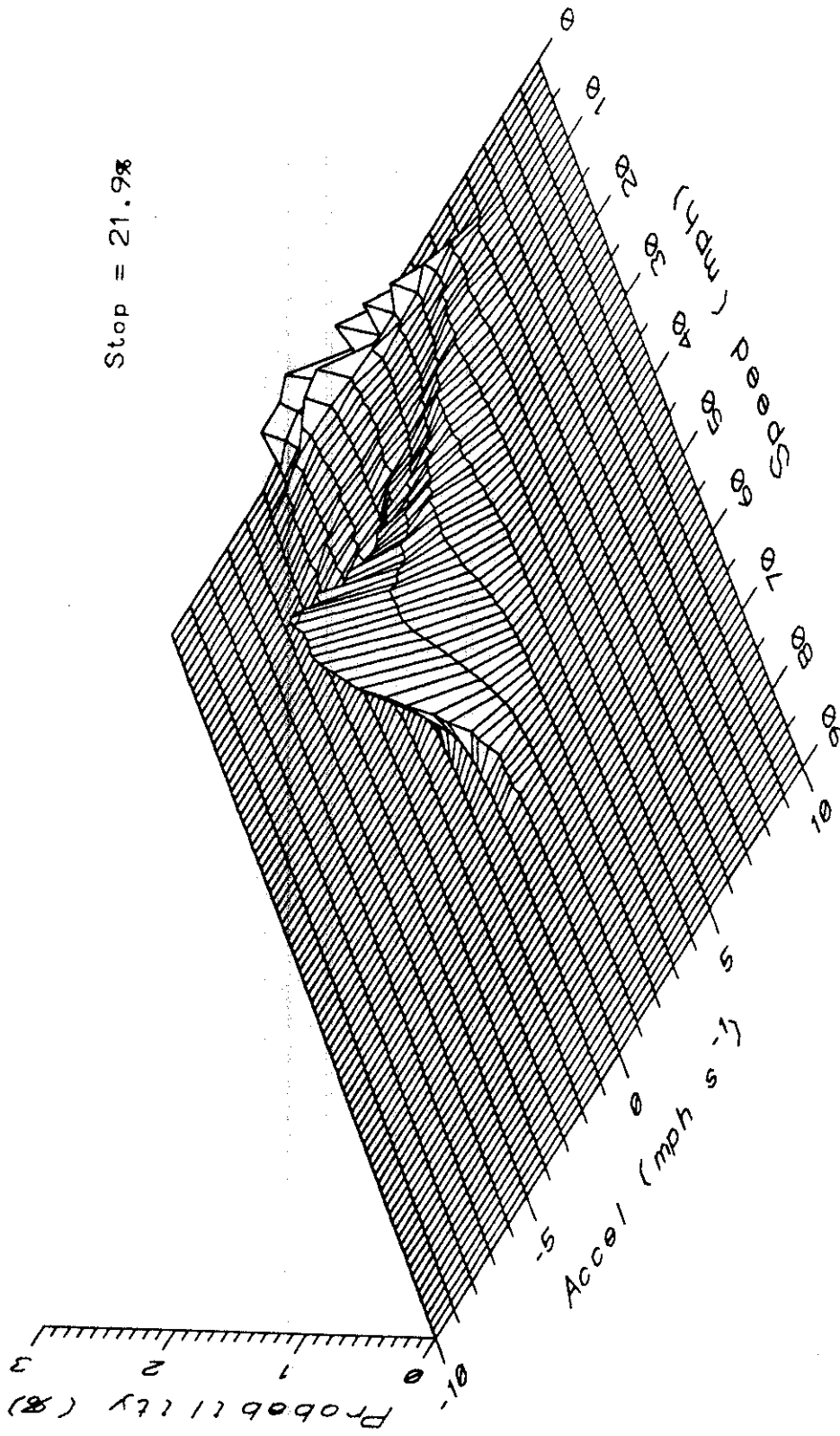


Figure 3.2.6.7 Probability plot of conservative urban driving pattern data.

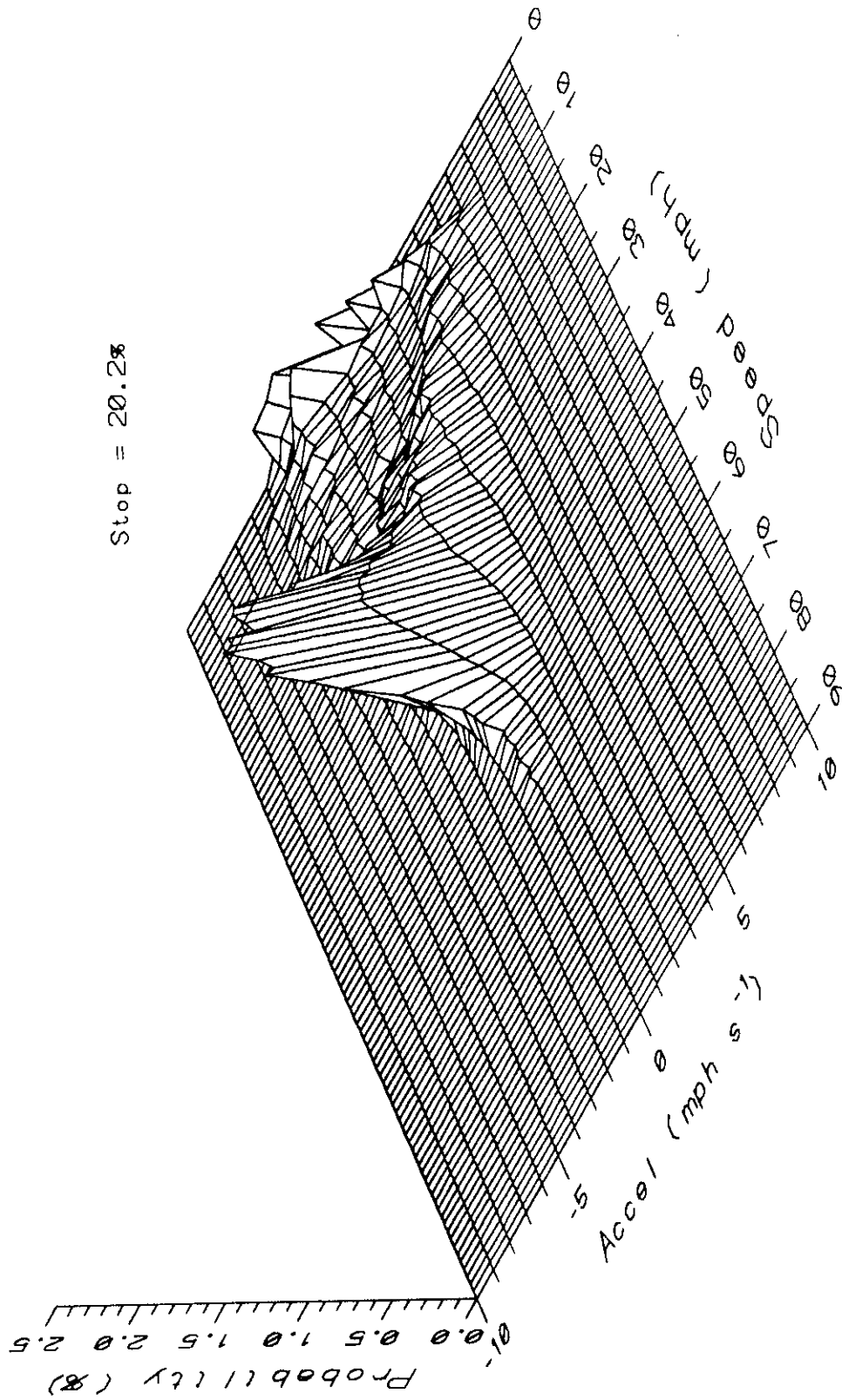


Figure 3.2.6.8 Probability plot of conservative morning urban driving pattern data.

Probability (%)

0.1
0.5
1.0
1.5
2.0
2.5

Stop = 23.3%

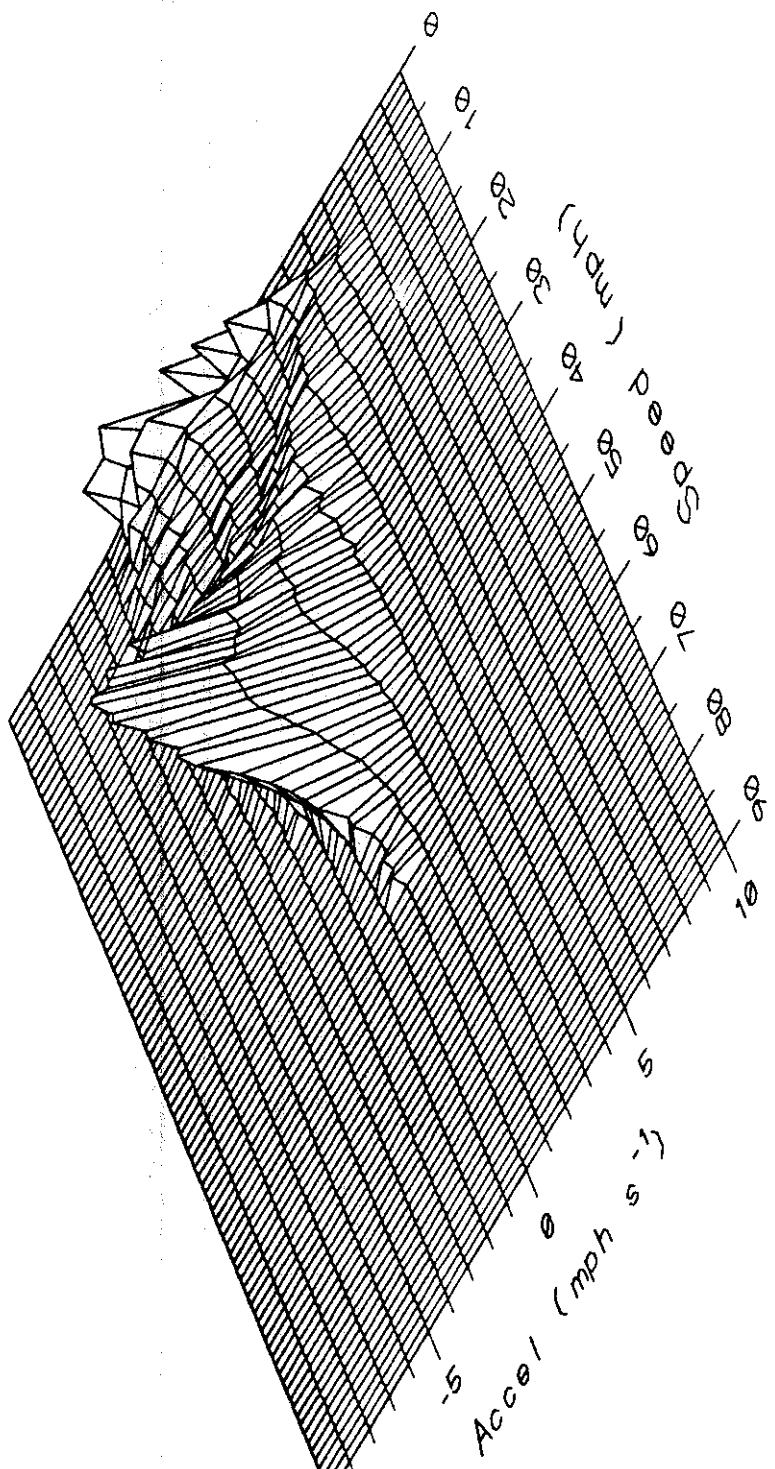


Figure 3.2.6.9 Probability plot of conservative evening urban driving pattern data.

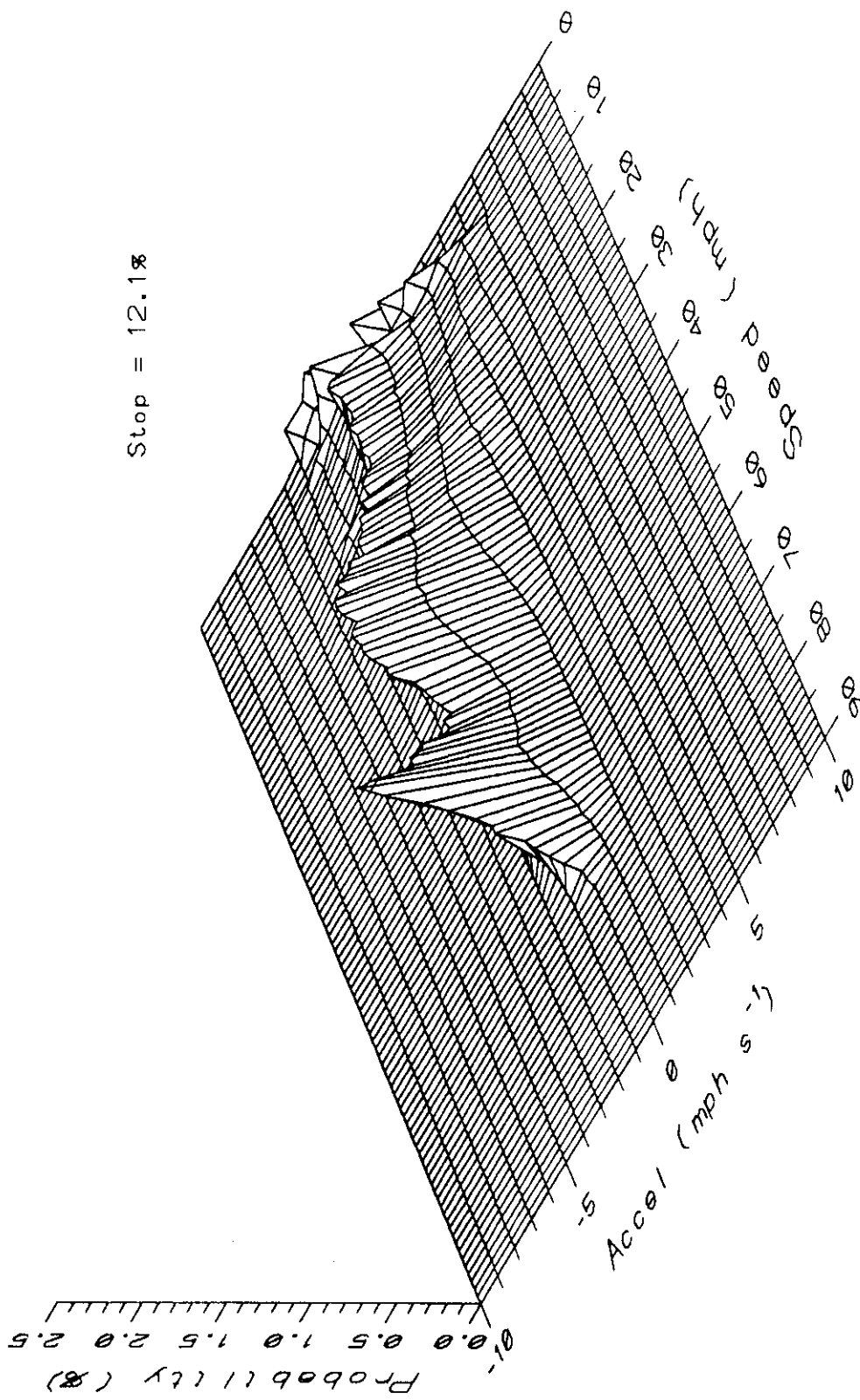


Figure 3.2.6.10 Probability plot of combined conservative freeway and urban driving pattern data.

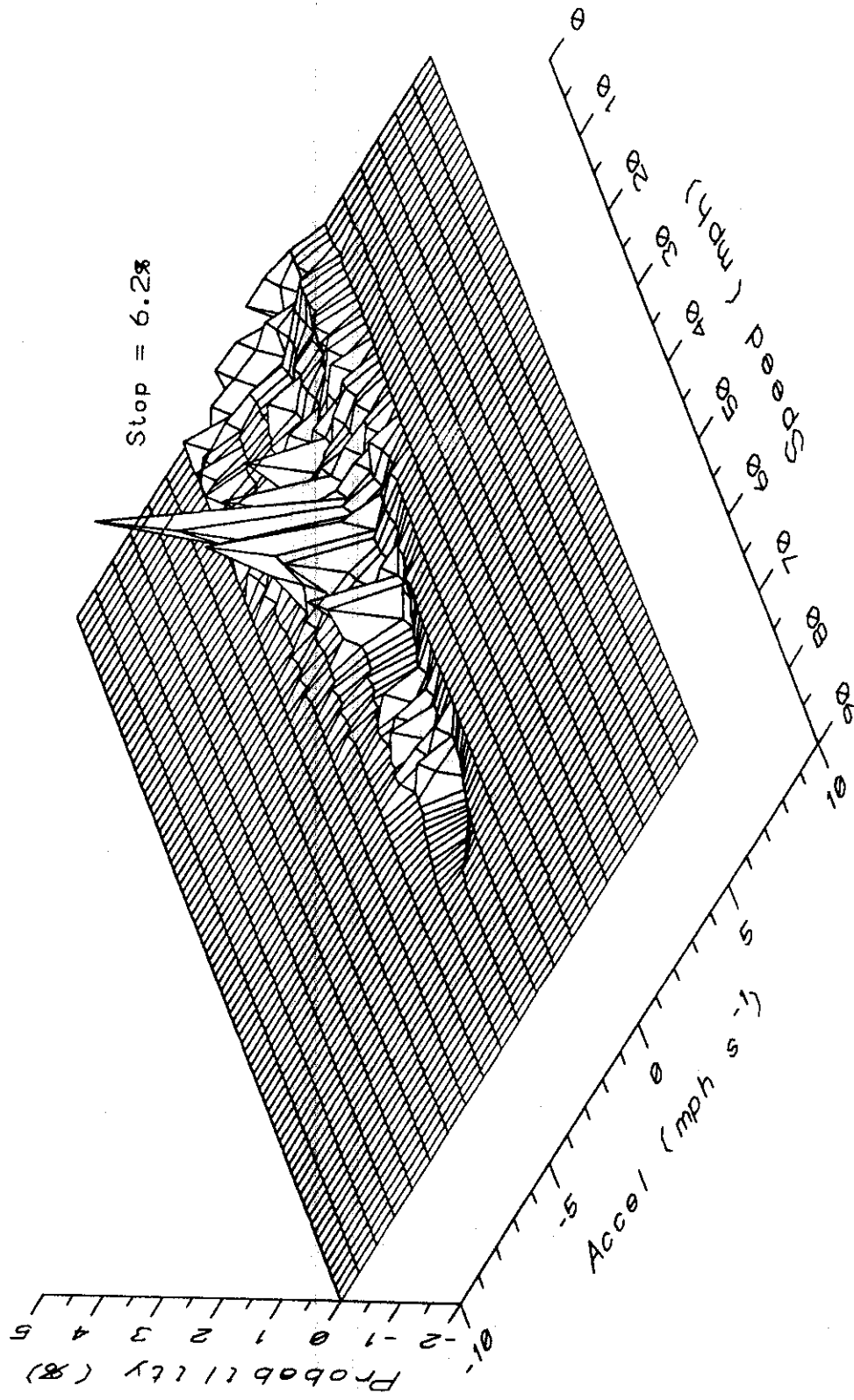


Figure 3.2.6.11 Probability plot of FTP minus combined conservative freeway and urban driving pattern data.

Table 3.2.7.1 Driving parameter data for on-road aggressive driving experiments.

Route	Depart	Travel	Travel	Avg	Max	Max	Max	Fuel	GM	Open	Open	Avg Dist
Number	Time	Time	Dist	Speed	Speed	Accel	Decel	Econ	Enrich	Loop	Loop	Per Stop
Dir, Expt#	hr:min	min	miles	mph	mph	mph s-l	mph s-l	mpg	%	Rich %	Lean %	miles
Freeway Routes												
1A-NS-54	7:30	64.98	50.02	46.20	76.73	4.72	9.04	32.4	6.59	0.87	1.77	16.67
1A-SN-55	16:30	65.23	49.94	45.95	77.27	4.74	6.31	30.1	5.09	0.23	0.92	4.54
6A-SN-60	7:30	75.13	39.77	31.77	80.25	6.91	7.49	27.2	3.11	0.18	0.13	1.53
6A-NS-61	16:30	64.10	40.26	37.69	75.45	5.14	6.36	29.0	4.55	0.47	0.47	4.47
Freeway Averages		67.36	45.00	40.40	77.43	5.38	7.30	29.7	4.84	0.44	0.82	6.80
Freeway Std. Dev.		5.20	5.76	6.98	2.03	1.04	1.28	2.2	1.44	0.31	0.71	6.73
Freeway Maxima		75.13	50.02	46.20	80.25	6.91	9.04	32.4	6.59	0.87	1.77	16.67
Freeway Minima		64.10	39.77	31.77	75.45	4.72	6.31	27.2	3.11	0.18	0.13	1.53
Urban Routes												
4A-WE-56	7:30	62.78	29.05	27.77	67.22	8.34	8.96	19.0	10.75	1.01	0.19	0.74
4A-EW-57	16:30	72.70	29.02	23.96	66.75	8.66	7.51	19.5	7.63	1.51	0.16	0.60
7A-SN-58	7:30	85.85	39.68	27.73	75.03	9.57	7.91	21.5	6.93	0.85	0.25	0.90
7A-NS-59	16:30	99.17	39.63	23.98	65.65	8.43	9.78	19.2	7.26	0.84	0.12	0.67
Urban Averages		80.13	34.35	25.86	68.66	8.75	8.54	19.8	8.14	1.05	0.18	0.73
Urban Std. Dev.		15.83	6.13	2.18	4.30	0.56	1.03	1.1	1.76	0.31	0.05	0.13
Urban Maxima		99.17	39.68	27.77	75.03	9.57	9.78	21.5	10.75	1.51	0.25	0.90
Urban Minima		62.78	29.02	23.96	65.65	8.34	7.51	19.0	6.93	0.84	0.12	0.60
Combined Averages												
Combined Averages		73.74	39.67	33.13	73.04	7.06	7.92	24.7	6.49	0.75	0.50	3.77
Combined Std. Dev.		12.87	7.92	9.13	5.62	1.96	1.26	5.5	2.31	0.44	0.58	5.47
Combined Maxima		99.17	50.02	46.20	80.25	9.57	9.78	32.4	10.75	1.51	1.77	16.67
Combined Minima		62.78	29.02	23.96	65.65	4.72	6.31	19.0	3.11	0.18	0.12	0.60

(24.7 versus 28.6 mpg) but was still higher than the FTP (23.1 mpg). There were also less frequent stops (3.77 versus 2.81 for conservative driving and 0.58 miles per stop for the FTP) for the aggressive driver experiments since the test vehicle was no longer restricted to a single lane, and the driver could pass the vehicle ahead if it decelerated quickly or stopped.

Data for the acceleration-based modes of operation for the aggressive driving routes are presented in Table 3.2.7.2. A comparison of the aggressive driving experiments to the "conservative" driving patterns for the same experiments and the FTP by mode of operation is shown in Figure 3.2.7.2. As expected, aggressive driving decreased the percent of time cruising and coasting (16.1 versus 18.5%, and 2.9 versus 5.6%) and increased the frequency of all accelerations relative to conservative driving with the largest increase in the percentage of time in hard accelerations (0.74 versus

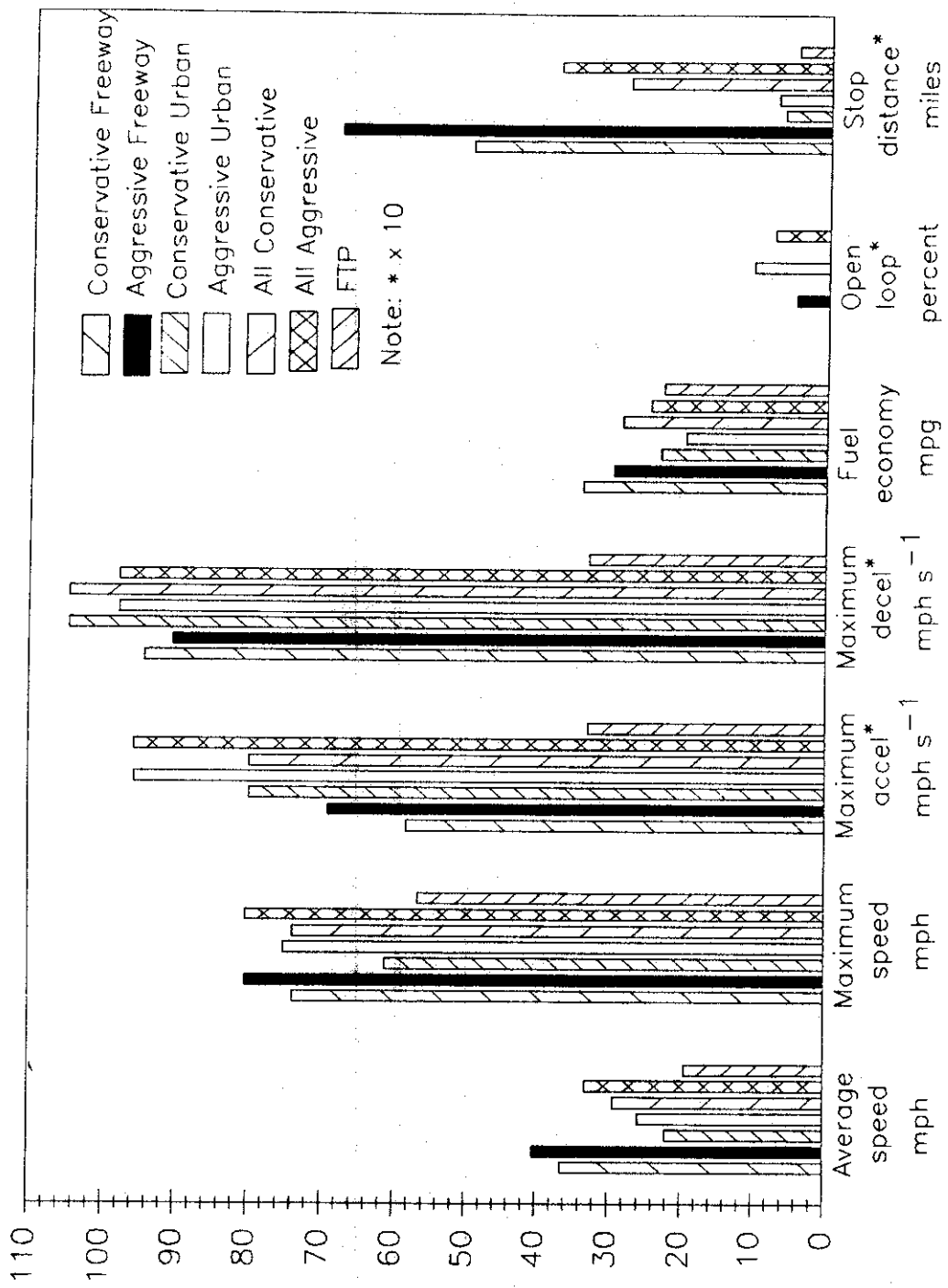


Figure 3.2.7.1 Comparison of vehicle operating parameters for the FTP, conservative driving and aggressive driving on-road data.

Table 3.2.7.2 Percent time in acceleration-based modes for on-road aggressive driving experiments.

Route Number	Depart Time	Modes									
		Cold Start	At Stop	Cruise	Coast	Hard Accel	Med Accel	Light Accel	Hard Decel	Med Decel	Light Decel
Dir, Expt#	hr:min										
Freeway Routes											
1A-NS-54	7:30	0.00	0.62	21.73	3.28	0.87	0.10	36.6	0.36	18.68	17.73
1A-SN-55	16:30	0.00	1.35	29.01	3.42	0.20	0.05	33.8	0.69	10.81	20.70
6A-SN-60	7:30	0.00	4.02	17.33	6.37	0.16	0.51	36.2	1.80	21.06	12.56
6A-NS-61	16:30	0.00	1.30	18.54	3.93	0.47	0.23	38.1	0.57	22.31	14.51
Freeway Averages		0.00	1.82	21.65	4.25	0.43	0.22	36.2	0.86	18.22	16.38
Freeway Std. Dev.		0.00	1.50	5.24	1.44	0.33	0.21	1.8	0.64	5.16	3.59
Freeway Maxima		0.00	4.02	29.01	6.37	0.87	0.51	38.1	1.80	22.31	20.70
Freeway Minima		0.00	0.62	17.33	3.28	0.16	0.05	33.8	0.36	10.81	12.56
Urban Routes											
4A-WE-56	7:30	0.00	20.15	10.57	0.96	1.01	3.00	31.9	3.35	21.64	7.43
4A-EW-57	16:30	0.00	20.84	10.39	2.50	1.51	2.34	28.9	3.14	22.86	7.57
7A-SN-58	7:30	0.00	20.27	12.04	1.30	0.85	2.39	29.4	2.31	20.52	10.91
7A-NS-59	16:30	0.00	23.82	9.14	1.51	0.84	2.87	29.8	3.26	21.73	7.01
Urban Averages:		0.00	21.27	10.54	1.57	1.05	2.65	30.0	3.02	21.69	8.23
Urban Std. Dev.		0.00	1.73	1.19	0.66	0.31	0.33	1.3	0.48	0.96	1.80
Urban Maxima		0.00	23.82	12.04	2.50	1.51	3.00	31.9	3.35	22.86	10.91
Urban Minima		0.00	20.15	9.14	0.96	0.84	2.34	28.9	2.31	20.52	7.01
Combined Averages:		0.00	11.55	16.09	2.91	0.74	1.44	33.1	1.94	19.95	12.30
Combined Std. Dev.		0.00	10.50	6.91	1.77	0.45	1.32	3.6	1.27	3.91	5.09
Combined Maxima		0.00	23.82	29.01	6.37	1.51	3.00	38.1	3.35	22.86	20.70
Combined Minima		0.00	0.62	9.14	0.96	0.16	0.05	28.9	0.36	10.81	7.01

0.01%). Also, because there was less time cruising and coasting, the percentage of time decelerating also increased.

The average time in the acceleration-based modes for aggressive driving is given in Table 3.2.7.3. When driving aggressively, the average time in cruise or coast was less than driving conservatively (1.7 versus 2.1 seconds, and 1.4 versus 1.7 seconds). The duration of hard and medium accelerations increased (1.8 versus 1.6 seconds and 1.8 versus 1.7 seconds) but the duration of light accelerations decreased due to the aggressiveness of the driving (4.1 versus 4.7 seconds). The duration of hard decelerations were approximately the same, but the duration of medium and light decelerations decreased (4.2 versus 4.9 seconds, and 2.1 versus 2.2 seconds).

The percent time in load-based modes for the aggressive driving experiments is

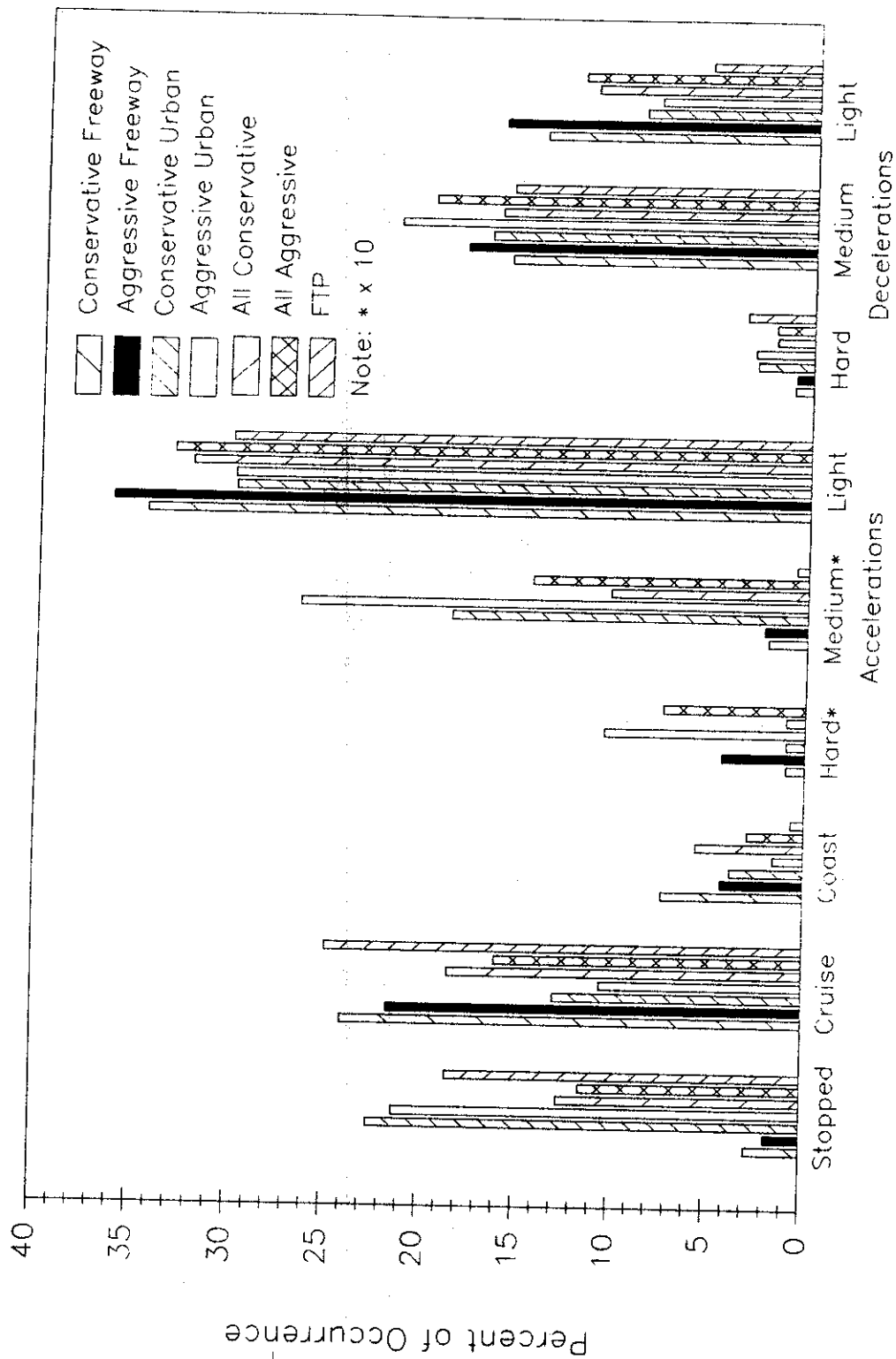


Figure 3.2.7.2 Comparison of the FTP, conservative driving and aggressive driving on-road data by mode of operation.

Table 3.2.7.3 Average time in acceleration-based modes for on-road aggressive driving experiments.

Route Number	Depart Time	Modes									
		Cold Start	At Stop	Cruise	Coast	Hard Accel	Med Accel	Light Accel	Hard Decel	Med Decel	Light Decel
Dir, Expt#	hr:min	Start	Stop			Accel	Accel	Accel	Decel	Decel	Decel
note: **** mode did not occur during driving of on-road route											
Freeway Routes											
1A-NS-54	7:30	****	8.00	1.84	1.54	2.62	1.33	4.45	1.56	3.94	2.53
1A-SN-55	16:30	****	4.82	2.15	1.81	1.60	1.00	3.63	1.59	3.28	2.78
6A-SN-60	7:30	****	6.96	1.84	1.65	1.75	1.77	4.34	1.80	3.81	2.19
6A-NS-61	16:30	****	5.56	1.65	1.40	1.80	1.50	4.08	1.69	3.76	1.82
Freeway Averages		****	6.34	1.87	1.60	1.94	1.40	4.13	1.66	3.70	2.33
Freeway Std. Dev.		****	1.42	0.21	0.17	0.46	0.32	0.36	0.11	0.29	0.42
Freeway Maxima		****	8.00	2.15	1.81	2.62	1.77	4.45	1.80	3.94	2.78
Freeway Minima		****	4.82	1.65	1.40	1.60	1.00	3.63	1.56	3.28	1.82
Urban Routes											
4A-WE-56	7:30	****	19.46	1.57	1.20	1.52	2.17	4.35	2.57	5.00	1.84
4A-EW-57	16:30	****	18.94	1.59	1.27	2.13	2.08	3.78	1.96	4.49	1.73
7A-SN-58	7:30	****	23.73	1.65	1.16	1.69	2.16	4.06	2.20	4.52	2.07
7A-NS-59	16:30	****	24.02	1.52	1.13	1.56	2.16	4.40	2.20	4.43	1.61
Urban Averages		****	21.54	1.58	1.19	1.73	2.14	4.15	2.23	4.61	1.81
Urban Std. Dev.		****	2.71	0.05	0.06	0.28	0.04	0.29	0.25	0.26	0.20
Urban Maxima		****	24.02	1.65	1.27	2.13	2.17	4.40	2.57	5.00	2.07
Urban Minima		****	18.94	1.52	1.13	1.52	2.08	3.78	1.96	4.43	1.61
Combined Averages		****	13.94	1.73	1.40	1.83	1.77	4.14	1.95	4.15	2.07
Combined Std. Dev.		****	8.37	0.21	0.25	0.37	0.45	0.30	0.35	0.55	0.41
Combined Maxima		****	24.02	2.15	1.81	2.62	2.17	4.45	2.57	5.00	2.78
Combined Minima		****	4.82	1.52	1.13	1.52	1.00	3.63	1.56	3.28	1.61

shown in Table 3.2.7.4. Similar to the hard, medium and light accelerations, the percentage of time in high and medium high load conditions increased (7.0 versus 1.3, and 34.3 versus 29.4) and the percent time in medium low and low load conditions decreased when driving aggressively (8.4 versus 11.3, and 49.0 versus 57.6). The percent time in open loop operation is discussed in Section 3.2.8.

The average, maximum and minimum vehicle operation parameter data for aggressive driving are given in Tables 3.2.7.5, 3.2.7.6 and 3.2.7.7 respectively. The average load on-road was only slightly higher for aggressive driving than conservative driving (0.29 versus 0.26). Although the maximum load for aggressive driving and conservative driving were the same, the maximum for all the aggressive driving experiments was the maximum recorded (0.75).

Table 3.2.7.4 Percent time in load-based modes for on-road aggressive driving experiments.

Route Number	Depart Time	Modes							
		Open Loop		High	Medium	Medium	Low	Hot	Cold
Dir. Expt#	hr:min	Rich	Lean	Load	High Load	Low Load	Load	Start	Start
Freeway Routes									
1A-NS-54	7:30	0.87	1.77	7.18	54.46	5.75	30.0	0.00	0.00
1A-SN-55	16:30	0.23	0.92	6.54	62.87	2.86	26.6	0.00	0.00
6A-SN-60	7:30	0.18	0.13	4.53	29.04	8.45	57.7	0.00	0.00
6A-NS-61	16:30	0.47	0.47	5.38	40.10	7.98	45.6	0.00	0.00
Freeway Averages		0.44	0.82	5.91	46.62	6.26	40.0	0.00	0.00
Freeway Std. Dev.		0.31	0.71	1.18	15.02	2.55	14.4	0.00	0.00
Freeway Maxima		0.87	1.77	7.18	62.87	8.45	57.7	0.00	0.00
Freeway Minima		0.18	0.13	4.53	29.04	2.86	26.6	0.00	0.00
Urban Routes									
4A-WE-56	7:30	1.01	0.19	11.39	26.18	9.80	51.4	0.00	0.00
4A-EW-57	16:30	1.51	0.16	6.56	17.20	10.25	64.3	0.00	0.00
7A-SN-58	7:30	0.85	0.25	8.00	25.36	10.64	54.9	0.00	0.00
7A-NS-59	16:30	0.84	0.12	6.69	19.11	11.72	61.5	0.00	0.00
Urban Averages		1.05	0.18	8.16	21.96	10.60	58.0	0.00	0.00
Urban Std. Dev.		0.31	0.05	2.25	4.48	0.82	5.9	0.00	0.00
Urban Maxima		1.51	0.25	11.39	26.18	11.72	64.3	0.00	0.00
Urban Minima		0.84	0.12	6.56	17.20	9.80	51.4	0.00	0.00
Combined Averages									
Combined Averages		0.75	0.50	7.03	34.29	8.43	49.0	0.00	0.00
Combined Std. Dev.		0.44	0.58	2.05	16.70	2.91	14.1	0.00	0.00
Combined Maxima		1.51	1.77	11.39	62.87	11.72	64.3	0.00	0.00
Combined Minima		0.18	0.12	4.53	17.20	2.86	26.6	0.00	0.00

The measured maximum lambda for all of the aggressive experiments was 1.70 and all experiments contained lean open loop operation. All of the conservative driving freeway experiments contained lean open loop operation and the maxima were all 1.70 with the exception of one reading of 1.71. For the urban experiments, all of the experiments which contained lean open loop operation had maxima of 1.70 with the exception of one experiment for which the maximum was 1.61. The maximum for experiments without lean open loop operation was 1.23.

The lambda minima for the aggressive experiments ranged from 0.82 - 0.84 and rich open loop operation occurred for all of the aggressive driving experiments. The

Table 3.2.7.5 Average vehicle operating parameter data for on-road aggressive driving experiments.

Route	Depart	Throttle		Stock	Horiba	%	Vehicle		Amb	Air	Eng	Exh	Cat	%	
Number	Time	Position	RPM	Load	A/F	A/F	MeOH	Accel	Gear	Temp	Charge	Coolant	Gas	Temp	Time
Dir, Expt#	hr:min							G's		deg F	Temp	Temp	Temp	deg F	Braking
Freeway Routes															
1A-NS-54	7:30	82.04	1756	0.29	1.00	1.01	0.11	0.03	3.55	62.92	77	200	912	1176	24.08
1A-SN-55	16:30	88.84	1733	0.31	1.00	1.00	0.14	0.06	3.46	79.11	99	203	920	1146	16.40
6A-SN-60	7:30	58.22	1455	0.27	1.00	1.00	0.14	0.25	2.91	****	82	203	835	1065	32.36
6A-NS-61	16:30	69.23	1562	0.28	1.00	1.00	0.15	-0.02	3.36	****	89	205	890	1128	27.67
Freeway Averages		74.58	1627	0.29	1.00	1.00	0.14	0.08	3.32	71.02	87	203	889	1129	25.13
Freeway Std. Dev.		13.60	143	0.02	0.00	0.01	0.02	0.12	0.28	11.45	9	2	38	47	6.73
Freeway Maxima		88.84	1756	0.31	1.00	1.01	0.15	0.25	3.55	79.11	99	205	920	1176	32.36
Freeway Minima		58.22	1455	0.27	1.00	1.00	0.11	-0.02	2.91	62.92	77	200	835	1065	16.40
note: **** sensor was not working															
Urban Routes															
4A-WE-56	7:30	85.80	1480	0.31	1.00	1.00	0.11	0.05	2.74	****	76	204	926	1203	47.52
4A-EW-57	16:30	68.24	1360	0.28	0.99	1.00	0.15	0.03	2.59	65.44	89	207	876	1147	50.09
7A-SN-58	7:30	70.85	1405	0.29	0.99	1.00	0.13	-0.33	2.83	****	74	204	892	1164	44.40
7A-NS-59	16:30	68.14	1355	0.28	0.99	1.00	0.15	-0.09	2.58	68.10	99	209	883	1155	51.36
Urban Averages		73.26	1400	0.29	0.99	1.00	0.14	-0.09	2.69	66.77	84	206	894	1167	48.34
Urban Std. Dev.		8.46	58	0.01	0.01	0.00	0.02	0.17	0.12	1.88	12	3	22	25	3.08
Urban Maxima		85.80	1480	0.31	1.00	1.00	0.15	0.05	2.83	68.10	99	209	926	1203	51.36
Urban Minima		68.14	1355	0.28	0.99	1.00	0.11	-0.33	2.58	65.44	74	204	876	1147	44.40
Combined Averages		73.92	1513	0.29	1.00	1.00	0.14	0.00	3.00	68.89	86	204	892	1148	36.74
Combined Std. Dev.		10.51	158	0.01	0.01	0.00	0.02	0.16	0.40	7.13	10	3	29	40	13.32
Combined Maxima		88.84	1756	0.31	1.00	1.01	0.15	0.25	3.55	79.11	99	209	926	1203	51.36
Combined Minima		58.22	1355	0.27	0.99	1.00	0.11	-0.33	2.58	62.92	74	200	835	1065	16.40

lowest two recorded lambdas for the conservative driving freeway routes were in experiments 7-EW-2 and 7-WE-3 (0.84 and 0.83) with the next lowest lambda for the freeway experiments of 0.87. Both of the low lambda experiments contained rich open loop operation. For the conservative driving urban experiments, experiment 4-EW-22 contained rich open loop operation and it was the lowest recorded lambda on-road for the urban experiments. Experiment 1-NS-6 also contained rich open loop operation however the minimum lambda was only 0.85, the same as three other experiments.

From the lean and rich open loop data, it appears the exhaust gas lambda could be used to determine if the vehicle is operating open loop. This would simplify determination of open loop operation for other vehicles because it would remove the need to directly access the EEC to read the open loop flag to determine open loop operation. This is discussed further in Section 3.3.4, Emissions During Open Loop

Table 3.2.7.6 Maximum vehicle operating parameter data for on-road aggressive driving experiments.

Route Number	Depart Time	Throttle Position	RPM	Load	Stock A/F	Horiba A/F	% MeOH	Vehicle Accel	Gear	Amb Temp	Air Charge	Eng Coolant	Exh Gas	Cat Temp
Dir, Expt#	hr:min							G's		deg F	Temp	Temp	Temp	deg F
Freeway Routes														
1A-NS-54	7:30	740.56	4385	0.75	2.00	1.70	0.12	0.51	4.00	72.49	132	216	1289	1376
1A-SN-55	16:30	627.70	3685	0.75	2.00	1.70	0.14	0.44	4.00	89.89	148	218	1284	1403
6A-SN-60	7:30	624.00	3965	0.75	1.86	1.70	0.15	0.57	4.00	****	108	216	1233	1345
6A-NS-61	16:30	696.30	4027	0.75	2.00	1.70	0.15	0.23	4.00	****	104	216	1261	1399
Freeway Averages		672.14	4015	0.75	1.97	1.70	0.14	0.44	4.00	81.19	123	217	1267	1381
Freeway Std. Dev.		56.44	288	0.00	0.07	0.00	0.01	0.15	0.00	12.30	21	1	26	27
Freeway Maxima		740.56	4385	0.75	2.00	1.70	0.15	0.57	4.00	89.89	148	218	1289	1403
Freeway Minima		624.00	3685	0.75	1.86	1.70	0.12	0.23	4.00	72.49	104	216	1233	1345
note: **** sensor was not working														
Urban Routes														
4A-WE-56	7:30	665.78	4529	0.75	2.00	1.70	0.13	0.49	4.00	66.79	132	218	1341	1445
4A-EW-57	16:30	719.78	4233	0.75	2.00	1.70	0.15	0.41	4.00	75.27	124	218	1257	1350
7A-SN-58	7:30	707.30	4379	0.75	2.00	1.70	0.15	0.10	4.00	****	122	218	1263	1369
7A-NS-59	16:30	659.09	4251	0.75	1.78	1.70	0.16	0.32	4.00	86.48	136	218	1307	1399
Urban Averages		687.99	4348	0.75	1.95	1.70	0.15	0.33	4.00	76.18	129	218	1292	1391
Urban Std. Dev.		30.07	137	0.00	0.11	0.00	0.01	0.17	0.00	9.88	7	0	40	42
Urban Maxima		719.78	4529	0.75	2.00	1.70	0.16	0.49	4.00	86.48	136	218	1341	1445
Urban Minima		659.09	4233	0.75	1.78	1.70	0.13	0.10	4.00	66.79	122	218	1257	1350
Combined Averages														
Combined Std. Dev.		42.71	274	0.00	0.09	0.00	0.01	0.16	0.00	9.70	15	1	34	33
Combined Maxima		740.56	4529	0.75	2.00	1.70	0.16	0.57	4.00	89.89	148	218	1341	1445
Combined Minima		624.00	3685	0.75	1.78	1.70	0.12	0.10	4.00	66.79	104	216	1233	1345

Operation.

The ambient temperatures for the aggressive driving experiments were in the range of the conservative driving experiments. The average temperature (69°F) was lower than the prescribed temperature for the FTP and the average on-road ambient temperature (75°F).

The average engine coolant temperature for freeway experiments was 3°F cooler than the urban experiments for aggressive driving (203°F versus 206°F). This was similar to the trend observed for the conservative driving routes where the engine coolant temperature on the freeway routes was 4°F cooler than on the urban experiments, and the average temperature for aggressive and conservative freeway experiments was the same (203°F). The maximum engine coolant temperature for all of the aggressive driving

Table 3.2.7.7 Minimum vehicle operating parameter data for on-road aggressive driving experiments.

Route	Depart	Throttle			Stock	Horiba	%	Vehicle		Amb	Air	Eng	Exh	Cat
Number	Time	Position	RPM	Load	A/F	A/F	MeOH	Accel	Gear	Temp	Charge	Coolant	Gas	Temp
Dir, Expt#	hr:min							G's		deg F	Temp	Temp	Temp	deg F
Freeway Routes														
1A-NS-54	7:30	0.97	702	0.06	0.83	0.80	0.11	-0.24	1.00	56.53	66	190	658	693
1A-SN-55	16:30	0.00	676	0.06	0.83	0.83	0.13	-0.15	1.00	64.39	74	188	578	780
6A-SN-60	7:30	0.00	647	0.06	0.84	0.86	0.13	-0.13	1.00	****	1	186	500	739
6A-NS-61	16:30	0.00	671	0.06	0.84	0.84	0.14	-0.34	1.00	****	78	194	645	890
Freeway Averages		0.24	674	0.06	0.84	0.83	0.13	-0.22	1.00	60.46	55	190	595	775
Freeway Std. Dev.		0.49	23	0.00	0.01	0.03	0.01	0.10	0.00	5.56	36	3	73	84
Freeway Maxima		0.97	702	0.06	0.84	0.86	0.14	-0.13	1.00	64.39	78	194	658	890
Freeway Minima		0.00	647	0.06	0.83	0.80	0.11	-0.34	1.00	56.53	1	186	500	693
note: **** sensor was not working														
Urban Routes														
4A-WE-56	7:30	0.98	659	0.07	0.82	0.84	0.10	-0.41	1.00	****	60	190	536	701
4A-EW-57	16:30	0.41	653	0.06	0.84	0.83	0.14	-0.39	1.00	59.87	74	190	618	763
7A-SN-58	7:30	0.00	653	0.06	0.84	0.83	0.12	-0.76	1.00	****	60	188	558	732
7A-NS-59	16:30	0.00	660	0.07	0.83	0.83	0.14	-0.59	1.00	62.00	78	194	562	763
Urban Averages		0.35	656	0.07	0.83	0.83	0.13	-0.54	1.00	60.94	68	191	569	739
Urban Std. Dev.		0.46	4	0.01	0.01	0.00	0.02	0.17	0.00	1.51	9	3	35	29
Urban Maxima		0.98	660	0.07	0.84	0.84	0.14	-0.39	1.00	62.00	78	194	618	763
Urban Minima		0.00	653	0.06	0.82	0.83	0.10	-0.76	1.00	59.87	60	188	536	701
Combined Averages														
Combined Averages		0.30	665	0.06	0.83	0.83	0.13	-0.38	1.00	60.70	61	190	582	757
Combined Std. Dev.		0.44	18	0.00	0.01	0.02	0.02	0.22	0.00	3.34	26	3	55	61
Combined Maxima		0.98	702	0.07	0.84	0.86	0.14	-0.13	1.00	64.39	78	194	658	890
Combined Minima		0.00	647	0.06	0.82	0.80	0.10	-0.76	1.00	56.53	1	186	500	693

experiments was either 216 or 218°F.

The average catalyst temperature for the aggressive driving experiments was more than 100°F higher than the average for the conservative driving experiments. Although the average catalyst temperature increased and the average exhaust gas temperature increased over conservative driving (892 versus 810°F), the maximum engine coolant temperature did not increase. This suggests the EEC is set to prevent the engine coolant temperature from exceeding 218°F.

There was a reversal from the conservative driving experiments for the highest average catalyst temperature with the freeway experiments having a lower average temperature than the urban experiments (1129 versus 1167°F). The maximum catalyst temperature for the aggressive driving routes was only slightly higher than the conservative driving experiments (1445 versus 1432°F) and the freeway experiments had

a lower maximum than the urban experiments (1403 versus 1445°F) similar to the conservative driving experiments.

The freeway and urban aggressive driving experiments had a similar trend to the conservative driving experiments with the freeway routes containing less time braking than the urban routes (25 versus 48%). The aggressive driving routes also had a higher average percent time braking than the conservative routes (37 versus 34%) possibly due to an increased amount of time necessary to slow down from higher speeds during the aggressive driving experiments.

The driving pattern data for the aggressive driving experiments were plotted as a function of probability of being at a specific speed and acceleration rate (Figure 3.2.7.3). The freeway route pattern data show a larger high speed peak which extends to higher speeds with less time at stop than the conservative driving experiments (1.4% versus 2.5%). For comparison of the morning and evening freeway data (Figures 3.2.7.4 and 3.2.7.5), a similar trend to the conservative driving experiments for freeway routes was observed with approximately twice the percent time at stop for morning driving compared to evening driving (2.0% versus 0.81%). The freeway driving patterns for evenings at high speeds was greater than for the morning experiments.

The driving pattern data for the urban routes driven aggressively (Figure 3.2.7.6) show higher rates of acceleration (to 10 mph s^{-1} at 12 mph) than the conservative driving urban experiments and the aggressive driving freeway experiments, and higher speeds than the conservative driving urban experiments. The symmetric "urban cruise" peak in for conservative driving urban experiments was flattened in the aggressive driving urban experiments, with more time in the low speed region (between 5 and 25 mpg) and at higher rates of acceleration at higher speeds. The aggressive driving urban experiments in the morning (Figure 3.2.7.7) had less time in the urban cruise peak (at approximately 40 mph) than for evening driving (Figure 3.2.7.8). The aggressive driving urban routes had less time at stop for the morning driving than for the evening driving (19.5% versus 21.4%) which was similar to the conservative driving urban experiments.

The aggressive driving freeway and urban probability plots were averaged 1:1 in

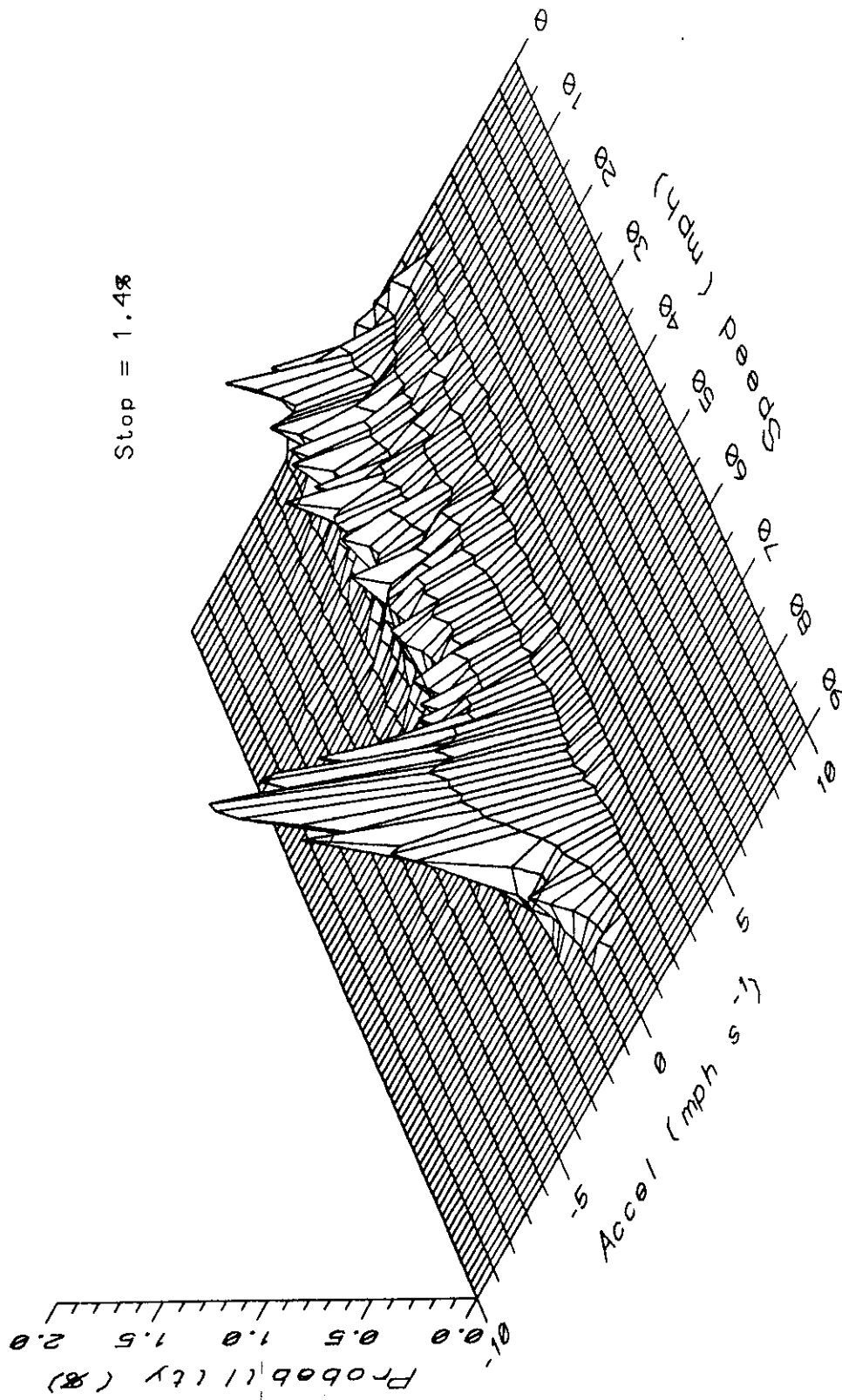


Figure 3.2.7.3 Probability plot of aggressive freeway driving pattern data.

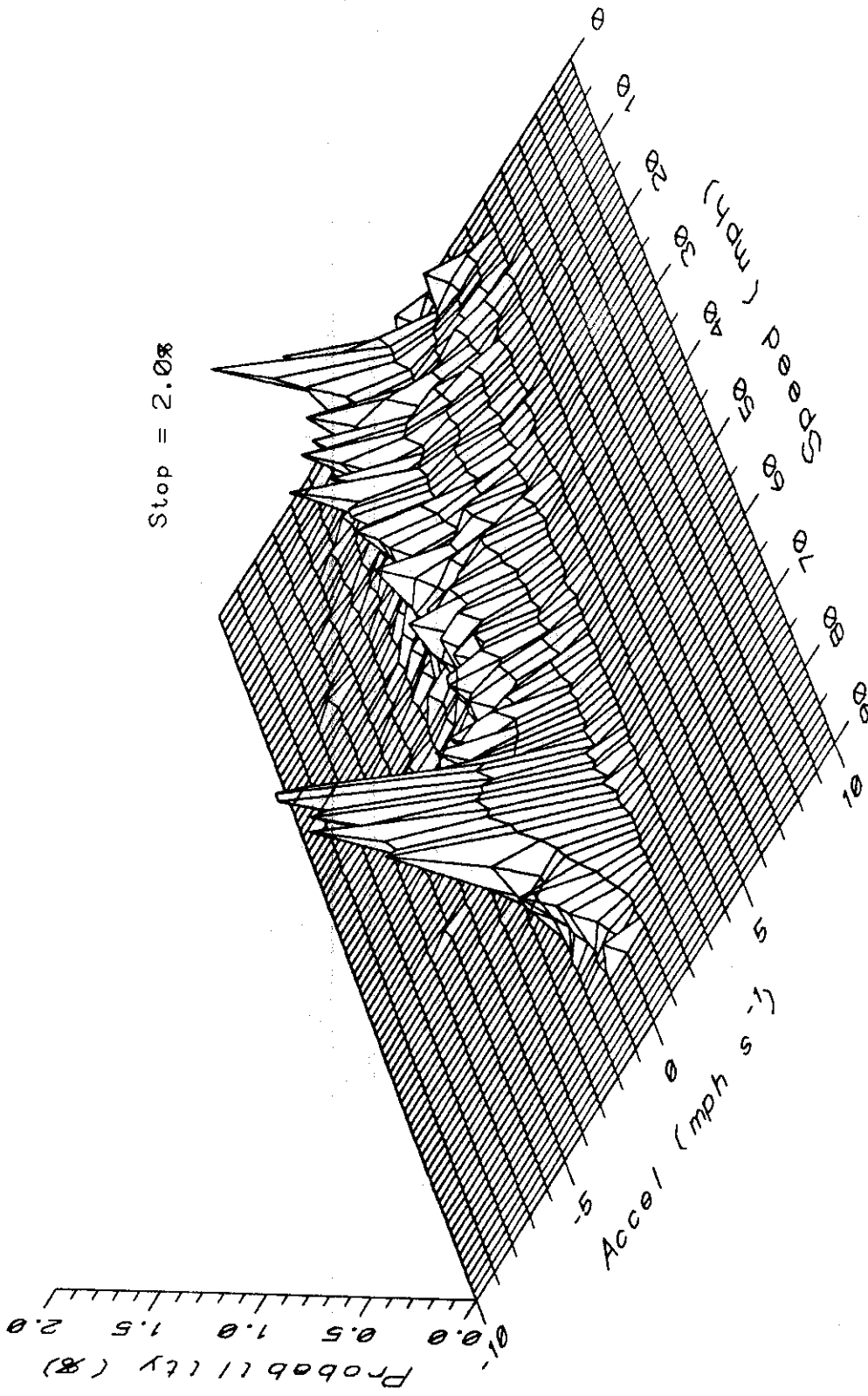


Figure 3.2.7.4 Probability plot of aggressive morning freeway driving pattern data.

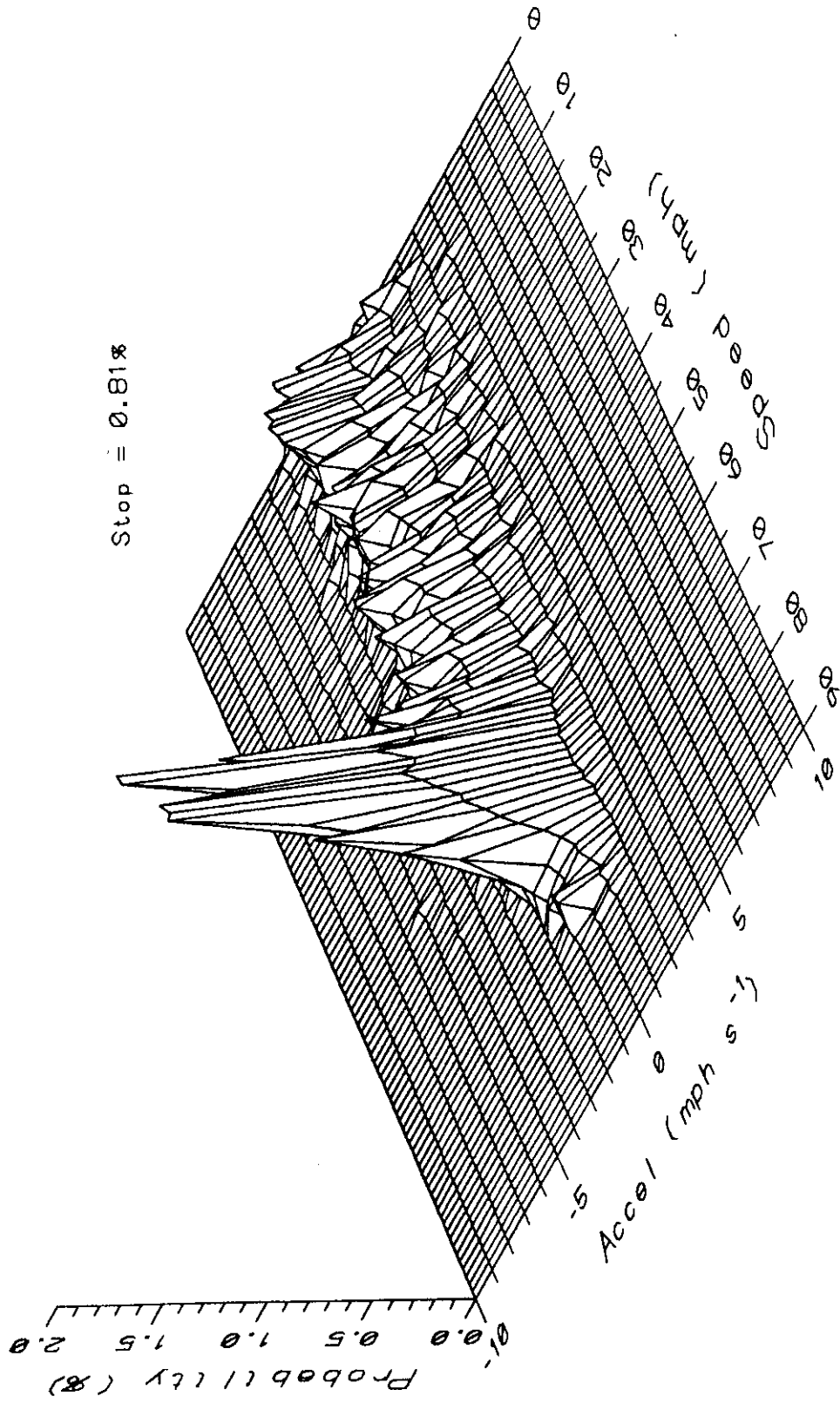


Figure 3.2.7.5 Probability plot of aggressive evening freeway driving pattern data.

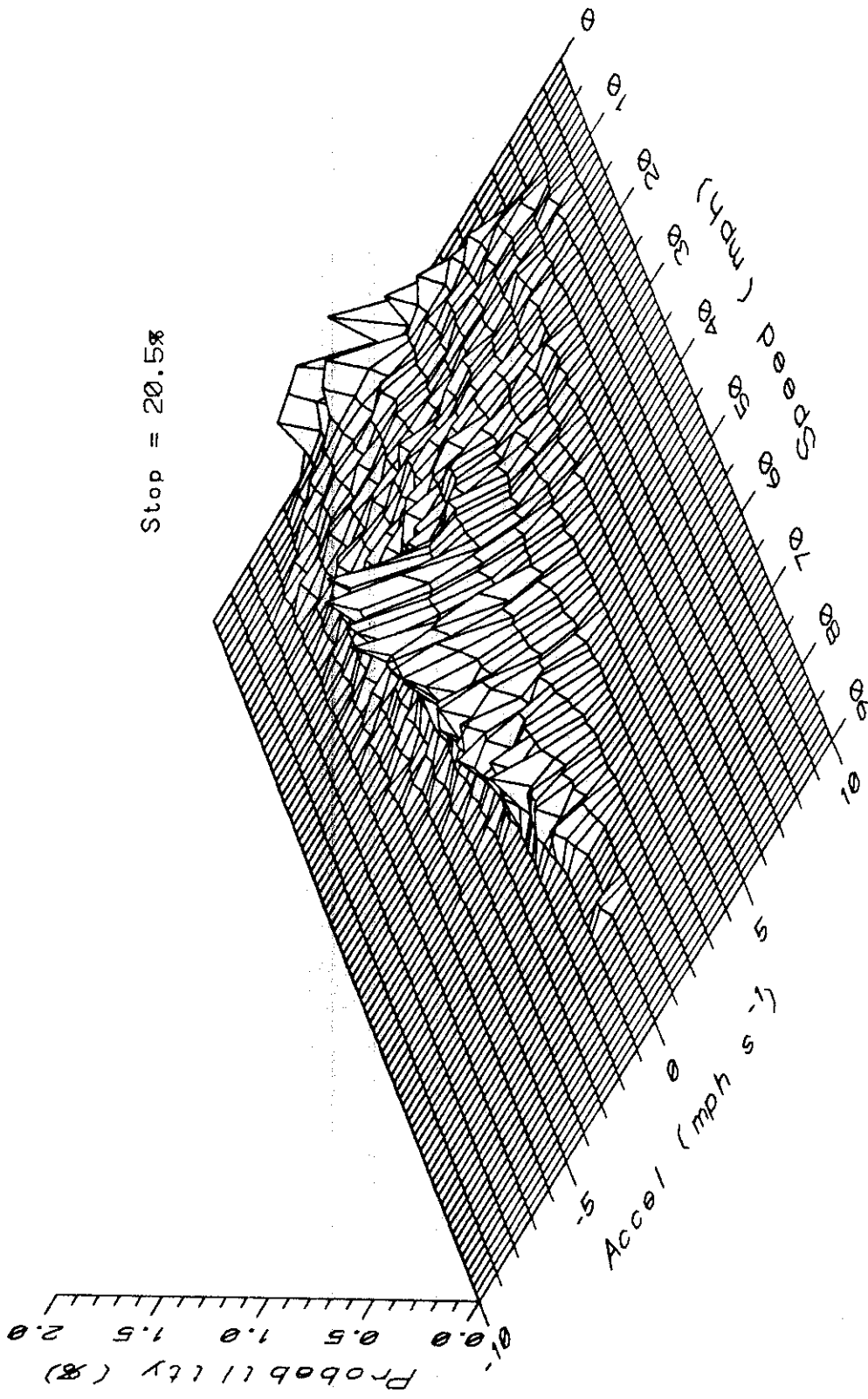


Figure 3.2.7.6 Probability plot of aggressive urban driving pattern data.

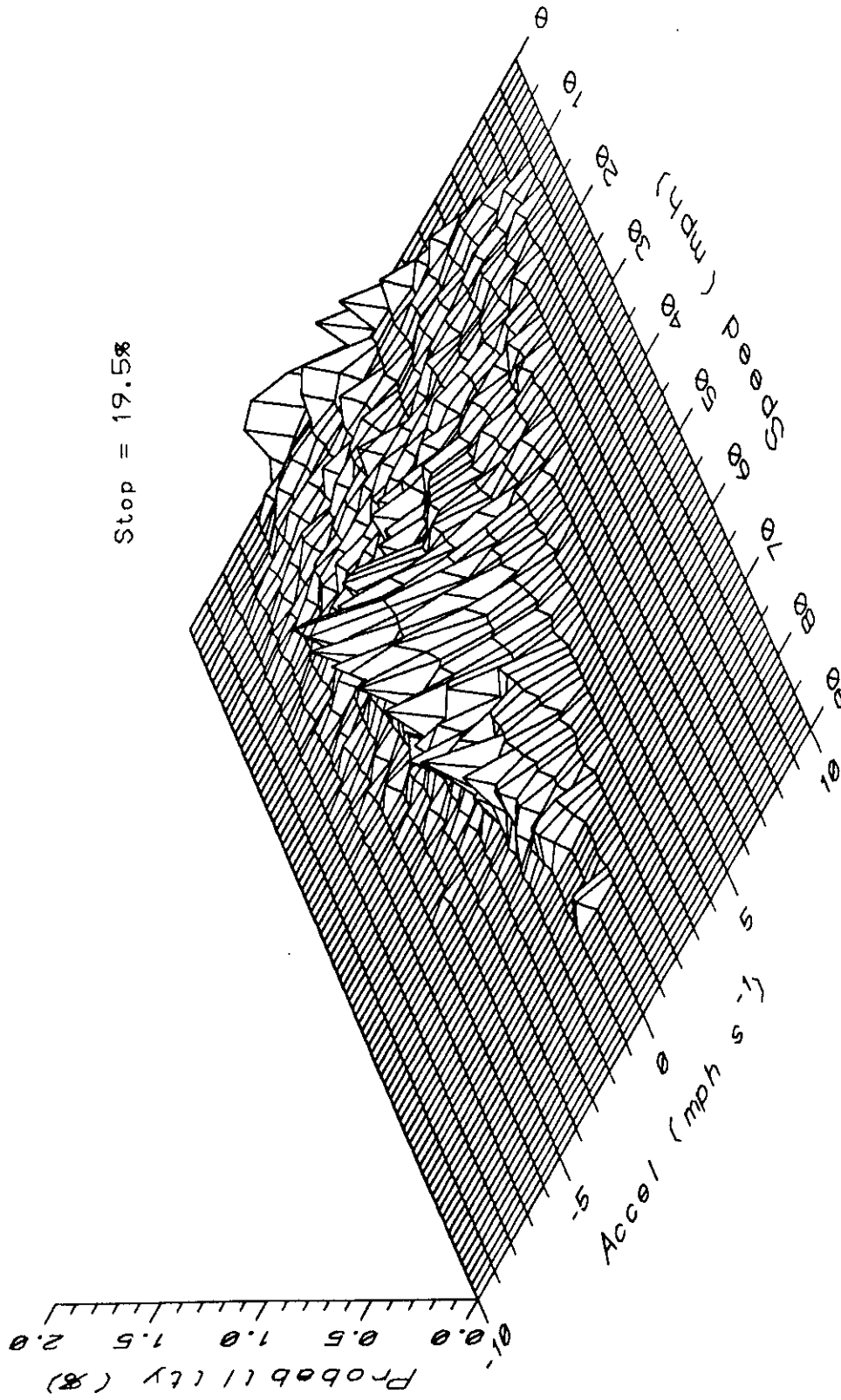


Figure 3.2.7.7 Probability plot of aggressive morning urban driving pattern data.

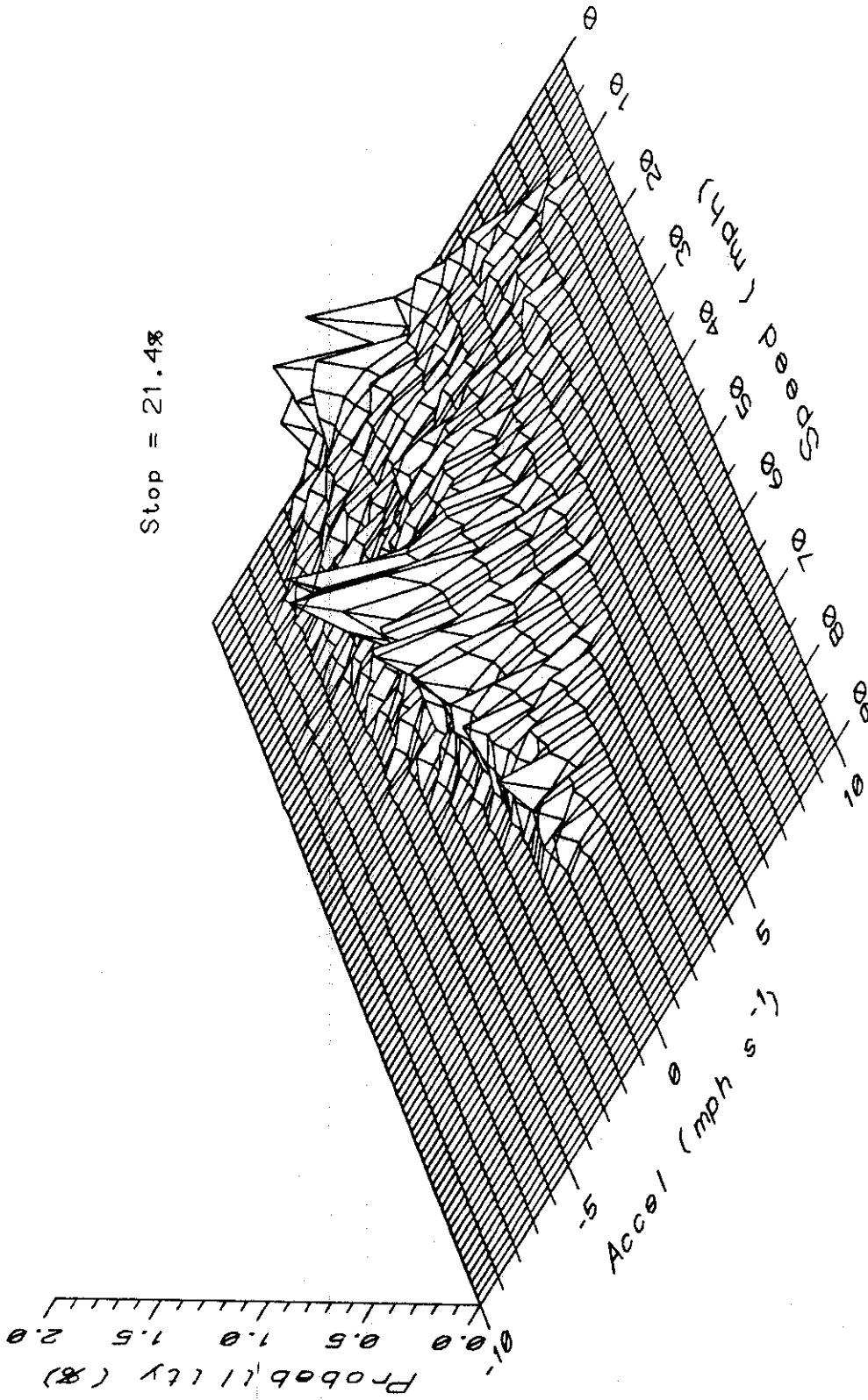


Figure 3.2.7.8 Probability plot of aggressive evening urban driving pattern data.

the same manner as the conservative driving plots to obtain the average on-road aggressive driving plot (Figure 3.2.7.9). The average aggressive driving plot covers a large area (high rates of acceleration and deceleration, and low to high speeds) and appears to be approximately equally distributed between 5 and 25 mph, 25 and 55 mph and has a high speed cruise peak from 55 to 80 mph. The average percent time at stop in the aggressive driving experiments was 11.0%.

The combined aggressive driving probability plot was subtracted in three dimensions from the FTP plot to show differences between aggressive driving and the FTP (Figure 3.2.7.10). The differences were similar to the FTP minus conservative driving patterns with the extremes slightly more exaggerated. The percent time at stop was 7.3% higher for the FTP than the aggressive driving patterns, and the under-estimation at high speeds and the over-estimation in the urban cruise peak (25 to 45 mph) were both slightly greater.

The aggressive driving probability plot was also subtracted in three dimensions from the averaged conservative driving plot to show differences between conservative and aggressive driving (Figure 3.2.7.11). The percent of time at stop for aggressive driving was lower than for the conservative driving experiments as expected due to the ability of the driver to change lanes to avoid stopping in the aggressive driving experiments. The other differences between the aggressive driving probability plot and the conservative driving was slightly more accelerations and higher speed freeway cruise peak for the aggressive driving patterns.

3.2.8 Open Loop Operation

3.2.8.1 Lean Open Loop Operation

Table 3.2.8.1.1 lists the frequency of lean open loop operation on-road by type of driving pattern, test procedure or on-road route type. Lean open loop operation occurred 0.77% of the time during the conservative freeway experiments and 0.036% of the time during the urban experiments. (Note: These values are slightly different than those presented in Section 3.2.6 because those were averaged by pattern, and these averages are

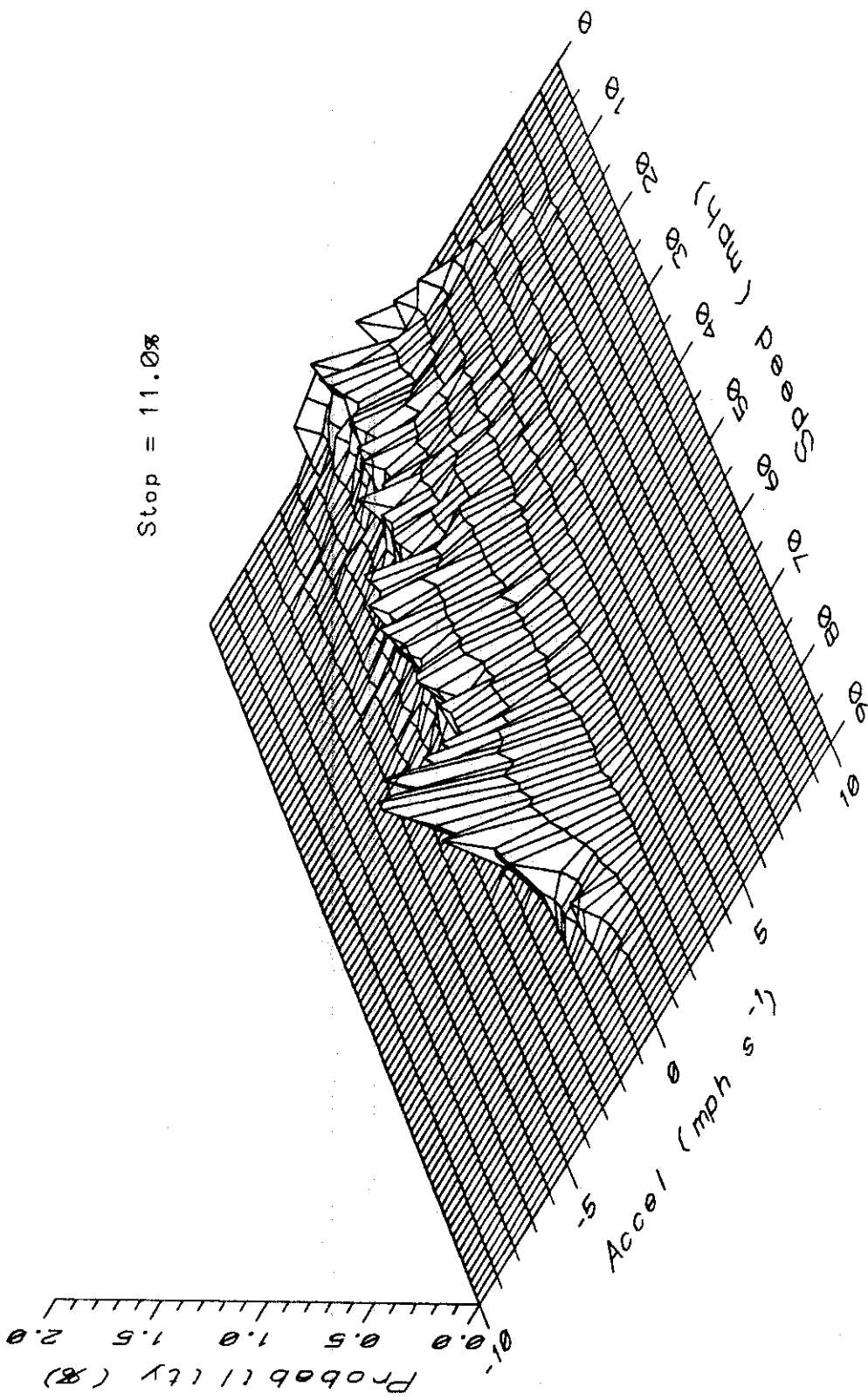


Figure 3.2.7.9 Probability plot of combined aggressive freeway and urban driving pattern data.

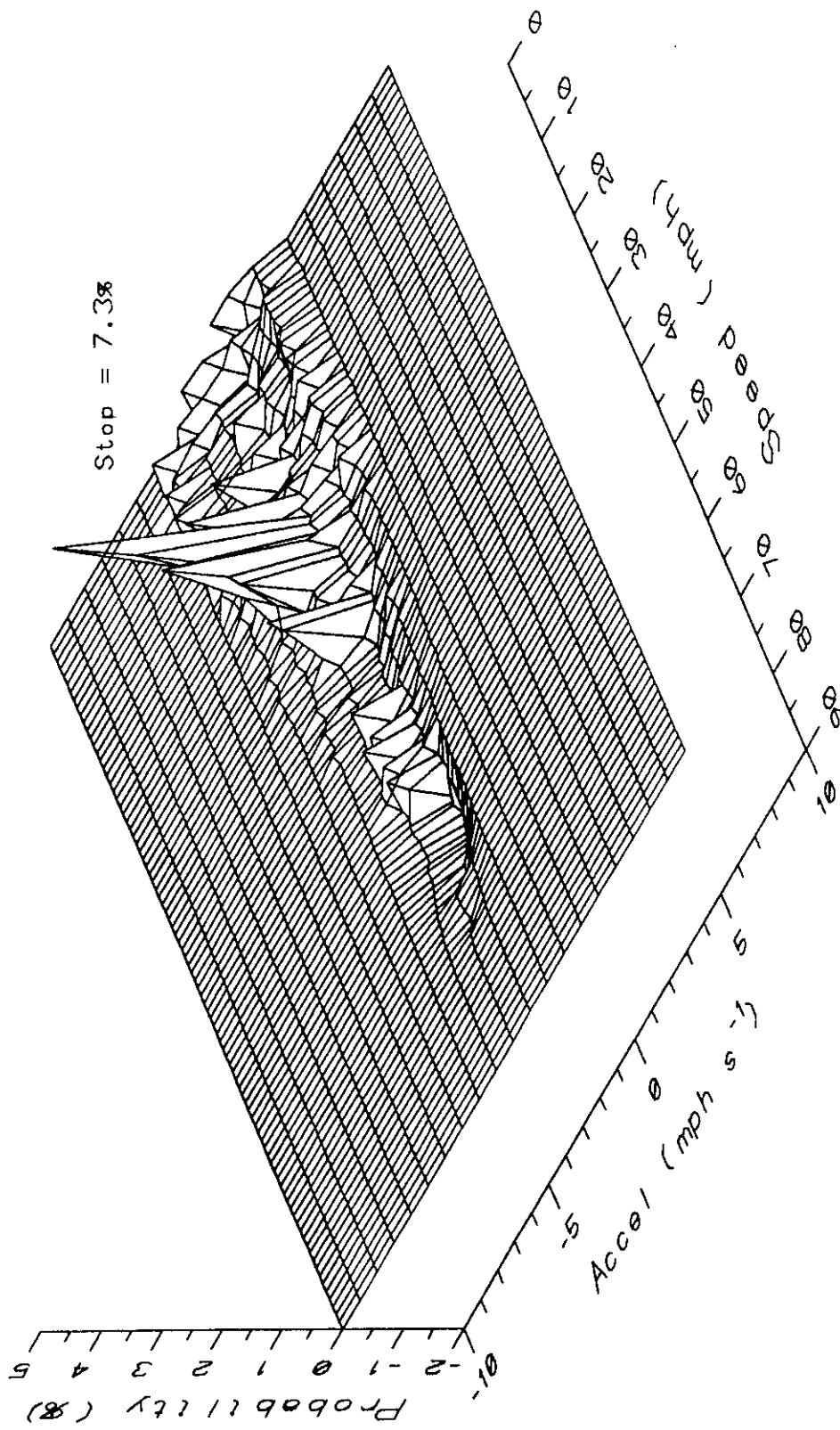


Figure 3.2.7.10 Probability plot of FTP minus combined aggressive freeway and urban driving pattern data.

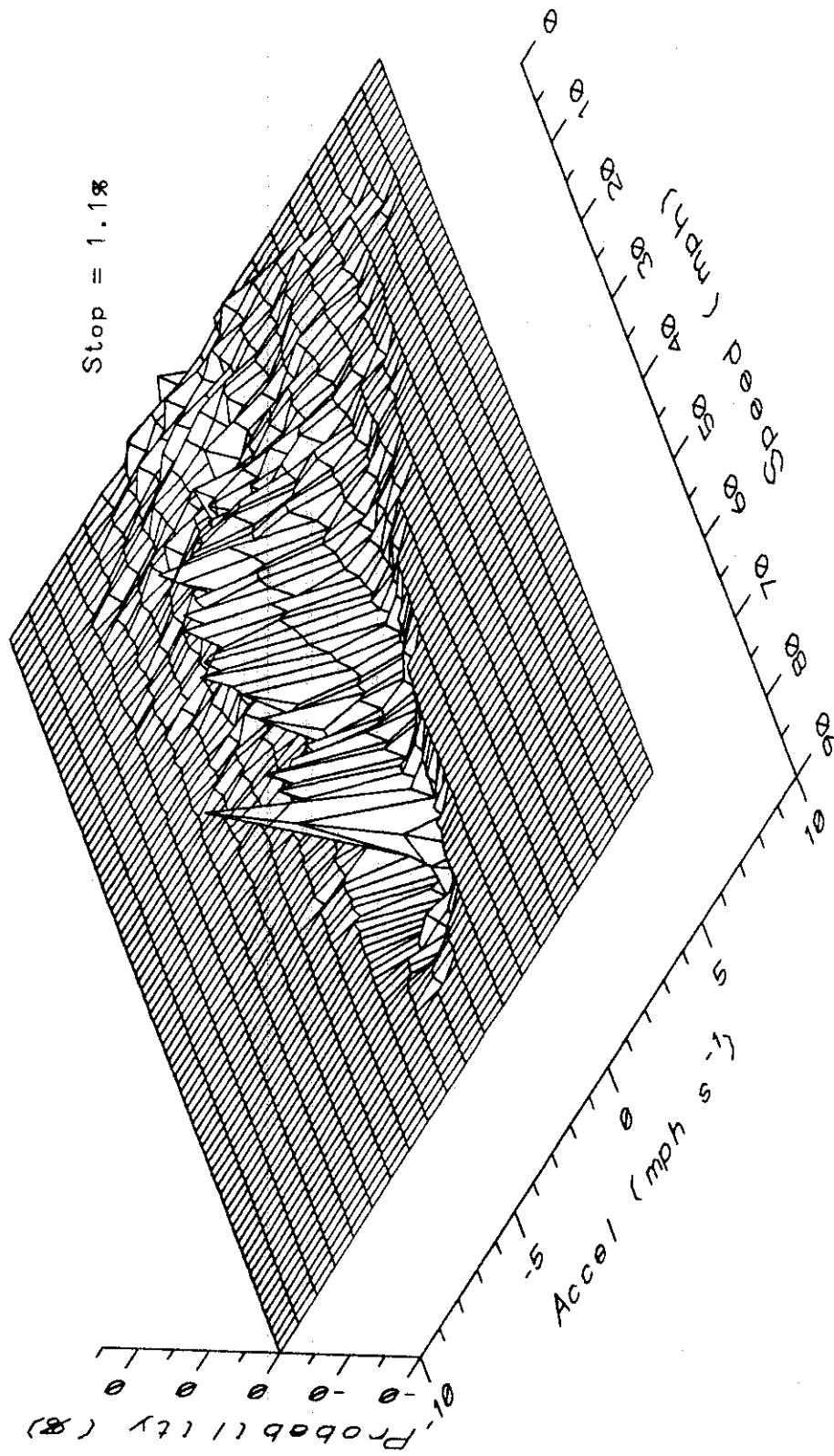


Figure 3.2.7.11

Probability plot of combined conservative freeway and urban driving on-road data minus combined aggressive freeway and urban driving pattern data.

weighted for the total seconds of data collection during each experiment). There were a total of 134 events which ranged from 1 to 26 seconds in duration with an average of 4.1 seconds. Figure 3.2.8.1.1 shows the speeds and accelerations associated with these events in relation to the maximum operating envelope. The duration, speed and acceleration rate for each of the events is given in Appendix A.4.3. All of the events except for one occurred during decelerations (0.42 to -3.62 mph s^{-1}) and between 42.4 and 68.9 mph.

For the aggressive driving experiments the frequency of lean open loop operation was much greater for the freeway experiments compared to the urban experiments, as in the conservative driving experiments, with a frequency of 0.80% for the freeway experiments and 0.18% for the urban experiments. There were a total of 62 events which ranged from 1 to 19 seconds long with an average of 2.6 seconds. Figure 3.2.8.1.2 shows the speeds and accelerations associated with these events in relation to the maximum operating envelope. The duration, speed and acceleration rate for each of the events is given in Appendix A.4.5. All of the events occurred during decelerations which ranged from -0.06 to -4.56 mph s^{-1} and occurred in a similar speed range to the conservative driving experiments (42.7 to 67.4 mph).

Figure 3.2.8.1.3 shows the 239 lean open loop events (4.0% of the time) as a function of speed and acceleration for the repeated freeway experiment. The duration, speed and acceleration rate for each of the events is given in Appendix A.4.1. The range in duration of the open loop events was much greater than for conservative or freeway experiments (1 to 69 seconds) and had an average of 6.8 seconds. The speed range (43.7 to 71.2 mph) and the range of deceleration rates (0.36 to -4.21 mph s^{-1}) were very close to the conservative and aggressive driving experiments.

3.2.8.2 Rich Open Loop Operation

Table 3.2.8.2.1 lists the frequency of lean open loop operation on-road by type of driving pattern, test procedure or on-road route type. The frequency of rich open loop operation recorded during the FTP and the HFET driven on a dynamometer are not included in Table 3.2.8.2.1 because the rich open loop operation did not occur during the

Table 3.2.8.1.1 Summary of on-road lean open loop operation.

Lean Open Loop					
	Average	Median	Std. Dev.	Minimum	Maximum
Duration (sec)					
Conservative	4.1	3	4.3	1	26
Aggressive	2.6	2	3.0	1	19
Repeated Freeway	6.8	4	9.9	1	69
Speed (mph)					
Conservative	55.0	54.6	5.6	42.4	68.9
Aggressive	54.6	53.9	6.3	42.7	67.4
Repeated Freeway	56.9	56.3	5.5	43.7	71.2
Accel rate (mph/s)					
Conservative	-0.87	-0.78	0.67	-3.62	0.42
Aggressive	-1.32	-1.04	0.93	-4.56	-0.06
Repeated Freeway	-0.54	-0.39	0.57	-4.21	0.36

tests.

For the conservative driving experiments, there were only five rich open loop events during more than 160,000 seconds of driving time. The events ranged from 1 to 4 seconds in duration with an average of 2 seconds. Frequency of rich open loop operation was 0.0044% for freeway routes and 0.0074% for urban routes. Figure 3.2.8.2.1 shows four of the events which occurred during accelerations near the maximum and lie outside the envelope of the FTP. The duration, speed and acceleration rate for each of the events is given in Appendix A.4.4. The fifth rich open loop event which was inside the envelope of the FTP occurred on a grade. Because there are no changes in load during the FTP (no "grades"), this rich open loop event would not be expected to occur during the FTP.

The frequency of rich open loop operation was greater for aggressive driver experiments than for passive driver experiments (0.43% for freeway routes and 1.03% for urban routes). However, the ratio of the frequency of open loop operation for freeway to urban routes was similar between conservative and aggressive routes (approximately two times more frequent for urban routes than freeway routes). As mentioned in Section

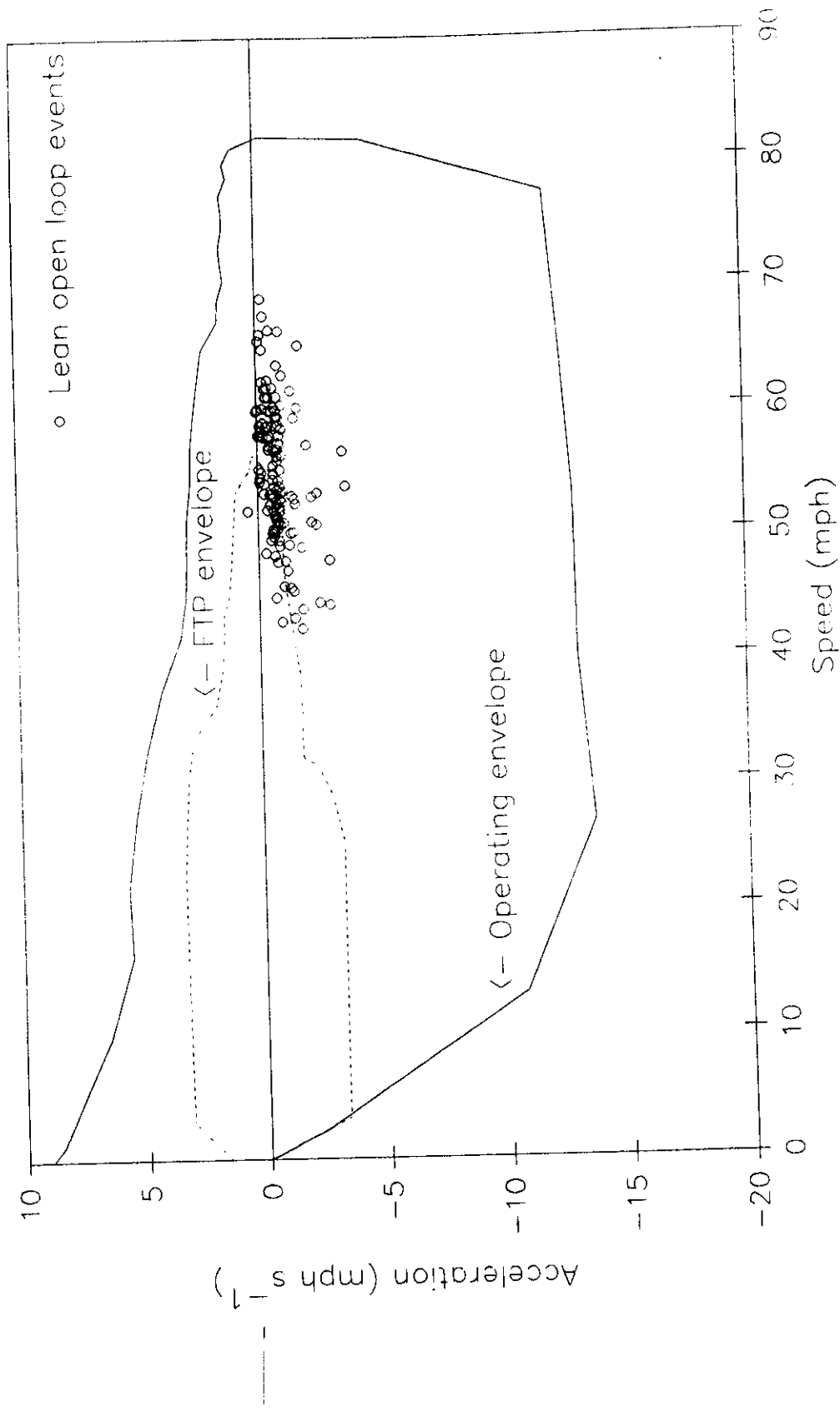


Figure 3.2.8.1.1 Occurrences of lean open loop operation for conservative driving freeway and urban matrix routes.

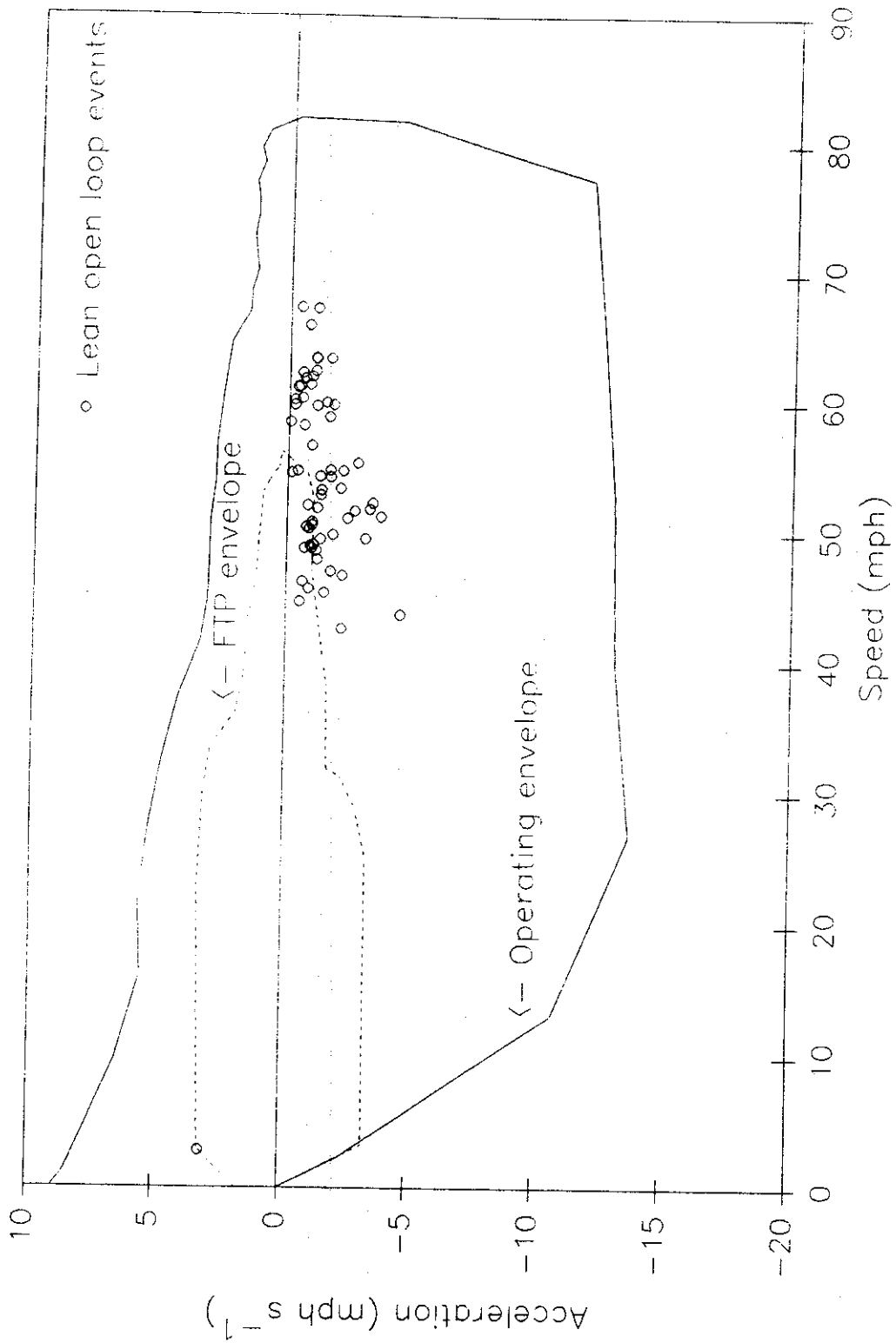


Figure 3.2.8.1.2 Occurrences of lean open loop operation for aggressive driving freeway and urban matrix routes.

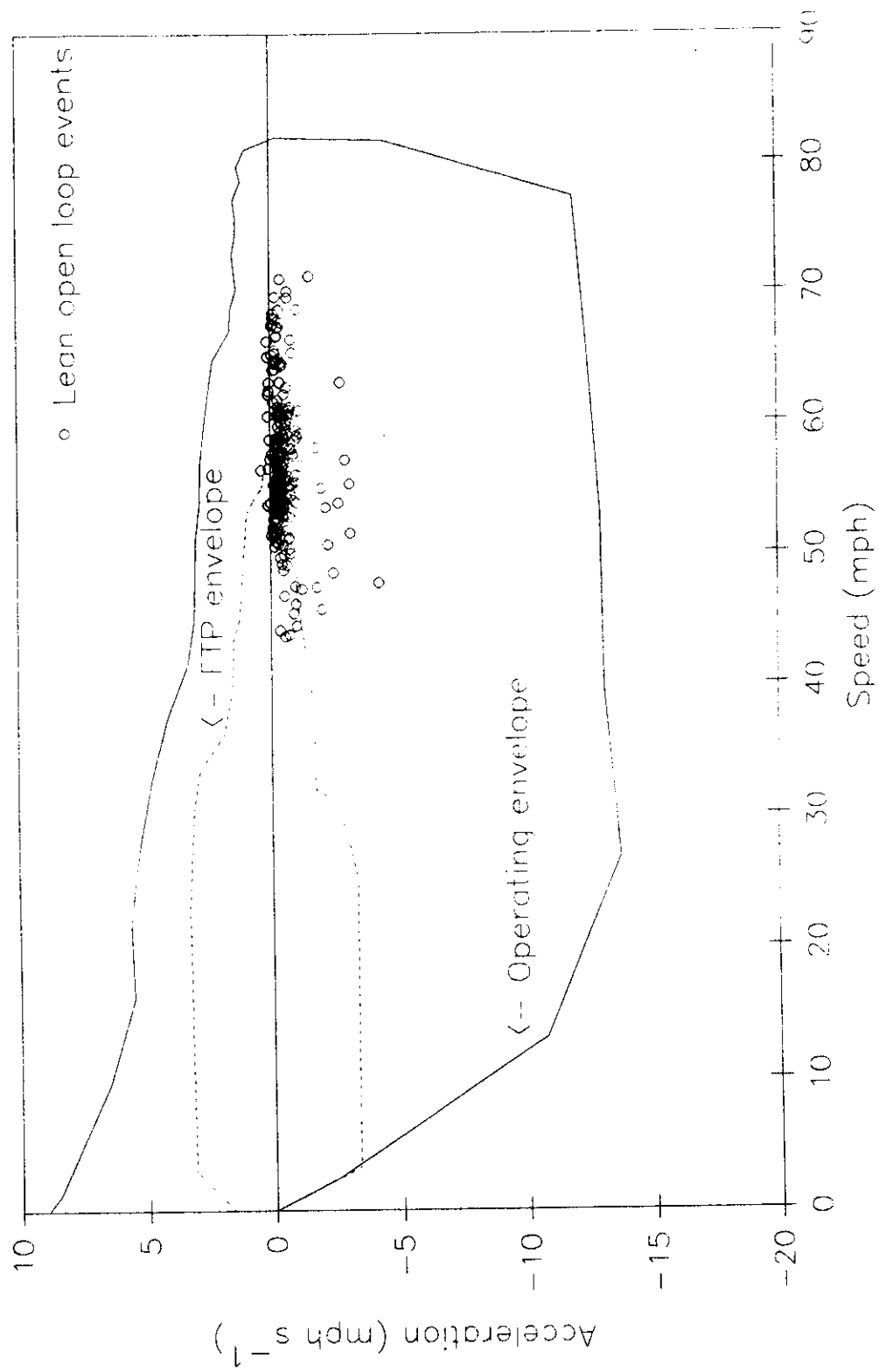


Figure 3.2.8.1.3 Occurrences of lean open loop operation for repeated freeway experiment.

Table 3.2.8.2.1 Summary of on-road rich open loop operation.

Rich Open Loop					
	Average	Median	Std. Dev.	Minimum	Maximum
Duration (sec)					
Conservative	2.0	2	1.2	1	4
Aggressive	1.8	1	1.3	1	8
Repeated Freeway	2.4	2	1.2	1	6
Speed (mph)					
Conservative	34.3	36.7	16.8	12.4	54.2
Aggressive	32.2	33.5	17.6	0.0	73.7
Repeated Freeway	49.6	54.4	11.6	26.2	63.2
Accel rate (mph/s)					
Conservative	2.79	3.43	1.66	0.71	4.77
Aggressive	3.37	2.93	2.05	-0.35	8.35
Repeated Freeway	1.64	1.35	0.85	0.31	3.13

3.2.4., in the grade experiments rich open loop operation uphill occurred an average of 3% of the time for three tests without the use of the cruise control and no open loop operation was observed when using the cruise control although the speed was maintained near 65 mph. This and the difference between conservative and aggressive driving suggests the frequency of open loop operation may be more dependent on the manner in which the driver operates the vehicle than on the vehicle control strategy.

There were a total of 148 rich open loop events for the aggressive driving experiments which ranged from 1 to 8 seconds in duration with an average of duration of 1.8 seconds. Figure 3.2.8.2.2 shows the rich open loop events and the duration, speed and acceleration rate for each of the events is given in Appendix A.4.6. . Some of the events occurred at speeds and accelerations which were outside the maximum operating envelope because the acceleration experiments were conducted on a level road and higher rates of acceleration are possible driving downhill. The events started at virtually all speeds from 0 to 65 mph with one event at 73.7 mph. Although some of the events occurred inside the envelope of the FTP, the majority of the events occurred outside the envelope. The events inside the envelope of the FTP may have been due to increased

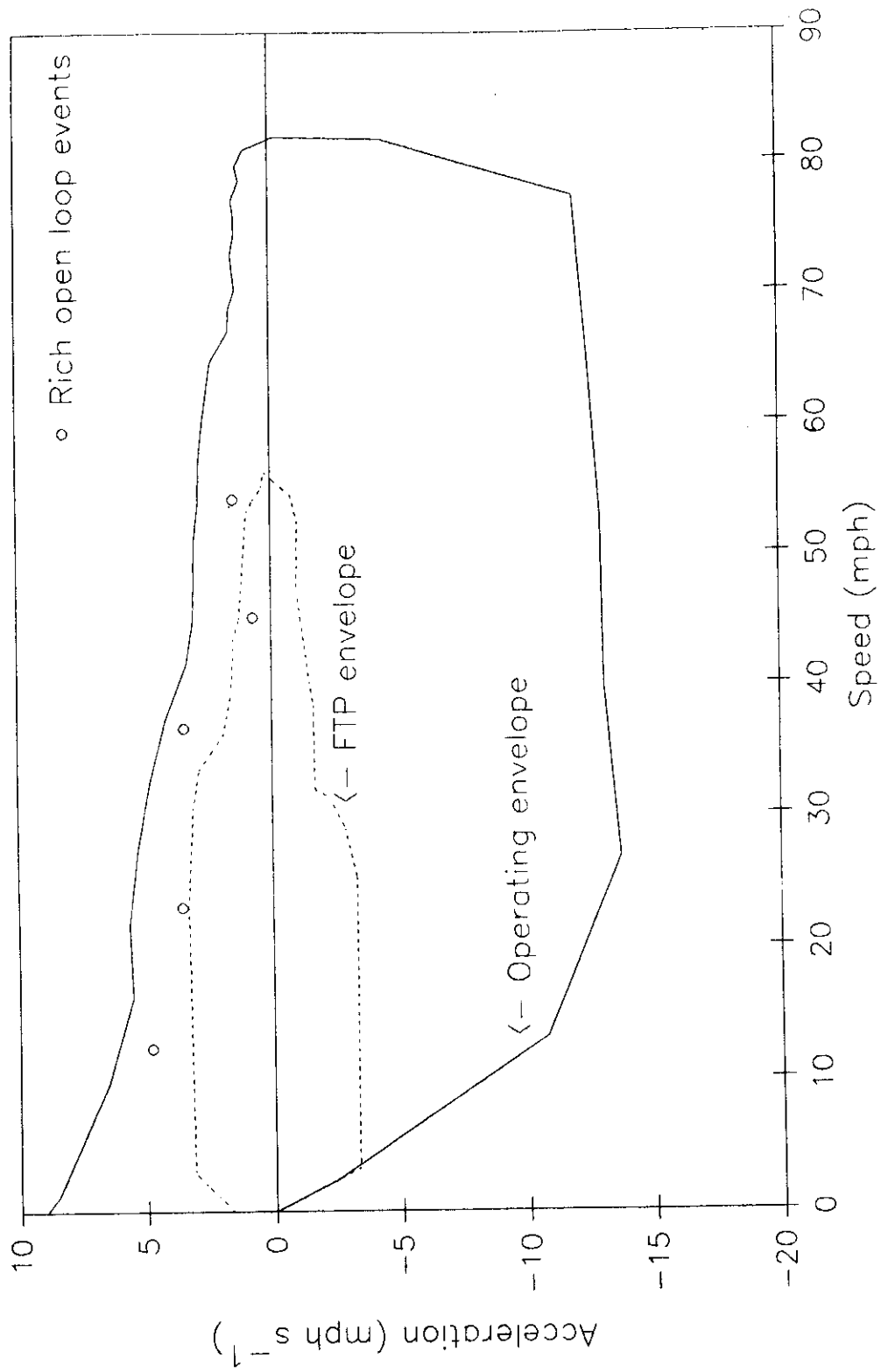


Figure 3.2.8.2.1 Occurrences of rich open loop operation for conservative driving freeway and urban matrix routes.

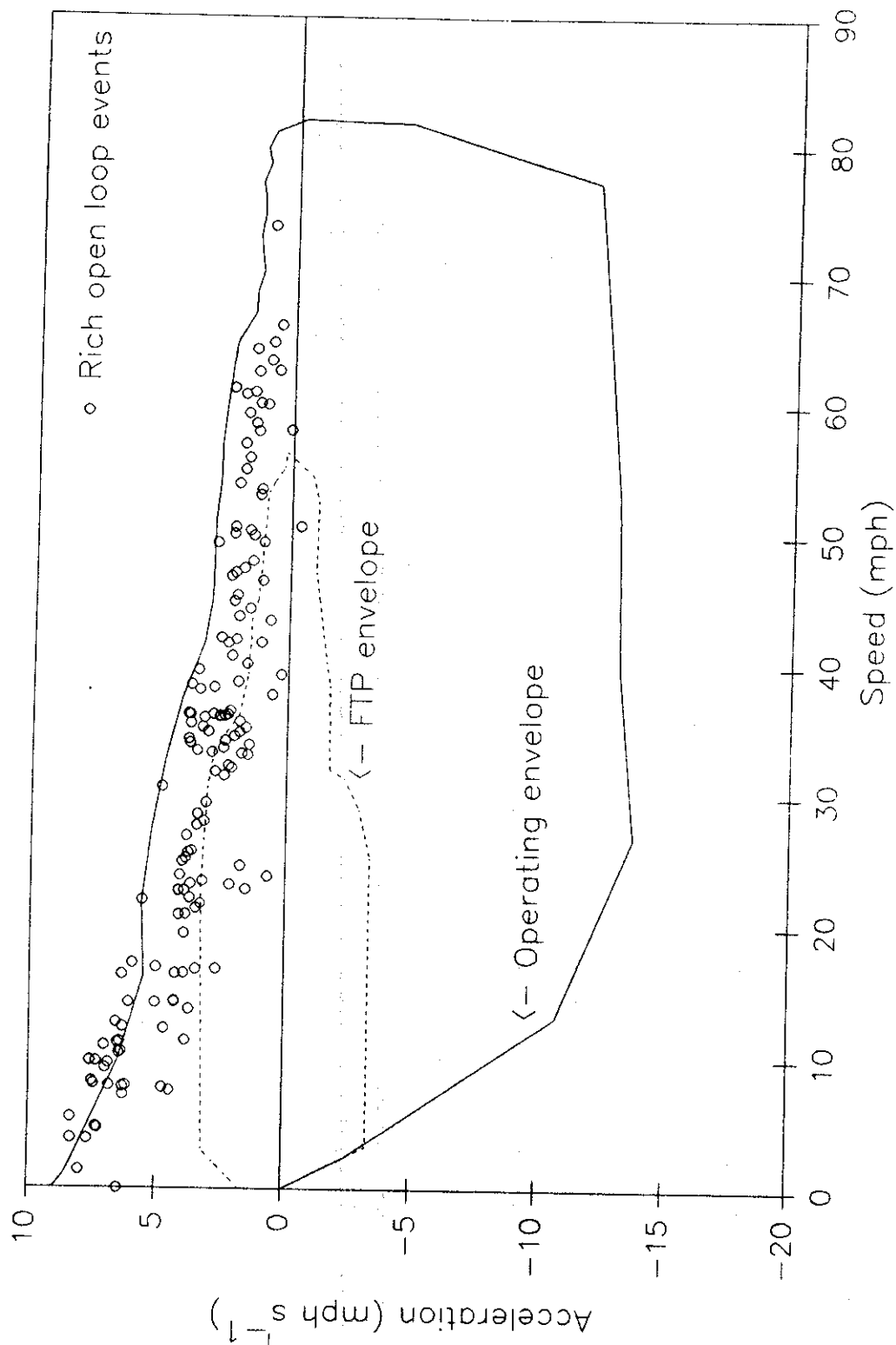


Figure 3.2.8.2.2 Occurrences of rich open loop operation for aggressive driving freeway and urban matrix routes.

loads caused by grades.

The 35 rich open loop events which occurred during the repeated freeway experiment are shown in Figure 3.2.8.2.3. The duration, speed and acceleration rate for each of the events is given in Appendix A.4.2. The duration of the rich open loop events ranged from 1 to 6 seconds with an average of 2.4 seconds. Approximately half of the events lie within the envelope of the FTP, probably due to the fact that the route contains a hill and the increased load, although at a low rate of acceleration, may have caused the open loop operation. The large number of open loop events may also be due to hard accelerations needed for merging during freeway entrances and exits combined with the increased load traveling up the on-ramps (there were 54 merges onto the freeway during the experiment).

The data from the experiment were analyzed to determine the influence of average speed on percent time rich open loop and rich open loop operation was found to increase as average speed increased (see Figure 3.2.5.1). This suggests that rich open loop operation is less frequent in congested driving conditions, possibly due to the close proximity and low speeds of the vehicles which prevented hard accelerations.

3.2.8.2.1 Comparison to Other Vehicles

Kelly and Groblicki (1992) conducted 10.6 hours (36,160 seconds) of driving in an instrumented Pontiac Boneville SSE with a 3.8L V6 engine in Los Angeles. Their driving included the LA-4, peak and off-peak freeway, driving up and down a steep hill, metered freeway on-ramps, and idling. Their test vehicle operated open loop rich 1.2% of the time and they concluded that the conditions which caused rich open loop operation were > 40% throttle and > 2000 rpm ("GM enrichment").

All the on-road data collected in our study were evaluated to determine the frequency of operation in this "GM enrichment". Comparison of the percent time in rich open loop operation for the Taurus to the percent time the vehicle would in principle operate rich open loop if the control strategy for the Taurus were the same as for the Boneville SSE is given in Table 3.2.8.2.1.1. The results indicate there are significant

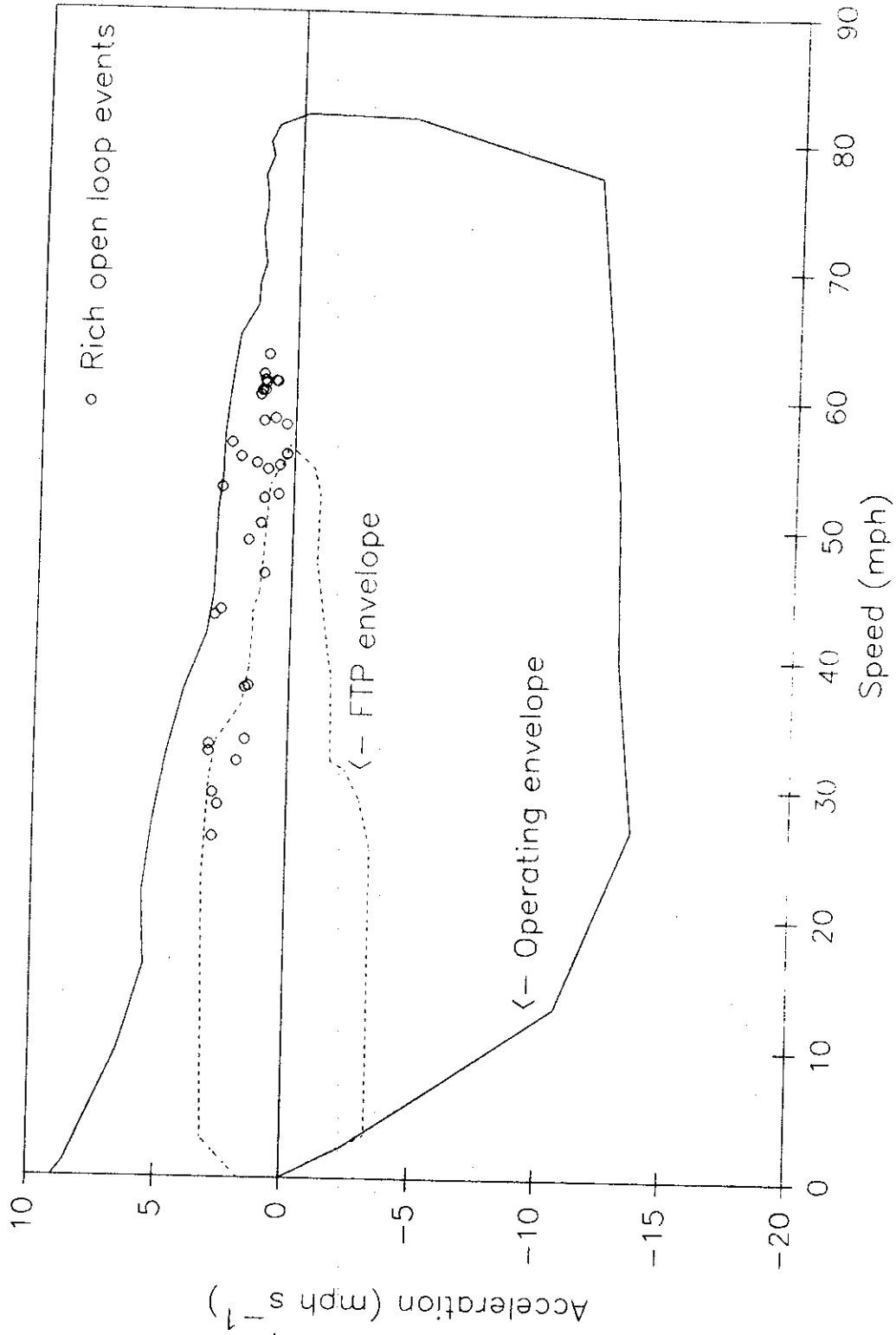


Figure 3.2.8.2.3 Occurrences of rich open loop operation for repeated freeway experiment.

Table 3.2.8.2.1.1 Comparison of experimental conditions vs. GM enrichment condition for the Taurus.

Experiment	Percent time in Rich Open Loop	Percent time in "GM Enrichment" ^a
Federal Test Procedure	0.0	0.27
Highway Fuel Economy Test	0.0	0.0
Conservative freeway driving	0.003	0.57
Conservative urban driving	0.007	0.98
Repeated freeway route	0.24	4.3
Aggressive freeway driving	0.44	4.8
Aggressive urban driving	1.1	8.2

^a >40% Full throttle and >2000 RPM

differences between the control strategies for these two vehicles.

For comparison, FTP tests were conducted with a 1992 Aerostar van which had the same 3.0L V6 engine as the Taurus (St. Denis et al., 1993, Jesion et al., 1993). The RCON data from the Aerostar was analyzed identically to the data for the Taurus using a modified version of the data analysis program. The results indicated that the engine operated rich open loop 0.43% of the time, and operated 0.96% of the time in the "GM enrichment condition". This was dramatically different than the results for the Taurus shown in Table 3.2.8.1.1. and suggests that not only are the results different for the same pattern for vehicles produced by different manufacturers, but that vehicles with the same engine may have different frequencies of rich open loop operation.